

Annex 2 – Feasibility Study

Climate Resilient Fishery Initiative for Livelihood Improvement
The Gambia (PROREFISH)

Part 1: Climate Rationale for GCF Investment

CHAPTER 1 OVERVIEW OF THE CLIMATE RATIONALE	5
INTRODUCTION	5
OVERVIEW OF THE CLIMATE RATIONALE FOR GCF INVOLVEMENT	6
REFERENCES.....	12
CHAPTER 2 FISHERIES VALUE CHAIN ANALYSIS IN THE GAMBIA	13
INTRODUCTION	13
ARTISANAL FISHERIES	15
SHELLFISH PRODUCTION AND MARKETING	20
INDUSTRIAL FISHERIES	21
POLICY AND LEGISLATIVE FRAMEWORKS	22
REFERENCES.....	26
CHAPTER 3 CLIMATE TREND ANALYSIS AND PROJECTED CLIMATE CHANGE IN THE GAMBIA AND OVER THE GAMBIA RIVER WATERSHED	27
INTRODUCTION	27
DATA.....	27
ANALYSIS	29
CONCLUSIONS	38
REFERENCES.....	39
CHAPTER 4 CLIMATE CHANGE AND THE OCEAN ENVIRONMENT	42
INTRODUCTION	42
OBSERVED CLIMATE CHANGE IMPACTS ON THE OPEN OCEAN.....	42
OBSERVED CLIMATE CHANGE IMPACTS ALONG THE CONTINENTAL SHELF AND COASTAL AREAS	47
PROJECTED IMPACTS AND TRENDS	51
NOTABLE ANTICIPATED IMPACTS IN THE OPEN OCEAN.....	51
NOTABLE ANTICIPATED IMPACTS ALONG THE CONTINENTAL SHELF AND COASTAL AREAS.....	52
CONCLUSIONS	53
REFERENCES.....	54
CHAPTER 5 THE GAMBIA RIVER, MANGROVE ECOSYSTEM AND CLIMATE CHANGE IMPACTS	60
INTRODUCTION	60
THE GAMBIA RIVER AND ESTUARINE ENVIRONMENT	61
ESTUARINE ECOLOGY AND MANGROVE ECOSYSTEM.....	64
MANGROVE ECOSYSTEMS SERVICES	66
GAMBIAN MANGROVE ECOSYSTEM COMPOSITION	67
CLIMATE CHANGE IMPACT	70
HUMAN ACTIONS AND CONCLUSIONS	77
REFERENCES.....	79
CHAPTER 6 SALINE INTRUSION IN THE GAMBIA RIVER	83
PART 1 – INTRODUCTION	83
PART 2 – RATIONALE FOR THE ASSESSMENT	83
PART 3 – THEORY ON SALT INTRUSION	85
PART 4 – METHODS AND MATERIALS	95
PART 5 RESULTS & DISCUSSION	115
PART 6 – LIMITATIONS	136
PART 7 – CONCLUSIONS.....	139
CONCLUSIONS	141
REFERENCES.....	142
APPENDIX A DISCHARGE MODEL.....	146
APPENDIX B HYDROPOWER DAM OPERATIONAL SCHEMES	147
APPENDIX C MODEL SCENARIOS	150

APPENDIX D MODEL RESULTS	151
CHAPTER 7 BIOLOGICAL IMPACTS OF CLIMATE CHANGE ON THE GAMBIAN FISHERIES	153
OBSERVED IMPACTS OF CLIMATE CHANGE ON THE FRESHWATER AND MARINE ENVIRONMENTS OF THE GAMBIA AND FORECAST OF FUTURE CHANGES	153
CLIMATE VULNERABILITY ASSESSMENT: METHODS	157
VULNERABILITY OF KEY SPECIES TO THE LIKELY IMPACTS OF CLIMATE CHANGE	161
VULNERABILITY TO CLIMATE CHANGE OF DIFFERENT SEGMENTS (HABITATS) OF THE GAMBIA FISHERIES AND AQUACULTURE.....	170
REFERENCES.....	174
APPENDIX 1A. VULNERABILITY SCORES FOR THE TEMPERATURE ATTRIBUTE.....	181
APPENDIX 1B. VULNERABILITY SCORES FOR SALINITY	187
APPENDIX 1C. VULNERABILITY SCORES FOR OXYGEN.....	191
APPENDIX 1D. VULNERABILITY SCORES FOR PH	195
APPENDIX 1E. VULNERABILITY SCORES FOR OCEAN CIRCULATION AND PRODUCTIVITY	198
APPENDIX 1F. VULNERABILITY SCORES FOR SEA LEVEL RISE.....	202
APPENDIX 1G. VULNERABILITY SCORES FOR EXTREME EVENTS	206
APPENDIX 1H. VULNERABILITY SCORES FOR PRECIPITATION	210
APPENDIX 2. EXAMPLES OF ADAPTIVE MODELS/ACTIVITIES APPLIED TO DIFFERENT SYSTEMS IN THE FISHERIES AND AQUACULTURE SECTORS.....	214

Chapter 1 Overview of the Climate Rationale

Introduction

1. **As a low lying coastal nation, and the smallest country on the African continent, The Gambia is particularly vulnerable to the impacts of climate change.** The country's physical location renders it highly exposed to climate change threats from both land and sea and, due to the small size of the economy, the country possesses limited capacity to autonomously undertake extensive adaptation efforts in response to threats for which it contributed little in creating.¹ In the Notre Dame Global Adaptation Initiative (ND-GAIN) index, Gambia is the 33rd most vulnerable country and the 53rd least ready country in the world, reflecting its high vulnerability score and low readiness score.
2. **The Gambia's climate vulnerability is also set in a complex development context.** The country is classified as low income by the World Bank², and it ranks 172nd in the 2020 Human Development Index. In addition, the Gambia is also now recognised as a Fragile and Conflict-affected Situation (FCS FY21) country, given its high institutional and social fragility. The average GDP growth of 2.9% over the last decade has proven insufficient to accelerate development, reduce poverty and improve food security. The Gambians, particularly the youth, continue to migrate from rural areas to the urbanised coastal zone, but more importantly to attempt to emigrate to developed countries. In addition, the economic shock induced by the Covid-19 pandemic on the tourism sector will erase some of the recent developmental gains.
3. **Agriculture continues to play an important role in the Gambia's development, even as its weight has been decreasing.** The agriculture sector, including forestry and fisheries (and related industries) employs nearly half—46 percent—of the labour force and represents the source of livelihood for 80 percent of the rural population, according to the latest 2015/16 Integrated Household Survey (IHS). For about 72 percent of poor households and 91 percent of extremely poor rural households, agriculture is the main source of income. In 2019, the sector contributed 23.7 percent of GDP and a third of all foreign exchange earnings from exports.
4. **Within the broader agriculture sector, the fisheries sub-sector presents both challenges and opportunities.** The sub-sector has generally received significantly less attention and investment from public, private and international financing sources, when compared with the focus on crops and livestock. For example, the majority of recent donor funded projects have responded to the Government's call to boost crop (particularly rice) production in order to reduce the country's food import bill. In parallel, the fisheries sector productive base has continued to deteriorate absent investment, and under pressure from resource over-exploitation by international vessels operating in the Gambian waters. On the other hand, in recent years the fisheries and aquaculture sub-sector has grown steadily. For the moment, the fisheries represent the most significant segment within the primary sector of the Gambian economy (see Chapter 2). This is partly explained by the significant declines in recent years for crops and livestock, while fishing

¹ Per capita GHG emissions in The Gambia is 1.11 Mt CO₂e, compared to the global average of 6.76 Mt CO₂e (source: https://www.climatewatchdata.org/ghg-emissions?breakBy=regions-PER_CAPITA&chartType=line&gases=all-ghg®ions=WORLD%2CGMB§ors=total-including-lucf accessed 3/8/2020).

² World Bank Country and Lending Groups 2020 (<https://datahelpdesk.worldbank.org/knowledgebase/articles/906519-world-bank-country-and-lending-groups>)

and aquaculture increased decidedly. In addition, fisheries present excellent opportunities for job creation, especially for youth and women, and for value addition in synergy with the tourism sector.

5. **In this context, the Government of the Gambia has requested FAO's support for the development of a project proposal for the *Climate Resilient Fishery Initiative for Livelihood Improvement*, to be considered for Green Climate Fund (GCF) financing.** FAO has been a long-standing partner of the Government for the agricultural and rural development of the Gambia. In particular, FAO has been particularly active in supporting the fisheries sub-sector through a series of technical assistance projects, which supported capacity development at central level, the introduction of a series of West African innovations and the promotion of aquaculture. Building on this collaboration, the present proposal seeks to urgently address the climate vulnerability of the fisheries sector and to build the resilience of fisher folk's livelihoods.

Overview of the Climate Rationale for GCF Involvement

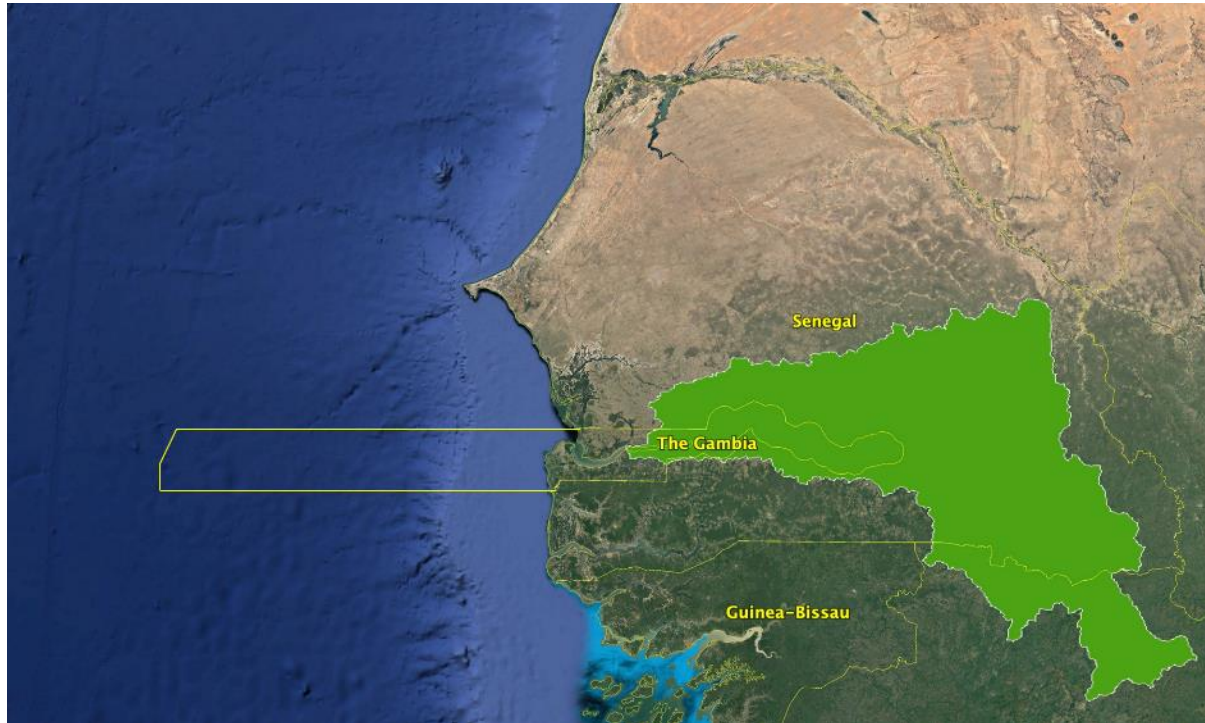
6. **The story of climate change impacts in The Gambia is largely one of water.** No other country has perhaps as close a relationship with a river's course than The Gambia. A majority of the national boundaries were drawn tracing lines 10 km north and south of the respective riverbanks of the Gambia River to the furthest navigable point upstream (see Figure 1-1). The water passing through the river originates as seasonal rainfall in the upland areas of the river's watershed, which aggregate and drain through the length of the country on the way to the sea. Along its path the growing volume of fresh water enters an increasingly saline estuarine environment, impacted by the daily tidal movements of the Atlantic Ocean, before emptying into the sea. This continuous, dynamic hydrologic system of fresh to saltwater bodies, and the habitats and species that it supports, is subject to and responds differently to the major climate change forces encountered along its transect.

7. **As illustrated in Figure 1-1, The Gambia has both an oceanic economic exclusion zone extending 200 nautical miles into the Atlantic Ocean, and an associated watershed situated predominantly in neighbouring countries, Senegal and Guinea.** From the starting point of the Gambia River, at an elevation of 1,125 m in the Fouta Djallon of Guinea, over 1,150 miles inland, to the depths of the economic exclusion zone 3,000 m below sea level, 370 km offshore, the geographic diversity of The Gambia's aquatic resource-base is immense (Agudo-Bravo and Mangas, 2015; ISL, 2014). In terrestrial systems, some of the greatest impacts of climate change – changes in temperature, precipitation and the atmospheric concentrations of greenhouse gases – are seen through their direct effects on crop and livestock species, with other effects felt indirectly through more intricate biotic relationships involving associated species (e.g., pests, diseases and pollinators).

8. **Aquatic systems are vastly more complex.** Climate impacts aquatic species at various levels. To take one example, ocean warming, increases in air temperature must first warm surface waters before this heat can be transferred into the ocean body and impact fish species at varying depths. The transfer of energy from air to sea, however, is mediated through a complex of interconnected processes involving differential rates of heating of land and water surfaces, along shore winds, and the confluence of currents, upwelling events and thermocline barriers, which can slow, even stop, or greatly accelerate the pace of warming in different locations and at different periods of time. In the same way changes in precipitation

and atmospheric CO₂ concentrations, the other drivers of direct climate change impacts, are also having important species-level effects, and in doing so they too must work through equally complex sets of physical and chemical reactions. Some of the greatest impacts of climate change on aquatic species are felt through the indirect effects on habitat and food chains, involving several trophic levels of biological diversity, each with their own requirements, tolerances and dependencies.

Figure 1-1 The Gambia, Gambia River watershed and economic exclusion zone³



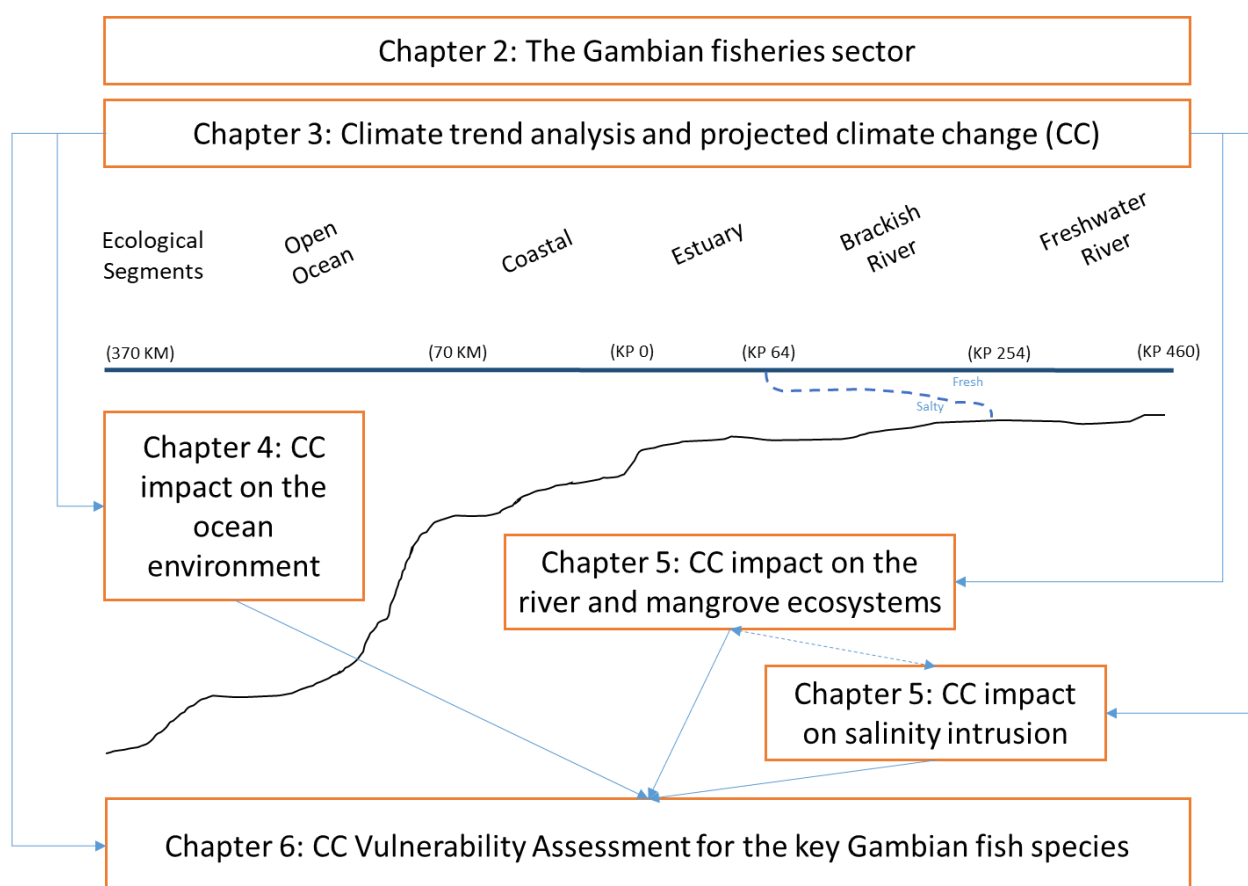
9. To address the range of climate change dynamics within the Gambian fisheries, a comprehensive climate analysis has been prepared as part of the project formulation process. Following this introduction, the subsequent six chapters each address a different facet of major impacts. **Chapter two** introduces and describes the various fisheries, their structure and economic importance, relative contributions to food security and employment, the sector's governance, policies and investments. **Chapter three** provides an overview of the historical and projected physical aspects of climate change in The Gambia and the Gambia River watershed. **Chapter four** examines the climate change impacts and threats on the oceanic environment. **Chapter five** explores the Gambia River and mangrove ecology and the climate change impacts and threats on these key fisheries habitats. **Chapter six** presents findings of a focused hydrologic assessment of saltwater intrusion into the Gambia River under climate change and the risks of the river experiencing a hypersaline disaster. **Chapter seven** assesses the overall biological impacts

³ Note that the watershed reflects those areas upstream of the maximal extend of permanent saltwater intrusion (KP 64) (Figure sources: the shape file for the Gambia Watershed was obtained from the HydroSHEDS database (<https://hydrosheds.org/page/overview>); The Gambian Economic Exclusion Zone from the Marine Regions Gazetteer (<https://www.marineregions.org/gazetteer.php?p=details&id=8370>); Base map, Google Earth Pro.

of major climate change threats on key target species in the various fisheries – oceanic, coastal, estuary and river – as presented in the earlier chapters.

10. **The climate analysis presents a complex pathway through which climate change will impact each of the ecological segments of the Gambian fisheries, which in turn will generate biological impacts on various fish species, resulting in reduced resource availability for the Gambian populations.** To begin with, the Gambian fisheries can be separated into five ecological segments: 1) the open ocean, 2) the coastal zone, 3) the estuary, 4) the brackish water segment of the river, and 5) the freshwater segment of the river (kilometre points (KP) are indicated in Figure 1-2 below). Climate change impacts each segment in different ways and magnitudes; given the very limited information and studies available on the topic of Gambian fisheries, new research was conducted for the present assessment.

Figure 1-2 Overview of the climate rationale



11. **The climate trend analysis and projections of climate change were conducted (see chapter 3 for full details), downscaling global circulation models to identify the best fit and forecast changes in temperature and precipitation.** Overall, across the projections there is a mixed through general agreement in the potential of declines in future precipitation, albeit modest, towards the end of the

century.⁴ Given the historical trend and virtual certainty of continued increases in temperature across all locations and time periods (demonstrated by the analysis), resulting in greater rates of evaporation, the conclusion indicates the likelihood of there being a decline in streamflow within the Gambia River in the decades ahead. Such a conclusion is consistent with a meta-analysis done on studies on river basin runoff in West Africa, which found that for the Gambia River basin future streamflow will likely decline by 4.5 percent (Roudier et al., 2014).

12. In the off-shore environment, the focus of the analysis was on documenting the impact of climate change on the open ocean, and on continental shelf and coastal areas (see chapter 4 for full details). A number of dimensions were investigated, including sea surface and ocean warming, dissolved oxygen, salinity changes, marine heatwaves, storms, harmful algal blooms, acidification, upwelling and sea level rise. **The findings indicate that the speed, magnitude and inertia of change occurring in the abiotic conditions in the North Atlantic and CCLME offer limited scope for taking adaptive actions.** These limitations are particularly acute for The Gambia given the extremely small size of the country's EEZ compared to the vastness of the oceanic environment and fluidity in movement of key fish stocks. Other than improved joint monitoring efforts of fish stocks with neighbouring countries and continued adjustments to fishing pressure and management of residential stocks, and the possible selective protection of seaward assets, there are few prospects for realizing returns to investments in adaptive measures in the fishery sector in the oceanic environment.

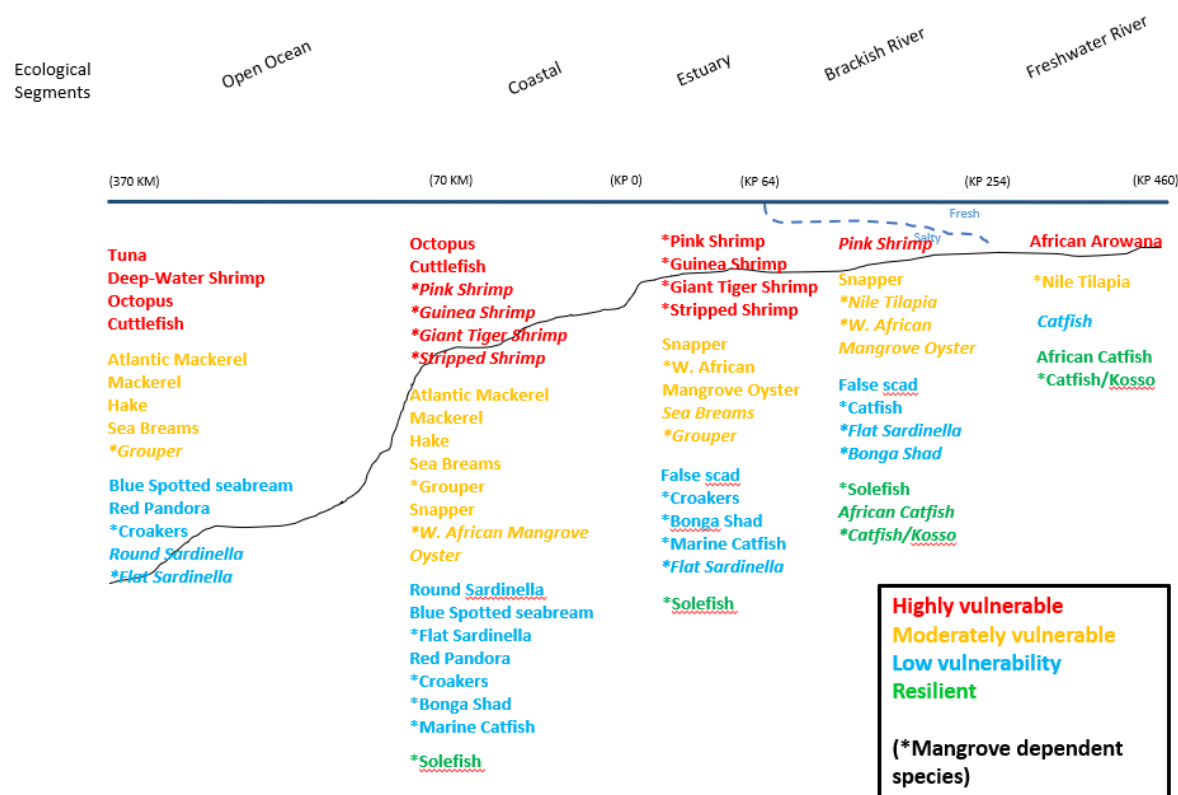
13. Moving into the estuary and the middle river (brackish water segment), the emphasis of the analysis turned to the mangrove ecosystems, which play a pivotal role in the lifecycle of major fish species (see chapter 5 for full details). The analysis documents the Gambia river and estuarine environments, and presents the mangrove ecosystems in detail, before diving into the climate change impacts (focused on sea level rise, salinity changes, CO₂ increase, pH decrease and soil acidification, dissolved oxygen (DO) and turbidity changes, and decreased stream flow and drought). In addition, human activity stressors were considered. Overall, the mangrove ecosystem in The Gambia faces both human and climatic pressures. Due to the varying sources of these pressures, mangroves may not be able to adapt or recover if attention is given to only individual stressors. Investments, therefore, need to address both human and climatic pressures.

14. Salinity intrusion in the Gambia river – a naturally occurring process expected to be exacerbated by climate change – received particular attention in the climate analysis (see chapter 6 for full details). This is due to both the direct impact of salinity intrusion on fish biology and their distribution, and the indirect effect on the mangrove ecosystems. The study commissioned for the present proposal fills an important knowledge gap for the Gambia and shows that climate change and a planned hydropower dam will have strong effects on the level of salt intrusion in the Gambia estuary. In the future, the pattern of salt intrusion will be heavily influenced by changes in precipitation and temperature, sea level rise and short-term anthropogenic alterations of river flow. This may result in a strong hypersaline estuary before the end of the century, which would be detrimental for the ecology and economy of The Gambia.

⁴ This conclusion is also supported by ensemble data from the CORDEX Africa models (<https://dap.climateinformation.org>). The analysis in the latter portal also finds variability between models, but 12 out of 18 models project a decrease in precipitation under RCP4.5 for the period 2041-2070.

15. Tying together the different strands of the above analysis, the climate change vulnerability assessment investigated the biological responses of the 28 most important (shell)fish species in the Gambia (see chapter 7 for full details). Building on the rest of the climate analysis, the vulnerability assessment identified eight key climate stressors (temperature, salinity, oxygen, pH, ocean circulation and productivity, sea level rise, extreme events and precipitation) and analysed the tolerance and response of the 28 most important (shell)fish species to the projected changes. A significant number of species, currently representing a majority of the catch in the Gambia, is projected to be negatively impacted by climate change in the medium term (see the visual summary in Figure 1-3 below).

Figure 1-3 Visual summary of the climate change vulnerability assessment for the main Gambian fish species



16. In addition to this impact pathway, it is important to note that climate change will also have other indirect effects on the Gambian fisheries by damaging the existing coastal fisheries infrastructure and the inland aquaculture facilities. The findings of the climate vulnerability assessment at each major landing site targeted for the project are presented together with the proposed climate-proofing interventions in part 2 of the Feasibility study.

17. Overall, the climate change impacts on the Gambian fisheries will translate into less fish availability for the local population, for whom this resource represents both a livelihood and food source (see chapter 2 for more details). As such, it is imperative to invest in adaptation measures to

preserve and improve the livelihoods of the Gambian fisher folk, as well as maintain availability of fish – the cheapest source of protein – for the general population.

References

Agudo-Bravo, L.M. and J. Mangas. 2015. Main Geomorphic Features in the Canary Current Large Marine Ecosystem. In: Oceanographic and Biological Features in the Canary Current Large Marine Ecosystem. Valdés, L. and I. Déniz-González (eds). Technical Series 115. Paris: IOC-UNESCO.

Oréade-Brèche and ISL Ingénierie (ISL). 2014. Etude d'Impact Environnemental et Social du Projet Energie (Revue du rapport COTECO 2008). Mission d'Appui Conseil a l'OMVG pour la Réalisation de son Projet Energie. Projet de Rapport Final. Dakar: OMVG.

Chapter 2 FISHERIES VALUE CHAIN ANALYSIS IN THE GAMBIA

Introduction

1. **The Gambia has one of West Africa's most productive fishing grounds with over 500 marine fish species recorded, mostly demersals and pelagics.** With a marine coastline of 80 km, The Gambia claims a continental shelf of 4,000 km² and an Exclusive Economic Zone of 10,500 km². As for inland fishing, the Gambia River, which runs through the entire length of the country (about 460 km), mainly harbours fresh water species (i.e. catfish or tilapia). The estuary areas are fringed by thick mangrove forests (covering an estimated 35,000 ha) on both the Northern and Southern sides and attract marine fish and crustacean species for feeding and spawning purposes, while serving as a refuge for most species too.
2. **Fisheries play an important role for the Gambian economy and society, making a significant contribution to people's nutrition and livelihoods.** Fish is the major source of animal protein for Gambians due to its low price. Indeed, it accounts for about 40 percent of total animal protein intake.⁵ The national annual per capita fish consumption is about has been estimated at 25 kg, though more recent estimates quote the figure of 18.4 kg, while some variability is observed between inland consumers (as low as 9 kg per capita) and coastal areas where the production is high.⁶ Generally, consumers prefer fresh small pelagic fish but in case these are not available, they purchase dried and smoked fish (small pelagic and low quality demersal).⁷
3. **According to The Gambia Bureau of Statistics, in 2019 the fishing and aquaculture sector accounted for 12.1 percent of GDP.** Given that the overall contribution of agriculture, forestry and fisheries is estimated at 23.7 percent of GDP, for the moment the fisheries represent the most significant segment within the primary sector of the Gambian economy. This is partly explained by the significant declines in recent years for crops and livestock, while fishing and aquaculture increased decidedly (19.6 percent in 2018, 18.4 percent in 2019). However, despite representing an important opportunity for employment and for increasing fish availability inland, aquaculture activities in the country are still at a nascent stage and their economic contribution is marginal.
4. **In terms of employment, it is estimated that about 200,000 people (76 percent of which are Gambian nationals) are directly or indirectly dependent on fisheries and related activities for their livelihoods.** The value chain engages about 41,000 self-employed fishers, processors, and traders; 158,000 workers in fish processing and distribution; and 1,500 workers in fish processing and export companies.⁸ Hence, the main wage providers in the value chain are fishers (59 percent) and processors (39 percent) while retailers accounts for only 2% of total wages.⁹ However, jobs in the production and processing segments are precarious and/or informal.¹⁰ The 2016 Frame survey reports that a fisher's household size is, on average, composed of 11 people.

⁵ Ragusa, 2014, p. 1.

⁶ FAO, <http://www.fao.org/fi/oldsite/FCP/en/gmb/body.htm>.

⁷ Avadí, A. et al., 2020, p. 39.

⁸ Ibid.

⁹ Ibid., p. 74.

¹⁰ Ibid., p. 13.

5. **Fisheries is a source of foreign exchange earnings for The Gambia.** Fish and fish products represent 13.6 percent of national exports. In terms of quantity, fresh, dried, or frozen fish accounts for 70.3 percent of the total fish exports.¹¹ The main importers of frozen fish are Korea, Vietnam, the United Kingdom, and the European Union, while fresh fish is exported mainly to Israel and to the United States, and dried fish to Korea and the United Kingdom.¹² Fishmeal accounts for the remaining 29.7 percent of total fish exports and is imported by Vietnam and Tunisia. The fisheries value chain gives a positive contribution to the balance of trade as it registers a trade surplus of around GMD 2.583 billion (US\$ 50.6 million).¹³ Nevertheless, the sectoral export performance is below its potential even though The Gambia is part of many bilateral trade agreements. Indeed, supply-side constraints hinder compliance with the World Trade Organization (WTO) sanitary and phytosanitary requirements, the WTO technical barriers to trade agreements, and the standards and technical requirements for exporting to the European Union. Market information gaps are an additional constraint. According to the World Bank, the unrealized export potential for Gambian frozen fish is estimated at 85 percent for OECD countries and 87 percent for non-OECD countries.¹⁴

6. **Gambian fisheries can be divided in two broad sub-sectors: artisanal fisheries, whose activities are dispersed, labour intensive, and characterised by low capital investment, and industrial fisheries, characterised by high capital investment and limited to the marine areas.** Overall, the two sub-sectors provide an average annual official landing of around 65,000 t, including both coastal marine and inland fishing.¹⁵ Figure 2-1 below outlines the flow of the fisheries value chain. Gambians consume about 32,000 t of fresh fish, smoked or dried fish per year for a total value of GMD 2,750 million (US\$ 53.9 million). Nationally consumed fish is artisanally sourced and processed, and distributed by fishmongers, processed fish traders or market operators. The industrial sub-sector is completely export-oriented. Foreign vessels land their catches abroad and industrial processors operating in The Gambia export the totality of their products although they source their raw material from artisanal fishers via fishmongers. Exported fish and fish products amount to around 19,000 t per year generating GMD 3,350 million (US\$ 65.7 million).¹⁶

7. **Although women's participation characterizes almost all segments of the value chain, there is a highly gendered division of labour reflecting social roles.** Indeed, the presence of women in production is limited to shellfish harvesting but they play a crucial role in domestic processing and marketing. It is estimated that women represent 80 percent of artisanal processors, 50 percent of fish retailers, and 65 percent of the processing plant workforce.¹⁷ Despite their involvement in different income-generating activities, women's contribution to economic growth is weak due to their limited access to credit and productive assets. In turn, this translates into lower wages and higher vulnerability to poverty.¹⁸

¹¹ Ibid., pp. 39-40, 72.

¹² Ibid.

¹³ Ibid., p. 12.

¹⁴ World Bank, 2019. p.14.

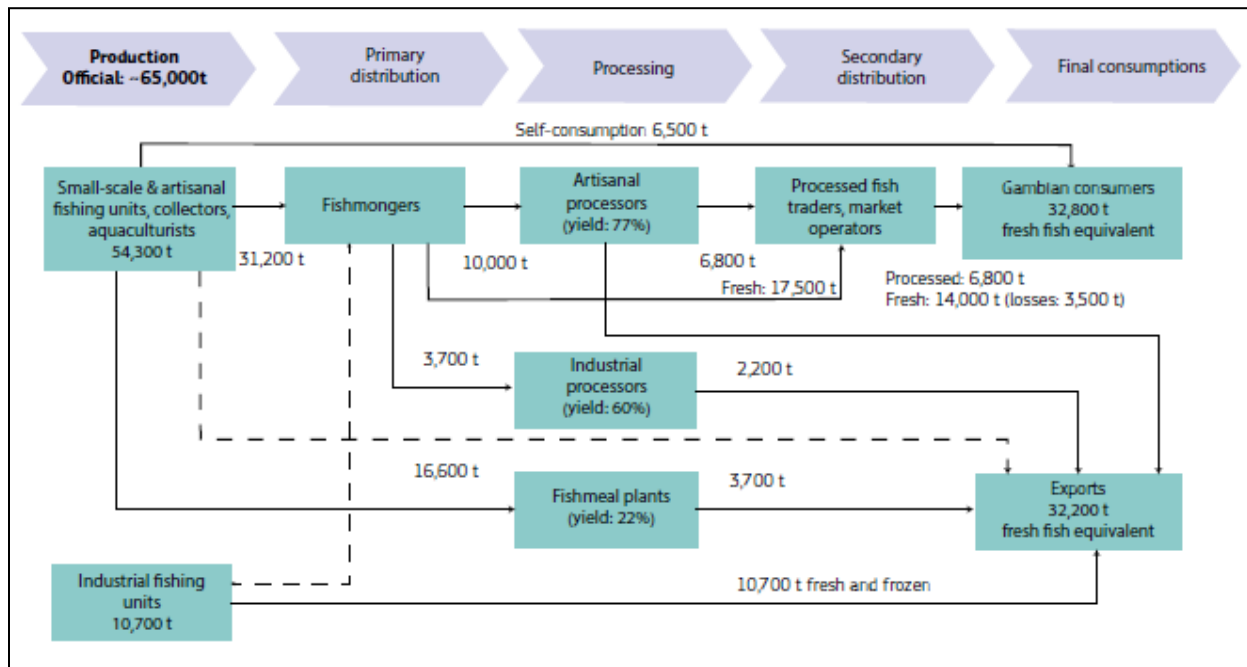
¹⁵ Avadí et al., 2020. p. 11. Average taken over the range 2014-2018.

¹⁶ Ibid., pp. 30, 44.

¹⁷ Ibid., p. 92.

¹⁸ Ibid., p. 13.

Figure 2-1 Flow chart of the fisheries value chain in the Gambia



Source: Jones, 2021

Artisanal Fisheries

8. Gambian artisanal fisheries are a multipurpose activity associated with a host of ancillary socio-economic activities. These activities range from boatbuilding and net making, fishing operations, offloading of catch, onshore auctioning/marketing, processing (both in-situ and/or at home) to distribution and marketing (national, regional and international). These processes involve inputs and outputs which are sourced and supplied accordingly, linking fisheries to other sectors' value chains. The artisanal sub-sector fully supplies the fresh and processed domestic fish market.¹⁹

9. Artisanal fishers can be classified into two categories, according to their working environment: marine and continental or estuarine. Fish capturing involves investing in a fishing unit: a canoe, an engine (motorized canoes) and fishing gears. While canoes are locally constructed, engines and fishing nets can be sourced within or outside the country.²⁰ Small-scale fishers use planked dug-out and fiberglass canoes (mostly along the coast) but dug-out canoes are used for shrimping, oyster harvesting, line fishing, and for inland fishing. The larger canoes (powered by an outboard engine) are employed in the coastal marine fishing, while the smaller dug-out canoes are used in the estuary and inland fishing. The crew number depends on the size of the canoe and the fishing gear-type being operated. Most common fishing gears used in the Gambia include: gillnets (set, bottom and suspended nets) for demersal and mid-water fish, drift nets surrounding or entangling nets for small pelagic, cast nets for pelagic, hook and lines for a variety of species, purse seines for schooling fish and, stow nets for shrimp fishing. Crew size ranges from 3 to 6

¹⁹ Jones S., 2021. p. 2.

²⁰ According to Avadí et al., 2020, people employed in related outboard motor mechanics and carpentry are around 500.

people (in canoes up to a length of 5 meters) to 10 to 15 people (for 17- to 25-meter-long canoes). Fishing ventures can be self-financed, financed through partnerships, from a funding agent or agencies. Partnerships or sponsorships may be conditional to some share of proceeds or to granting exclusive purchasing rights on the catch.

10. **The 2016 Frame Survey estimated the number of units operating at sea as 565 (2 812 fishers), while the number of those operating in the continental environment was estimated at 658 units (1420 fishers).** Shellfish collectors are estimated to be 756. Fishing is predominantly carried out by men and women are only involved directly in shellfish harvesting within the estuarine areas. However, some women have their own fishing unit and/or provide funding and equipment to other fishers.

11. **Sea fishing in The Gambia is carried out mainly by foreigners.** The 2016 Frame Survey identified 300 Senegalese units out of 502 motorised units. Conversely, Gambians dominate mainland fishing as this sector employs only 63 Senegalese and 31 Malians out of 728 units. The majority of fishers do not seasonally migrate. Senegalese fishers are mainly engaged in sardinella, shrimp, and demersal species while Malians in Clarias species.²¹

12. **Fishers' average wage is estimated at GMD 42,760 per month ranging from GMD 13,200 for fishers on board a purse seine up to GMD 87,560 for fishers on board a bottom gillnet.**²² Hence, the income of many fishery workers is much higher than the guaranteed minimum professional wage in the formal sector, standing at GMD 15,000.²³ Only the income generated by pure seine fishers is not sufficient to cover operating expenses of the fishing units.²⁴ The 2016 Frame Survey estimates that the average fisherman's household size is composed of 11 people.

13. **The artisanal annual average catch is around 54,300 t, which accounts for about 83 percent of total landing.**²⁵ Atlantic and inland shares account respectively for 67 percent and 16 percent of the total artisanal landing. The main species landed by artisanal vessels are bonga shad (about 26 percent), sardinella species (21 percent), and demersal fish such as catfishes, rays and sharks (about 8 percent).²⁶ Most key commercial species are either fully exploited or overexploited. Artisanal catches are landed and sold for direct consumption and transformation in the country. However, a marginal part of artisanal captures (4.6 percent of total artisanal catch) consisting mainly of small pelagic is landed abroad.²⁷

14. **Artisanal catches are loaded on board the canoes.** Ice is used depending on its price and on the duration of the fishing trips, which can last for several days. The production capacity of ice-making plants in the landing sites are low and cannot satisfy the sector needs. Moreover, artisanal operators complain about the high unit cost per ice kilo, due to the prohibitive cost of energy in The Gambia. All catches (100%) are landed in base or other fish landing sites. There are over 150 landing in the Gambia, eleven in

²¹ Jones S., 2021. p. 2.

²² Avadí et al., 2020. p. 10.

²³ Ibid., p. 12.

²⁴ Ibid., p. 11.

²⁵ Ibid.

²⁶ Ibid., p. 33-34.

²⁷ Ibid., p. 43.

the marine coastline and the rest inland. Generally, they are characterized by minimal infrastructure accommodating numerous artisanal processing facilities.²⁸

15. Catches are offloaded by crew members or by a group of men and women with plastic pans or baskets on their heads known as “dunular” in Mandinka dialect. The number of fish off-loaders per canoe depends on the canoe gear: small pelagics canoes attract more people than demersal canoes whose crew members normally offload the catch. The off-loaders are primarily paid in kind, a few fish, which they sell in-situ/on the beach for cash or take home for family consumption. Catches are landed in poor sanitary conditions at landing sites where they are insufficiently protected from contact with the soaked soil and/or poorly conditioned. The fish is occasionally loaded directly into trucks with layers of ice scattered over the product. The lack of adequate facilities and appropriate practices for fish handling and storage increases the incidence of fish degradation and hinders the development of fish distribution. Depending on the season, post-harvest losses are estimated at 20-30 percent. Prearranged sales of catch is a normal practice in the artisanal fisheries sub-sector. Wheelbarrows are used to transfer sold fish to other transports or to be directly brought to smokehouses. Most catches are marketed fresh (the one bought by distributors), while some are smoked and sundried before being sold.²⁹ Once fish is landed from the canoes, its auctioning or marketing is largely done by fishers’ wives or close relatives. The preferred fish by Gambian consumers, the bonga, is marketed at GMD 25,000 per t at the landing sites while substitute species (i.e. flat and round sardinella of quality 1) are sold at GMD 20,000 per t. However, the price for all species (quality 2) goes down to GMD 10,000 for fishmeal plants.³⁰

16. A large number of agents participates in the primary distribution segment. Fishmongers and retailers buy the bulk of the artisanal catch (57 percent), while fishmeal plants buy 31 percent and the rest (12 percent) is left for self-consumption. Some artisanally caught high-value fish (shrimp, soles, sea bream, lobster) is bought by fish merchants appointed by industrial fishing companies for processing and export abroad. Both fishmongers and retailers register a positive net operating profit.³¹ They mainly deal with small pelagic and demersal species. The Department of Fisheries estimates a total of 10,330 fishmongers. However, this number reaches 30,399 if their employees are included. Indeed, each fishmonger hires an average of three employees to assist them at different stages of the distribution process (conditioning fish, driving trucks, sailing fish).³² They are usually self-employed and self-financed. Moreover, they often finance small-scale fisheries conditional on the exclusivity of the catch. Fishmongers buy their fish at landing sites and according to the amount of fish bought, they are classified as large (5 to 10 t of fish per day) or medium (3 t of fish per day). Large fishmongers are almost exclusively men while 30% of medium fishmongers are women.³³ Mostly Senegalese, large fishmongers distribute fish to central points in townships and inland markets using either insulated trucks with ice for fresh fish or open trucks for processed products. However, product loss often occurs as trucks are old and not adequate to fish

²⁸ Jones S., 2021. p. 2.

²⁹ Avadí et al., 2020. p. 35.

³⁰ Ibid.

³¹ Avadí et al. (2020) report a net operating profit of GMD 7 528 000 for large fishmongers, GMD 681 000 for medium fishmongers, and GMD 1 947 240 for retailers.

³² Ibid., p. 64.

³³ Ibid., p. 26.

transportation. Similarly, Gambians account only for 30% of medium fishmongers.³⁴ However, medium fishmongers deliver fish kept under ice to inland or neighbouring markets within the urban areas using a personally hired land rover or a collectively hired truck. They sell their fish either to retail buyers, to restaurants and hotels, or directly to consumers displaying their product on cement tables provided by markets authorities.³⁵

17. **Fish retailers, called *Banabanas*, are mostly Gambian women, facing competition from fishmongers.**³⁶ The low presence in the big distribution compared to the small one is justified by their very weak financial base and by fish trade requirements such as long absences away from the family or overnight stays in the country hinterland.³⁷ Generally, they buy smaller quantities of fish (3 to 4 baskets of 50 kg each per day carried in with ice) from fishers at the landing beaches. They supply fish to markets in the immediate environment and nearby villages and towns. Depending on the distance to the sale point, retailers may use public (i.e. bush taxis) or private transportation (bicycles or motorcycles). They do not have cooling facilities and fish is laid either on wooden tables, on the floor, or on plastic sheets, normally without ice. However, in addition to selling directly to consumers, retailers also deliver to hotels and restaurants.

18. **Distributors include also factory buyers.** Mostly independent and self-financed, these traders buy high value fish from different small-scale fishers. In turn, they aggregate the collected product and sell it to industrial processors, which provide them with ice and private transport.³⁸

19. **Artisanal catches undergo both artisanal (62 percent of artisanal landings) and industrial processing (7 percent of artisanal landing except fishmeal).**³⁹ The Department of Fisheries counted 25,420 fish processors. However, as each processor employs around five people, the total number of people involved in processing activities reaches 127,100. Gambian nationals, particularly women (80 percent), dominate the processing segment. However, women processors have limited cash availability and handle small volumes of fish and consequently, they are forced to buy their raw materials at the prevailing market rates.⁴⁰ There are more than 350 artisanal processing units, mostly located at the landing sites.⁴¹ Artisanal fish processing mainly consists of smoking and drying, predominantly carried out using traditional methods. Fresh fish processed by artisanal smoking amounts to 5, 212 t per year, while 4, 614 t per year are processed by artisanal drying.⁴² However, artisanal process yield is only 77 percent. Several drying and smoking technologies have been tried and a few are being used such as the modified Gambian Banda oven. While drying processors record a positive net operating profit, the smoking processors are characterised by negative net operating profit.⁴³ There are about 86 artisanal smoking units divided between those exclusively producing smoked bonga, the most important product of the artisanal

³⁴ Ibid.

³⁵ Ibid.

³⁶ Ibid. Women account for 95% of retailers.

³⁷ Ibid., p. 63.

³⁸ Ibid., p. 35.

³⁹ Ibid., p. 43.

⁴⁰ Ibid., pp. 15, 62.

⁴¹ Ibid., p. 37.

⁴² Ibid., p. 11.

⁴³ Ibid., p. 12.

fisheries sector, and those processing different species like catfish, skate and ray.⁴⁴ While the first group is composed by men and women, the second group consists only of women. Women processors mostly use pit and barrel ovens with low capacity and poor hygienic conditions because of cultural practices and the high cost of improved smoking facilities and. However, some major landing sites also operate some community-owned ovens.⁴⁵

20. **Large quantities of fuelwood are used in fish smoking operations.** The Department of Fisheries estimates that men operating in two main landing sites (Tanji and Gunjur) use over 8,000 tonnes of forest resources per year. The overall impact of the use of such large quantities of firewood in highly inefficient processes is depletion of forest resources and emission of large quantities of carbon dioxide (CO₂) resulting in environmental degradation and climate change. Moreover, because of the increasingly scarce supplies and high cost of firewood, women smokers may use other fuels such as carton or plastic materials to smoke their fish releasing toxic substances. This practice exposes them to a high health hazard and results in highly toxic compounds in the traditionally smoked fish products.⁴⁶

21. **There are about 259 artisanal units involved in fish drying.** Artisanal driers are mostly women (95 percent) operating in all major landing sites.⁴⁷ They predominantly process high-value fish landed as spoilt (e.g. sharks, skates, and rays). The drying process includes fermentation, cleaning, gutting, dripping, salting, and drying. Drying racks are locally made from materials taken in the forest. Pest infestation of products and rain are the main problems causing product loss.⁴⁸ However, both drying and smoking practices reduce the high level of fish waste and ensure supply of fishery products for domestic consumption and export. Indeed, some high-value fish is smoked fresh for international markets (i.e. North America).

22. **The secondary distribution segment is carried out by either processing fish wholesalers or retailers.** Wholesalers sell large quantities to the semi-wholesalers at the primary and secondary national markets and to sub-regional markets, where profit margins are higher. Generally, they are men as they can travel long distances to sell smoked and dried fish products with a longer shelf life. Their substantial financial resources allow them to afford transportation and storage costs to reach rural areas and cities in the hinterland.⁴⁹ On the other hand, processed fish retailers are generally women who trade hot-smoked fish with a relatively short shelf life in urban and domestic markets. Given their low financial capacity, they are involved in small-scale marketing on a daily basis using public transport. They source their products directly from processors, wholesalers, or semi-wholesalers and sell them to the consumer on stalls. Their profit margins are usually low.⁵⁰

⁴⁴ Ibid., p. 37. The bonga, the preferred fish of Gambians consumers, is marketed on average at GMD 25 000 per t against GMD 20 000 for substitute species (i.e. sardinella).

⁴⁵ Ibid.

⁴⁶ Ibid., p. 46.

⁴⁷ Ibid., p. 37.

⁴⁸ Ibid.

⁴⁹ Ibid., pp. 39, 46.

⁵⁰ Ibid.

23. Overall, Gambians consume about 32,300 t of fish products each year for a value of GMD 2,750 million.⁵¹ Smoked fish products are mainly sold in urban markets. In The Gambia, there are 28 registered markets trading fresh, smoked, and dried fish products in addition to other food such as vegetables and meat. They are characterised by inadequate infrastructures and poor hygienic conditions.⁵² Generally, Gambian consumers show a preference for fresh small pelagic fish followed by dried or smoked small pelagic and low-quality demersal fish.⁵³

Shellfish Production and Marketing

24. Shellfish harvesting happens in the Tanbi Wetlands National Park (TWNP) and in other mangrove areas along the estuary of the Gambia River. It involves mostly wild oysters but also cockles. The Gambia granted exclusive rights to manage shellfish resources in the TWNP to a community-based organization of women shellfish harvesters, the TRY Oyster Women's Association. Generally, the sector is dominated by Gambian women but men are also involved. Indeed, the 2016 Frame Survey identified 397 women and 359 men practicing oyster collection, but the TRY women's association alone lists more than 600 female members.⁵⁴ Women take control over all segments of the oyster value chain, from production to retailing. However, sometimes marketing is done by harvesters' family members.

25. Wild oysters and cockles are collected by cutting mangroves using axes or knives. Harvesting sites are mostly reached by walking at low tide. However, few harvesters use small non-motorized dug-out which are 3- or 4-meter long and can carry from 1 to 3 women who paddle from their base to the harvesting areas. The harvesting season last from March to June for oysters and from July to November for cockles. Bivalves represent an important source of livelihood for women. Nevertheless, they are involved in other activities outside the harvesting season, such as farming or fish trading. Wild oyster and cockle collection amounts to an average of 273 t per year.⁵⁵ Oyster aquaculture practice is still limited.⁵⁶

26. Oyster and cockles processing takes place at the landing sites or in makeshift quarters lacking hygiene and potable water. Processing consists of steaming, boiling, or roasting on metal grill or sheet by using fuelwood (mostly mangroves) to ease the extraction of the flesh from the shell. In particular, roasting is time consuming and requires a large amount of firewood. Hence, both harvesting and processing use a substantial quantity of mangroves leading to significant cover loss. The flesh is extracted with knives, collected in woven baskets, and marketed often after being washed or even reheated. Sometimes, before being marketed, the flesh is preserved by salting and sun drying to low moisture contents. Marketing of processed products takes place in processing sites, neighbourhoods, urban market places, weekly market days ("loumo"), and along roadsides.⁵⁷ Buyers include individual consumers, street food vendors. and restaurant operators. Limited quantities of oysters are exported by the Gambian Diaspora as gift to relatives or to be sold in niche markets in the European Union and the United States.

⁵¹ Ibid., p. 44. This estimate also includes shellfish products.

⁵² Ibid., p. 39.

⁵³ Ibid.

⁵⁴ Ibid., p. 44.

⁵⁵ Ibid., p. 11. Annual average is taken over the period 2014-2018.

⁵⁶ Ibid., p. 44.

⁵⁷ Ibid., p. 56.

Oyster shells are gathered in heaps and sold to industries producing white lime, brick, chicken feed and fertilisers for horticulture.

Industrial fisheries

27. Foreign or foreign-operated industrial vessels completely dominate the Gambian industrial capture fishery. Foreign vessels are licensed to fish in Gambian waters conditional on landing 10 percent of their total catch (by weight and species) in the shores of the country. This license condition also provides for the option of paying the equivalent in cash. However, inadequate rule monitoring and enforcement has resulted in discharges of species with low commercial value which are consumed locally. Moreover, it has been argued that foreign industrial vessels land their catches in foreign ports, especially in Senegal, because the Banjul Fisheries Jetty lacks appropriate landing and handling facilities and the industrial processing capacity is limited. Besides, foreign vessel owners enter into contract with Gambian fishing companies to meet national licensing requirements. The industrial fleet is mainly composed of shrimp (5 units registered under the Gambian flag and one unit under the Senegalese flag) and demersal trawlers (49 units, out of which 39 flying the Gambian flag and the rest flying Ivory Coast, Chinese or Egyptian flags).⁵⁸ Industrial production accounts for about 10,700 t per year or 17 percent of total annual landings, 90 percent of which is landed in foreign ports of origin or other.⁵⁹

28. Industrial fish processors purchase their raw material, mainly high-value fish, from artisanal fishery. Sourcing fish from foreign vessels operating in Gambian waters is uncommon as the unfavourable exchange rate makes it very costly. Industrial processing mainly consists of 10 plants freezing high value demersal fish for export to regional and international markets (mainly to the EU, North America and Asia). However, there are three Chinese-owned, export-oriented fishmeal companies.⁶⁰ Processing plants are mostly located around Banjul due to better access to water, electricity and services. Industrial processing employs 1,500 workers and women represent 65 percent of this workforce. The industrial processing segment records positive net operating profit.⁶¹

⁵⁸ Ibid., p. 32-33.

⁵⁹ Jones S. 2021, p.1.

⁶⁰ Avadí et al., 2020. p. 37.

⁶¹ Ibid, p. 12. The net operating profit is GMD 77,542,000 for a freezing plant and GMD 12.153 million for a fishmeal plant.

Policy and legislative frameworks

International policy commitments

29. **As reflected in its policy commitments, the Government of the Gambia recognizes the importance of addressing the strongly interlinked issues of livelihood improvement and climate change mitigation and adaptation.** Indeed, it has ratified the United Nations Framework Convention on Climate Change (UNFCCC) in 1994, the Kyoto Protocol in 2002, and the Paris Agreement in 2016. In fulfilment of The Gambia's obligations under the UNFCCC, The Gambia has submitted its Nationally Appropriate Mitigations Actions (NAMAs) in 2011, its National Adaptation Programme of Action (NAPA) in 2008 outlining appropriate measures to adapt to the negative impacts of climate change in the fisheries sector, and its first Nationally Determined Contributions (NDC) in 2016 and in the recently submitted Second NDC⁶². It has also submitted three National Communications (the last one in 2020) which document the status of socio-economic and ecological conditions as they relate to greenhouse gas emissions and vulnerability to climate change, particularly for some key affected sectors such as fisheries. Furthermore, these communications include some adaptation measures to be taken and identifies implementation problems.

30. In 2016 the Government of the Gambia has signed its third United Nations Development Assistance Framework (UNDAF) 2017-2021 describing the strategic direction, programme areas, and results to be achieved from cooperation between the Government of the Gambia and the United Nations Country Team. The UNDAF mainstreams the international development agenda guided by the Sustainable Development Goals (SDGs), Africa Agenda 2063, other international declarations such as the 2015 Paris Climate Conference (CoP 21), and national development priorities. Mentioning fisheries as part of the critical agricultural and natural resource sector, the UNDAF aims to ensure, among other outcomes, that *"sustainable, inclusive and integrated natural resource and environment management is enhanced for food security, income generation and, safe environment"*. This will be achieved through institutional capacity and system strengthening in planning and implementation of programmes to increase opportunities, efficiency and effectiveness in addressing development and humanitarian challenges.

National legislative framework

31. The significant role played by the fishery sector in the growth of the Gambian economy has been stated in the long-term vision and overarching plan of the Third Republic, the National Development Plan 2018-2021 (NDP). Closely aligned with the Sustainable Development Goals (SDGs) and the Agenda 2063 of the African Union, the NDP goal is to *"deliver good governance and accountability, social cohesion, and national reconciliation and a revitalized and transformed economy for the wellbeing of all Gambians"*. To achieve this goal, the Plan sets out eight strategic priorities to pursue, the third being *"Modernizing our agriculture and fisheries for sustained economic growth, food and nutritional security and poverty reduction"*. Complementing these priorities, the NDP identifies seven crosscutting critical enablers, among which there are the promotion of environmental sustainability, climate resilient communities, and

⁶² Second Nationally Determined Contribution of The Gambia (2021) – available [at this link](#).

appropriate land use; and the empowerment of Gambian women to realize their full potential.⁶³ Furthermore, the NDP outlines an accountability framework with the unprecedented involvement of regional-, ward- and village-levels structures. Finally, it elaborates a financing strategy for the whole plan.

32. Regarding the fisheries and aquaculture sector, the NDP's goal is to promote a vibrant sector through research, sustainable environmental management and utilization of the fisheries resources that would enhance employment and livelihood opportunities, income and foreign exchange earnings, food, and nutrition security. To attain this goal, the Plan identifies the key issues to address: the poor management of fisheries (involving fish resources and fishing activities), the inadequate post-harvest handling of catches, and the increased frequency and severity of climate-related hazards. In this respect, proposed interventions focus on the strengthening of the institutional development (legislative, policy and regulatory framework, human resources, systems and tools) which shall, among others, include a strong incentive to attract the youth to the sector; the enhancement of fisheries infrastructure; and the improvement of value chains for fisheries and aquaculture.

33. Nationally, the Government of The Gambia has initiated various policies, plans and strategies to support climate change mitigation and adaptation. In line with the UNFCCC, the Gambia's Intended Nationally Determined Contribution, and its NDP, the National Climate Change Policy (NCCP) 2018 is the overarching policy framework to steer the transition to a climate-resilient society within a thriving low-emissions economy *"through systems and strategies that mainstream climate change, disaster risk reduction, gender and environmental management, for sustainable social, political and economic development"*. Its goal is *"by 2025, to achieve the mainstreaming of climate change into national planning, budgeting, decision-making, and programme implementation, through effective institutional mechanisms, coordinated financial resources, and enhanced human resources capacity"*. For this purpose, the NCCP specifies *"comprehensive and crosscutting policy directions to implement national development strategies in a climate resilient manner, drawing on all sectors of the population in a spirit of partnership and collaboration"*. It also promotes the principle of community-based management as a cost-effective approach to support the sustainable management of natural resources. Furthermore, it outlines enhanced institutional arrangements for coordination and mainstreaming such as the National Climate Change Council, a new integrated approach to resource mobilisation, a clear policy direction for human resource development. Finally, the NCCP advocates for the adoption of a national climate change response strategy and action plan to serve as the NCCP implementation framework.

34. Recognizing the fisheries sector as particularly vulnerable to climate change, the NCCP identifies various measures to promote the sustainable adaptive management of the fisheries resources such as strengthening the Fisheries Department to integrate climate change risks into planning; promoting of awareness of climate change risks, and capacity building and strengthening of fishing communities; facilitating access to finance to enhance the resilience against climate change and disaster recovery of industrial and artisanal fishermen, and young women processors; increasing collaborative research and

⁶³ It is worth to note that the Government of the Gambia recognizes the pivotal role of its youth in the country's development including their potential in the fisheries and aquaculture sector. Indeed, rather than being a critical enabler, the NDP considers their empowerment a strategic priority of its own.

information exchange among national and international research institutions; or upgrading onshore fishing infrastructure to withstand more severe weather linked to climate change.

35. The Agriculture and Natural Resources (ANR) Policy 2017-2026 sets out the long-term vision for the sector, that is *“the creation of a marketed-led commercialized, efficient, competitive and dynamic ANR sector in the context of sustainable development”*. As for the fisheries and aquaculture sector, the ANR policy puts high priority on: aquaculture development through the facilitation of access to funds, equipment, technical expertise and support to conduct research activities; the improvement of the artisanal and industrial fisheries production systems through enhanced institutional capacity, regulatory and licensing mechanisms, quality assurance, harvesting and post-harvesting infrastructure, and the facilitation of private sector participation.⁶⁴ It also advocates for the active participation of fishermen’s associations to modernize the ANR sector. In this respect, the ANR policy provides for measures mitigating the low capital base and lack of technical and managerial expertise.

36. To provide a legal framework for the management of the fisheries sector, the Government of the Gambia enacted the Fisheries Act 2007 and its attendant Fisheries Regulations 2008. Incorporating international trends in fisheries such as the principles of the Code of Conduct for Responsible Fisheries (CCRF), the Act aims *“to provide for the conservation, management, sustainable utilisation and development of fisheries and aquaculture in the fisheries waters and in the territory of The Gambia”*. Hence, the provisions of the Act relate to the artisanal, industrial and aquaculture sub-sectors. In particular, its policy objectives are: a rational and long-term utilization of the fisheries resources while promoting bio-diversity enhancement and preventing environmental degradation; the use of fish as a means to improve the nutritional standards of the population; the increase of employment opportunities for Gambians in the sector and specifically the participation of women and youth; the increase of foreign exchange earnings; the development of aquaculture; and the strengthening of regional and international collaboration in the management and sustainable exploitation of shared stocks.

37. The Fisheries Act outlines the institutional and administrative responsibilities for the sector. Indeed, the overall authority is the Ministry of Fisheries and Water Resources, while the Director of Fisheries is responsible for its technical implementation. The Act identifies the Gambia Navy as the responsible for the enforcement of licensing conditions. It also provides for the establishment of a Fishery Advisory Committee and the Community Fisheries Centres (CFCs) for advisory purposes and decentralized fisheries co-management.

38. To enhance the effective implementation of the NDP, the Fisheries Act, and other sectoral and national policies, the Department of Fisheries in collaboration with the FAO developed the Fisheries and Aquaculture Sector Strategy (FASS) 2017-2021. The FASS aims to develop the sector to *“be recognized one of three most critical contributors to national economic growth, food and nutrition security, employment creation and exchange earnings”* by 2021. This vision will be achieved *“through the recognition of fisheries and aquaculture potentials as natural economic resources and by ensuring responsible and ecologically sustained fishing and aquaculture practices, to optimally harness The*

⁶⁴ For instance, the ANR policy recommends the adoption of improved fish curing kilns that do not use fuel wood (e.g. mangroves vegetation) so as to minimize health hazard and to preserve coastal forests.

Gambia's fisheries and aquaculture resources and to deliver employment, foreign exchange support, food and nutrition security in achieving accelerated national growth and development". Special emphasis is placed on the empowerment of the Gambian women and youth in the sector to eradicate gender poverty in a sustainable way.

39. To accomplish its mission, the FASS identifies three strategic priorities. First, it envisages institutional restructuring, rearrangements and capacity strengthening. This includes the transformation of the Department of Fisheries into a National Fisheries Commission for increased operational and financial autonomy. Second, it provides for key sector stakeholder capacity building and sensitisation. Third, it advocates the improvement of inter-sectoral linkages and the optimisation of the overall value chain advantages of the fisheries and aquaculture sector for increased government and donor budgetary support and better alignment with relevant key sectors. Besides, emphasis is put on improving the collaboration and partnership with key international, regional, and national stakeholders. Finally, the FASS includes a detailed strategy coordination, financing, implementation and monitoring framework.

References

Avadí, A., Dème, M., Mbaye, A., Ndenn, J. 2020. Fisheries Value Chain Analysis in The Gambia. Report for the European Union, DG-DEVCO. Value Chain Analysis for Development Project (VCA4D CTR 2016/375-804).

Department of Fisheries. 2016. The 2016 Fishery Frame Survey Final Report. The Islamic Republic of the Gambia. Banjul.

Jones S., 2021. The Gambia fisheries study brief. European Commission.

<https://europa.eu/capacity4dev/value-chain-analysis-for-development-vca4d-/documents/gambia-fisheries-study-brief>.

Ragusa, G. 2014. Overview of the Fisheries Sector in the Gambia. Fisheries and Aquaculture Journal 5:107. doi:10.4172/2150-3508.1000107.

National Accounts Units, 2019. Annual Bulletin- Gross Domestic Product-Production and Expenditure for 2018 and 2019. The Gambia Bureau of Statistics. <https://www.gbosdata.org/downloads/gdp-2019-69>.

United Nations Conference on Trade and Development, 2014. The fisheries sector in the Gambia: trade, value addition and social inclusiveness, with a focus on women. United Nations, New York and Geneva.

World Bank. 2019. The Gambia Agriculture Engagement Note: Fostering agriculture-led inclusive growth. World Bank. <http://documents1.worldbank.org/curated/en/814691560411931505/pdf/The-Gambia-Agriculture-Engagement-Note-Fostering-Agriculture-Led-Inclusive-Growth.pdf>

Chapter 3 CLIMATE TREND ANALYSIS and PROJECTED CLIMATE CHANGE in The GAMBIA and OVER the GAMBIA RIVER WATERSHED

Introduction

1. **As part of the global hydrologic system, the Gambia River is directly affected by changes occurring in the principal drivers of climate change.** From the global to national scales, changes in temperature and rainfall regimes, and associated changes in moisture loss through evaporation, are altering the movement of water within the river and watershed, and subsequently impacting key ecological segments along the river and Gambian fisheries. To understand the magnitude and rate of current and future changes, it is necessary to interrogate appropriate datasets for the presence of important trends, historically, as well as those that are reasonable to anticipate in the coming decades.
2. **This chapter presents a summary of a detailed analysis undertaken to identify the underlying physical attributes of historical and projected changes of temperature and precipitation within the watershed.** This analysis was further used to inform the assessment of climate change impacts on the ocean environment and river ecologies, and in modelling the impact of climate change on the saline intrusion into the Gambia River, presented in the following chapters. These additional chapters, together and separately, are used in assessing the likely biological impacts of climate change on the various fisheries, and individual species, as well as aiding in the physical location of specific adaptive activities.

Data

3. **Over two-thirds of the Gambia River watershed is located within Senegal, with the remaining portion split near evenly between The Gambia and Guinea.**⁶⁵ Due to the cross-border nature of the watershed, in order to undertake a trend analysis of possible changes in historical weather patterns that might be affecting the basin's hydrology, as well as projecting future trends, it is necessary to rely on weather records at a commensurate spatial scale, above national level. The EWEMBI (Earth2Observe, WFDEI and ERA-Interim data Merged and Bias-corrected for ISIMIP) dataset was selected for this purpose (Lange, 2018; Dee et al., 2011; Weedon et al., 2014; Dutra, 2015). The EWEMBI dataset is a robust, global dataset compiled and maintained by the Inter-Sectoral Impact Model Intercomparison Project (ISIMIP) in support of impact assessment teams contributing to the Intergovernmental Panel on Climate Change (IPCC) assessment reports. The dataset provides daily precipitation and temperature data, covering the period from 1979-2018, at a global scale with 0.5° resolution (roughly 55.5 km² at the equator).
4. **In assessing climate trends in the Gambia River watershed, daily temperature (maximum, minimum and average) and precipitation values were reconstructed as monthly averages.** This reconstruction was carried out for two reasons. First, it simplified the dataset for use in trend detection, where seasonal changes in magnitude and spatial distribution of precipitation within the watershed are the primary concerns. Secondly, use of monthly timescale was adequate for the data inputs needs of the

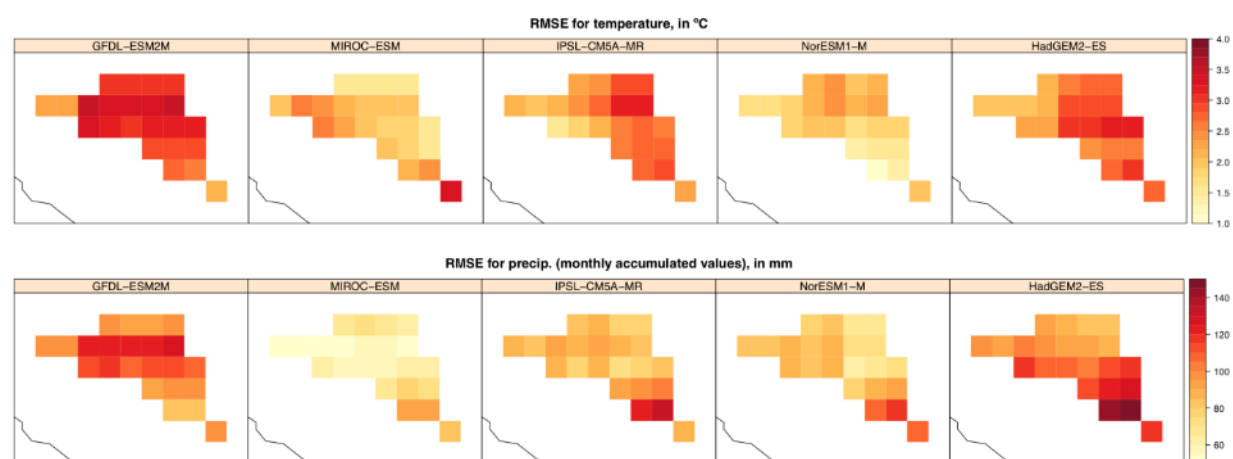
⁶⁵ 14 percent of the watershed lays in The Gambia, 71 percent in Senegal and 15 percent in Guinea (Oréade-Brèche and ISL Ingénierie, 2014). The shape file for the Gambia Watershed was obtained from the HydroSHEDS database (<https://hydrosheds.org/page/overview>). The watershed includes those areas upstream from the extent of permanent saltwater intrusion into the river at KP 64.

SALNST salinity model being used to project changes in the saltwater intrusion into the Gambia River (see Chapter 6). For this later purpose, in addition to precipitation data, daily maximum and minimum temperatures were used to calculate potential evapotranspiration values using Thornthwaite's equation, which is based on temperature (Thornthwaite, 1948).

5. **For future climate projections, five global circulation models (GCMs) used by FAO in other national assessments were selected.** The models selected are: the GFDL-ESM2M (Geophysical Fluid Dynamics Laboratory – Earth System Model 2M)(Dunne et al., 2012); the MIROC-ESM (Model for Interdisciplinary Research on Climate – Earth System Model)(Watanabe et al., 2011); the IPSL-CM5a-MR (Institut Pierre-Simon Laplace-Climate Model 5a-Mid-Resolution)(Dufresne et al., 2013); the NORESM (Norwegian Earth System Model 1-M)(Bentsen et al., 2013), and the HadGEM2-ES (Hadley Centre Global Environment Model ver.2-Earth System)(Martin et al., 2011). All of these models are part of the Coupled Model Intercomparison Project 5 (CMIP5), used in conducting analysis for the IPCC Fifth Assessment Report (AR5).⁶⁶

6. **To assess the correlation between the different GCMs and the EWEMBI dataset, a quality control check was performed.** The Root Mean Square Error (RMSE) was used to determine the best fit between each of the models' re-creation of historical daily precipitation and temperature values for the period 1979 to 2016 covered by the EWEMBI dataset. Figure 3-1 shows the RMSE by geographic location for each of the models, and Figure 3-2 shows the RMSE by months. The MIROC-ESM, developed by the University of Tokyo, the National Institute for Environmental Studies (NIES) and the Japanese Agency for Marine-Earth Science and Technology (JAMSTEC), had the lowest RMSE values for precipitation and close to lowest for temperature. Based on the low RMSE, the MIROC-ESM was selected for use in generating the projected weather for use in the SALNST salinity assessment.⁶⁷

Figure 3-1 GCM to EWEMBI Root Mean Square Error values (1979-2016) for temperature and precipitation across the Gambia River watershed (lighter colors denote smaller RMSEs)

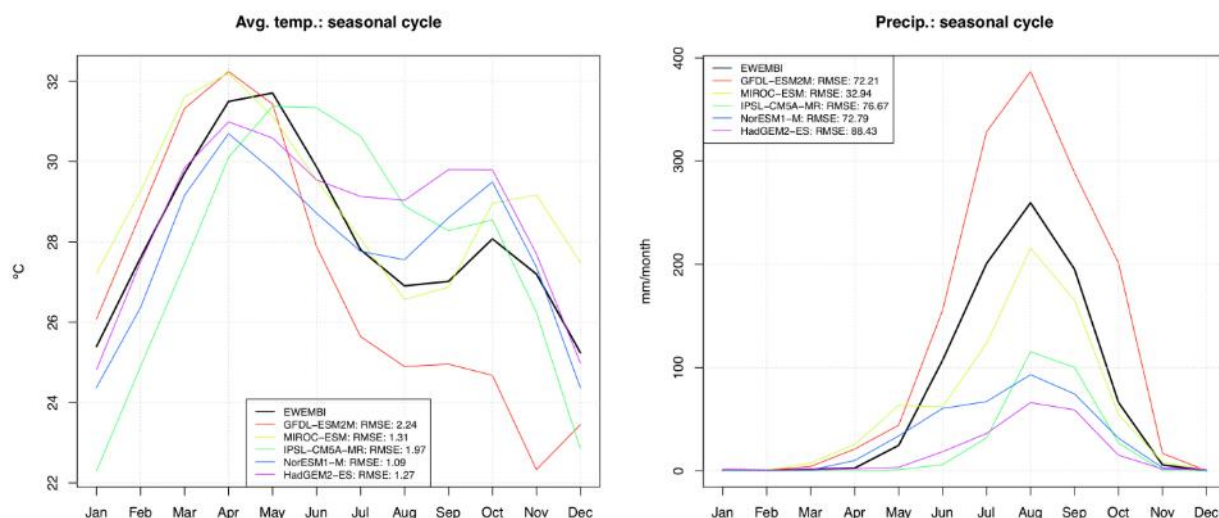


Source: FAO analysis of EWEMBI dataset

⁶⁶ For further details see the IPCC AR5 Chapter 9 "Evaluation of Climate Models" (https://www.ipcc.ch/site/assets/uploads/2018/02/WG1AR5_Chapter09_FINAL.pdf) and IPCC Data Distribution Center AR5 Reference snapshot http://www.ipcc-data.org/sim/gcm_monthly/AR5/Reference-Archive.html

⁶⁷ For further details on data processing for the SALNST assessment, see chapter 6.

Figure 3-2 GCM to EWEMBI Root Mean Square Error values for monthly temperature and precipitation (1979-2016) in the Gambia River watershed

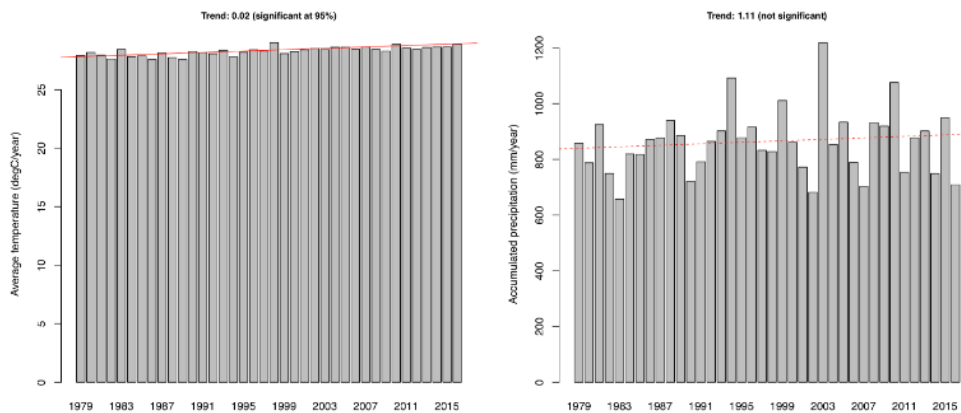


Source: FAO analysis of EWEMBI dataset

Analysis

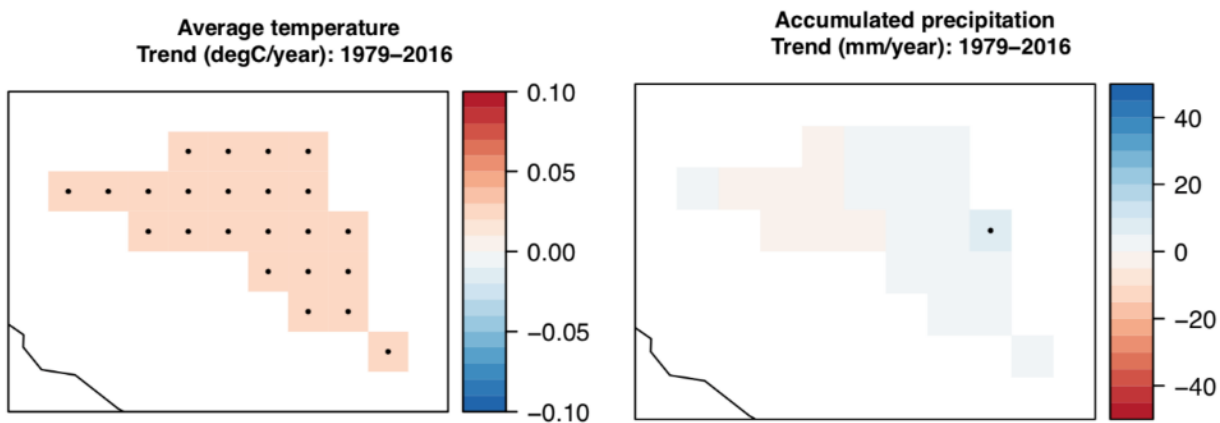
7. **Historical trends.** Considering the whole of the Gambia River watershed over the period 1979-2016, average annual precipitation has shown a non-significant increase of about 1 mm per year, while temperatures have increased on average 0.02°C per year, or about 0.74°C in total over the period (statistically significant at the 95 percent confidence interval) (see Figure 3-3). This rate of warming is approximately 40 percent less than the average rate of temperature increase for Africa, which warmed at the rate of 0.028 C/yr over the same time period, or 1.06 °C total (NOAA, 2020). Geographically, temperatures have increased uniformly over the entire watershed, while precipitation have declined slightly in the central watershed, with slight increases seen in the upper reaches of the watershed, and along the coast (see Figure 3-4).

Figure 3-3 Annual changes in temperature and precipitation within the watershed, 1979-2016 (the solid line indicates a statistically significant trend)



Source: FAO analysis of EWEMBI dataset

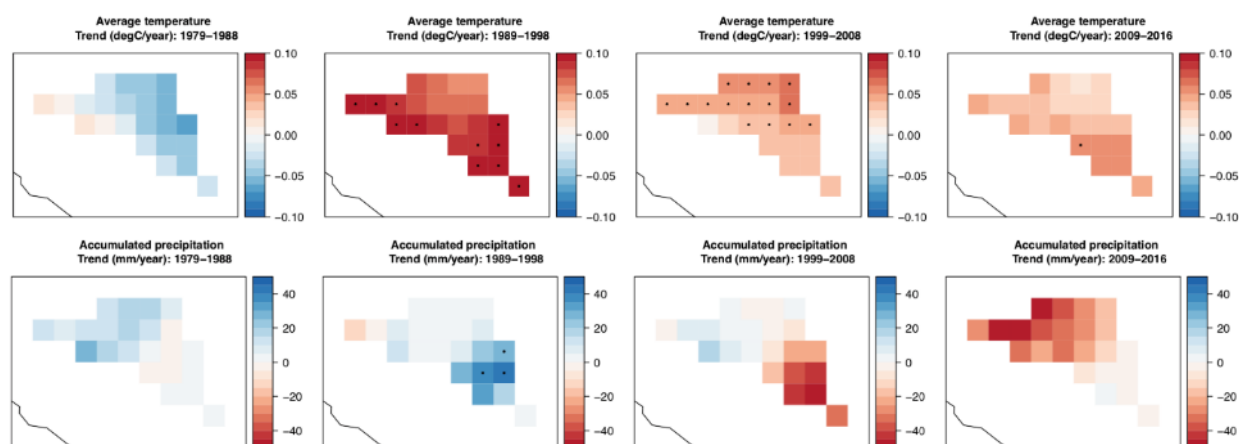
Figure 3-4 Average annual change in temperature and precipitation, 1979-2016 (grid cells with black dots indicate statistically significant trends)



Source: FAO analysis of EWEMBI dataset

8. When viewed at decadal time intervals between 1979 and 2016 (1979-1988; 1989-1998; 1999-2008; 2009-2016), the data show a strong evolution in spatial trends in both precipitation and temperature. As seen in Figure 3-5, the general cooler and relatively wet decade of the 1980s is followed by consecutive decades of sustained warming and an initial shifting and subsequent decades of decline in precipitation. Of particular importance with regards to precipitation is the shift from increases in the 1979-1988/1989-1998 period, to declines in 1999-2008/2009-2016 period. The plans for the Sambangalou dam used historical rainfall patterns (1970 - 2001) (ISL, 2014) for modelling future hydrology of the watershed. The lower current and potential future rainfall may, therefore, lead not only to an under performance of the dam in generating hydroelectric power but also hold significant implications for the hydrologic dynamics and biological communities downstream within The Gambia (more details on this issue area presented in Chapter 6 on saline intrusion).

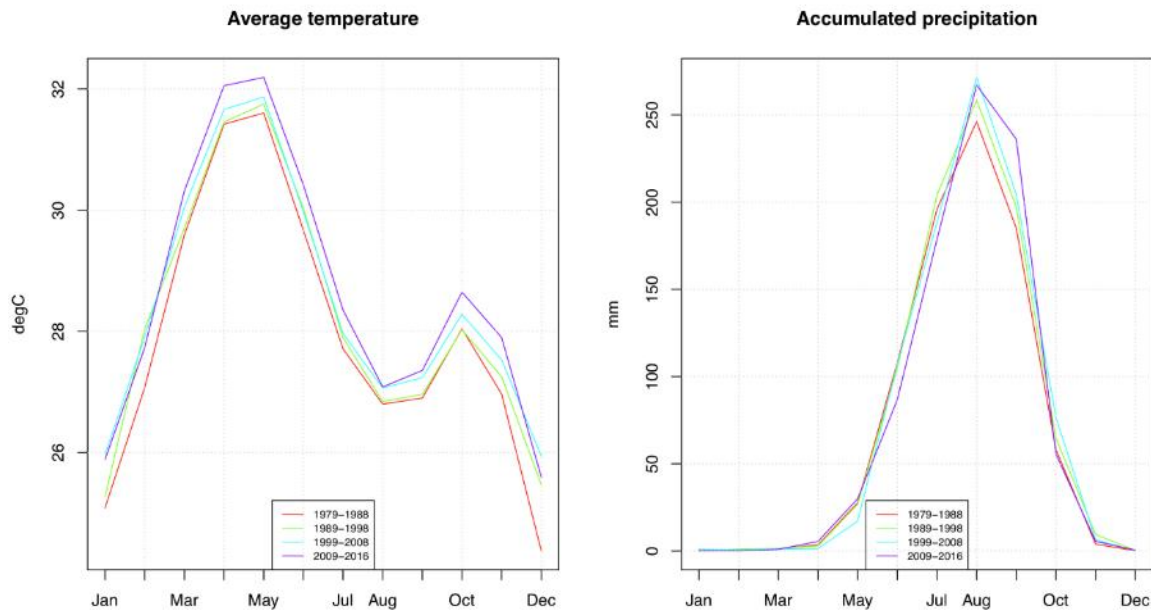
Figure 3-5 Decadal average temperature and rainfall within the Gambia River watershed (grid cells with black dots indicate statistically significant trends)



Source: FAO analysis of EWEMBI dataset

9. From a temporal perspective, Figure 3-6 shows a general increase in temperature and slight shifting in timing for precipitation by decade. The slight delay in onset of the rainy season and lengthening in the peak rainfall period in the most recent decade (2009-2016), suggests a somewhat later, but longer wet season flood, delaying the entry of saline water into the upper reaches of the estuary.

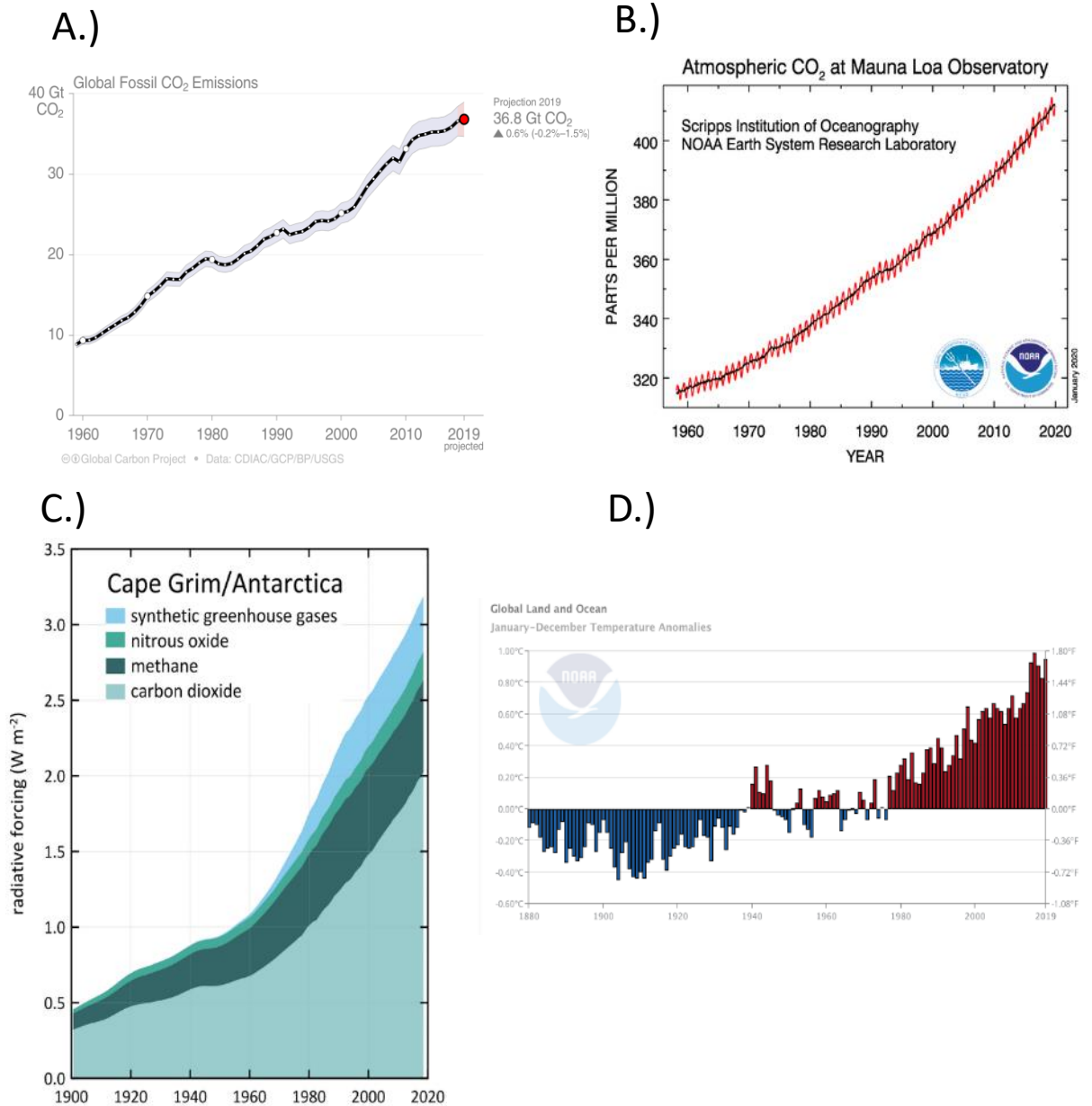
Figure 3-6 Decadal average monthly temperature and precipitation (1979-2016) in the Gambia River watershed



Source: FAO analysis of EWEMBI dataset

10. **Future projections.** Each of the five GCMs were used to generate future downscaled temperature and precipitation projections for the watershed, reported here at three future time intervals, near (2011-2040), medium (2041-2070) and far (2071-2099) future. For this report, it was decided to include only references to projected impacts resulting from Representative Concentration Pathway (RCP) 8.5, a high emissions business as usual scenario resulting in 8.5 watts/m² of additional energy being retained within the earth's atmosphere. Projections under the more moderate emission scenarios, e.g., RCP 4.5, can be assumed to be similar in sign with possible modest variance in intensity, geographic and temporal distribution. The decision to use RCP 8.5 for projecting possible future climate is based on the metrics presented in Figure 3-7 (where it is indicated that (fig. A) Rates of emissions have continue to increase (Global Carbon Project, 2019); (fig. B) Observed atmospheric concentrations of CO₂ continue to rise (NOAAa, 2020); (fig. C) Radiative forcing of the global climate system, from all greenhouse gases, continues to rise (CISRO, 2019); (fig. D) Global air and sea surface temperatures (SST) continue to rise – 2019 witnessed the second highest average global temperature, and the highest sea surface temperatures – the past five years are the hottest five years on record (air and sea surface temperatures), and the past decade the hottest decade ever recorded (air and sea surface temperatures) (NOAAb, 2020; Cheng, et al., 2020).

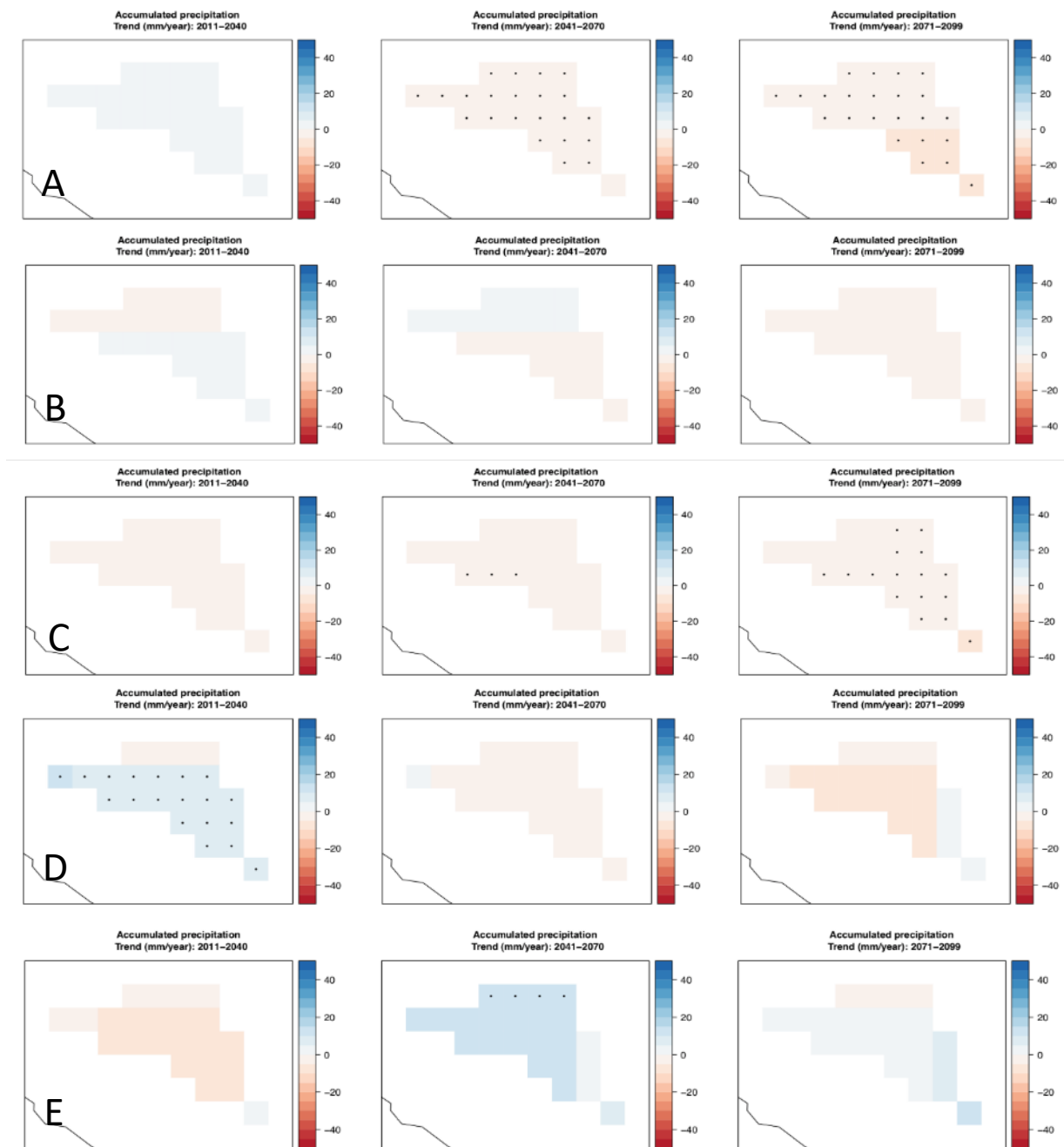
Figure 3-7 Indicative metrics for climate change



11. **Currently, global warming is at 1.1 C° above pre-industrial times (range among the five global datasets 1.05 – 1.2 C°) (WMO, 2020), and on-track for 2.3 – 4.7 C° of warming by 2060 (90 percent confidence interval) (Sherwood et al., 2020).** The voluntary nationally determined commitments to reduce greenhouse gas emissions under the Paris Agreement, if implemented to 100 percent effectiveness, are assessed to allow global temperatures to rise to 2.8 – 3.5 C° by 2100 (Climate Action Tracker, 2019), consistent with an RCP8.5 trajectory. The vast majority of countries are assessed to be lagging behind in implementing their current national commitments (FEU-US and ACT, 2019). Evidence emerging from the new generation of global circulation models (CMIP6) being used in preparing the upcoming IPCC 6th assessment report suggest that climate sensitivity may have been seriously underestimated, by over 30 percent, with the potential warming equilibrium (and rate of warming) from a doubling of CO₂ over 2 degrees warmer than previously thought (e.g., Zelinka et al., 2020). In sum, based upon the evidence, there is currently no empirical basis for anticipating anything other than the projected impacts associated with an RCP 8.5 future. Should future progress be made in reducing greenhouse gas emissions, various projected impacts can be assumed to be somewhat less, but consistent in sign, to those indicated in this report.

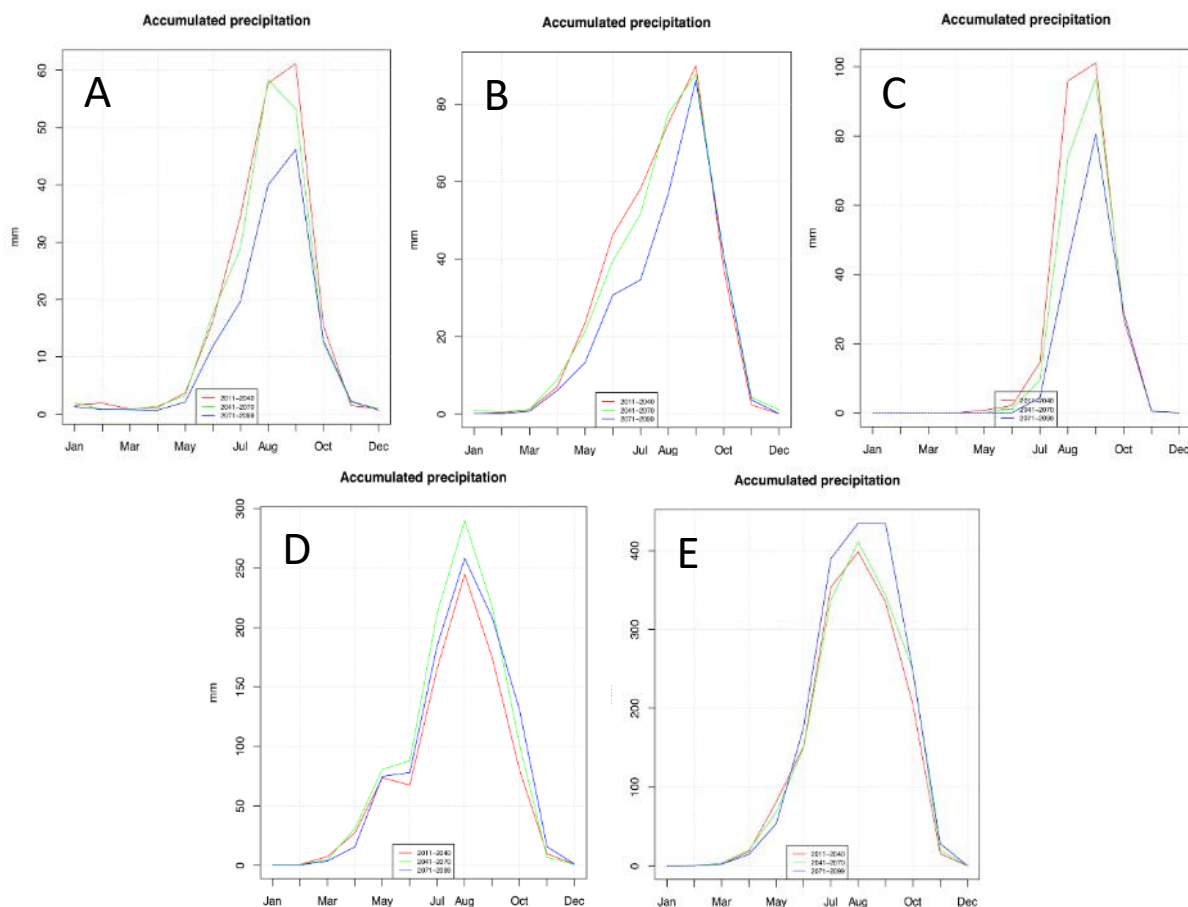
12. **Below, Figure 3-8 shows the generally mixed projections for precipitation, with both mixed results between the models at each time interval, and within each model across the three periods.** Only one model projects a consistent, though slight, declining trend in precipitation across all three time periods, while most models show a decline in precipitation in the medium and far future time periods. This divergence in model output is consistent with studies focusing on projected precipitation within the Sahelian zone, where models generally split between those predicting precipitation increases and decreases (Giannini, 2016). Figure 3-9 shows the various projected changes in the seasonal distribution of precipitation across the different time periods, with three models indicating an increasingly later start to the rainy season, and two showing a slight lengthening of the rainy period. Again, variance in model output and the seasonal shifting in precipitation is high, and is to be expected.

Figure 3-8 Projected geographic trend in precipitation for RCP 8.5 across three time periods (near (2011-2040), medium (2041-2070) and far (2071-2099) future) for five GCMs – (A) HADGEM2-ES; (B) NORESM1-M; (C) IPSL-CM5a; (D) MIROC-ESM; (E) GFDL-ESM2M)(grid cells with black dots indicate statistically significant trends)



Source: FAO analysis

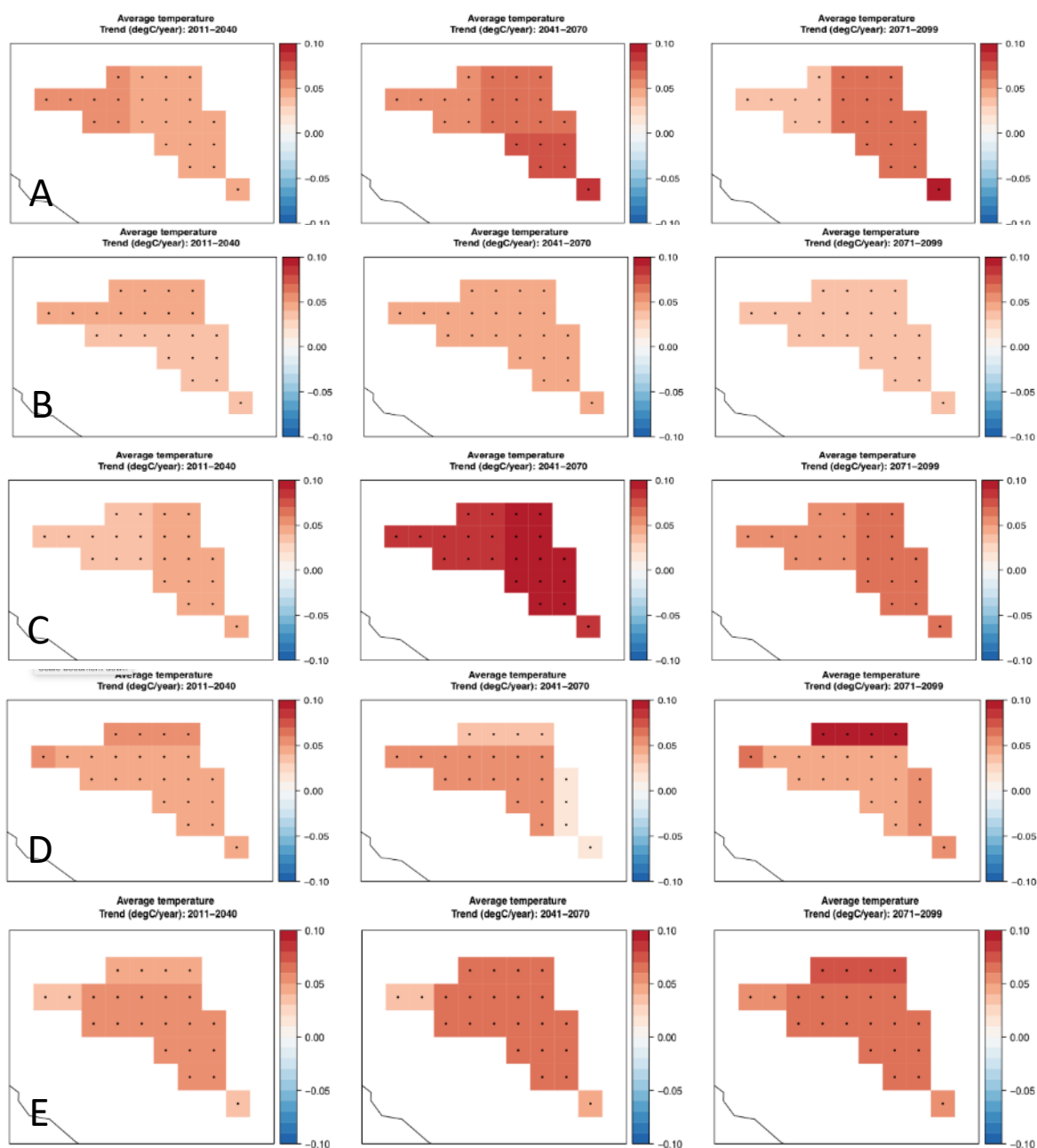
Figure 3-9 Projected trend in seasonal precipitation for RCP 8.5 across three time periods (near (2011-2040), medium (2041-2070) and far (2071-2099) future) for five GCMs – (A) HADGEM2-ES; (B) NORESM1-M; (C) IPSL-CM5a; (D) MIROC-ESM; (E) GFDL-ESM2M)



Source: FAO analysis

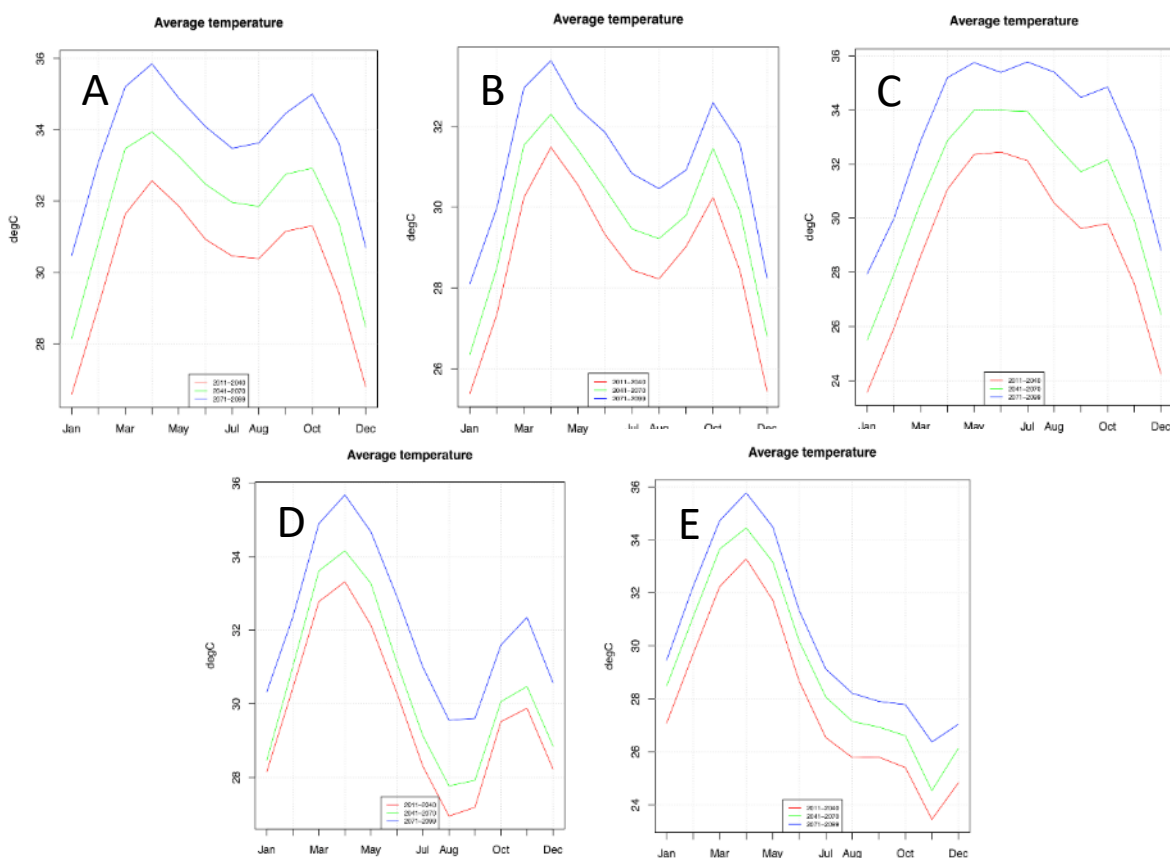
13. In contrast to the projected trends for precipitation, the trends for temperature change show a much higher degree of consistency across both the different models and time periods (Figure 3-10). All models, across all time periods, show a sustained upward trend in mean temperatures, consistent with what is known about the future of global climate change, with mean minimum temperatures rising at roughly twice the rate as mean maximum temperatures. The output from all models is statistically significant at a 95 percent confidence interval. There do not appear to be any important trends in terms of the temporal distribution of rising temperatures as shown in Figure 3-11.

Figure 3-10 Projected geographic trend in temperature for RCP 8.5 across three time periods (near (2011-2040), medium (2041-2070) and far (2071-2099) future) for five GCMs – (A) HADGEM2-ES; (B) NORESM1-M; (C) IPSL-CM5a; (D) MIROC-ESM; (E) GFDL-ESM2M)(grid cells with black dots indicate statistically significant trends)



Source: FAO analysis

Figure 3-11 Projected trend in temperature for RCP 8.5 across three time periods (near (2011-2040), medium (2041-2070) and far (2071-2099) future) for five GCMs – (A) HADGEM2-ES; (B) NORESM1-M; (C) IPSL-CM5a; (D) MIROC-ESM; (E) GFDL-ESM2M)



Source: FAO analysis

Conclusions

14. Overall, across the model projections there is a mixed though general agreement in the potential of declines in future precipitation, albeit modest, towards the end of the century.⁶⁸ Given the historical trend and virtual certainty of continued increases in temperature across all locations and time periods, resulting in greater rates of evaporation, one conclusion to be gained from this analysis is the likelihood of there being a decline in streamflow within the Gambia River in the decades ahead. Such a conclusion is consistent with a meta-analysis done on studies on river basin runoff in West Africa, which found that for the Gambia River basin future streamflow will likely decline by 4.5 percent (Roudier et al., 2014). Human activities that contribute to greater removal of water from the river (e.g., irrigation) and increased evaporation (e.g., from irrigated surfaces and dam reservoir), will accelerate the process of climate change driven moisture loss. For example, Gambia's National Water Management Strategy estimates a 7 percent reduction in stream flow in the Gambia River at Kedougou, immediately

⁶⁸ This conclusion is also supported by ensemble data from the CORDEX Africa models (<https://dap.climateinformation.org>). The analysis in the latter portal also finds variability between models, but 12 out of 18 models project a decrease in precipitation under RCP4.5 for the period 2041-2070.

downstream from the Sambangalou dam under construction in Senegal, due to evaporation from the dam's reservoir (GoTG, 2015). This volume of moisture loss translates roughly into a 3.5 percent reduction in stream flow as the river enters The Gambia.⁶⁹

15. **From the perspective of ecological niches and the life cycle of individual species, the potential shifting in the seasonality (timing and length) of the annual flood/recession cycle, within a context of declining overall streamflow, may have even greater effect.** Such trends, when combined with the offtake of water for irrigation in the freshwater portions of the river, increased evaporation and further alterations in the flood cycle imposed by the water retention and release schedule of the Sambangalou dam, will greatly amplify the impacts of climate change alone (these issues are explored in greater detail in Chapters 6 and 7).

References

Bentsen, M., et al. 2013. The Norwegian Earth System Model, NorESM1-M – Part 1: Description and basic evaluation of the physical climate, *Geosci. Model Dev.*, 6, 687-720.

Bruyère C.L., et al. 2014. Bias corrections of global models for regional climate simulations of high-impact weather. *Climate Dynamics* 43(7-8):1847–1856.

Cheng, L., et al. 2020. Record-Setting Ocean Warmth Continued in 2019. *Advances in Atmospheric Sciences* Vol. 37: 137-142.

Climate Action Tracker. 2019. https://climateactiontracker.org/documents/698/CAT_2019-12-10_BriefingCOP25_WarmingProjectionsGlobalUpdate_Dec2019.pdf. (accessed 29/01/2020).

CSIRO (Commonwealth Scientific and Industrial Research Organization). 2019. <https://blog.csiro.au/more-greenhouse-gas-in-atmosphere-than-you-may-have-realised/>. (accessed 29/01/2020).

Dee, D.P., et al. 2011. The era-Interim Reanalysis: Configuration and performance of the data assimilation system. *Quarterly Journal of the Royal Meteorological Society*, 137(656, Part a), 553–597.

Dufresne, J., et al. 2013. Climate change projections using the IPSL-CM5 Earth System Model: from CMIP3 to CMIP5. *Clim Dyn* 40, 2123–2165.

Dunne, J.P., et al. 2012. GFDL's ESM2 global coupled climate–carbon Earth System Models. Part I: Physical formulation and baseline simulation characteristics. *Journal of Climate* 25:6646–6665.

⁶⁹ Stream flow in the Gambia River at Sambangalou has been measured as 48 percent of the volume at Gouloumbou, Senegal, 32 km upstream from where the river enters The Gambia (Oréade-Brèche and ISL Ingénierie, 2008).

Dutra, E. 2015. Report on the current state-of-the-art Water Resources Reanalysis. Deliverable 5.1 of the project Global Earth Observation for integrated water resource assessment (earth2Observe). Available at <https://earth2observe.eu/files/PublicDeliverables>.

Frieler, K., et al. 2017. Assessing the impacts of 1.5oC global warming—Simulation protocol of the Inter-Sectoral Impact Model Intercomparison Project (ISIMIP2b). *Geoscientific Model Development*, 10(12), 4321–4345.

FEU-U and ACT (Fundación Ecológica Universal FEU-US and Acting on Climate Together). 2019. <https://drive.google.com/file/d/1nFx8UKTyjEteYO87-x06mVEkTs6RSPBi/view>. (accessed 29/01/2020).

Giannini, A. 2016. 40 Years of climate modelling: The causes of late-20th century drought in the Sahel. In: Behnke R. and Mortimore M. (eds.) *The End of Desertification? Disputing Environmental Change in the Drylands*. Springer Earth System Sciences. Berlin Heidelberg: Springer-Verlag.

Global Carbon Project. 2019. <https://www.globalcarbonproject.org/carbonbudget/> (accessed 29/01/2020).

Government of The Gambia. 2015. National Water Resources Assessment and Management Strategy. Prepared by, NIRAS. Consulting Services for the National Water Sector Reforms Studies for The Gambia. Banjul: Ministry of Environment, Climate Change, Water Resources, Parks and Wildlife.

Gutiérrez, J.M., et al. 2019: An intercomparison of a large ensemble of statistical downscaling methods over Europe: Results from the VALUE perfect predictor cross-validation experiment. *International Journal of Climatology*, Vol. 39(9): 3750-3785.

Lange, S. 2018. Bias correction of surface downwelling longwave and shortwave radiation for the EWEMBI dataset. *Earth System Dynamics*, 9(2), 627–645.

Martin, G.M., et al. 2011. The HadGEM2 family of Met Office Unified Model climate configurations, *Geosci. Model Dev.*, 4, 723–757.

NOAA (National Oceanic and Atmospheric Administration). 2020a. Mouna Loa CO₂ Record. <https://www.esrl.noaa.gov/gmd/ccgg/trends/full.html>. (accessed 29/01/2020).

NOAA (National Oceanic and Atmospheric Administration). 2020b. Global Land and Sea Surface Temperature Record. https://www.ncdc.noaa.gov/cag/global/time-series/globe/land_ocean/ytd/12/1880-2019. (accessed 29/01/2020).

Oréade-Brèche and ISL Ingénierie (ISL). 2014. Etude d’Impact Environnemental et Social du Projet Energie (Revue du rapport COTECO 2008). Mission d’Appui Conseil a l’OMVG pour la Realisation de son Projet Energie. Projet de Rapport Final. Dakar: OMVG.

Roudier, P., A. Ducharne and L. Feyen. 2014. Climate Change Impacts on Runoff in West Africa: A review. *Hydrology and Earth System Sciences* Vol. 18: 2789-2801.

Sherwood et al., 2020. An Assessment of Earth’s Climate Sensitivity Using Multiple Lines of Evidence. *Review of Geophysics* doi: 10.1029/2019RG000678

Themessl, M.J., et al. 2012: Empirical-statistical downscaling and error correction of regional climate models and its impact on the climate change signal. *Climatic Change* 112(2):449–468.

Thornthwaite, C. W. (1948). "An approach toward a rational classification of climate". *Geographical Review* 38(1): 55–94.

Watanabe, S., et al. 2011. MIROC-ESM 2010: Model description and basic results of CMIP5-20c3m experiments. *Geoscientific Model Development* 4(4):845-872.

Weedon, G.P., et al. 2014. Watch forcing data methodology applied to ERA-Interim reanalysis data. *Water Resources Research*, 50, 7505–7514.

WMO, 2020. WMO Confirms 2019 as Second Hottest Year on Record. <https://public.wmo.int/en/media/press-release/wmo-confirms-2019-second-hottest-year-record>. (accessed 29/01/2020).

Zelinka, M.D., A.M. Myers, D.T. McCoy, S. Po-Ghedley, P.M. Cadwell, P. Ceppi, S.A. Klein and E. Taylor. 2020. Causes of Higher Climate Sensitivity in CMIP6 Models. *Geophysical Research Letters* Vol. 47(1).

Chapter 4 CLIMATE CHANGE and the OCEAN ENVIRONMENT

Introduction

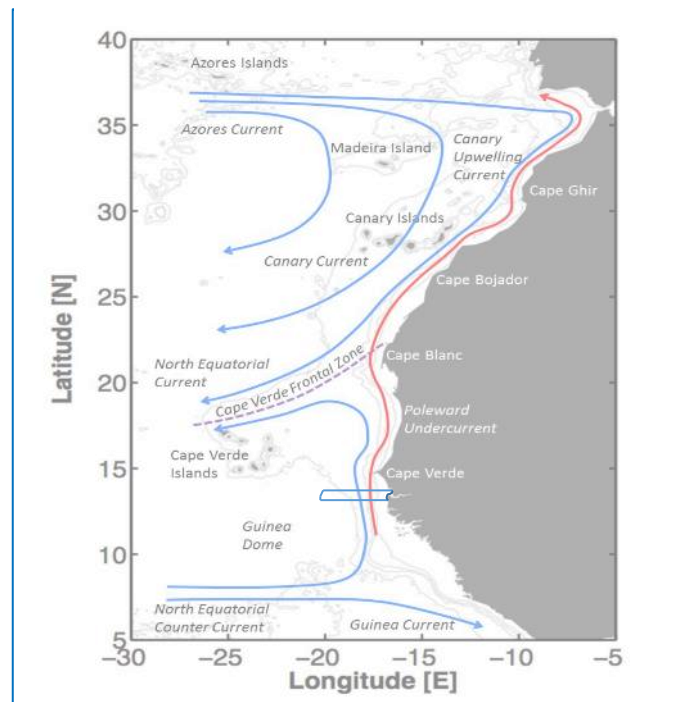
1. **The world's oceans occupy 71 percent of the planet's surface and contain 97 percent of earth's water.** This vast volume serves as the primary sink of additional energy trapped by the anthropogenic release of greenhouse gases, absorbing approximately 93 percent of the additional heat (Cheng et al., 2019; IPCC, 2019a). The connected global oceans also serve as one of the major sinks of atmospheric CO₂, having absorbed between 20-30 percent of CO₂ emissions since the 1980s (IPCC, 2019a). These primary responses of the world's ocean to changes in atmospheric chemistry are driving a number of associated abiotic changes in the ocean environment, which in turn have set in motion an even greater number of direct and indirect effects on oceanic biological systems.
2. **In considering the major abiotic changes effecting The Gambia's fisheries, this review begins with the major impacts occurring in the open ocean and moves shoreward to consider the continental shelf and coastal environment.** The oceanic environment ultimately connects with the mangrove dominated estuary and freshwater ecosystems of the Gambia River covered in the following chapter. Each of these environmental segments supports different fisheries – oceanic, coastal, estuary, riverine – and are exposed to differing climate change threats, while exhibiting varying sensitivities, and will each receive dedicated attention in the chapters ahead.

Observed Climate Change Impacts on the Open Ocean

3. **The ocean environment along the West African coast is a dynamic body.** In addition to tidal surges, the ocean is in constant motion driven by a complex of shifting gyres, currents and eddies, as well as vertical upwellings and subsidence. The result is a heterogeneous mixing of waters along different spatial and temporal scales (from hourly to decadal) although, as shall be illustrated, this mixing is imperfect with regards to some key effects of climate change forcing. With relevance to The Gambia, the most important macro feature of the ocean environment is the North Atlantic Tropical Gyre, an important feature of the Eastern Boundary currents off the West African coast, referred to most commonly in the literature (and in this section) in the context of the Canary Current Large Marine Ecosystem (CCLME) within which The Gambia is located (Pelegrí and Peña-Izquierdo, 2015a). Situated within the southern half of the CCLME (see Figure 4-1), The Gambia lays claim to a band of coastline approximately 65 km in width. Extended seaward 200 nautical miles (370 km) this narrow band demarcates the country's exclusive economic zone (EEZ).⁷⁰ Due to the small size of the EEZ, dynamic nature of the larger physical environment within which it is situated, and the paucity of local data, the climate change evidence presented here, and assumed to be impacting The Gambian waters, is drawn principally from global, North Atlantic and CCLME references.

⁷⁰ The maximum width of The Gambia's EEZ is approximately 65 km (Zeller and Pauly, 2015; see also Flanders Marine Institute, 2019).

Figure 4-1 Ocean currents of the CCLME and the relative position of The Gambia EEZ

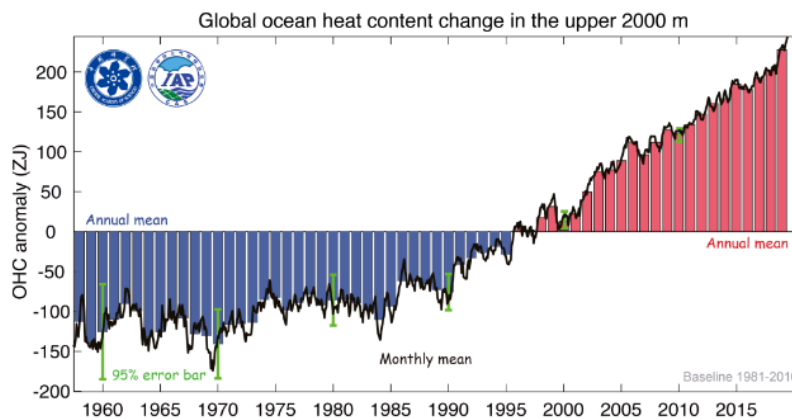


Source: adapted from: Pelegri and Pena, 2015a

4. **Ocean warming.** The Atlantic Ocean covers 20 percent of earth surface (106.5 million sq km). Across this vast expanse off The Gambia's Western coast, several important physical exchanges take place. The first and most significant is the gradual heating of the ocean surface, the top few meters, and the transfer of this heat into deeper ocean layers. Without this thermal transfer taking place, average global temperatures would have already warmed at nearly twice the current rate, or at the same rate as land surface temperature rise (IPCC, 2019b), pushing global warming well above the 1.5 °C threshold. As outlined in recent global assessment reports the impacts of this level of warming would be nothing short of catastrophic (IPCC, 2019a, b; IPCC, 2018; Steffen et al., 2018).

5. **Overall, average ocean temperatures have risen steadily since 1970 (IPCC, 2019a), with the rate of increase rising dramatically over the past three decades** (see Figure 4-2). Between 1955-1986 ocean warming grew at a rate of 2.1 +/- 0.5 ZJ/year. From 1987 to 2019, the rate of warming increased to 9.4 +/- ZJ/year – approximately 450 percent faster (Cheng et al., 2020). Average global ocean temperatures in the upper 2000 m in 2019 were the highest ever recorded; the past five-years, the warmest ever recorded; the past decade, the warmed 10-years on record (Cheng et al., 2020). In the CCLME, upper ocean temperatures (0-200 m depth) have risen on average 0.28 °C per decade over the 32-year period of 1982-2013 (Vélez-Belchí et al., 2015), or 0.9 °C of total warming, with areas within this zone warming at double this rate, at 0.65 °C per decade. The warming of surface waters within the CCLME exhibit a strong seasonal trend, with the highest values observed during periods of greater downwelling, especially in locations where this occurs during the summer months, leading to observed warming trends of over 0.90 °C per decade during peak warming periods of the year. The areas off The Gambian coast are reported to have increased downwelling (Vélez-Belchí et al., 2015), thus indicating the potential for higher warming trends, although *in situ* measurements are lacking to substantiate this trend.

Figure 4-2 Trend in Global Warming of the Upper Ocean (1955-2019)



Source: NOAA, 2020a

6. **The increase in sea surface temperatures is associated with three corresponding abiotic changes.** The first is an increase of **salinity levels**. As seawater warms its density decreases. To maintain equilibrium, salinity levels increase as temperatures rise.⁷¹ Measurements in the CCLME show both, an increase in temperatures of the surface layer, and a corresponding increase in salinity of 0.03 +/- 0.023 per decade (Vélez-Belchí et al., 2015).

7. Secondly, the rise in surface temperatures increases the **stratification of the water column**, resulting in less mixing of upper and lower water layers (IPCC, 2019a). Stratification has increased globally 5 percent in recent decades, with over 70 percent of the increase occurring in the upper 200 m (Li et al, 2020). The decrease in vertical mixing has important implications for the cycling of inorganic ocean nutrients and dissolved oxygen levels. Measurements within the CCLME, while documenting the increase in surface temperatures, show little or no changes in water temperatures at intermediate depths and the deep ocean (Vélez-Belchí et al., 2015), suggesting weak vertical mixing.

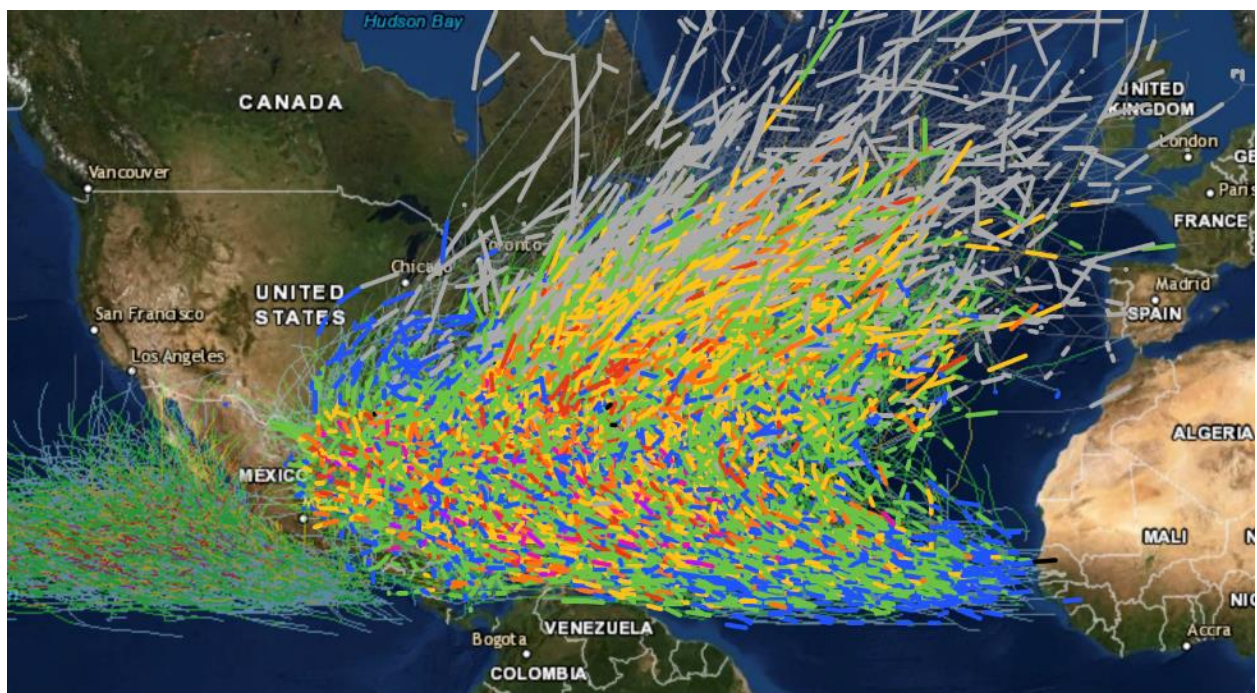
8. Third, there is the decrease in **dissolved oxygen** content within the more rapidly warming surface waters. As water warms, it is able to hold less oxygen due to changes in gas solubility. Greater stratification of surface waters increases residency times and prevents mixing. Stratification is responsible for 80 percent of global deoxygenation of surface waters (Li et al., 2020). Globally, dissolved oxygen levels have decreased by 2 percent since the 1950s, with the volume of water completely devoid of oxygen quadrupling since the 1960s (IPCC, 2019a; Laffoley and Baxter, 2019). Over this same time period the number of ocean sites suffering from low oxygen levels has grown from 45 to over 700 in 2011 (Laffoley and Baxter, 2019). These changes mean that although the oxygen content of the ocean is only 0.6 percent of that in the atmosphere the ocean has become a net source of atmospheric oxygen, due to the rise in sea surface temperatures and ability of warm water to hold less oxygen, (Laffoley and Baxter, 2019). Eastern boundary upwelling systems (EBUS) are known for their low levels of dissolved oxygen. Of the major EBUS the oxygen minimum zone in the CCLME is the least hypoxic globally, but the rate of decline in dissolved oxygen levels observed in the CCLME is twice as fast as other oxygen minimum zones (Pelegri and Peña-Izquierdo, 2015b; Stramma et al., 2008).

9. **Imbedded within this general, slow-onset trend of increasing sea surface temperatures, and associated secondary effects, is a commensurate increase in the potential of marine heatwaves,**

⁷¹ Increased salinization in the Atlantic is also linked to a basin-wide freshwater transfer from the Atlantic to Pacific resulting from an intensification in the hydrologic cycle (evaporation and precipitation) (Li et al., 2020).

violent storms and harmful algal blooms. As with land surfaces, the ocean environment is also subject to extreme, rapid on-set, heating events in the form of marine heatwaves. Globally the frequency of **marine heatwaves** have doubled since 1982, becoming increasingly intense, with longer-duration and covering larger areas (IPCC, 2019a). As example of the magnitude and effect of these events, in 2015/16 during a particularly strong *el niño* event, a major marine heatwave occurred in the North Pacific that raised sea surface temperatures 1-2 °C killing an estimated one million seabirds through impacts on the food chain beginning with a decline in plankton primary productivity (Piatt et al., 2020). The energy transfer from periods of gradual and rapid heating of the sea surface is stored within the ocean and feeds the formation of **major storms**. In the same year, 2015/16, Hurricane Patricia formed over the eastern Pacific, with wind speeds of over 320 km/hr, the strongest storm ever recorded. The paucity of data specific to the CCLME do not allow observations to be made on trends, however, in general the tropical North Atlantic is the source of tropical depressions, storms and hurricanes, which once formed, strengthen and are pushed westward by the overlaying trade winds, striking North America (see Figure 4-3). Due to the connectedness of the global ocean and consistency in drivers, it is likely that similar tendencies are occurring in the CCLME environment as well.

Figure 4-3 Tropical Depressions (blue), Storms (green) and Hurricane Tracks (yellow, orange, red) in the North Atlantic Ocean (1842-2018)



Source: NOAA, 2020b

10. Due to the high level of nutrients in upwelling water, the major EBUSs worldwide are susceptible to the development of **harmful algal blooms** (Pitcher and Jacinto, 2019). Four main types of harmful algal blooms – paralytic shellfish poisoning, diarrhetic shellfish poisoning, amnesic shellfish poisoning, ciguatera fish poisoning and cyanobacteria poisoning – have been reported in the CCLME (Pitcher and Fraga, 2015). The principle species responsible for these blooms are all regular components of the phytoplankton communities found in the CCLME upwelling zones. Depending on the emergence of favorable conditions found along the upwelling system, individual populations of toxin producing species can dominate, leading to an outbreak in one of the poisoning related harmful blooms noted. The main species of marine life affected by harmful algal blooms are shellfish, whereas

ciguatera poisoning occurs through the consumption of affected fish, principally top-predators who have assimilated high levels of toxins, accumulated through several trophic levels of biomagnification. Human consumption of either contaminated shellfish or sea fish can lead to serious health consequences even death. Cyanobacteria blooms, which can occur in ocean, brackish or fresh water, produce toxins that can directly affect human or livestock coming into contact.

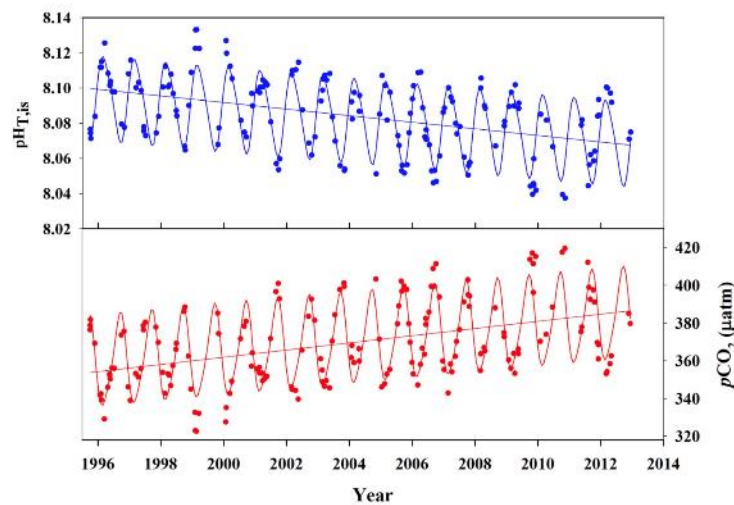
11. The increased appearance of ciguatoxic fish within the CCLME is interpreted as another indicator of the shift in bioregions northwards towards higher latitudes brought on by higher sea surface temperatures (Dickey and Plakas et al., 2010; Otero et al., 2010). It has been noted that the first recorded cyanobacteria blooms in the CCLME appeared in association with the highest seasonal temperatures since 1912 and the occurrence of significant Saharan dust storms that deposited Fe laden dust in offshore waters required for the growth of the bacteria (Pitcher and Fraga, 2015).⁷²

12. **Acidification.** The second major exchange taking place at the sea surface is the diffusion of atmospheric CO₂ into the ocean body. Between one-fifth and a third of total CO₂ emissions since the 1980s have been sequestered in the global ocean (IPCC, 2019a). The impact on seawater pH (acidification) of this vast amount of sequestered CO₂ is the resulting balance of a complex set of interactions. Increasing atmospheric concentrations of CO₂ raise the CO₂ partial pressure (pCO₂) with respect to seawater, leading to more CO₂ entering the ocean and a decrease in pH at the sea surface (see Figure 4-4). In contrast, as sea surface temperatures warm, the solubility of CO₂ declines, lowering the amount of additional CO₂ that can be absorbed (González-Dávila and Santana-Casiano, 2015). In upwelling areas the induction of cold water, rich in inorganic nutrients and high in CO₂, rising to the surface supports the development of massive phytoplankton blooms, which assimilate carbon dissolved in seawater through photosynthesis, resulting in a raise in pH and a lowering of pCO₂ (Loucaides et al., 2012; Lachkar and Gruber, 2013), allowing more CO₂ to enter the ocean.

13. Due to the induction of cold water through upwelling events, containing high levels of dissolved CO₂, coastal areas such as the CCLME naturally have among the most extreme pH levels in the world with pH reported as low as 7.6-7.7 (Feely et al., 2008). Since pre-industrial times, the pH of the global ocean has declined by 0.1 units, equivalent to a 30 percent increase in acidity (Caldeira and Wickett, 2003). In the CCLME, monitoring data collected at a site in the Canary Islands since 1994, shows a decline in pH of -0.0013/yr to -0.0025/yr, roughly double the global rate of ocean acidification. That said, the ocean waters in the CCLME are highly heterogenous, the result of complex processes associated with varying upwelling intensities, sea surface temperatures, mixing with underlying water layers and rate of phytoplankton uptake of dissolved carbon, each of which are influenced by various attributes of climate change, making generalized statements about changes to pH beyond global trends difficult to substantiate (Santana-Casiano and González-Dávila, 2015).

⁷² Over half (55 percent) of the global atmospheric dust input comes from the Saharan desert and Sahel. "Atmospheric dust deposition is an important source of essential and limiting nutrients and metal to the oceans, affecting the oceanic carbon uptake, phytoplankton growth and productivity...dust inputs may promote nitrogen fixation, by providing iron and other trace metals" (Gelado-Caballero, 2015; internal citations withheld).

Figure 4-4 Change in Ocean pH and CO₂ Partial Pressure



Source: González-Dávila and Santana-Casiano, 2015

Observed Climate Change Impacts along the Continental Shelf and Coastal Areas

14. Shifting focus from the open ocean shoreward, to the continental shelf and coastal environment, the most important abiotic forces influencing fish populations and biological habitat are upwelling events and sea level rise. The coastal environment of the CCLME is one of four major global EBUS (see text box). Along the Gambian coast, the continental shelf begins to drop away approximately 70 km from shore, with head of the slope in roughly 200 m of water and base at 2500-3000 m (Agudo-Bravo and Mangas, 2015). Upwelling occurs along the declining slope of the continental shelf, whereas sea level rise is felt most acutely along the shore and the extent of seawater intrusion into the Gambia River estuary.

15. **Upwelling.** The differential rates of warming of adjacent sea and coastal land surfaces give rise to increased alongshore winds, the driver of upwelling events (Bakun, 1990; Bakun et al., 2010). The nutrient rich waters brought to the surface through upwelling events along the continental shelf feed the oceanic food chain through the stimulation of massive blooms of phytoplankton, visible in satellite images as filaments, the signature of upwelling areas, and subsequently blooms of zooplankton (Demarcq and Somoue, 2015; Berraho et al., 2015) (see Figure 4-6).⁷³ Measurements in the CCLME have detected an increase in alongshore wind, favorable to producing upwelling events (Benazzouz et al., 2015), yet remote sensing data has not detected a corresponding decrease in sea surface temperature associated with increased coastal winds (ibid). A drop in sea surface temperatures is normally associated with upwelling events as cooler water is brought to the surface. Satellite imagery have also not detected an increase in filaments of plankton bloom down current from traditional upwelling areas.⁷⁴ Primary productivity has been assessed as generally stable across the CCLME, with

⁷³ Surface waters in the CCLME are "...characterized by high temperatures and salinities, high dissolved oxygen and low nutrient concentrations" (Pastor et al., 2008; 2015).

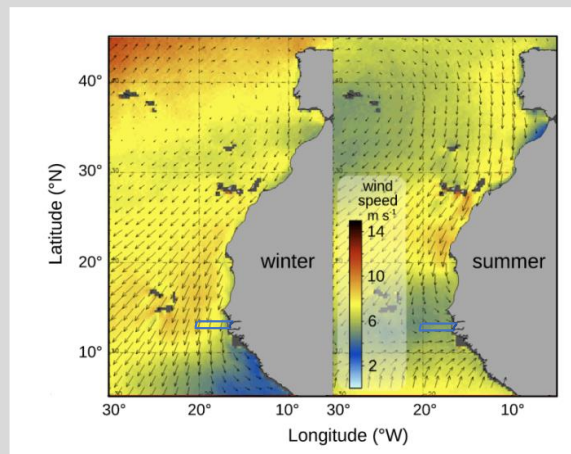
⁷⁴ Measurements in the CCLME observe that between 30 – 60 percent of the primary productivity is exported horizontally off of the continental shelf, moved by Ekman transport (Álvarez-Salgado, 2015; Sangrá, 2015).

a possible slight decrease in productivity in the southern portion off the Gambian coast as evident in the data analyzed from 1998 to 2014 (Demarcq and Benazzouz, 2015).

Eastern Boundary Upwelling

EBUS occupy less than 3 percent of the global ocean surface (Large and Danabasoglu, 2006), but contribute from between 20 to 40 percent of the total fish catch (Pauly and Christensen, 1995; Capone and Hutchins, 2013; Laffoley and Baxter, 2019), comprised primarily of small pelagic species^{f.n.} and those that feed upon them (e.g., tunas). EBUS are driven by three primary factors: alongshore wind, the Coriolis effect and Ekman transport mechanism (Bakun, 1990; Ekman, 1905). Alongshore winds create friction over the ocean surface, tending to pull surface waters with it. The combined forces of the Coriolis effect and Ekman transport mechanism in turn act on these moving waters, deflecting their path of travel to 45° of the wind direction. In the northern hemisphere, water moves to the right of the wind direction (Chelton et al., 2004; Pelegrí and Benazzouz, 2015). Surface water that are drawn away from shore, create nearshore suction, pulling deeper waters to the surface – forming an upwelling event (Mann and Lazier, 2006). In contrast, surface waters pushed further shoreward are forced downwards, creating an area of downwelling. Along the Gambian coast upwelling occurs most frequently during the autumn and winter months, when prevailing winds are towards the equator, whereas downwelling occurs during the spring and summer when winds turn poleward (ibid) (see Figure 4-5).

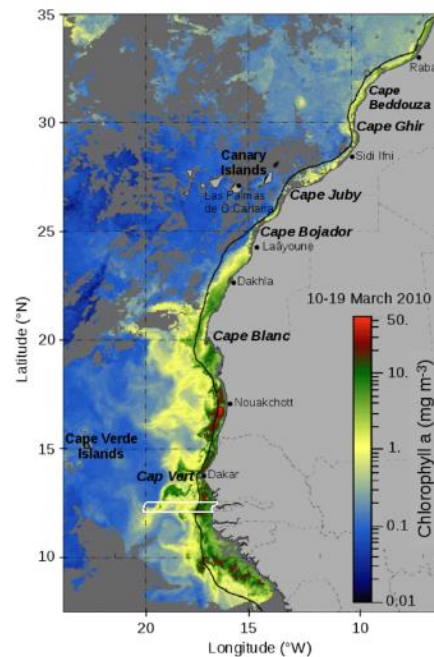
Figure 4-5 Seasonal Wind Directions and Intensities in the CCLME and Relative Position of the Gambian EEZ



Source: adapted from Pelegrí and Benazzouz, 2015

f.n. In slow and very rapid upwelling currents, small phytoplankton species dominate delaying somewhat the buildup of grazing populations of zooplankton and larger organisms that in turn feed higher trophic levels in the food chain. Populations of large-sized plankton thrive in moderate upwelling currents, leading to more rapid buildup of zooplankton, filter feeders and small pelagic species within the food chain (van der Lingen et al., 2009 and 2006; Rykaczewski, 2018). Productivity of the CCLME is such that small pelagic biomass can double in the course of a single season.

Figure 4-6 Phytoplankton Filament Detected from the MODIS Sensor, 10-19 March, 2010, and relative position of the Gambian EEZ



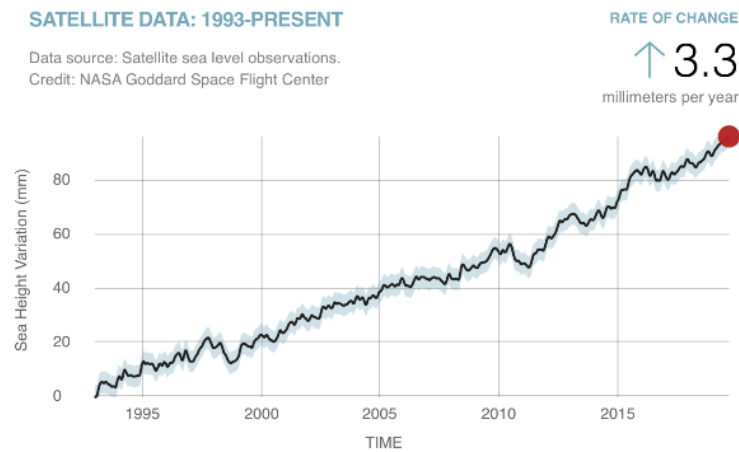
Source: adapted from Demarcq and Somoue, 2015

16. Although the dynamics are not fully understood, it is believed that rapidly increasing sea surface temperatures have increased the strength of the thermocline barrier between the upper and intermediate ocean layers. The observed increase in the alongshore winds, normally associated with an increase in upwelling events, are thought to not exert sufficient vertical lifting force for subsurface waters to break through the temperature gradient. As a result, there has been no observable increase in upwelling activity, with observable decreases in sea surface temperatures (from upwelled cooler water) or visible plankton blooms down current (Demarcq and Benazzouz, 2015).

17. **Sea level rise.** The other important abiotic impact of climate change on the coastal zone is sea level rise. Although sea level rise affects the entire ocean environment, the most meaningful point of reference is when the ocean comes into contact with shore, and in the case of The Gambia, where the ocean meets the outgoing river estuary. From 1900 - 2013, sea levels rose risen by approximately 22 cm, with close to half this increase (9.6 cm; 3.3 mm/yr) occurring since 1993 (NASA, 2020) (see Figure 4-7). Across the CCLME the rate of sea level rise confirms the global trend, although the southern portion has risen more quickly with recorded increases of up to 4.5 mm/yr for the period 1992-2013 (Pérez-Gómez et al., 2015). The rapid increase in the global rate of sea level rise, more than doubling in recent decades, obscures an important shift occurring in the source of sea level rise. Initial increases were driven primarily by thermal expansion; the warming of the oceans (warmer water takes up more volume). More recently, however, the contribution of additional fresh water from melting glaciers and ice sheets have come to dominate. Over the period 1993 to 2018, thermal expansion contributed 42 percent of the recorded sea level rise, while melting glaciers and ice sheets contributed 44 percent (IPCC, 2019a). Over the recent decade, 2007-2016, the rate of additional fresh water from the Greenland ice sheet has doubled, and those from the Antarctic ice sheets have tripled, relative to 1997-2006 (IPCC, 2019a). The exceptional melting in 2019 saw the Greenland ice sheet alone

contribute 40 percent, 1.5 mm, of the total 3.75 mm observed sea level rise (Tedesco and Fettweis, 2020).

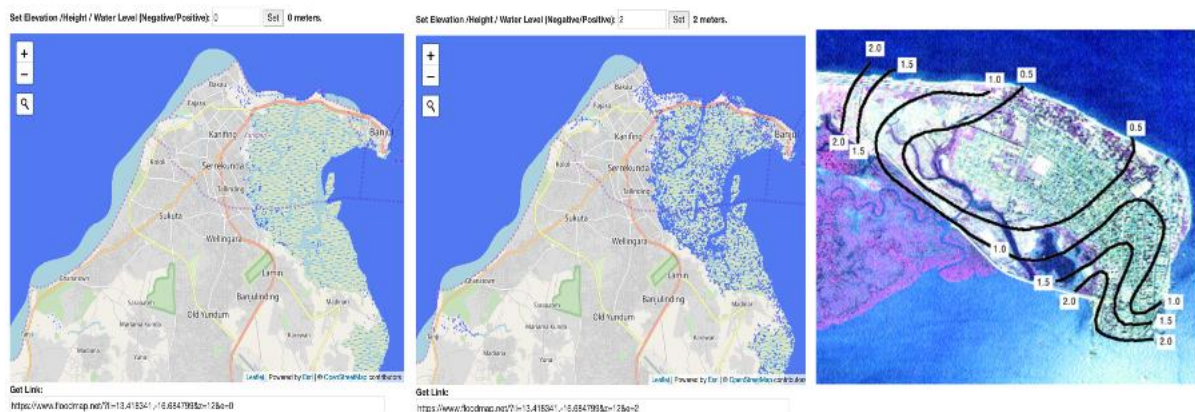
Figure 4-7 Sea Level Rise since 1993



Source: NASA, 2020

18. The Gambia's capital, Banjul, sits perilously close to historical sea level, with the port and much of the city within 2 m of sea level (see Figure 4-8). Extreme wave heights in the South Atlantic have increased on average by 1 cm per year since 1985, over 30 cm total, further threatening coastal lands and infrastructure (IPCC, 2019a).⁷⁵ Also exposed to rising sea levels, the Gambia River has an extremely flat profile, falling less than one meter (57 cm) over the final 500 km of length (ISL, 2014). Such a flat profile exposes the river environment to substantial impacts from continued sea level rise; in the absence of river discharge, each additional centimeter of sea level rise potentially allows seawater to reach many kilometers further inland. Assessments of the mangrove along river estuary have detected a decline of 47 percent in the mangroves tree cover between 1981-92 and 2009-10, due changes in salinity levels from drought, sea level rise and human activities (GoTG, 2010).

Figure 4-8 Banjul and Surrounding Coastline with Approximate Impacts of 0 - 2 m of Sea Level Rise (<https://www.floodmap.net/?ct=GM>); accessed 29/01/2020)



Source: Jallow et al., 1999

⁷⁵ Globally, “nearly 50 percent of coastal wetlands have been lost in the last 100 years, as a result of the combined effects of localized human pressures, sea level rise, warming and extreme events” (IPCC, 2019a).

Projected Impacts and Trends

19. Stated most simply, all of the impacts of climate change noted in the previous sections are anticipated to worsen in the coming decades. As our understanding improves on how the various dynamics and interrelations of abiotic features of the earth system respond to increased CO₂ concentrations and global warming, estimates on future impacts, the relative timing of their onset and geographic precision of where impacts will be felt, will become more exact. With regards to the CCLME, and areas off the Gambian coast, the impact of future changes are best guided by estimates at the global level, keeping in mind that with regards to many measures the CCLME has shown itself to be more sensitive than other non-EBUS environments.

Notable Anticipated Impacts in the Open Ocean

20. **Sea surface and ocean warming.** As a principle driver of many other abiotic changes occurring within the ocean environment, what happens with regards to sea surface temperatures is of utmost importance. The IPCC anticipates that under RCP 8.5, the upper 2000 m of the ocean will take up 5-7 times more heat by 2100 (IPCC, 2019a). For even the slowest warming areas of the CCLME, this will mean an increase of sea surface temperatures of 1.4 to 1.9 °C per decade. The cumulative effect of this rate of warming makes it difficult to conceive of any of the major existing fisheries being sustained without significant impact. Given that warming of the ocean body is not reversible over meaningful time periods, taking millennia to stabilize (IPCC, 2019a; Laffoley and Baxter, 2019; Cheng et al., 2020), what happens in the coming decades in terms of emission reductions will have a profound effect on the future of ocean biological systems.

21. The ongoing assessment of a possible underestimation of the relative sensitivity of the climate system to levels of atmospheric forcing (i.e., the global temperature response to greenhouse gas emissions) makes the attention given to reducing emissions all the most important. Outputs from the new generation of global circulation models being used in preparation of the IPCC sixth assessment report show an upward trend in both the predicted rate of warming and ultimate equilibrium as compared to those used in the past (e.g., Zelinka et al., 2020; Nijssen et al., 2020). If such an underestimation has occurred, expected global warming from greenhouse gas emissions already released (as well as those anticipated) will require that even more aggressive actions are taken to reduce greenhouse gas emissions to meet the target set by the Paris Agreement.

22. **Dissolved oxygen.** As sea surface continues to warm, ocean circulation is expected to slow, leading to a 50 percent reduction in oxygen levels in the upper 1000 m, and a 98 percent reduction at depths greater than 1000 m (IPCC, 2019a). Implications for the CCLME are that deep ocean waters, the source of upwelling currents, already noted to be low in oxygen, will become even more oxygen deprived. In terms of general sensitivities, it is noted that “[o]cean deoxygenation...affects marine systems as soon as conditions depart from full aeration” (Laffoley and Baxter, 2019). The loss of viable habitat due to oxygen depletion will threaten the pelagic fisheries across the entire CCLME (Arístegui et al., 2006; Stramma et al., 2012). [Note: The global oxygen minimum zones are also a major source of N₂O⁷⁶ (Garçon et al., 2019), responsible for approximately 22 percent of the annual global N₂O emissions. It is predicted that an expansion of oxygen depleted zones will intensify global nitrous oxide

⁷⁶ N₂O is a powerful greenhouse gas, exerting 298 times more warming over a 100-year period than CO₂ (IPCC, 2013).

(N₂O) fluxes (Capone and Hutchins, 2013), further contributing to global warming and its related impacts on the marine environment.]

23. **Salinity changes.** No specific projections are made regarding changes to salinity levels. Due to the relationship between sea surface temperatures, water density and salinity, and the major influences of surface evaporation and precipitation, it can generally be anticipated that salinity levels in the upper oceans will continue to rise as waters warm and evaporation relative to precipitation intensifies.

24. **Marine heatwaves.** By 2100, marine heatwave frequency is projected to increase by 50 times, relative to 1900 under RCP 8.5, with an increase in intensity of 10 times (IPCC, 2019a).

25. **Storms.** Globally it is projected that oceanic storms will increase with the continued warming of sea surfaces, leading to increased storm frequency and intensity and propagation of more category 4 and 5 hurricanes (IPCC, 2019a). The IPCC (IPCC, 2019a) predicts a decrease in maximal wave height in the North Atlantic, however, it is unclear whether this pertains to the CCLME as well. In any event, the combined forces of sea level rise, increased storm and highwater events will likely have a progressive and greater impact on coastal erosion and shoreline infrastructure.

26. **Harmful algal blooms.** The decreasing intensity of the Atlantic Meridional Overturn Circulation is expected to lead to a decrease Sahelian rainfall (IPCC, 2019a), which, due to its teleconnection with the CCLME, would be expected to contribute to greater dust transport and deposition, effectively seeding the CCLME with Fe and potentially contributing to an increase in harmful algal blooms associated with dust deposits and warmer water temperatures.

27. **Acidification.** Ocean pH levels are projected to continue to decline by an estimated 0.3 – 0.4 units under RCP 8.5. These pH levels will threaten keystone shell-forming species, by crossing aragonite stability thresholds by 2100 (IPCC, 2019a), thus effecting shellfish along the Gambian coast and saltwater estuary. Recent analysis indicates that the oceans may be absorbing 25 percent more CO₂ than previously thought (Watson et al., 2020), underscoring the likelihood of pH levels exceeding critical biological thresholds more rapidly than anticipated.

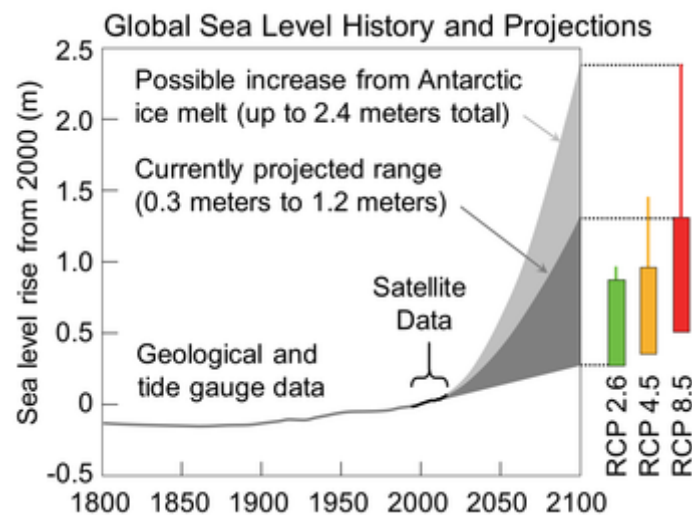
Notable Anticipated Impacts along the Continental Shelf and Coastal Areas

28. **Upwelling.** Stratification of the upper 200 m of surface water is expected to intensify by an additional 12-30 percent, thus further limiting the mixing and exchange of dissolved oxygen, nutrients and carbon within the water column (IPCC, 2019a; see also Li et al., 2020). Due to the impacts of increased stratification, net primary productivity is predicted to decline 7-16 percent by 2081-2100 (IPCC, 2019a), thus precluding a doubling of net primary productivity of phytoplankton in response to a doubling of upwelling inducing wind speed predicted by some models for the central and northern CCLME (Lachkar and Gruber, 2013).

29. **Sea level rise.** Concerning sea level rise, the normative and admittedly conservative projections of the IPCC are for sea level rise of 0.84 m by 2100 under RCP 8.5, potentially increasing at a rate of 15 mm per year (IPCC, 2019a). In contrast, a growing body of evidence (see Sieger et al., 2020) places anticipated sea level rise associated with high levels of warming at over 2 m by 2100 (NOAA, 2017; Bamber et al., 2019) (see Figure 4-9). Historically, the last time global temperatures were 2-3 °C warmer than pre-industrial levels, sea surface levels were over 16 m higher than present (Dumitru et al., 2019). New research indicates that 2.3 °C of total warming by 2100 is already

committed through the GHG emissions currently in the atmosphere (Zhou et al., 2021). The volume of water held in the Antarctic and Greenland ice sheets, which if melted, has the potential of rising sea levels an additional 58.3 m and 7.4 m respectively (WCRP, 2018). Recent studies have assessed that the Greenland ice sheet and arctic permafrost have crossed tipping points of sustained melting, which will continue for several centuries regardless as to efforts in reducing GHG emissions (King et al., 2020; Randers and Goluke, 2020). In the near term, through 2100, and depending on other hydrological changes within the Gambia River watershed, .84 m to 2 m of sea level rise can be anticipated, allowing sea water to enter well into the Gambia River (chapter xx presents a detail analysis of saltwater intrusion associate with sea level rise), as well as potentially contributing to hypoxia conditions within estuary (IPCC, 2019a) and hypersaline conditions in the brackish segments of the river (e.g., Savenije and Pages, 1992), and would inundate much of the capital city (see Fig. X above). In addition, under RCP 8.5, the frequency of extreme sea levels events, which have occurred once per century in the past, are projected to occur annually by 2050 in many locations (IPCC, 2019a); The Gambia’s vulnerability to this additional threat is unclear.

Figure 4-9 Projected Sea Level Rise Under Different Emission Pathways



Source: NOAA, 2017

Conclusions

30. To summarize, in the oceanic environment the combined direct and indirect impacts of rising concentrations of atmospheric CO₂, increasing ocean temperatures, declining pH levels, strengthening of thermocline barriers affecting nutrient cycling and oxygen levels have led to an overall poleward shift in the physical parameters that provide suitable habitats for major marine species. The IPCC (2019a) notes a global poleward movement of individuals species at a rate of between 52 +/- 33 km per year to 29 +/- 16 km per year for species in the upper 200 m and seafloor, respectively, as well as the likely vertical and horizontal compression of viable habitat for the marine species that remain (Braham and Corten, 2015; Laffoley and Baxter, 2019). Additional impacts on the entire upwelling system foodchain of the CCLME, as well as potential damage due to sea level rise and highwater events on coastal infrastructure and further saltwater intrusion into the Gambia River estuary, are imminent.

31. **One conclusion to be taken from these findings is that the speed, magnitude and inertia of change occurring in the abiotic conditions in the North Atlantic and CCLME offer limited scope for taking adaptive actions.** These limitations are particularly acute for The Gambia given the extremely small size of the country's EEZ compared to the vastness of the oceanic environment and fluidity in movement of key fish stocks. As will be detailed further in the biological assessment of climate change impacts on key fish stocks, beyond improved joint monitoring efforts of fish stocks with neighboring countries and continued adjustments to fishing pressure and management of residential stocks, and the possible selective protection of seaward assets, there are few prospects for realizing returns to investments in adaptive measures in the fishery sector along the country's coast and in the oceanic environment.

References

Agudo-Bravo, L.M. and J. Mangas. 2015. Main Geomorphic Features in the Canary Current Large Marine Ecosystem. In: Oceanographic and Biological Features in the Canary Current Large Marine Ecosystem. Valdés, L. and I. Déniz-González (eds). Technical Series 115. Paris: IOC-UNESCO.

Álvarez-Salgado, X.A. and J. Arístegui. 2015. Organic Matter Dynamics in the Canary Current. In: Oceanographic and Biological Features in the Canary Current Large Marine Ecosystem. Valdés, L. and I. Déniz-González (eds). Technical Series 115. Paris: IOC-UNESCO.

Arístegui, J., X.A. Álvarez-Salgado, E.D. Barton, F.G. Figueiras, S. Hernández-León, C. Roy and A.M.P. Santos. 2006. Oceanography and Fisheries of the Canary Current/Iberian Region of the Eastern North Atlantic (18a,E). In: Robinson, A.R. and K.H. Brink (eds). The Sea: The global coastal ocean. Interdisciplinary Regional Studies and Synthesis, Vol. 14B. Boston (MA): Harvard University Press.

Bakun, A. 1990. Global Climate Change and Intensification of Coastal Ocean Upwelling. *Science* (247): 198-201.

Bakun, A., D.B. Field, A. Redondo-Rodriguez and S.J. Weeks. 2010. Greenhouse Gas, Upwelling-favorable Winds, and the Future of Coastal Upwelling Ecosystems. *Global Change Biology* Vol. 6(4): 1213-1228.

Bamber, J.L., M. Oppenheimer, R.E. Kopp, W.P. Aspinall and R.M. Cooke. 2019. Ice Sheet Contributions to Future Sea-Level Rise from Structured Expert Judgement. *Proceedings of National Academy of Sciences* Vol. 116(23):11195-11200.

Berraho, A., I. Somoue, S. Hernández-Léon and L. Valdés. 2015. Zooplankton in the Canary Current Large Marine Ecosystem. In: Oceanographic and Biological Features in the Canary Current Large Marine Ecosystem. Valdés, L. and I. Déniz-González (eds). Technical Series 115. Paris: IOC-UNESCO.

Benazzouz, A., S. Mordane, A. Orbi, M. Chagdali, K. Hilmi, A. Atillah, J.L. Pelegrí and H. Demarcq. 2014. An Improved Coastal Upwelling Index from Sea Surface Temperature Using Satellite-based Approach – The case of the Canary Current upwelling system. *Continental Shelf Research* Vol. 81: 38-54.

Benazzouz, A. H. Demarcq and G. González-Nuevo. 2015. Recent Changes and Trends of the Upwelling Intensity in the Canary Current Large Marine Ecosystem. In: Oceanographic and Biological Features in the Canary Current Large Marine Ecosystem. Valdés, L. and I. Déniz-González (eds). Technical Series 115. Paris: IOC-UNESCO.

- Braham, C.-B. and A. Corten, 2015. Pelagic Fish Stocks and Their Response to Fisheries and Environmental Variation in the Canary Current Large Marine Ecosystem. In: Oceanographic and Biological Features in the Canary Current Large Marine Ecosystem. Valdés, L. and I. Déniz-González (eds). Technical Series 115. Paris: IOC-UNESCO.
- Caldeira, K. and M.E. Wickett. 2003. Oceanography: Anthropogenic Carbon and Ocean pH. *Nature* Vol. 425: 365.
- Capone, D. and D.A. Hutchins. 2013. Microbial Biogeochemistry of Coastal Upwelling Regimes in a Changing Ocean. *Nature Geoscience* Vol. 6: 711-716.
- Chelton, D.B. M.G. Schlax, M.H. Freilich and R.F. Milliff. 2004. Satellite Measurements Reveal Persistent Small-Scale Features in Ocean Winds. *Science* Vol. 303: 978-983.
- Cheng, L., J. Abraham, Z. Hausfather and K.E. Trenberth. 2019. How Fast are the Oceans Warming? *Science* Vol. 363(6423): 128-129
- Cheng, L., et al. 2020. Record-Setting Ocean Warmth Continued in 2019. *Advances in Atmospheric Sciences* Vol. 37: 137-142.
- Demarcq, H. and L. Somoue. 2015. Phytoplankton and Primary Productivity off Northwest Africa. In: Oceanographic and Biological Features in the Canary Current Large Marine Ecosystem. Valdés, L. and I. Déniz-González (eds). Technical Series 115. Paris: IOC-UNESCO.
- Dickey, R.W. and S.M. Plakas. 2010. Ciguatera: A public health perspective. *Toxicology* Vol. 55: 123-136.
- Dumitru, O.A. et al., 2019. Constraints on Global Mean Sea Level during Pliocene Warmth. *Nature* Vol. 575: 233-236.
- Ekman, V.M. 1905. On the Influence of the Earth's Rotation on Ocean-Currents. *Arkiv För Matematik, Astronomi Och Fysik* Vol. 2(1): 1-52.
- Feely, R.A., B.A. Seibel, J.M. Hernandez-Ayon, D. Lanson and B. Hales. 2008. Evidence of Upwelling of Corrosive 'Acidified' Water onto the Continental Shelf. *Science* Vol. 320: 1490.
- Flanders Marine Institute. 2019. Maritime Boundaries Geodatabase: Maritime Boundaries and Exclusive Economic Zones (200NM), version 11. (accessed 12/10/2020: <https://www.marineregions.org/gazetteer.php?p=details&id=8370>)
- Garçon, V., B. Dewitte, I. Montes and K. Goubanova. 2019. Land-Sea-Atmosphere Interactions Exacerbating Ocean Deoxygenation in Eastern Boundary Upwelling Systems (EBUS). In: In: Laffoley, D. and J.M. Baxter (eds). 2019. Ocean Deoxygenation: Everyone's Problem – Causes, Impacts, Consequences and Solutions. Full Report. Gland, Switzerland: International Union of Concerned Scientists.
- Gelado-Caballero, M.D. 2015. Saharan Dust Inputs to the North Atlantic. In: Oceanographic and Biological Features in the Canary Current Large Marine Ecosystem. Valdés, L. and I. Déniz-González (eds). Technical Series 115. Paris: IOC-UNESCO.
- González-Dávila, M. and J.M. Santana-Casiano. 2015. Inorganic Carbon, pH and Alkalinity in the Canary Current Large Marine Ecosystem. In: Oceanographic and Biological Features in the Canary Current Large Marine Ecosystem. Valdés, L. and I. Déniz-González (eds). Technical Series 115. Paris: IOC-UNESCO.
- Government of The Gambia. 2010. The Gambia. National Forest Assessment 2008-2010. Banjul: Ministry of Forestry and Environment.

IPCC (Intergovernmental Panel on Climate Change). 2013. *Climate Change 2013: The Physical Science Basis. Contributions of the Working Group I to the Fifth Assessment Report on the Intergovernmental Panel on Climate Change* [Stocker et al., eds.] Cambridge University Press: Cambridge, U.K.

IPCC (Intergovernmental Panel on Climate Change). 2014: *Climate Change 2014: Synthesis Report. Contribution of Working Groups I, II and III to the Fifth Assessment Report of the Intergovernmental Panel on Climate Change*. Geneva, Switzerland: IPCC.

IPCC (International Panel on Climate Change). 2018. *Global Warming of 1.5°C. An IPCC Special Report on the impacts of global warming of 1.5°C above pre-industrial levels and related global greenhouse gas emission pathways, in the context of strengthening the global response to the threat of climate change, sustainable development, and efforts to eradicate poverty* [Masson-Delmotte, V. et al. (eds.)]. Geneva, Switzerland: World Meteorological Organization.

IPCC (Intergovernmental Panel on Climate Change). 2019a. *Special Report on the Ocean and Cryosphere in a Changing Climate* [H.-O. Pörtner, et al. (eds.)]. Geneva, Switzerland: IPCC.

IPCC (Intergovernmental Panel on Climate Change). 2019b. *Climate Change and Land: an IPCC special report on climate change, desertification, land degradation, sustainable land management, food security, and greenhouse gas fluxes in terrestrial ecosystems* [P.R. Shukla, et al. (eds.)]. Geneva, Switzerland: IPCC.

Jallow, B.P., S. Toure, M.M.K. Barrow and A.A. Mathiew. 1999. Coastal Zone of The Gambia and the Abidjan Region in Côte d'Ivoire: Sea level rise vulnerability, response strategies, and adaptive options. *Climate Research* Vol. 12: 129-136.

James, L.A.W. 1992. Ecological and Economic Change along the Middle Reaches of the Gambia River, 1945-1985. *Africa Affairs* Vol. 91(365): 543-565.

King, M.D., Howat, I.M., Candela, S.G. et al. 2020. Dynamic Ice Loss from the Greenland Ice Sheet Driven by Sustained Glacier Retreat. *Nature Communications Earth and Environment* 1, 1 (2020). doi:10.1038/s43247-020-0001-2.

Lachkar, Z. and N. Gruber. 2013. Response of Biological Production and Air-sea CO₂ Fluxes to Upwelling Intensification in the California and Canary Current Systems. *Journal of Marine Systems* Vol. 109: 149-160.

Laffoley, D. and J.M. Baxter (eds). 2019. *Ocean Deoxygenation: Everyone's Problem – Causes, Impacts, Consequences and Solutions. Full Report*. Gland, Switzerland: International Union of Concerned Scientists.

Large, W.G. and G. Danabasoglu. 2006. Attribution and Impacts of Upper-Ocean Biases in CCSM3. *Journal of Climate* Vol. 19(11): 2325-2346.

Li, G., L. Cheng, J. Zhu, K.E. Trenberth, M.E. Mann and J.P. Abraham. 2020. Increasing Ocean Stratification Over the Past Half-century. *Nature Climate Change*. doi: 10.1038/s41558-020-00918-2.

Loucaides, S., T. Tyrrell, E.P. Archterberg, R. Torres, P.D. Nightingale, V. Kitidis, P. Serret, M. Woodward and C. Robinson. 2012. Biological and Physical Foricng of Carbonate Chemistry in an Upwelling Filament off Northwest Africa: Results from a Lagrangian study. *Global Biogeochemical Cycles* Vol. 26. BG3008. doi:10.2029/2011GB004216.

Mann K.H. and J.R.N. 2006. Dynamics of Marine Ecosystems: Biological-physical Interactions in the Oceans. Oxford: Blackwell Publishing.

NASA (National Aeronautics and Space Administration). 2020. <https://climate.nasa.gov/vital-signs/sea-level/>. (accessed 29/01/2020).

Nijse, J.M.M.F., P.M. Cox and M.S. Williamson. 2020. An Emergent Constraint on Transient Climate Response from Simulated Historical Warming in CMIP6 Models. Earth Systems Dynamics Discussion. <https://doi.org/10.5194/esd-2019-86>, in review, 2020.

NOAA (National Oceanic and Atmospheric Administration). 2017. Global and Regional Sea Level Rise Scenarios for the United States. NOAA Technical Report NOS CO-OPS 083. Silver Springs (MD): NOAA.

NOAA (National Oceanic and Atmospheric Administration). 2020a. Global Land and Sea Surface Temperature Record. https://www.ncdc.noaa.gov/cag/global/time-series/globe/land_ocean/ytd/12/1880-2019. (accessed 29/01/2020).

NOAA (National Oceanic and Atmospheric Administration). 2020b. <https://coast.noaa.gov/hurricanes/>. (accessed 29/01/2020).

Otero, P. et al., 2010. First Toxin Profile of Ciguateric Fish in Madeira Arquipelag (Europe). Analytical Chemistry Vol. 82: 6032-6039.

Pastor, M.V., J.L. Pelegrí, A. Hernández-Guerra, J. Font, J. Salat, and M. Emelianov. 2008 Water and Nutrient Fluxes off Northwest Africa. Continental Shelf Research Vol. 28(7): 915-936.

Pastor, M.V., P. Vélez-Belchi and A. Hernández-Guerra. 2015. Water Masses in the Canary Current Large Marine Ecosystem. In: Oceanographic and Biological Features in the Canary Current Large Marine Ecosystem. Valdés, L. and I. Déniz-González (eds). Technical Series 115. Paris: IOC-UNESCO.

Pauly, D. and V. Christensen. 1995. Primary Production Required to Sustain Global Fisheries. Nature Vol. 374: 255-257.

Pelegrí, J.L. and A. Benazzouz. 2015. Coastal Upwelling off North-West Africa. In: Oceanographic and Biological Features in the Canary Current Large Marine Ecosystem. Valdés, L. and I. Déniz-González (eds). Technical Series 115. Paris: IOC-UNESCO.

Pelegrí, J.L. and J. Peña-Izquierdo. 2015a. Eastern Boundary Currents off North-West Africa. In: Oceanographic and Biological Features in the Canary Current Large Marine Ecosystem. Valdés, L. and I. Déniz-González (eds). Technical Series 115. Paris: IOC-UNESCO.

Pelegrí, J.L. and J. Peña-Izquierdo. 2015b. Inorganic Nutrients and Dissolved Oxygen in the Canary Current Large Marine Ecosystem. In: Oceanographic and Biological Features in the Canary Current Large Marine Ecosystem. Valdés, L. and I. Déniz-González (eds). Technical Series 115. Paris: IOC-UNESCO.

Pérez-Gómez, B., E. Álvarez-Fanjul, M. Marco, B. Puyol and M.J. García. 2015. Sea Level Variability and Trends in the Canary Current Large Marine Ecosystem. In: Oceanographic and Biological Features in the Canary Current Large Marine Ecosystem. Valdés, L. and I. Déniz-González (eds). Technical Series 115. Paris: IOC-UNESCO.

Piatt J.F., J.K. Parrish, H.M. Renner, S.K. Schoen, T.T. Jones, M.L. Arimitsu, et al. 2020. Extreme mortality and reproductive failure of common murrelets resulting from the northeast Pacific marine heatwave of 2014-2016. PLoS ONE 15(1): e0226087. <https://doi.org/10.1371/journal.pone.0226087>

- Pitcher, G.C. and S. Fraga. 2015. Harmful Algal Bloom Events in the Canary Current Large Marine Ecosystem. In: Oceanographic and Biological Features in the Canary Current Large Marine Ecosystem. Valdés, L. and I. Déniz-González (eds). Technical Series 115. Paris: IOC-UNESCO.
- Pitcher, C. and G.S. Jacinto. 2019. Ocean Deoxygenation Links to Harmful Algal Blooms. In: Laffoley, D. and J.M. Baxter (eds). 2019. Ocean Deoxygenation: Everyone's Problem – Causes, Impacts, Consequences and Solutions. Full Report. Gland, Switzerland: International Union of Concerned Scientists.
- Randers, J. and U. Goluke. 2020. An Earth System Model Shows Self-sustaining Melting of Permafrost Even if Man-made GHG Emissions Stop in 2020. *Nature* <https://doi.org/10.1038/s41598-020-75481-z>
- Rykaczewski, R.R. 2018. Changes in Mesozooplankton Size Structure Along a Tropic Gradient in the California Current Ecosystem and Implications for Small Pelagic Fish. *Marine Ecology Progress Series*, doi.org/10.3354/meps12554.
- Sangrá, P. 2015. Canary Island Eddies and Coastal Upwelling Filaments off North-West Africa. In: Oceanographic and Biological Features in the Canary Current Large Marine Ecosystem. Valdés, L. and I. Déniz-González (eds). Technical Series 115. Paris: IOC-UNESCO.
- Santana-Casiano, J.M. and M. González-Dávila. 2015. Ocean Acidification in the Canary Current Large Marine Ecosystem. In: Oceanographic and Biological Features in the Canary Current Large Marine Ecosystem. Valdés, L. and I. Déniz-González (eds). Technical Series 115. Paris: IOC-UNESCO.
- Savenije, H.H.G. and J. Pages. 1992. Hypersalinity: A dramatic change in the hydrology of Sahelian estuaries. *Journal of Hydrology* Vol. 135: 157-174.
- Siegert, M., R.B. Alley, E. Rignot, J. Englander and R. Corell. 2020. Twenty-first Century Sea-level Rise Could Exceed IPCC Projections for Strong-warming Futures. *One Earth* Vol. 3 (6): 691 DOI: [10.1016/j.oneear.2020.11.002](https://doi.org/10.1016/j.oneear.2020.11.002)
- Steffen, W. et al. 2018. Trajectories of the Earth System in the Anthropocene. *Proceedings of the National Academy of Sciences* Vol. 115(33): 8252-8259.
- Stramma, L., P. Brandt, L. Schafstall, F. Schott, J. Fischer and A. Körtzinger. 2008. Oxygen Minimum Zone in the North Atlantic South and East of the Cape Verde Islands. *Journal of Geographical Research* Vol. 113(C4), C04014.
- Tedesco, M. and X. Fettweis, 2020. Unprecedented Atmospheric Conditions (1948-2019) Drive the 2019 Exceptional Melting Season Over the Greenland Ice Sheet. *The Cryosphere* Vol. 14(4): 1209-1223.
- van der Lingen, C.D., L. Hutching and J.G. Field. 2006. Comparative Trophodynamics of Anchovy *Engraulis encrasicolus* and Sardine *Sardinops sagax* in Southern Benguela: Are Species Alternations Between Small Pelagic Fish Trophodynamically Mediated? *African Journal of Marine Sciences* Vol. 28(3&4); 465-477.
- van der Lingen, C.D. et al. 2009. Tropic Dynamics. In: Checkley, D.M., Roy, C., Alheit, J. and Y. Oozeki (eds), *Climate Change and Small Pelagic Fish*. Plymouth (UK): GLOBEC Project Office.
- Vélez-Belchí, P., M. González-Carballo, M.D. Pérez-Hernández and A. Hernández-Guerra. 2015. Open Ocean Temperature and Salinity Trends in the Canary Current Large Marine Ecosystem. In: Oceanographic and Biological Features in the Canary Current Large Marine Ecosystem. Valdés, L. and I. Déniz-González (eds). Technical Series 115. Paris: IOC-UNESCO.

Watson, A.J., U. Schuster, J.D. Shutler, T. Holding, I.G.C. Ashton, P. Landschützer, D.K. Woolf and L. Goddijn-Murphy. 2020. Revised Estimates of Ocean-Atmosphere CO₂ Flux are Consistent with Ocean Carbon Inventory. *Nature Communication*, doi.org/10.1038/s41467-020-18203-3.

WCRP (World Climate Research Program). 2018. Global Sea-level Budget 1993-present. *Earth System Science Data* Vol. 10(3): 1551-1590.

Zelinka, M.D., A.M. Myers, D.T. McCoy, S. Po-Ghedley, P.M. Cadwell, P. Ceppi, S.A. Klein and E. Taylor. 2020. Causes of Higher Climate Sensitivity in CMIP6 Models. *Geophysical Research Letters* Vol. 47(1).

Zeller, D. and D. Pauly. 2015. The Sea Around Us: Area Parameters and Definitions. Accessed 12/10/2020: <http://www.seaaroundus.org/doc/Methods/Area/Methods-EEZ-LMEs-shelf-etc-New-June-11-2015.pdf>.

Zhou, C., M.D. Zelinka, A.E. Dessler and M. Wang. 2021. Greater Committed Warming After Accounting for the Pattern Effect. *Nature Climate Change* <https://doi.org/10.1038/s41558-020-00955-x>

Chapter 5 THE GAMBIA RIVER, MANGROVE ECOSYSTEM and CLIMATE CHANGE IMPACTS

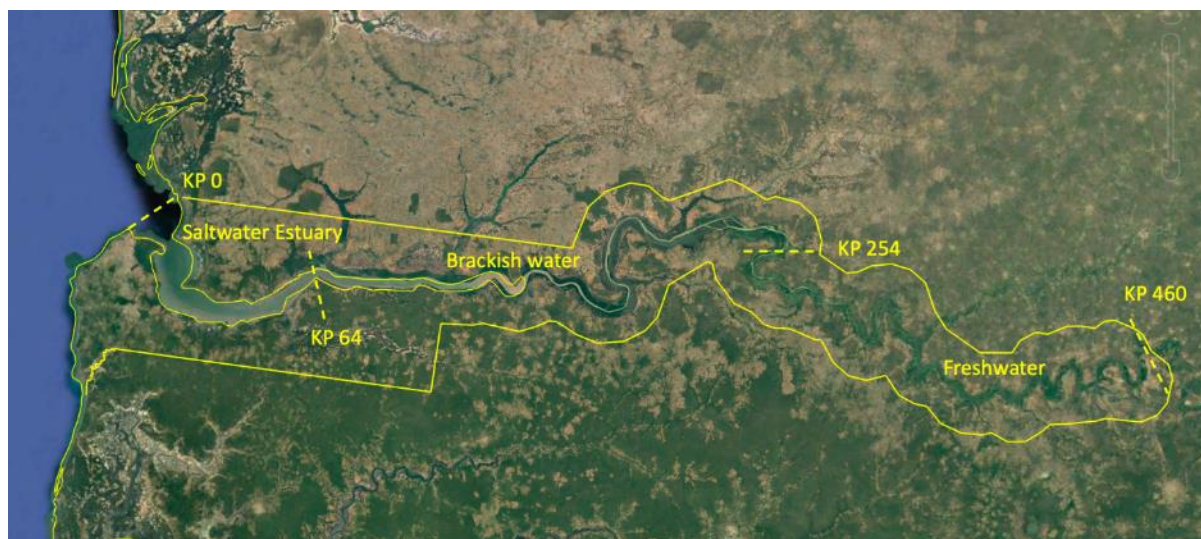
Introduction

40. **The Gambia river transitions through three distinct segments as it descends through the length of the country on its way to the sea.** In the first segment, furthest upstream, the river is entirely freshwater. The extent of the freshwater segment begins at the upstream border with Senegal at Kilometer Point (KP) 460 to a point downstream approximately at Kuntaur (KP254), the historical average maximum extent of annual saltwater intrusion.

41. The next segment alternates between freshwater and saline and is demarcated by the maximal extent and retreat of saltwater intrusion into the river, as determined by the position of the 1-part-per-thousand (ppt) saline front, with increasing levels of salinity on the downstream side of the front. The position of the saline front, and its movement, reflect the annual cycle of dry and rainy seasons, and the amount of rainfall received within the watershed during the wet period. This segment, referred to as brackish in this analysis, begins at or around KP254, reaching above KP300 during exceptionally dry periods, and descends to a point downstream, KP64, traditionally used to demarcate the extent of permanent seawater intrusion (Risley et al., 1993).

42. The final segment is that of the permanent saltwater estuary beginning at Kemoto (KP64; KP100 is alternatively referenced as the extent of permanent seawater) and extending to the river mouth and the open ocean at KP 0 (see Figure 5-1).

Figure 5-1 Relative locations of River segments based on salinity



Source: FAO analysis on Google Earth map

43. **The mangrove ecosystem is found throughout the saltwater estuary and brackish portions of the river.**⁷⁷ The mangroves are home to a great diversity of residential fish and aquatic species, and

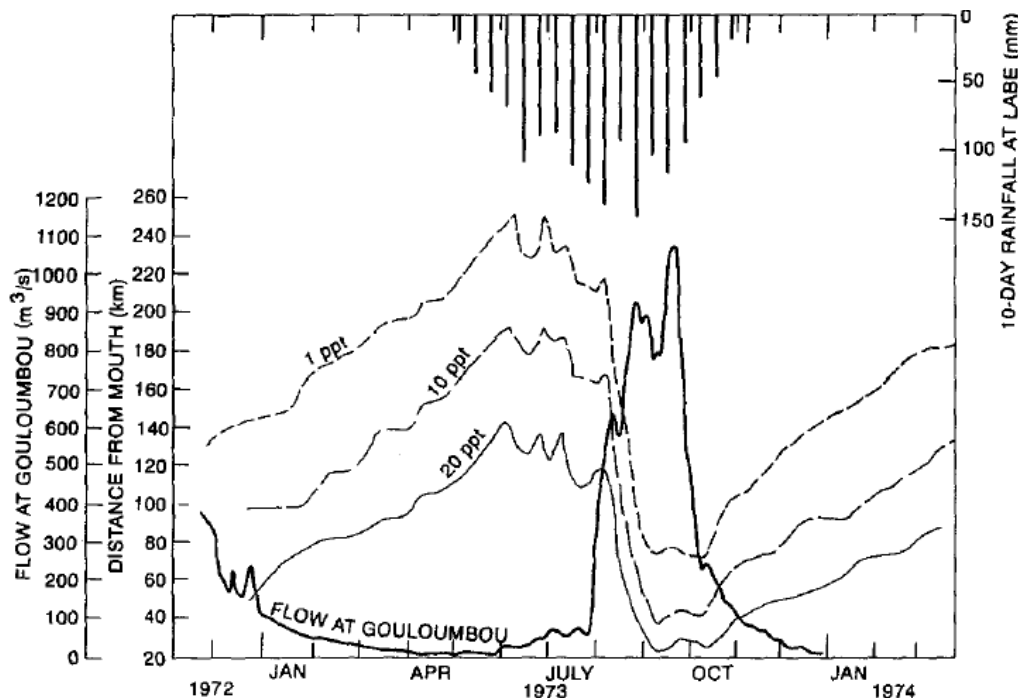
⁷⁷ A mangrove is a tree or shrub which grows in tidal, chiefly tropical, coastal swamps and estuaries, having numerous tangled roots that grow above ground and form dense thickets. The latter function as spawning grounds and nurseries for many fish and other aquatic species. The term mangrove is also used for the vegetation consisting of such trees and shrubs.

support an even larger number of species who are transitory, residing in the mangroves for a portion of their lifecycle, often during their reproductive or early developmental stages, while still other species depend on the productivity of the mangrove as the base of their food chain.⁷⁸ The tree species composition of the mangroves varies along the river, and with it the associated communities of organisms. Species distribution is influenced by the hydrologic regime, both in terms of water depth and salinity. These diverse mangrove communities in turn shape the immediate environment and water quality in the river more broadly.

The Gambia River and Estuarine Environment

44. **Hydrology of the Gambia River.** The Gambia River saltwater and brackish estuary, and estuarine ecosystems in general, are predominantly shaped by the annual hydrologic cycles of the watershed and by daily tidal movements. Discharge from the Gambia River watershed typically reaches its maximum in September with the flow decreasing progressively until the end of the dry period and start of the subsequent rainy season, generally in May. Roughly half of the river's volume as it enters The Gambia originates in the Guinea highlands, while the remainder is added from rainfall occurring in the portion of the watershed located elsewhere in Senegal (ISL, 2014). It is estimated that less than 10 percent of the river's flow (Risley, 1987) comes from rainfall occurring within The Gambia's borders. The river's outward flow of freshwater keeps the intrusion of saltwater from reaching further inland. The relative dynamics of the timing of rainfall, river flow downstream and positioning of the saline front are shown in Figure 5-2.

Figure 5-2 Rainfall at Labe, Guinea, River Flow at Gouloumbou, Senegal (KP492), and position of the 1-ppt Salinity front within The Gambia (year 1973)



Source: Risley et al., 1993

⁷⁸ See: Blader, 2013; White et al., 2012; Louca et al., 2009; DeGeorge and Reilly, 2007; Manson et al., 2005; Albaret et al., 2004; Panfili et al., 2004; Vidy et al., 2004.

45. Throughout the year the diurnal tide heights at the river mouth (KP 0) vary from 0.9 m to 1.6 m, with maximal spring tides exceeding 2 m (ISL, 2014). Tidal surges are felt the entirety of the river's 460 km length within the country, with recorded tide heights of 1 m at Basang, 310 km upstream, and tides of 10 – 30 cm extending beyond the border with Senegal to Gouloumbou (KP 492)(ISL, 2014). The resulting variation in daily and annual flood depth and concentration of salinity at different points in the river estuary influence the extent and dominance of herbaceous species along the shore and the associated communities of aquatic and terrestrial species.

46. The Gambia River has a catchment area of 77,000 km², spread across The Gambia (14 percent), Senegal (71 percent) and Guinea (15 percent) (ISL, 2014). From its origins in the Fouta Djallon plateau, the river flows 1,150 km to sea at Banjul. In its final portion, the Gambia River is nearly flat, its most distinct characteristic, falling a mere 57 cm over the last 500 km (ibid). In addition to tidal surges felt across the entirety of this flat topography, the river's hydrology is driven by the short monomodal rainy season in the upper watershed, resulting in one of the most widely variable salinity regimes in the world with saltwater penetrating nearly 200 km upstream (from KP64 to KP254) into the river during the dry season each year (Ceesay et al., 2017). The rainy season in the watershed occurs from May through October with the highest precipitation received in August. Peak river discharge occurs in September and declines rapidly with little discharge from January to the beginning of July (Albaret et al., 2004). The outflow of the Gambia River is influenced by the morphology of the river's large mouth, flat topography, rainfall intensity and timing upstream, sea level and evaporation. This natural equilibrium is being increasingly altered through human activities, particularly the abstraction of water for irrigation and, in the near future, the anticipated completion and operation of the Sambangalou dam in Senegal.

47. **Water chemistry and quality characteristics of the Gambia River.** For aquatic species, individual species niches are most strongly associated with characteristics of water quality and chemistry. Withing the floodplains the water quality factors most strongly associated with species preferred habitat are salinity, water depth, vegetative cover and pH (Louca et al., 2009), with dissolved oxygen and temperature exerting a critical overall influence. In the river's main channel, salinity, temperature, turbidity, depth, strength of the current and dissolved oxygen have been identified as critical factors (Albaret et al., 2004). In addition to those parameters directly associated with species habitat, other water quality variables are essential for supporting the food chain upon which riverine species depend (e.g., phosphate, nitrogen, silica). Most variables are influenced by the seasonal variations in river flow (e.g., salinity, temperature, dissolved oxygen, pH, turbidity), while others are directly or indirectly associated with the tidal surge (water depth, strength of the current, vegetative cover).

48. The water in the Gambia River is high in reactive phosphate in the lower part of the estuary, due to tidal mixing and the resuspension of river-borne organic waste products. The concentration of nitrates, carried downstream, ranges from 7.7 to 54 µg/L from the beginning to the end of the flood season. The Gambia River also carries down Silica, which is needed for diatoms development, in high concentrations (Binet et al., 1995). Together, phosphorus, nitrogen and silica are essential for phytoplankton growth and are responsible for the high phytoplankton productivity within the river estuary and in areas immediately offshore, which in turn supports key fisheries.

49. Seasonal flooding into the upper reaches of the “bolong” (shifting river channels) during the rainy season has been observed to coincide with a drop in river acidity (pH). This annual dip in pH results from the flushing of iron sulphates that accumulate in the mangrove soils. The regular removal of sulphates maintains mangrove soil health and is associated with the annual shifting in species richness and biomass within the floodplain environment (Louca et al., 2009).

50. There are important annual fluctuations in the movement of floodwater and the presence of suspended particles, influencing water transparency in the Gambia Estuary. The latter ranges from 0.1 m to 1.8 m with an overall mean of 0.6 m. During the wet season, transparency decreases rapidly to 0.2 m starting at KP20 and remains low upstream. During the dry season, with decreased streamflow, higher transparency is observed in the upper river (Albaret et al., 2004). The transparency of water in the estuary determines the relative exposure of larvae and juveniles of key fisheries species to predators. The period of lowest transparency corresponds with the main breeding period of many key species (Manson et al., 2005; Louca et al., 2009; Panifili et al., 2004).

51. River salinity, while generally well mixed within the water column, shows a wide range in temporal and geographical variation. During the dry season (ending annually in May), and periods of drought, the salinity front reaches and may exceed KP254 upstream, at Kuntaur, while being pushed back as far as KP64, at Kemoto, during the peak of rainy season discharge. Savenije and Pagès (1992) describe the similarities between the Casamance and Gambia Rivers in terms of their hydrologic characteristics, and the potential for the latter experiencing a hypersaline disaster similar to what occurred in the Casamance. The Casamance river became hypersaline during the early 1980s, with saline levels exceeding 100 ppt within the river estuary resulting in the death of most river life. Similarities between the two rivers suggest the potential of the same fate for the Gambia River should a minimum water outflow not be maintained. In fact, during the dry season, and periods of drought, salinity levels in the upper reaches of some of the bolong exceed that of seawater (Ceesay et al., 2017). Due to the importance of the issue, a specific study on the positioning of the saline front under future weather conditions, sea level rise and water management regimes, and the risk of a hypersaline disaster, was commissioned in preparation for this proposal, the results of which are presented in detail in the following chapter.

52. As with salinity, river water temperature is also well mixed, differing less than 1°C between surface and river bottom. The mean surface temperature is 27.4°C, with a mean bottom temperature of 26.9°C. There is, however, a significant longitudinal gradient maintained throughout the year with higher temperatures occurring upstream in the river. Sea water intrusion plays an important role in cooling the river's freshwater discharge, regulating water temperature. During the flood period, in summer and early autumn, water temperatures in the river vary from 28°C downstream to 30°C upstream. At this time of year, seawater intrudes least and is at its warmest (approximately 24.5°C), while during the dry season, seawater intrudes most and is at its coldest (approximately 20.5°C), resulting in river temperatures that vary from 24°C downstream to 26°C upstream (Albaret et al., 2004; Vélez-Belchí et al., 2015).

53. Dissolved oxygen levels in the river are generally non-limiting for the growth and development of aquatic organisms. Oxygen saturation ranges from a low of 60 percent in September at the peak of the flood, when biological activity is at its highest, rising to 95 percent by the end of the dry season (April). A minimum of 20% oxygen saturation is needed to allow biological development in the River (Albaret et al., 2004), a level that is maintained within the river throughout the year.

Estuarine Ecology and Mangrove Ecosystem

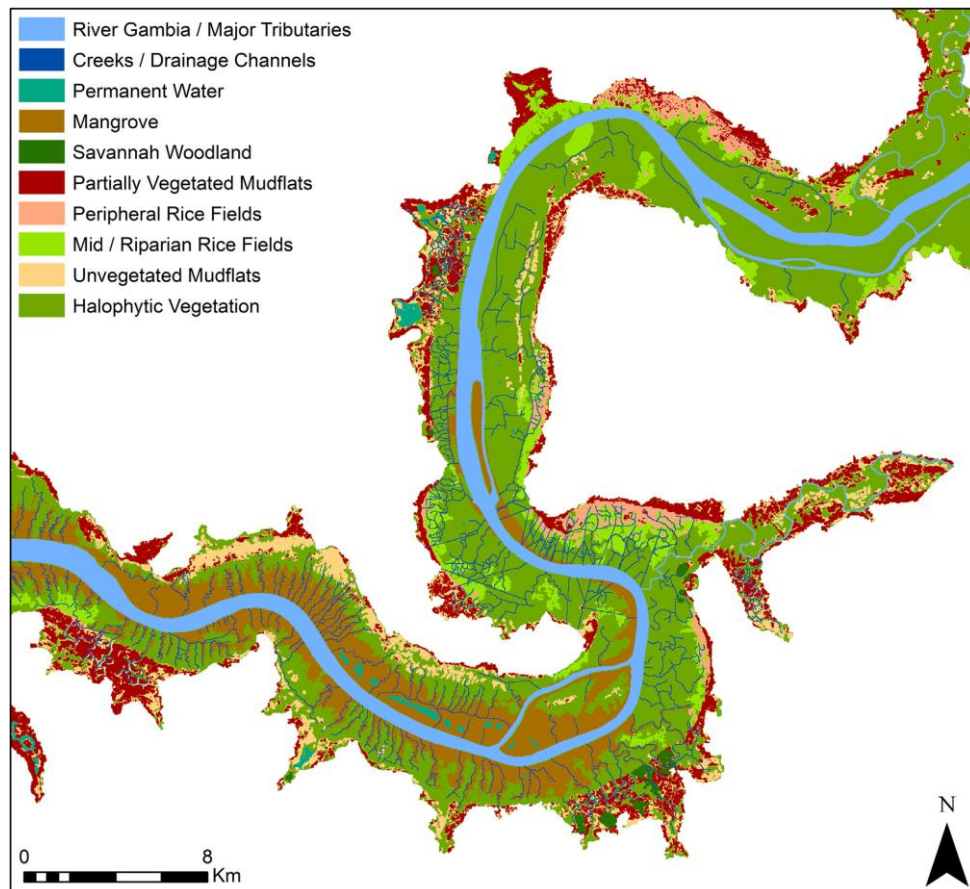
54. The estuarine ecology is characterized by its high primary productivity driven by two complementary sources of nutrient supply emanating from the water bodies feeding the system. River flooding carries with it organic material washed down from upstream and from along the river bank (Binet et al., 1995). Mangrove roots and accumulated debris catch up to 80% of the sediment flow (Krauss et al., 2014). These sediments, and the addition of mangrove leaf litter and wood residues, are fed upon by herbivores, especially crabs, considered as the “architects” of the mangrove, detritivores and bacteria. The decomposition and release of nutrients from this material in turn feeds the development of phytoplankton blooms (Binet et al., 1995), which form the base of the mangrove estuary food chain (Saifullah et al., 2015). As flood waters recede through the dry season, seasonal upwelling events along the coast, most common during the winter months, are carried further upstream into the estuary bringing nutrients from the oceanic side, as well as populations of zooplankton which had been limited by river outflow during the rainy season. Zooplankton feed on the rich concentration of riverine phytoplankton, forming the second level of the estuarine food chain. This seasonal shift in nutrient source and plankton populations drives the foodchain and overall productivity of the River’s mangrove ecosystem.

55. The physical extent of the mangrove ecosystem is shaped by three boundaries – terrestrial, water depth and water quality (salinity levels) – that are driven by the natural rhythm of tidal inundation, varying salinity levels and shifting sediments. Seasonal flooding and daily tides influence the diversity of the herbaceous landscape more than 2 km inland from each riverbank. Due to the dynamic nature of the mangrove environment the notion of river course and bank are relative, being comprised of a permanent river channel, seasonally inundated areas, networks of creeks and drainage channels (bolong), permanent water pools, associated mangrove areas and halophyte communities and unvegetated mudflats (Ettritch et al., 2018) (see Figure 5-3).

56. **The current extent of the mangrove vegetation in The Gambia is estimated at approximately 35,700 ha (GoTG, 2010).**⁷⁹ The Tanbi wetlands, located near the River’s mouth, contain the largest concentration of mangrove in the country, over 4,100 ha (Ceasay et al., 2019). Across its range, two principal mangrove sub-systems are distinguished, fringe mangroves and the riverine mangroves. The fringe mangrove sub-system is found along the coast with direct exposure to open ocean and storms, providing protection against coastal erosion. This system is concentrated in the Niumi National Park on the Northern side of the river, and the Tanji Bird Reserve to the South, whereas most of The Gambia’s coastline is open, unprotected and subjected to erosion (McLeod and Salm, 2006). The riverine mangrove sub-system includes areas found along both sides of the river from the mouth up to the border with Senegal 460 km upstream (Lee et al., 2009). Other major riverine mangrove sections include those in the secondary tidal canals, known locally as bolongs. The Mandina, Jaleh Cassa, Bulok, Brefet, Payama and Bitang bolongs are the principal bolongs located on the Southern riverbank, while the Sami, Surrunku, Tabirereh, Tambana, Mini Minium and Kerewan bolongs are found on the Northern riverbank. The riverine mangroves are the most productive due to the high concentration of nutrients, dissolved oxygen and sediments found in the river (McLeod and Salm, 2006).

⁷⁹ The National Forest Assessments of 1981/82 and 1997/98 reported 66,900 ha and 58,800 ha of mangrove respectively (GoTG, 2010). The 2009/10 Assessment found that mangrove forest cover had declined by 47 percent since 1983, representing 73 percent of all forest loss in the country (GoTG, 2010).

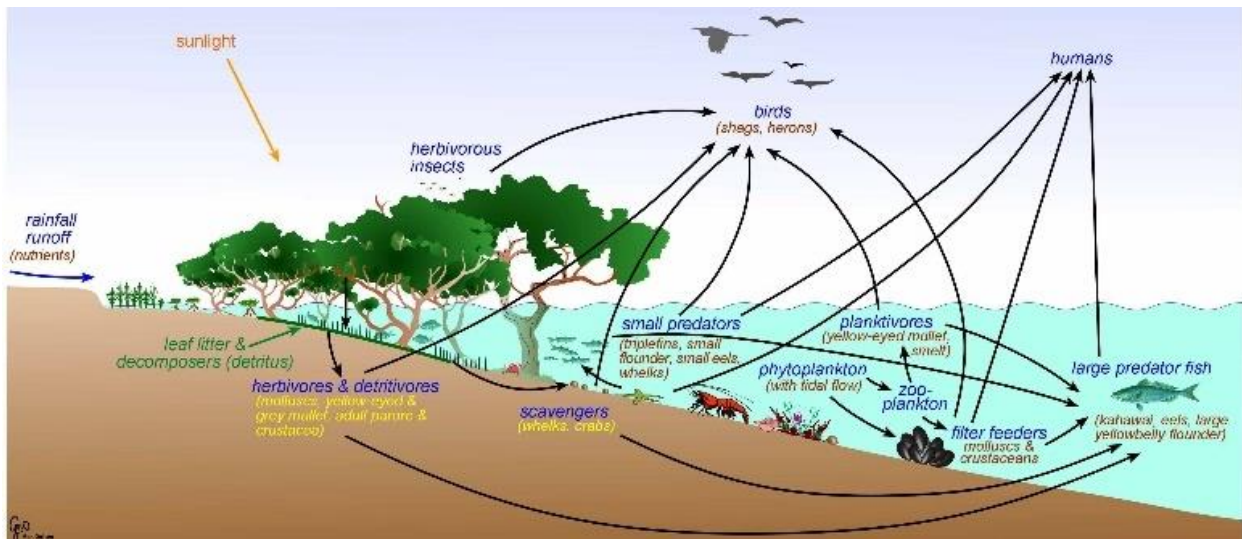
Figure 5-3 Land cover classification based on the multi-temporal analysis of Landsat imagery (1986–2016) at upper Balingho



Source: Ettritch et al., 2018

57. The roots of riverine mangrove trees (esp. *Rhizophora* spp.) are especially important in providing suitable habitat for the larvae of aquatic species and juveniles, through direct protection, leaf shade and important seasonal variations in water quality. The annual retreat downstream of the salinity front during the seasonal flooding, for example, serves as a barrier for saltwater predators, while the increased turbidity of flood waters and low light penetration within the mangroves limit predators' opportunities at a time of year when many species are spawning (Albaret et al., 2004). For terrestrial fauna, including avifauna, mangrove is also an important habitat due to prolific sources of food and low human presence (see Figure 5-4).

Figure 5-4 Mangroves ecosystem interactions

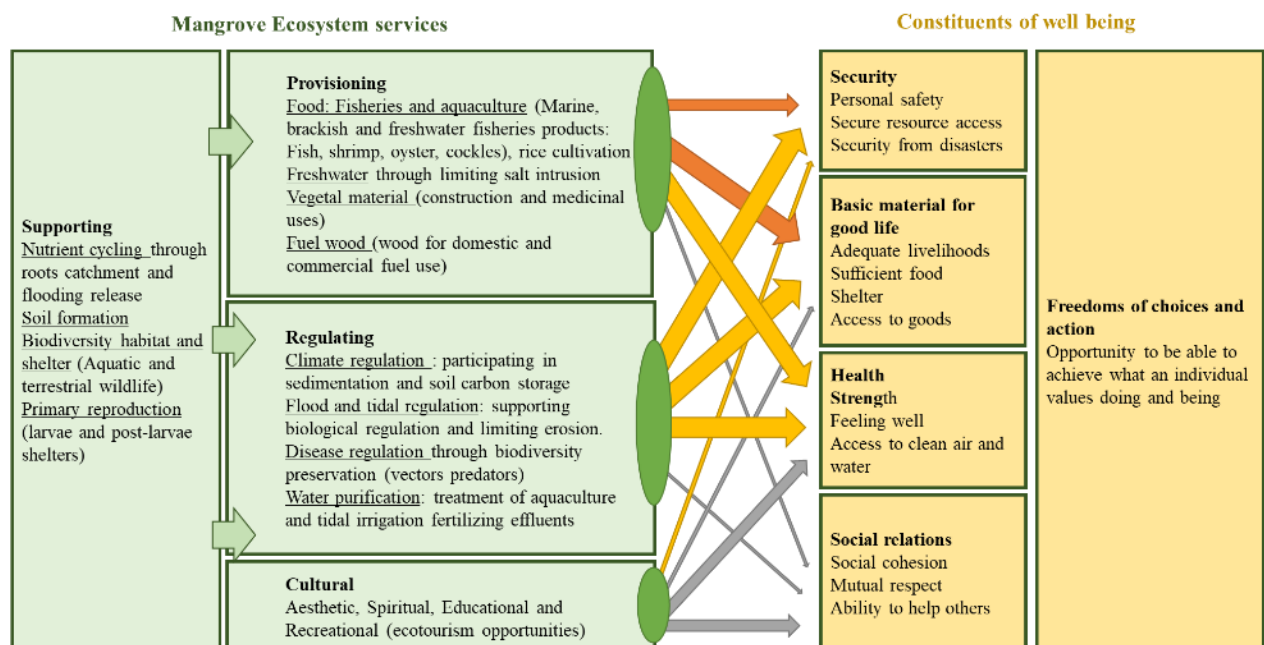


Source: Christy Ramsey

Mangrove Ecosystems Services

58. By supporting nutrient cycling, soil formation, biodiversity habitat and food chain productivity, mangroves serve as shelters, spawning grounds and feeding zones for both residential and migratory aquatic and terrestrial species. As such, birds, mammals, and more than 3,000 aquatic species are found in mangrove systems that provide a wide range of ecosystem services.

Figure 5-5 Ecosystem services assessment of the Gambian mangroves based on Millennium ecosystem assessment (2005)



59. **Provisioning services.** The most valuable fisheries for local communities are found in and depend on the mangrove ecology, for example the pink shrimp (*Peneaus notialis*), bonga shad

(*Ethmolosa fimbriata*), mangrove oyster (*Crassostrea gasar*) and cockles (*Anadara senilis*), among other marine and brackish water species. Most shrimp aquaculture in the tropics depends on wild-harvested fry.

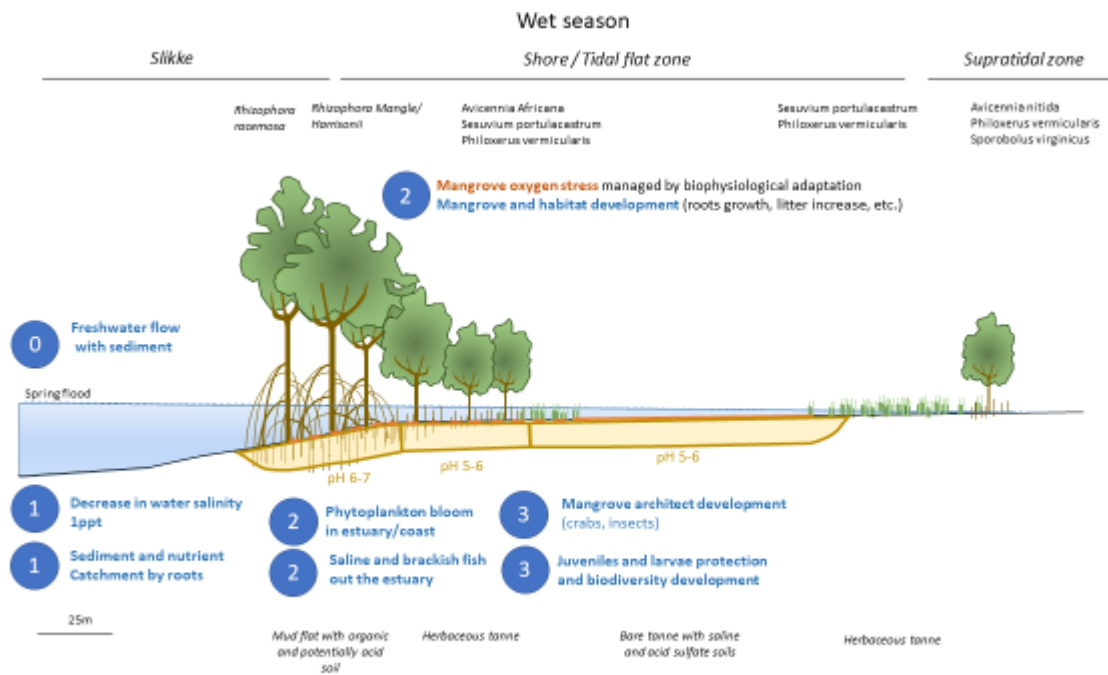
60. **Regulating services.** Mangroves help mitigate climate change through carbon sequestration, with a per hectare carbon storage potential of 3 to 5 times that of tropical dry forests, especially soil storage (Donato et al., 2011). Mangroves can also help to mitigate the effects of flood and tidal events by increasing soil height and limiting shore and riverbank erosion through trapping sediment as water levels rise. Mangroves have been found to be 5 times more effective than other barriers, such as breakwaters, in protecting coastlines (e.g., Narayan et al., 2016). Mangroves also provide water filtration and purification functions, especially for aquaculture effluents, where 2-5 ha mangroves were able to treat the effluence from 1 ha of aquaculture production (Primavera et al., 2007).

Gambian Mangrove Ecosystem Composition

61. The flora of the mangrove ecosystem is composed of mangrove tree and shrub species and other halophytes. Species are located along two gradients, from fresh to saltwater (from up to downstream) and water depth, from the riverside inland. Along these gradients, mangrove faces two main sources of stress: water stress, due to their exposure to saline waters, and oxygen stress due to waterlogged soil. The various mangrove species have different biophysiological adaptations and tolerance levels to salinity and flooding. According to their anatomic features, they adapt to anaerobic conditions in waterlogged soil through creating a vertical oxygen transport through their woody tissue, and, varying by species, they adapt to salinity through three strategies: salt exclusion, excretion and accumulation (Parida, 2010).

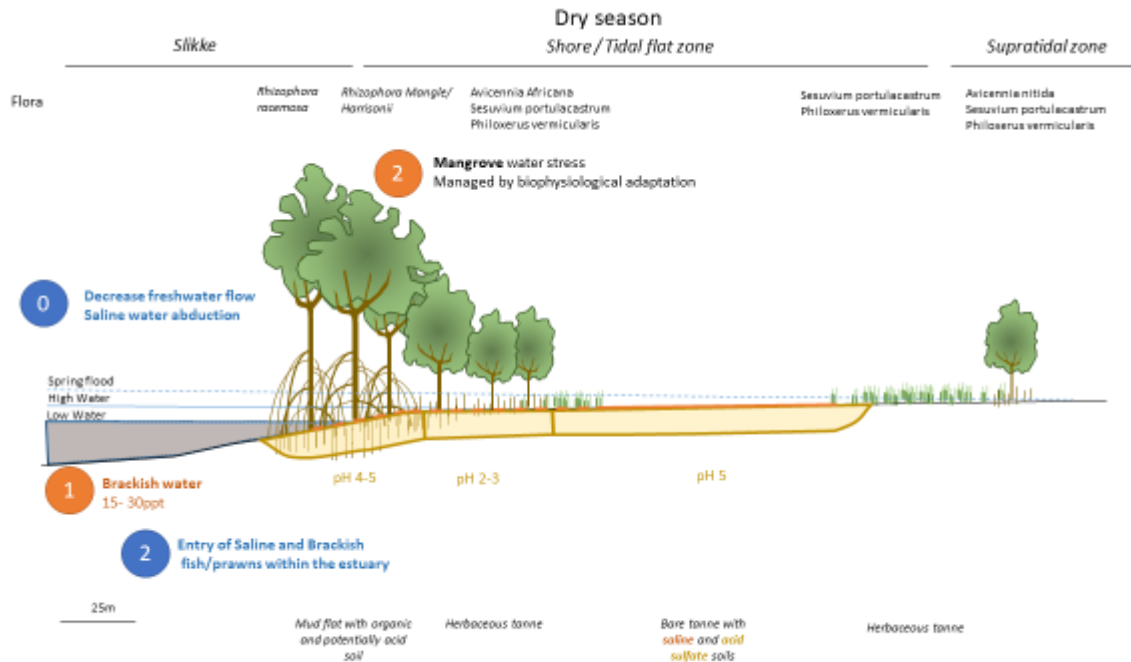
62. **Mangrove flora and tolerances.** In the Gambia, due to the high salinity, fewer mangrove species are found than in other estuarine environments, with 7 major mangrove species reported (Lee et al., 2009). The riverine mangrove sub-system is composed of a mangrove succession that begins within the tidal zone (estuarine slikke). Here, mangroves reach the height of 7 meters or more and are dominated by *Rhizophora racemosa* in locations within its salinity tolerance. At the high tidal line, *Rhizophora harrisonii* and *Rhizophora mangle* are the dominant species, which, in association with *Avicennia africana*, form a closed woodland. Further inland, above the tidal line, *Avicennia africana* becomes the sole species remaining with the mangrove height decreasing to below 7 meters. Along the flat tidal flood areas, acidic sulphate tanne and hypersaline soils prevent mangroves from developing, with herbaceous development constrained to the edges of the bare salty and acidic tanne. At higher elevations, above the tanne, mangrove trees (*Avicennia nitida*) reappear (Claude, 1985; Diop et al., 2002). A general profile of the mangrove environment and associated features, during the wet and dry seasons, is presented in Figure 5-6 and Figure 5-7 below.

Figure 5-6 Mangrove profile within the estuary during the flood period (September)



Source: Diop et al., 2002

Figure 5-7 Mangrove profile within the estuary at the end of the dry period (May-June)



Source: Diop et al., 2002

63. Mangroves in the fringe sub-system along the coast, such as the Niimi national park, have a similar profile and slightly more diverse species composition, including: *Rhizophora mangle*, *Rhizophora harrisonii*, *Rhizophora racemosa*, *Laguncularia racemosa*, *Avicennia germinans* and *Avicennia africana*. Here too, the profile gradient of mangrove species is influenced by the extent of tidal flooding. Red mangroves (*Rhizophora mangle*) are the most tolerant, withstanding flooding 50-70 percent of the year, while black mangrove (*Avicennia germinans*) and white mangrove (*Laguncularia racemosa*) are less tolerant to flooding duration (<50 percent) (McLeod and Salm, 2006). These species-specific tolerances and niche requirements underscore the point that the various mangrove species do not offer one-to-one replacement options, and in turn provide suitable environments for varying communities of associated organisms.

64. **Mangrove fauna and tolerances.** The flora of the mangrove ecosystem serves as the base of the estuary food chain and as an important breeding ground and nursery area for the larvae and juveniles for many species (e.g., Diop et al., 2002), each with their own requirements and tolerances to physical parameters. In addition to the more than 30 species of fish that directly and indirectly depend on the mangrove ecosystem (Louca et al., 2009; DeGeorges and Reilly, 2007; Viday et al., 2004; Albaret et al., 2004) (see assessment presented in Chapter 7), the mangrove habitat is home to cockles (*Anadara senilis*) and others gastropods (e.g., *Murex* spp and *Cymbium* spp.), shrimp (*Macrobrachium vollenhovenii*, *Penaeus notialis*) and crab (*Callinectes amnicola*) and many other species. The Mangrove Oyster (*Crassostrea gasar/tulipa*), for example, attaches itself to roots and branches of mangroves in the intertidal zone and is resistant to a broad range of salinity levels from 5 ppt to 50 ppt, with higher survival and growth rates around 25 ppt (Gosling, 2015). Survival rates under 5 ppt and over 50ppt are low, making oysters highly sensitive to changes in the hydrologic regime involving freshwater and hypersaline water events (Funo et al., 2015). Gonad development and reproduction of oysters peak when seawater temperature increases close to 30 °C and salinity declines to 24 ppt (Gomes et al., 2014; Diadhiou, 1995), corresponding to the flooding period in September. Cockles, in contrast, are found in the mud in the intertidal area in-between mangroves roots, with densities reaching several hundred cockles per square meter. A general decline in their populations, however, has been observed, with local communities noting the impact of rainfall on cockle production (Descamps, 1991). Tidal variation and dry periods decrease both oysters' and cockles' exposure to predation (Jaiteh and Sarr, 2011). Based on individual species' environmental requirements, Chapter 7 takes up a detailed assessment of the current and likely future impacts of climate change on key species in the different fisheries.

65. It is important to note that in addition to the aquatic species, the Gambian mangrove environment is also home to a high diversity of wildlife, some rare, including large marine mammals, such as the dolphin (*Soussa teuszii*), manatee (*Trichechus senegalensis*), clawless otter (*Aonyx capensis*) and hippopotamus (*Hippopotamus amphibius*), reptiles such as crocodiles (*Crocodylus niloticus*) and turtles (*Kinixys belliana*), antelopes (*Tragelaphus scriptus scriptus* and *Tragelaphus spekei*), small terrestrial mammals such as monkeys (*Cercopithecus aethiops*) and honey badger (*Mellivora capensis*), and avifauna of international importance, with more than 362 species identified (Diop et al., 2002; Lee et al., 2009).

Climate Change Impact

66. **Historical changes to the mangrove environment.** The changing extent of mangrove forest cover in The Gambia has been the focus of several investigations. Except for the earlier National Forest Assessments, carried out in 1981/82 and 1997/98 where aerial photography and ground surveys were used (GoTG, 2010), more recent estimates of mangrove cover have been derived through remote sensing using various sources of data and analytic techniques (e.g., Corcoran et al., 2007; Spalding et al., 2010; Fent et al., 2019). These studies, and those of the National Forest Assessments, have reached widely different conclusions (see Figure 5-8). For the preparation of this proposal, basic statistics from the National Forest Assessments will be used due to their primary reliance on ground-based data, supplemented by findings from specialized change detection studies not benefiting from ground-truthing (e.g., Fent et al., 2019).

Figure 5-8 Estimates of Mangrove extent (km²) by year and source

	GoTG, 2010	Corcoran et al., 2007	Spalding et al., 2010	Fent et al., 2019
1980		704		
1981/82	669			
1988				574
1997/98	588			
1999				699
2006		581		
2009/10	357		581	722
2018				868

67. The most recent National Forest Assessment conducted in 2009/10, using remote sensing data (Aster 15 m resolution) and extensive ground surveys, shows a 47 percent decline in mangrove forest cover since the 1981-82 Assessment, representing 73 percent of all forest loss in the country over this time period. Change in the extent of mangrove cover, however, is not unidirectional. The most recent analysis of mangrove surface area (Fent et al., 2019), using 30m resolution Landsat imagery, indicates significant changes in mangrove extent over the 30-year period from 1988 to 2018, with evidence of mangrove re-establishment occurring upstream within the bolong and along areas of the riverside (Figure 5-9). In contrast, a decadal view from the middle of this 30-year period, 1999 to 2009, shows evidence of mangrove loss, likely due to short-term droughts and human pressures (Figure 5-10).

68. The dynamic expansion and contraction of mangrove forested area reflects the relative sensitivity of the mangrove environment to changes in hydrology and salinity. The Gambia River watershed, as across the Sahel, has experienced tremendous changes in the rainfall regime over the past fifty years. Following an unusually wet period, during the 1950s and 60s, the subregion was stricken by a devastating drought beginning in most locations in 1968-70 (see Figure 5-11). Over the ensuing three decades, rainfall levels declined by 20-25 percent, and stayed there. Stream gauge measurement at Gouloumbou, Senegal, where the river enters The Gambia, recorded a 35 percent

decline in average streamflow from 1953 – 1970 to 1970 – 2001 (GoTG, 2015). The precipitation in the most recent decade in the record shows a return in roughly half of the years with rain levels above the long-term average, yet with a high degree of interannual variability. A detailed study of the fringe sub-system mangrove community in the Tanbi Wetland National Park found an increasing aged population (>60 years), dating roughly to the downturn in sub-regional fall in 1970, with little evidence of rejuvenation, exhibited by low seedling survival, stunting and dwarfism, attributed to the enduring, unstable hydrologic conditions of more recent decades (Ceesay et al., 2017).

Figure 5-9 Major recovery of the mangrove between 1988-2018 upstream bolong and upland, based on (Fent et al., 2019)

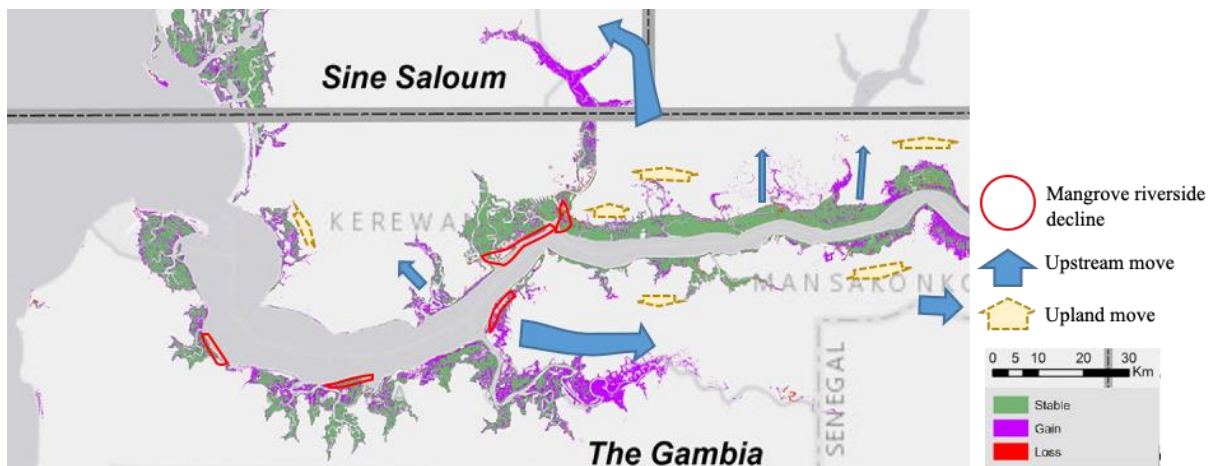


Figure 5-10 Mangrove dynamics between 1999-2009 and drought impact on upstream mangroves and upland mangroves, based on (Ashley Fent, 2019)

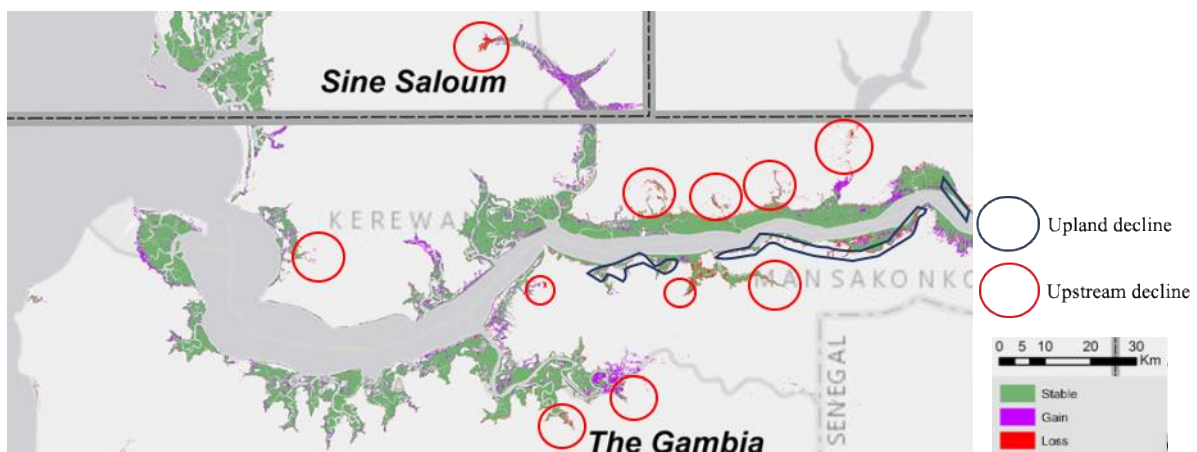
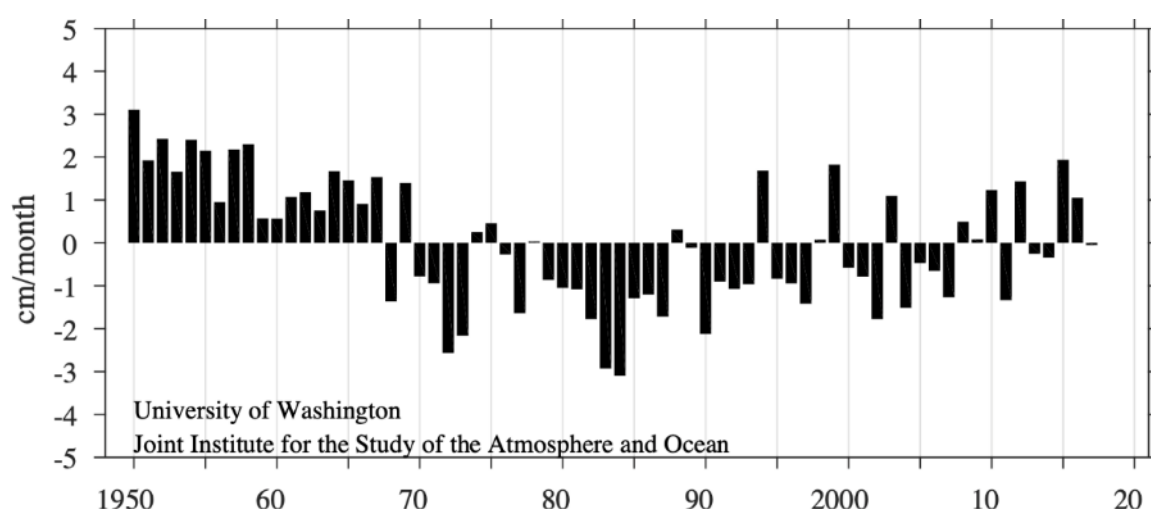


Figure 5-11 Sahelian annual precipitation anomalies 1950-2017



Source: University of Washington Joint Institute for the Study of Atmosphere and Ocean⁸⁰

69. The future extent and condition of mangrove forest cover will depend on a number of factors, including the pace of sea level rise, future trends in rainfall within the watershed, the multiple effects of temperature increase, as well as the success of preservation efforts, mangrove restoration initiatives, and a decrease in the cross-border wood trade (Fent et al., 2019; Carney J., 2014). The profile of potential mangrove expansion fits quasi perfectly with the mapping of inundated areas resulting from 1 m of sea level rise (Jaiteh and Sarr, 2011). Such observations underline the adaptive capacities for mangrove to move upstream along the river and bolongs. No data are available, however, on the potential for changes in the proportions of mangrove forest species between upland *Avicennia* spp and lowland *Rhizophora* spp, in response to changing abiotic conditions.

70. **Sea level rise.** A 1 m rise in sea level would submerge about 8 percent of The Gambia's land area, including 61 percent of the current mangroves, and 33 percent of swamps (Jaiteh and Sarr, 2011; Jallow et al., 1999). Mangroves can adapt to sea level rise in two ways: (i) by vertical gain or (ii) through horizontal expansion inland. The mechanics of vertical adaptation are based on mangrove's capacity to trap sediment in the root zone, especially *Rhizophora* spp. (Kathiresan, 2003), the accretion of organic matter with low decomposition rates and benthic mat development. Nevertheless, if the rate of sea level rise exceeds that of sedimentation and soil elevation increase, the flooding of air lenticels in mangrove roots will lead to oxygen stress, root die-off and subsurface root decomposition, resulting in soil compaction and a reduction in sediment retention in a positive feedback loop of system degradation.

71. In the riverine mangrove sub-system, soil surface levels can increase up to 6 mm/yr (Ken W. Krauss, 2014) suggesting a potential for vertical adaptation that would keep pace with current rates of sea level rise of +4.5 mm/yr (Pérez-Gómez et al., 2015). This assumes, however, that sediment loads and transport within the river are maintained and that the mangroves do not come under additional stresses that would interfere with their normal growth. For the Gambia river, a decrease in sediment transport resulting from the construction of the Sambagalou dam is highly likely, as is the increase in

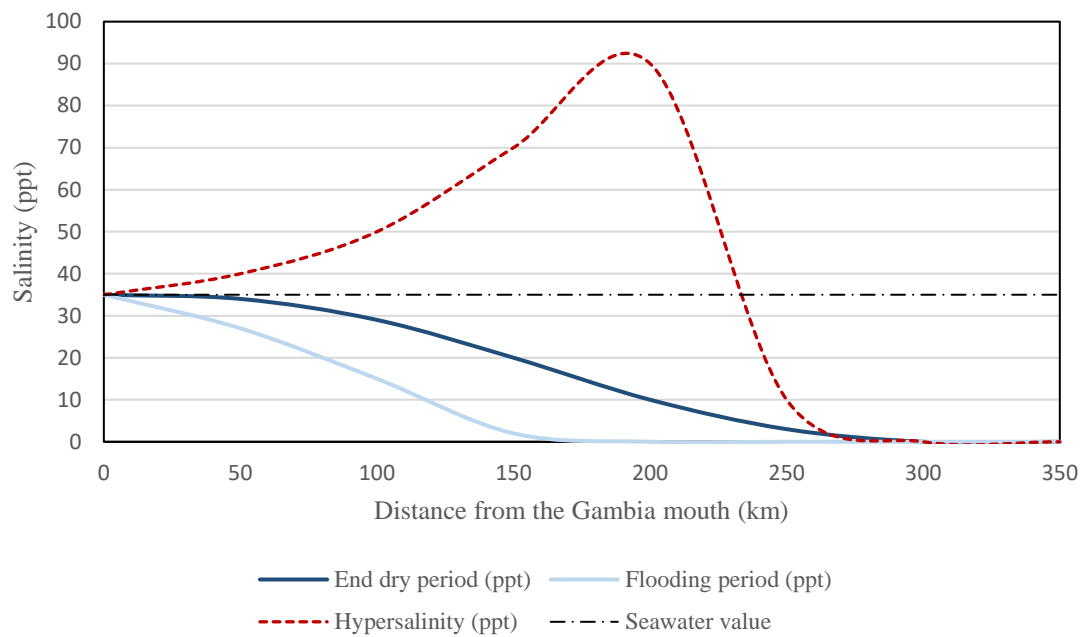
⁸⁰ http://research.jisao.washington.edu/data_sets/sahel/, doi: 10.6069/H5MW2F2Q, accessed 1/09/2020.

air and water temperatures and salinity levels due to climate change, thus placing the mangrove under biological stress, and limiting their ability to continue to adapt to sea level rise through vertical growth. The anticipated increase in the rate of sea level rise, reaching 15 mm/yr by 2100 (IPCC, 2019a), indicates that at some point, regardless as to the health status of the mangrove, the rate of sea level rise will exceed the mangrove's capacity for vertical adaptation.

72. Alternatively, mangroves might potentially adapt to sea level rise through horizontal expansion, landward, as well as movement upstream/downstream in response to changes in salinity levels if local conditions, such as soil, infrastructure and topographical features do not block their expansion. The vegetative succession of mangrove species place *Rhizophora racemosa* and mangle as pioneers, occupying the most inundated locations. Their expansion towards higher ground inland, with a potential movement of 1 m per decade, would in most locations be constrained by the presence of *Avicennia* (Semeniuk, 1994). *Avicennia* expansion in turn, would be limited by inland areas of barre tanne, with saline and acid sulfate soils. The possible expansion through propagule recruitment is another mechanism through which mangrove might adapt to sea level rise, although studies indicate that higher salinity levels and periods of hyper-salinity inhibit successful mangrove colonization through propagule establishment (Ceesay, et al., 2017).

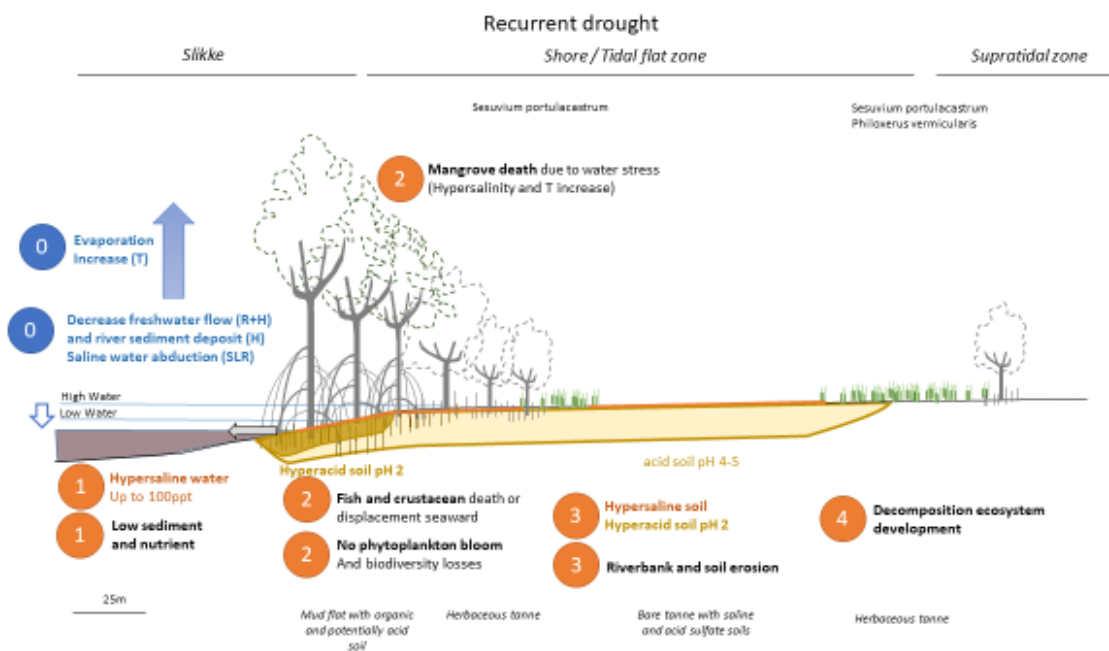
73. **Salinity change.** The convergence and combined influence of multiple forces determine the location and relative salinity level within the river at any one time. Principal drivers include the rate of river discharge, sea level, abstraction of river water for irrigation and the evaporation of water within the river and watershed. The salinity gradient is the main factor determining species composition for mangrove, fish and invertebrates within the estuarine environment (Ceesay et al., 2017; Albaret et al., 2004; Darboe, 2002), and would have tremendous impacts along major portions of the river course should major changes occur (see Figure 5-12). For example, the optimum salinity tolerance for *Rhizophora* growth is reported to be from 8 ppt to 26 ppt (Duke and Allen, 2006). In general, estuaries with higher salinity level, such as found in The Gambia, support less biodiversity (e.g., Blader, 2013; DeGeorge and Reilly, 2007). Mangroves are generally adapted to saline conditions, however, when species-specific salinity thresholds are exceeded, individuals become stressed, resulting in stunting and dwarfism, with slowed or no growth, smaller leaves, lowered reproduction and establishment, and ultimately mangrove death (Diop, 1991; Ceesay et al., 2017). Salinity and hypersaline stress within the estuary is highest at low tide due to overheating and desiccation of the exposed soil surface, and the evapotranspiration of any remaining available water (Asish Kumar Parida, 2010). The homogenous high clay content soils found in the Gambia River, in contrast to others regional rivers, reinforces this negative effect especially during the dry season (Claude, 1985). The potential of an accumulated "memory" of previous hypersaline events, in terms of salt accumulation in estuarine soils, is a potential that has not be explored (Savenije and Pagès, 1992).

Figure 5-12 Salt intrusion in the Gambia River under hypersaline conditions (based on Savenije, 1992)



74. The annual change in salinity levels in the river, due to the passing of the rainy season and cycle of river discharge, is a major factor affecting the distribution of aquatic species and plays a role in their lifecycle. The higher nutrient and lower salinity levels in the estuary associated with the flooding period supports the development of phytoplankton populations (Binet et al., 1995). Lower salinity is also favored by larvae and juveniles of many species and plays a protective role, acting as a barrier keeping out large marine predators (Binet et al., 1995). The progressive increase in salinity through the dry season leads to seasonal changes in the distribution of fish and invertebrate species, for example the entry of adult shrimp further upstream (Binet et al., 1995). Due to its extremely flat topography, with seasonally low dry season flow, the increased residency time of saline water within the estuary can result in saline levels rising above those of pure seawater as the evaporative removal of water results in a concentration of salt. Reduced stream flow due to drought/dry years is typically the trigger of hyper salinity (see Figure 5-13). Depending on the extent of the elevated salt level, hypersaline events can have disastrous effects, with the number of fish species decreasing proportionally to the increase in salinity from more than 45 species at a 35 ppt to no species remaining as salinity levels exceed 90 ppt (Binet et al., 1995), as happened in the Casamance estuary during the 1980s (DeGeorge and Reilly, 2007; Savenije and Pagès, 1992).

Figure 5-13 Mangrove potential profile within the estuary following recurrent drought within dry period



Source: FAO analysis based on Diop, 2002; Claude, 1985; Duke et al., 2017; Savenije, 1992

75. Air and seawater temperatures increase. Air and seawater temperatures both directly affect mangrove health and influence other important abiotic parameters. Mangrove temperature stress begins to occur when seawater temperatures rise above 25°C resulting in a decline in the leaf formation rate. Air temperature above 35°C cause a decline in root development and depresses propagules establishment. Above 38-40°C photosynthesis stops. Surface water temperature currently range from 24°C to 30°C during the year with low temperature during the dry season and higher temperature at the end of the flooding period when warmer water from upstream dominates the estuary. Spatially, temperature increase regularly from the mouth of the estuary to upstream. Therefore, the adaptive strategy of mangroves moving upstream to avoid increased salinity downstream may be limited by warmer upstream waters. Other aquatic life is equally sensitive to increase in water temperature. Shrimp species, for example, will not tolerate increases of more than 3°C to 5°C over current temperatures, and would move seaward (Lee et al., 2009).

76. **CO₂ increase.** CO₂ increase would support the growth of mangrove at low salinity levels for most of the mangrove species, except for *L. racemose*. The reproduction cycle of *Rhizophora mangle*, for example, was found to decrease from 2 years to 1 year under higher CO₂ levels (McLeod and Salm, 2006). In the Gambia case, however, these biological benefits from an increase in CO₂ will be limited by a rise in salinity associated with sea level rise and a possible decrease in river flow.

77. **pH decrease and soil acidification.** Soil pH in the mangrove ecosystem is mainly acid from the riverbank upland. Due to annual flooding, pH changes within areas forested by *Rhizophora* from 5 to 7, and in *Avicennia* areas from 3 to 6, respectively during the dry and flood periods. The higher tolerance to low pH by *Avicennia* spp. indicates that they are more adapted to acid soils. Nevertheless, in highly salty and acid sulphuric tannes, where pH range from 3 to 5, little vegetation is found (e.g., *Sesuvium portulacastrum* ou *Philoxerus vernicularis*) except for the border of such areas (Thornton and Gigliole, 1965; Claude, 1985). Recurrent drought might exacerbate and lead to an expansion of

areas where low pH conditions are found. Soils under *Rhizophora* spp. along the riverbank are high in pyrite, which oxidates after mangroves die-off during periods of intense drought. When this occurs, pH can drop as low as 2; no herbaceous species are able to tolerate such low pH. Once acidified, such areas would remain bare (Thornton and Gigliole, 1965; Claude, 1985).

78. **Dissolved oxygen (DO) and turbidity changes.** Dissolved Oxygen (DO) is a critical parameter for aquatic life and is a standard measure of river water quality. In the Gambia River, DO is close to saturation and is not limiting, ranging from 100 percent saturation in the dry season down to 60 percent at the end of the flooding period (Albaret et al., 2004). DO, however, is sensitive to higher temperature with warmer water capable of holding less oxygen. Continued air temperature increases across the watershed may lead to future reductions in DO, and would be exacerbated by decreased stream flow, leading to longer residency times, and a greater exposure to warming. Should DO fall as low as 20 percent, species of shrimp will die out, and most aquatic life of commercial value would disappear (Lee et al., 2009).

79. **Decreased stream flow and drought.** Periods of sustained drought, as documented in the case of the neighboring Casamance river (see Textbox below) and elsewhere (Duke et al., 2017), show mangroves' high vulnerability to changes in streamflow. As indicated in the summary descriptions of water parameters above, a significant reduction in streamflow can have a catalytic effect on several key chemical and water quality values affecting the mangrove habitat, as well as the physical structure of the mangrove environment.

80. A reduction in river flow, when combined with temperature increase, and related evaporation, and sea level rise will lead to a fundamental alteration in the aquatic environment, with greater salt-water intrusion and the likelihood of a regime shift towards hypersaline conditions later in the century. Human activities, such as the removal of river water in support of expanded irrigation and changes to the natural flood cycle resulting from the operation of the Sambangalou dam (covered in the following chapter), will lead to further decreases in the extent and timing of freshwater river flow, as well as a decrease in sediment availability. A primary impact of these changes will be a reduction in mangroves' vertical adaptive capacity, resulting in the exceedance of both water depth and saline tolerances of individual species. A significant die-off in the mangrove root zone would lead to soil subsidence and erosion of shoreline substrate, triggering a cycle of further decrease in soil elevation and an increase in inundated areas. Such consequences are based on observations of the aftermath of the 1970s drought in the Casamance.

81. A drastic decrease in river flow, resulting from drought conditions within the watershed, will lead to less freshwater, fewer nutrients and a decline in sediment transported downstream. The river would become more saline, with greater saltwater intrusion trending towards establishment of an inverse estuary hydrology, with a greater volume of water entering from the sea than moving downstream through the river due to high evaporative losses along the river course. Downstream, under such a scenario, riverine phytoplankton development would be severely limited due to high salinity and lack of nutrients. Salinity increase and reduced flood cycle will favor the entry of marine species and predators within the estuary throughout the year. A decrease in turbidity and phytoplankton concentration, and the increased presence of predators, will disrupt the food chain resulting in a reduction of survival rates of juveniles, larvae and mollusk's within the estuary. Further upstream, a combination of low waterflow, increased temperatures and evaporation and sea level rise would lead to warmer river water and an increase in potential of hypersaline conditions. Such an event

would first lead to mangrove death with a subsequent loss of habit (herbaceous and mangroves) and associated biodiversity richness. Secondary impacts would be the acidification of soil under previous *Rhizophora* and *Avicennia* groves resulting in increased extent of barre tanne, which would not allow reestablishment of *Rhizophora* along the river edge once drought conditions subsided. In parallel, only highly saline and warm tolerant fish would remain in areas where salinity levels reach 80 ppt. Cockles would lose their habitat due to high erosion, mud acidification and losses in nutrient. Oyster colonies would lose their habitat due to mangrove die-off. Those remaining would face salinity, warm and nutrient stresses. Where salinity levels exceed 90 ppt only orange algae would survive; no information is available on other potential long-term impacts. The purely freshwater portion of the river, furthest upstream, would contract and potentially disappeared from within The Gambia's boarder during portions or all of the year.

Box 1 Changes to water flow - the case of hypersalinity in the Casamance River

In the Casamance river, located immediately to the south of The Gambia, the abrupt changes in freshwater discharge during the 1970-1980 drought had a tremendous impact on the river's biological diversity, resulting in: i) the loss of all fish species in areas where water salinity rose above 90 ppt, even the most saline tolerant species, *Sarotherodon melanotheron*; ii) a collapse in pink shrimp catch numbers; iii) the retreat seawards of oysters and cockles populations (*Crassostrea gasar* and *Anadara senilis*); iv) blocked movement of migrant species travelling from the sea upstream by the warm and hypersaline water; and v) the death of large vertebrates (hippopotamus, crocodile and manatee) due food shortages. Riverian flora was also greatly affected. Freshwater reed swamps (*Phragmites communis*) retreated 100 km upstream. *Rhizophora* mangrove totally disappeared, only remnant communities of *Avicennia* survived far from the riverbanks (Savenije and Pagès, 1992; Claude, 1985) which remained bare years after the event (Savenije and Pagès, 1992).

A comparison of aquatic biodiversity found in the Casamance and Gambia rivers suggest that the hypersaline event caused a shift in dominant species from freshwater fauna to marine, with an overall decrease in the fauna abundance (Binet et al., 1995). While massive mortalities are to be expected during hypersaline events, some fish species (e.g., *Ethmolosa fimbriata*, *Sarotherodon melanotheron* and *Tilapia guineensis*) showed themselves to be tolerate of salinity levels as high as 82 ppt (Binet et al., 1995). Other freshwater fish species (e.g., *Gymnarchus niloticus*, *Herterotis niloticus*, *Clarids*, and *Cichlids*), however, suffered systematic spawning and recruitment failures, resulting in reduced populations as their spawning grounds turned hypersaline (Jaiteh and Sarr, 2011). Overall, high salinity levels reduced fish spawning success and growth rates (Binet et al., 1995). Oyster and cockles lost habit due to the disappearance of mangrove substrate, and a shift towards acid sulphate and saline soils.

Human Actions and Conclusions

82. There is a general consensus that the major decline of mangrove forest cover seen in the aftermath of the 1968-1974 Sahelian drought was due to water and salinity stress (Carney et al., 2014). The effects, however, of various human pressures on the mangrove habitat cannot be ignored. Of these additional pressures, the construction of the Sambangalou dam in Senegal is the most important.

83. The Environmental and Social Impact Assessment (ESIA) for the dam's construction, prepared in 2004 and updated in 2014 (ISL, 2014), did not identify significant negative environmental impacts downstream. In contrast, however, a growing body of independent studies make clear the many likely negative impacts resulting from dam's construction and operation on the river's hydrology, especially the highly productive bolong, the mangrove ecosystem generally, fish assemblages and individual species (Savenije and Pagès, 1992; White et al., 2012; DeGeorge and Reilly, 2007; Louca et al., 2009; Ceasay et al., 2017; Panfili et al., 2004). A 2005 study on saline intrusion (Verkerk and van Rens, 2005) clearly shows the potential ecological disaster related to the dam's construction and calls for a preventive strategy by insuring a continuous and a minimum water streamflow of 40m³/s for the Gambian water. In addition to the effects to the dam, the impacts of other human activities also warrant attention, including potential expansion of irrigated rice production, aquaculture and unsustainable oyster harvesting practices, urban growth, and the harvesting of fuelwood and construction materials

84. **Expansion of agriculture and aquaculture.** Tidal rice cultivation and aquaculture on the riverbanks can cause significant degradation to mangroves. In Asia, for example, shrimp aquaculture is known to be responsible for 38 percent of mangrove loss through the creation of extensive pond systems. The release of effluence from tidal rice fields or aquaculture ponds, rich in organic matter and nutrients into the river can cause secondary problems through the development of algae blooms and eutrophication, drastically decreasing DO and potentially killing aquatic life. The oxidation of soil pyrite that occurs when ponds or fields are drained and exposed to air leads to soil acidification, with pH dropping to as low as two, resulting in the need to abandon such sites, replacing them through expansion into new areas.

85. **Urbanization pressure.** Impacts from the expansion of the built environment is mainly an issue along coastal areas and around the Tanbi wetland mangrove due to the growth of Banjul and increased discharge of grey water effluent.

86. **Fuelwood and construction material.** *Rhizophora* species are the most impacted species by deforestation due to their prized qualities as building material and firewood. *Rhizophora* colonizes predominantly populate the banks of tidal creeks and estuaries and are easily reached by cutters using pirogues, whereas *Avicennia* covers areas of higher ground more readily reached through the expanding road network (Carney et al., 2014; Fent et al., 2019).

87. In sum, the mangrove ecosystem in The Gambia face both human and climatic pressures. Due to the varying sources of these pressures, mangroves may not be able to adapt or recover if attention is given to only individual stressors. Investments, therefore, need to address both human and climatic pressures.

References

- Albaret, J.J., M. Simier, F.S. Darboe, J.-M. Ecoutin, J. Raffray and L.T. de Moraes. 2004. Fish diversity and distribution in the Gambian Estuary, West Africa, in relation to environmental variables. *Aquatic Living Resources*, Vol. 17:35-46.
- Blader, S.J.M. 2013. Fishes and Fisheries in Tropical Estuaries: The last 10 years. *Estuarine, Coastal and Shelf Science*, Vol.135:57-65.
- Brown, S., A.S. Kebede and R.J. Nicholls. 2011. Sea-Level Rise and Impacts in Africa, 2000 to 2100. School of Civil Engineering and the Environment. Southampton, U.K.: University of Southampton.
- Carney, J., T.W. Gillespie and R. Rosomoff. 2014. Assessing Forest change in a priority West African mangrove ecosystem : 1986-2010. *Geoforum*, Vol. 53:126-135.
- Ceesay, A., N.D.H. Dibi, E. Njie, M. Wolff and T. Know. 2017. Mangrove Vegetation Dynamics of the Tanbi Wetland National Park in The Gambia. *Environment and Ecological Research* 5(2): 145-160.
- Cessay, A., K.Y. Aristide, N. Ebrima and K. Tidiani. 2019. Diversity and spatial variation of benthic macroinvertebrates in the River Gambia estuary, West Africa. *International Journal of Fisheries and Aquatic Studies*. - Vol. 7(1): 83-88.
- Claude, M. 1985. Mangroves du Sénégal et de la Gambie. *Ecologie - Pédologie - Géochimie. Mise en valeur et aménagement [Report] : Travaux et Document n.193 / Université Louis Pasteur. - Paris : ORSTOM.*
- Conchedda, G., E.F. Lambin and P. Mayaux. 2011. Between land and sea: livelihoods and environmental changes in mangrove ecosystems of Senegal. *Annals of the Association of American Geographers*, Vol. 101(6):1259-1284.
- Corcoran, E., C. Ravilious, and M. Skuja. 2007. *Mangroves of Western and Central Africa*. UNEP, Cambridge, UK.
- Crow, B. and J. Carney. 2013. Commercializing Nature: Mangrove conservation and female oyster collectors in The Gambia. *Antipode* Vol. 45(2):275-293.
- Darboe, F.S. 2002. Fish species abundance and distribution in The Gambia Estuary. The United Nations University. Fisheries Training Program. Final Report. 40pp.
- DeGeorge, A. and B.K. Reilly. 2007. Eco-Politics of Dams on the Gambia River. *Water Resources Development*, Vol. 23(4):641-657.
- Denis Binet, D., L. Le Reste and P.S. Diouf 1995. The influence of runoff and fluvial outflow on the ecosystems and living resources of west african coastal. In, *Effects of riverine inputs on coastal ecosystems and fisheries resources*. FAO Fisheries Technical Paper Vol. 349. Department of Fisheries. Rome: Food and Agriculture Organization of the United Nations.
- Descamps, C. 1991. La collecte des arches, une activité bi-millénaire dans le Bas-Saloum (Sénégal). In, M.-C. Cormier-Salem (ed.) *Dynamique et usages de la mangrove dans les pays des rivières du sud*. Marseilles: Éditions IRD.
- Diankha, O., Ba, A., Brehmer, P., Brochier, T., Sow, B. A., Thiaw, M., et al. 2018. Contrasted optimal environmental windows for both sardinella species in Senegalese waters. *Fish. Oceanogr.* 27, 351–365.
- Diadiou, H.D. 1995. Biologie de l'huître de palétuvier *Crassostrea gasar* (Dautzenberg) dans l'estuaire de la Casamance (Sénégal): reproduction, larves et captage du naissain. Ph.D. Dissertation. Brest, France : Université de Bretagne Occidentale.

- Diop, E.S. and J.-P. Barousseau. 1991. Synthèse sur les facteurs climatiques, hydrologiques et hydrodynamiques ; conséquence sur les phénomènes de sédimentation. In, M.-C. Cormier-Salem (ed.) Dynamique et usages de la mangrove dans les pays des rivières du sud. Marseilles: Éditions IRD.
- Diop, E.S., C. Gordon, A.K. Semesi, A. Soumaré, N. Diallo, A. Guissé, M. Diouf, and J.S. Ayivor. 2002. Mangroves of Africa. In, de Lacerda, L.D. (ed) Mangrove Ecosystems. Environmental Science. Berlin: Springer.
- Donato, D.D., J.B. Kauffman, D. Murdiyarso, S. Kurnianto. 2011. Mangroves among the most carbon-rich forest in the tropics. *Nature geoscience*, Vol. 4:293-297.
- Duke, N.C. and J.A. Allen. 2006. *Rhizophora mangle*, *R. samoensis*, *R. racemosa*, *R. harrisonii* (Atlantic-East Pacific red mangrove). Species Profiles for Pacific Island Agroforestry. (www.traditionaltree.org).
- Duke, N.C., J.M. Kovacs, A.D. Griffiths, L. Preece, D.J.E. Hill, P. van Oosterzee, J. Mackenzie, H.S. Morning and D. Burrows. 2017. Large-scale dieback of mangroves in Australia's Gulf of Carpentaria: a severe ecosystem response, coincidental with an unusually extreme weather event. *Marine and Freshwater Research*, Vol. 68(10):1816-1829.
- Equator Initiative TRY Oyster Women's Association. 2013. [Online] // Equator initiative. - TRY Oysters Women Association. The Gambia. Equator Initiative Case Studies. Local sustainable development solutions for people, nature and resilient communities. - December 2019. - https://www.equatorinitiative.org/wp-content/uploads/2017/05/case_1370356657.pdf.
- Ettritch, G., A. Hardy, L. Bojang, D. Cross, P. Bunting and P. Brewer. 2018. Enhancing digital elevation models for hydraulic modelling using flood frequency detection. *Remote Sensing of Environment*, Vol. 217:506-522.
- Fent, A., R. Bardou, J. Carney and K. Cavanaugh. 2019. Transborder political ecology of mangroves in Senegal and The Gambia. *Global Environmental Change*, Vol. 54: 214-226.
- Funo, I.C.dS., I.G. Antonio, Y. Ferreira-Marinho, A.O. Galvez. 2015. Influence of salinity on survival and growth of *Crassostrea gasar*. *Boletim do Instituto de Pesca*, Vol. 41(4): 837-847.
- Gomes, C., F.C. Silva, G.R. Lopes and C.M.R. Melo. 2016. The reproductive cycle of the oyster *Crassostrea gasar*. *Brazilian Journal of Biology*, Vol. 74(4): 967-976.
- Gosling, E. 2015. Ecology of bivalves. *Marine Bivalve Molluscs*. Second Edition. Wiley-Blaackwell.
- Government Gambia The Gambia (GoTG). 2010. National Forest Assessment 2008-2010. Banjul, The Gambia : Forestry Department.
- IPCC (Intergovernmental Panel on Climate Change). 2019a. The Ocean and Cryosphere in a Changing Climate. Summary for Policy Makers. In: Special Report on the Ocean and Cryosphere in a Changing Climate [H.-O. Pörtner, et al. (eds.)]. Geneva, Switzerland: IPCC.
- Jaiteh, M.S. and B. Sarr. 2011. Climate Change and Development in the Gambia. Challenges to Ecosystem Goods and Services.
- Jallow, B.P., S. Toure, M.M.K. Barrow and A.A.Mathieu. 1999. Coastal zone of The Gambia and the Abidjan region in Cote d'Ivoire: sea level rise vulnerability, response strategies and adaptation options. *Climate Research*, 12(2):129-136.
- Kandasamy, K. 2003. How do mangrove forests induce sedimentation? *Rev Biol Trop*, Vol. 51(2):355-359.
- Krauss, K.W., K.L. McKee, C.E. Lovelock, D.R. Cahoon, N. Saintilan, R. Reef and L. Chen. 2014. How mangrove forests adjust to rising sea level. *New Phytologist*, Vol. 202(1):19-34.
- Kristensen, E. 2008. Mangrove crabs as ecosystem engineers: with emphasis on sediment processes. *Journal of Sea Research*, Vol. 59(1-2):30-43.

- Lee, V., J. Tobey, K. Castro, B. Crawford, M.D. Ibrahima, O. Drammeh and T. Vaidyanathan. 2009. Marine Biodiversity Assets and Threats Assessment. Gambia-Senegal Sustainable Fisheries Project. Coastal Resources Center. Kingston, Rhode Island: University of Rhode Island.
- Louca, V., Lindsay, S.W., Majambere, S. and M.C. Lucas. 2009. Fish community characteristics of the lower Gambia River floodplains: a study in the last major undisturbed West African river. *Freshwater Biology*: 254–271.
- Manson, F.J., N.R. Loneragan, G.A. Skilleter and S.R. Phinn. 2005. An Evaluation of the Evidence for Linkages Between Mangroves and Fisheries: A synthesis of the literature and identification of research directions. *Oceanography and Marine Biology: An annual review*, Vol. 43:483-513.
- McLeod E. and V.R. Salm. 2006. Managing Mangroves for Resilience to Climate Change. Gland, Switzerland: IUCN.
- Muzaffar, M. A., Inam, M. Hashmi, K. Mehmood and I. Zia. 2017. Impact of reduction in upstream fresh water and sediment discharge in Indus deltaic region *Journal of Biodiversity and Environmental Sciences*, Vol. 10(4):208-216.
- Noor, T., N. Batool N., R. Mazhar R., N. Ilyas. 2015. Effects of siltation, Temperature and Salinity on Mangrove Plants. *European Academic Research*, Vol. II (11):14172-14179.
- Oréade-Brèche and ISL Ingénierie (ISL). 2014. Etude d'Impact Environnemental et Social du Projet Energie (Revue du rapport COTECO 2008). Mission d'Appui Conseil a l'OMVG pour la Realisation de son Projet Energie. *Projet de Rapport Final*. Dakar: OMVG.
- Panfili, J., A. Mbow, J.-D. Durand, K. Diop, K. Diouf, D. Thior, P. Ndiaye and R. Laë. 2004. Influence of Salinity on the Life-history Traits of the West Africa Black-chinned Tilapia (*Sarotherodon melanotheron*) : Comparison between The Gambia and Saloum estuaries. *Aquat. Living Resour.*, Vol.17 :65-74.
- Parida, A.K. and B. Jha. 2010. Salt Tolerance Mechanisms in Mangroves: a review. *Trees*, Vol. 24:199-217.
- Risley, J.C. 1987. Applications of the SSARR Model in the Gambia River basin. Technical Document No. 12. Gambia River Basin Development Organisation. Dakar, Senegal: United States Agency for International Development.
- Risley, J.C., D.P. Guertin and M.M. Fogel. 1993. Salinity-Intrusion Forecasting System for Gambia River Estuary. *Journal of Water Resource Planning and Management* Vol. 119(3): 339-352.
- Rossi, R.E. 2018. The Role of Multiple Stressors in a Mangrove Die-off: A Case Study in The Bahamas. PhD Dissertation. Raleigh, North Carolina: North Carolina State University.
- Saifullah, A.S.M., A.H.M. Kamal, M.H. Idris, A.H. Rajae and Md.K.A. Bhuiyan. 2016. Phytoplankton in tropical mangrove estuaries: role and interdependency. *Forest Science and Technology*, Vol. 12(2):104-113.
- Savenije, H.H.G. and J. Pagès. 1992. Hypersalinity: a dramatic change in the hydrology of Sahelian estuaries. *Journal of Hydrology*, Vol. 135(4): 157-174.
- Semeniuk V. 1994. Predicting the Effect of Sea-level Rise on Mangroves in Northwestern Australia. *Journal of Coastal Research*, Vol. 10(4): 1050-1076.
- Spalding, M., M. Kainuma, M. and L. Collins. 2010. World Atlas of Mangroves. Earthscan, London.
- Thornton, I. and M.E.C. Giglioli. 1965. The Mangrove Swamps of Keneba, Lower Gambia River Basin. II Sulphur and pH in the Profiles of Swamp soils. British Ecological Society. *Journal of Applied Ecology* Vol. 2(2): 257-269.

Vélez-Belchí, P., M. González-Carballo, M.D. Pérez-Hernández and A. Hernández-Guerra. 2015. Open Ocean Temperature and Salinity Trends in the Canary Current Large Marine Ecosystem. In: Oceanographic and Biological Features in the Canary Current Large Marine Ecosystem. Valdés, L. and I. Déniz-González (eds). Technical Series 115. Paris: IOC-UNESCO.

Verkerk M.P. and C.P.M. Van Rens. 2005 Saline intrusion in Gambia River after dam construction. Solutions to control saline intrusion while accounting for irrigation development and climate change [Book]. Twente, The Netherlands: University of Twente.

Vidy, G., F.S. Darboe and E.M. Mbye. 2004. Juvenile Fish Assemblages in the Creeks of the Gambian Estuary. *Aquat. Living Resour.*, Vol.17: 56-74

White, S.M., M. Ondračková and M. Reichard. 2012. Hydrologic Connectivity Affects Fish Assemblage Structure, Diversity and Ecological Traits in the Unregulated Gambia River, West Africa. *Biotropica*, Vol. 44(4):521-530.

World Bank Climate change knowledge portal. 2019. <https://climateknowledgeportal.worldbank.org/country/gambia/climate-data-historical> (accessed 2/21/2019).

Chapter 6 SALINE INTRUSION in the GAMBIA RIVER

Part 1 – Introduction

1. Due to fish species' specific water quality requirements, sea level rise and changes to the hydrologic regime of the Gambia River affecting the extent of saline intrusion is a critical issue for the future of capture fisheries – both within the river, and species dependent on the riverain environment for some portion of their lifecycle – as well as the selection and placement of aquaculture activities within the country. The most recent study on saline intrusion into the Gambia River was conducted in 2005, using data from the 1990s and earlier.

2. A re-analysis of saline intrusion, using the SALNST model, has been commissioned as part of the preparation of the funding proposal. The new analysis uses updated sea level rise estimates, updated precipitation and temperature records from the past 20 years, and utilizes downscaled projections of future precipitation and temperature drawn from the most recent generation of global circulation models, further bias corrected to ensure the most accurate fit possible. The recent historical and projected data covers the entire river watershed, not just the section of river within The Gambia's national borders, while comparing a historical reference scenario with 29 simulated combinations, involving two representative concentration emission pathways (RCP 4.5 and 8.5), two rates of sea level rise (.84 m and 2 m), three levels of irrigation development and two dam release schedules, and a reservoir filling scenario. The analysis places particular attention on assessing the risk of hypersaline condition emerging due to climate change and the construction of the dam at Sambangalou.

Part 2 – Rationale for the Assessment

3. Previous studies on saline intrusion in the Gambia River were commissioned by the Organisation pour la Mise en Valeur du fleuve Gambie (OMVG) as part of the Gambia River Basin Hydraulic Masterplan (1999) and of the feasibility studies for the construction of the Sambangalou dam (2004).⁸¹ Both computational irregularities and deficiencies were noted in these earlier studies (summarized in Table 6-1 Comparison of the salinity intrusion studies). For example, the 1999 Masterplan did not take into consideration sea level rise, while the 2004 feasibility study did not include water use for irrigation. Both of the earlier studies relied on historical (rainfall and temperature) data as the basis for estimating future precipitation and evaporation, and not climate projections. Given these shortcomings, a reanalysis of the extent of salinity intrusion was justified (Verkerk and van Rens, 2005).

⁸¹ The dam project, financed by the African Development Bank, has been much delayed, with initial pre-feasibility studies carried out in 2002-2004, and a second round of feasibility studies carried out in 2006-08, subsequently reviewed and verified in 2014. The OMVG website mentions the issuing of three contracts in early 2019 for construction on the dam. The latest satellite imagery available on Google Earth (10/31/2019), shows no obvious signs of physical work taking place.

Table 6-1 Comparison of the salinity intrusion studies

	OMVG Master Plan (1999)	Dam Feasibility Study (2004)	University of Twente (2005)	FAO (2021)
Model	SALNST	SALNST	SALNST	SALNST
Hydroelectric cap.	40 MW	128 MW	n/a	n/a
Precipitation data	Historical station data – future changes not considered	Historical station data – future changes not considered	Projected (2070-2100) – downscaled precipitation and temperature (HadCM3)	Historical station data – for model calibration; Projected (MIROC-ESM) 2 scenarios: RCP 4.5 RCP 8.5
Evapotranspiration	Historical values – future changes not considered	Historical values – future changes not considered	Comparison using projected precip/temp (HadCM3): -Thornthwaite -Linacre	Thornthwaite using projected weather data
Stream flow	Historical values – future changes not considered	Historical values – future changes not considered	Historical (Gouloumbo) and Projected (with release scenarios)	Historical (Gouloumbo) and Projected (with release scenarios)
Irrigation	3 scenarios: Operating 1,500 ha rice; Total existing 3,000 ha rice; All possible 14,000 ha rice, 3,700 ha other crops	Not considered	3 Scenarios: No irrigation; All tidal on swamp land (6,600 tidal, 8,800 pump); All pump (15,300).	3 pump irrigation scenarios: Current (2,625 ha), Expected (5,635 ha), Maximum (14,727 ha)
Geomorphology	Future changes not considered	Future changes not considered	2 scenarios: River widens proportional to 60 cm sea level; River widens disproportionately to 60 cm sea level rise	1 scenario, widening in response to sea level rise of .84 m and 2 m
Sea level rise	Not considered	2 scenarios: 20 cm (0.21 mm/yr); 50 cm (0.51 mm/yr)	60 cm/95 yrs (6.3 mm/yr)	2 Scenarios: .84 m to 2100 (8.9 mm/yr)(conservative) 2 m to 2100 (21.3 mm/yr)(max expected)
Dam release			4 scenarios from OMVG and 1 additional	2 Scenarios: -environmental power generation (OMVG); -power maximization (ensuring minimum 20 m ³ /sec flow at KP460)

Source (authors)	OMVG Master Plan, 1999	Dam Feasibility Study, 2004	Verkerk and van Rens, 2005	van der Scheer, 2021
Noted errors	Reference point used is 13 km upstream from actual	Uses decreased ET; increased elevation in estuary of 6 m	Current rate of sea level rise 3.3mm/yr; 10.5 mm/yr projected	

Sources: OMVG, 1999; IRD, 2004; Verkerk and van Rens, 2005; FAO, 2021

Part 3 – Theory on salt intrusion

1. To understand how this study deals with salt intrusion in the Gambia river the necessary theory is presented in this chapter. The theory of salt intrusion starts with the use of geography and followed by the formulas for determining steady state and unsteady state dispersion and salinity, both the theory and model are explained. This chapter follows the reasoning of Savenije (2012). The chapter will finish with an explanation of several types of salt intrusion and hyper salinity and its effects.

3.1 Geography of the Gambia estuary

2. The Gambia estuary is a coastal-plain estuary. It consists of small sediment that based on the sediment supply and flow can erode or build up. Since an estuary is the transition between river and ocean hydraulics of both play a role. Waves and tides from the ocean transport sediment up and downstream while the river supplies the estuary with fresh sediment.

3. The clear shape in The Gambia estuary can be described by the ‘ideal estuary theory’ of Pillsbury (1956). He relates the often-clear funnel shape in coastal-plain estuaries to the dampening of tidal forces while waves travel upstream. The width and area reduce in such a way, increasing the wave amplitude, that they match the amount of friction that decreases wave amplitude. This results in a constant wave amplitude. In cases where this theory cannot be applied the estuary is often shaped differently, either by bound by geography (e.g. rivers in rocky layers) or by manmade structures such as the Dutch river system.

4. The funnel shape according to the ideal estuary theory has a clear geometry. It starts wide and converges while following the river upstream. This can be described mathematically (e.g., Savenije, 1986; Davies and Woodroffe, 2010) by:

$$B(x) = B_0 \cdot e^{-\frac{x}{b}}$$

Where B_0 is the width at the mouth, x the distance from the mouth and b the width convergence length. Similarly, the cross-sectional area can be described:

$$A(x) = A_0 \cdot e^{-\frac{x}{a}}$$

Where A_0 is the cross-sectional area at the mouth and a is the area convergence length. These parameters are dependent on the dominant hydraulics at the location x in the estuary. The hydraulics at the mouth of the river are often dominated by the ocean, although there are cases of steep rivers and rivers with large flows that are dominated by river hydraulics. In the case of ocean dominated hydraulics, a deflection point exists after a distance x_1 . The distance x_1 is the distance in which the energy of ocean waves has been dissipated and riverine hydraulics determine new parameters for the cross-sectional area and width. These describe the further course of the estuary. Therefore, formulas for the width and cross-sectional area become respectively:

$$B(x) = \begin{cases} B_0 \cdot e^{-\frac{x}{b_1}} & x \leq x_1 \\ B_1 \cdot e^{-\frac{x-x_1}{b_2}} & x > x_1 \end{cases}$$

$$A(x) = \begin{cases} A_0 \cdot e^{-\frac{x}{a_1}} & x \leq x_1 \\ A_1 \cdot e^{-\frac{x-x_1}{a_2}} & x > x_1 \end{cases}$$

5. If further upstream the riverine hydraulics change significantly again more deflection points can be determined. Zhilin Zhang [2019] improved these relations for width and cross-sectional area for more riverine estuaries, by letting the area and width converge towards the cross-sectional area and width of the river far upstream. These improved relations have not been used in this study since The Gambia estuary is tidally dominated.

6. If one assumes the depth to be relatively constant over the width the depth can be determined with the formulas above, resulting in:

$$h(x) = \frac{A(x)}{B(x)} = \frac{A_0}{B_0} \cdot e^{\frac{x(a-b)}{ab}}$$

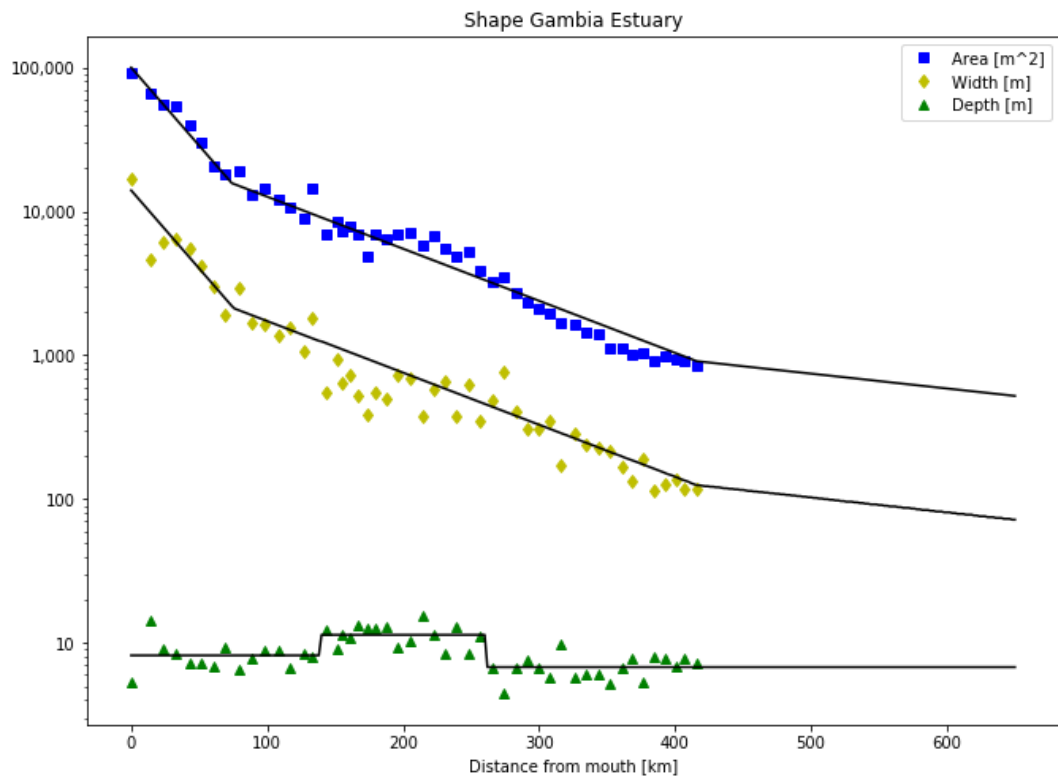
This shows that if the area convergence length is larger than the width convergence length the depth increases and vice versa. However, it has been found by Savenije (1992) that these convergence lengths are often close to each other. In the case of the Gambia estuary they are the same. This results in a more or less constant depth over the estuary. Figure 6-1

Figure 6-1 Geometrical results from the survey in 1971

7. The inflection point is clearly visible in the cross-sectional area and width. Furthermore, it can be seen that the depth is more or less constant throughout the estuary. below, shows the shape of the Gambia estuary with two inflections points. A survey in 1971 supervised by H.H.G. Savenije measured the cross-sectional area, the width, the depth and took salinity measures which will be presented later. Since the area convergence length and the width convergence length are equal, the extended area after 420 km has the same assumption and by using areal imagery the modelled river length has been increased to 650 km.

Figure 6-1 Geometrical results from the survey in 1971

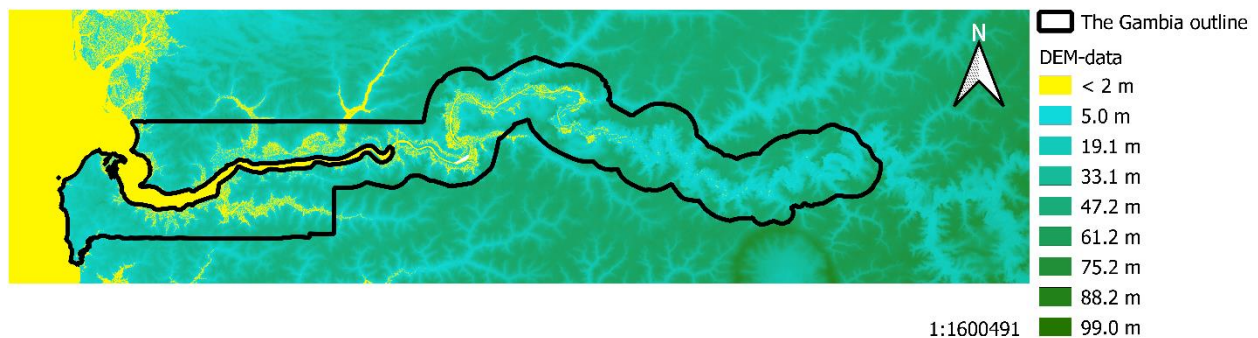
The inflection point is clearly visible in the cross-sectional area and width. Furthermore, it can be seen that the depth is more or less constant throughout the estuary.



Additional geographical changes

8. The Gambia is a flat country, especially alongside the river. A stroke on both sides of the river of multiple kilometres is close to sea level (see Figure 6-2 **Error! Reference source not found.**). This continues up to the border of Senegal where the river banks as well as the surrounding area slowly elevate. Farmers make smart use of these low elevations next to the river. When high tide pushes up freshwater to the level of their fields, they open small gates which allows freshwater to wet their fields. At low tide they open the gates once more to let the excess water escape.

Figure 6-2 Digital elevation map of The Gambia, showing elevation with respect to sea level



Source: <https://www.diva-gis.org/gdata>

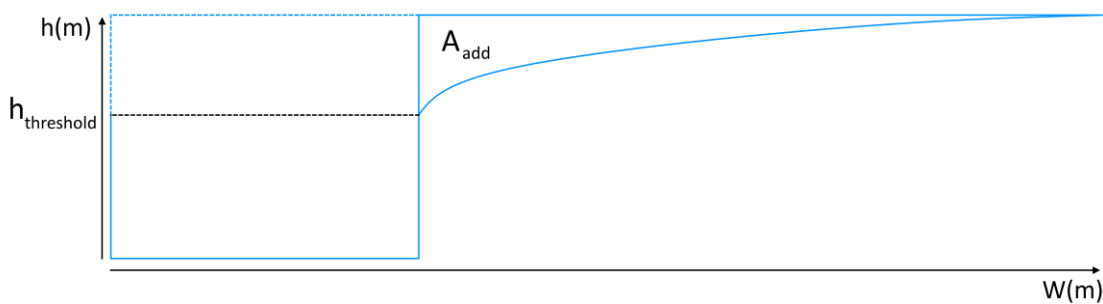
9. Since the amount of sea level rise this century is unknown a worst-case scenario should be taken into account. Therefore, two stages in the Gambia river can be distinguished. Below a certain threshold value, the river majorly increases in depth with increasing sea level. Above this threshold value the river also increases in width. A study of Ettritch et al. (2018) focused on the widening (flooding) due to sea level rise and compared two digital elevation models. This study took place on the Gambia river albeit on a relatively short section. Nonetheless their results have been used to create relations for the additional width and cross-sectional area. Where SLR is the sea level rise in meters, Hthreshold the threshold value for sea level rise and c1 and c2 constants deducted from Ettritch et al. (2018) their research. These relations have been visualized in

10. Figure 6-3. It can be seen that a small increase in water level above the threshold value accounts for a significant increase in width. This results in a strong increase in surface area once the threshold value is exceeded.

$$W_{add} = \ln\left(\frac{SLR}{c_1}\right) \cdot \frac{1}{c_2}$$

$$A_{add} = \frac{SLR}{c_2} \cdot \left(\ln\left(\frac{SLR}{c_1}\right) - 1\right) - \frac{H_{threshold}}{c_2} \cdot \left(\ln\left(\frac{H_{threshold}}{c_1}\right) - 1\right)$$

Figure 6-3: Effect of sea level rise



11. Another change that should not be overlooked is the possible increase in irrigated surface. Agriculture is an important sector in The Gambia and effort is being made to increase the work done in this sector. Studies in The Gambia as well as Senegal determined several scenarios on the possible development in irrigated surface. Since crops do not like saline water the water extraction is upstream of the saline front. Therefore, an increase in irrigated surface decreases the amount of freshwater discharge in the river. This could potentially have a significant influence on the salt intrusion length and concentration.

3.2 Advection and dispersion

12. Salt distribution along the river can be described by two processes: advection and dispersion. Advection, where salt is transported by river flow, is the most effective at distributing salt. This process is predominantly noticeable during the wet season, when large volumes of water flush the salt from upstream towards the mouth of the river. However, also during the dry season advection has a significant role. Due to the high evaporation and limited freshwater availability, there is a point along the river where all freshwater has been evaporated. Further evaporation of water results in seawater being sucked inlands thereby having the opposite effect as the advection during the wet season, where salt is flushed to sea.

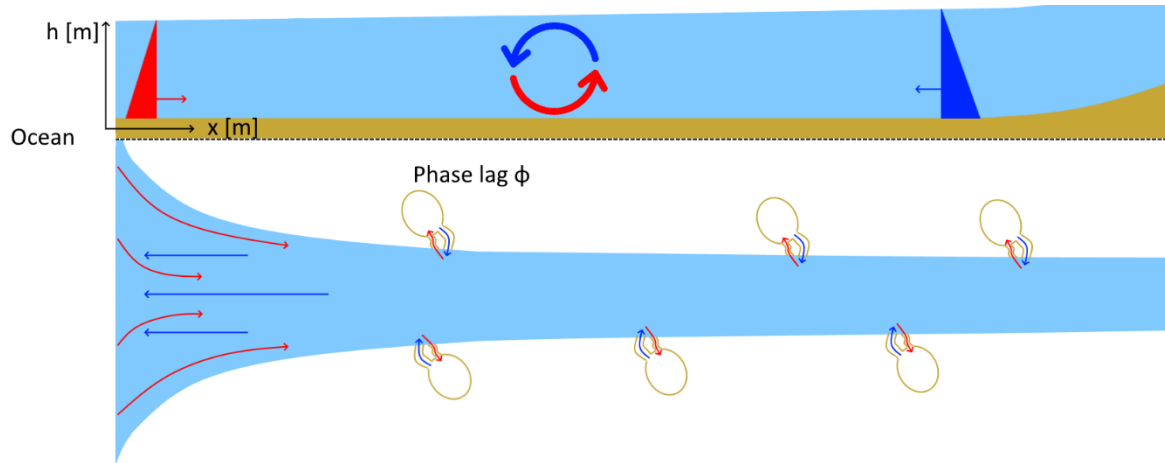
13. Dispersion can be seen as a combination of diffusion and mixing. Diffusion is the process where areas of high salinity diffuse into areas of low salinity. Mixing contains several processes where water fluxes actively bring volumes of higher salinity in contact with areas of lower salinity which are then mixed. The process of dispersion is only dominant during the dry season, when there is little flow. Several types of mixing can be distinguished, here the main processes are described and visualized below.

14. The three main mixing types are gravitational mixing, trapping and tidal pumping and are visualized in Figure 6-4. Gravitational mixing occurs due to saline water having a higher density than freshwater. To balance water pressures the water level at the freshwater side is a little higher than at the saline side. The pressures are equal but work on different elevations, therefore creating a flux in which salt water is transported on the bottom of the river in upstream direction while freshwater is transported on top of the river in downstream direction.

15. Trapping consists of areas that flood when there is high tide. When the tide reverses and water flows back to these small areas a small phase lag compared to the tide in the river is introduced. Therefore, the water that flows back has a different salinity and density than the river water it flows into.

16. Tidal pumping has to do with how water is flowing in and out of the river mouth. During high tide when sea water flows into the river the water comes from all directions however during low tide the river water forms more a waterjet and penetrates deeper into the ocean. Therefore, the water that is flowing back into the river during the next high tide is more saline.

Figure 6-4: The visualization of the main mixing mechanisms that contribute to dispersion



17. Earlier research tried describing individual dispersion components and adding them together but to no avail. There are always processes that are overlooked or overlap. Simultaneously such a bottom-up approach is sensitive to equifinality (e.g. Sivapalan, 2003; Savenije, 2005). Therefore, to counter equifinality all dispersion mechanisms are captured in Van der Burgh's K value. The Van der Burgh K value is an empirical value that links the effective dispersion to the freshwater discharge under steady-state conditions (Van der Burgh, 1972).

18. Secondly, two types of dispersion can be distinguished, steady-state dispersion and unsteady-state dispersion. During steady-state conditions the flow in the river does not differ much and Van der Burgh's method for steady-state dispersion can be applied. However, during part of the year the flow in the river varies significantly due to the difference in water availability between the dry and wet season. The system then lags behind the steady-state and an unsteady-state solution needs to be applied. The difference between the two methods is that the steady-state solution solely depends on hydraulic properties while the unsteady-state is dependent on the salinity gradient. In addition to that, if hyper saline conditions prevail the unsteady-state dispersion takes this into account as well. The formula for unsteady-state dispersion used in the 1-D SALNST model was first introduced by Savenije in 1992.

Steady-state dispersion: $\frac{dD}{dx} = K \frac{Q_f}{A}$

Unsteady-state dispersion: $\frac{D}{D_0} = \left(\frac{s}{s_0}\right)^K$

Where:

Dispersion:

$D \quad L^2/t$

Van der Burgh's parameter:

$K \quad -$

River discharge:

$Q_f \quad L^3/t$

Cross-sectional area:

$A \quad L^2$

Dispersion at the mouth of the river:

$D_0 \quad L^2/t$

Salinity:	s	M/L ³
Salinity at the mouth of the river:	s ₀	M/L ³

19. To determine the unsteady-state dispersion the dispersion at the mouth of the river is required. The definition of the dispersion at the mouth of a river has been described by Savenije in 1993, who based his relation on observations in 13 estuaries over the world. He related several non-dimensional parameters which were known to affect the dispersion. This empirical relation depends on the ratio of the tidal excursion at the mouth of the river (E_0) to the cross-sectional convergence length (a), the tidal flow velocity amplitude (v_0), the depth at the mouth of the river (h_0) and the Estuarine Richardson number (N_R). The latter being the ratio of potential energy provided to the estuary by the river discharge through buoyancy of fresh water and the kinetic energy provided by the tide during a tidal period (Savenije, 1992). The Estuarine Richardson number depends on amongst others the density of salt water (ocean) and freshwater (ρ_s, ρ_f), the freshwater discharge (Q_f), the tidal period (T) and the tidal prism (P_t). The latter being the volume of water being transported by the tide, which is approximately the tidal excursion at the mouth of the river multiplied by the cross-sectional area at the mouth of the river.

$$\frac{D_0^{HWS}}{v_0 h_0} = 1400 \frac{E_0}{a} N_R^{0.5}$$

Where:

Tidal excursion at the mouth of the river:	E_0	L
Cross-sectional convergence length:	a	L
Tidal flow velocity amplitude:	v_0	L/t
Depth at the mouth of the river:	h_0	L
Estuarine Richardson number:	N_R	-

$$N_R = \frac{\Delta \rho g h Q_f T}{\rho v_0^2 P_t}$$

$$\Delta = \frac{\rho_s - \rho_f}{\rho_f}$$

Where:

Salt water density:	ρ_s	M/L ³
Freshwater density:	ρ_f	M/L ³
Tidal period:	T	t
Tidal prism:	P_t	L ³

$$P_t \approx A_0 E_0$$

Where:

Cross-sectional area at the mouth of the river:	A_0	L ²
---	-------	----------------

20. Since the dispersion at the mouth of the river makes use of the depth at the mouth of the river, h equals h_0 . Therefore, the dispersion at the mouth of the river can, with the help of the previously introduced formulas, be rewritten to:

$$D_0 = 220 \sqrt{g} \frac{E_0}{a} \sqrt{\frac{Q_f T}{P_t}} h_0^{1.5}$$

3.3 Salt intrusion

21. Just as dispersion salt intrusion can distinguish steady-state and unsteady-state. Looking at the formula for steady-state salinity (Savenije, 1989) one can see similarities with the formula for unsteady-state dispersion. However, steady-state dispersion is applied which makes the steady-state salinity again fully dependent on hydraulic properties. The steady-state salinity is the equilibrium of salt concentration and salt intrusion. Unsteady-state salinity is calculated by solving the salt balance equation (Savenije, 2012).

$$\text{Steady-state salinity: } s - s_r = \left(\frac{D}{D_0}\right)^{\frac{1}{K}} \cdot (s_0 - s_r)$$

$$\text{Unsteady-state salinity: } r_s \frac{\partial s}{\partial t} - (1 - K) \frac{Q_f}{A} \frac{\partial s}{\partial x} - (1 - K) r_s \frac{P_n b}{\bar{h}} \frac{\partial s}{\partial x} + \frac{D}{a} \frac{\partial s}{\partial x} - D \frac{\partial^2 s}{\partial x^2} + r_s \frac{P_n}{h_0} s = 0$$

Where:

River salinity far upstream, uninfluenced by salt intrusion:	s_r	M/L ³
Width convergence length:	b	L
Average depth along the width:	\bar{h}	L
Cross-sectional storage coefficient:	r_s	-
Net precipitation:	P_n	L/t

$$r_s = \frac{B_s}{B_c}$$

$$P_n = P - E$$

Storage width:	B_s	L
Conveyance width:	B_c	L
Precipitation:	P	L/t
Evaporation:	E	L/t

22. As can be seen in the first term of the salt balance equation, the unsteady-state salinity is dependent on time. Salinity at a location x_i and a time t_i influence the salinity at the same location x_i for time $t_{i+\Delta t}$. The salt balance equation can be rewritten to:

$$r_s \frac{\partial s}{\partial t} - q \frac{\partial s}{\partial x} - D \frac{\partial^2 s}{\partial x^2} + r_s \frac{P_n}{h_0} s = 0$$

Where:

$$q = (1 - K) \cdot \frac{Q_f + r_s B P_n b}{A} - \frac{D}{a}$$

Effects of sea level rise and irrigation development

23. The beforementioned sea level rise has multiple effects when looking at dispersion and the salt balance. Due to the larger depth the cross-sectional area increases while the width stays constant. This reduces the gradient of the steady-state dispersion thereby increasing the salt dispersion over the whole estuary. At the same time the increased cross-sectional area increases the effectivity of the advective term in the salt balance equation. Similarly, an increase in irrigated surface leads to less freshwater discharge which decreases the advective term in the salinity equation as well as decreasing the dispersion gradient even more.

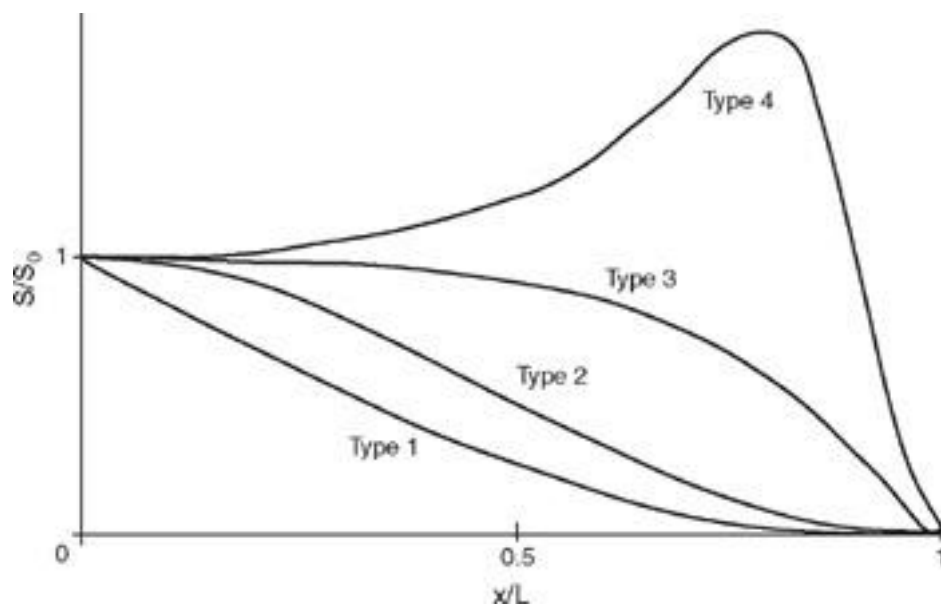
Salt intrusion types and hyper salinity

24. There are different kinds of salt intrusion. These are distinguished in three types based on how well mixed the salt in a vertical column of water is. The stratified type, the partially mixed type and the well mixed type. Based on the river discharge and tidal flows an estuary has a certain degree of mixing. When the tidal flows dominate it is well mixed and vice versa.

25. The stratified type is badly mixed, at the ocean side the water is saline and at the river side the water is fresh, in between there is a very short range in which the saline water goes to freshwater. Often a saline wedge is present underneath a layer of freshwater. The partially mixed type and well mixed type have increasingly a more gradual transition. However, the difference between partially mixed and well mixed is not objectively defined. In practice the well-mixed theory can be used up to a stratification of 20-30% (the difference between the salt concentration at the top and bottom of the river divided by their average) (Van Os, Abrahams; 1990).

26. In an estuary of the well mixed type the salinity changes gradually over distance. This can be seen best when measuring the salt concentration while traveling with low water slack, high water slack or the tidal average, the last being very hard to detect. If done correctly a smooth salinity curve shows the gradual change in salinity. There are four types of salt intrusion curves presented in Figure 6-5 below.

Figure 6-5: The four types of salt intrusion curves



Type 1: recession shape

Type 2: bell shape

Type 3: dome shape

Type 4: humpback shape

27. The first three types are largely linked to the geometric relations. Type 1 occurs in straight and narrow estuaries, such as the Chao Phya in Thailand and the Limpopo in Mozambique. Type 3 are wide channels with a pronounced funnel shape, such as the Gambia river. Type 2 is a mixture of type 1 and type 3, with a narrow river upstream but a strong funnel shape near the ocean.

28. Type 4 has nothing to do with the geometric relations. Any of the previously mentioned types can turn into a humpback shape, either when there is a rainfall deficit, evaporation excess or when too much freshwater is removed from the system (e.g. for irrigation purposes). Type 4 is the shape of the salt intrusion curve when the estuary turns hypersaline, with a higher salinity than the source.

Part 4 – Methods and Materials

29. The aim of this study is to provide insight into the magnitude of salt intrusion change due to climate change and the implications of the construction of a new hydropower dam. This chapter will start by repeating the research questions. Secondly, the required data to answer these questions and where this data comes from is treated followed by the calibration and validation of the model. Afterwards, practical differences between the model and theory are dealt with. Finally, an overview of all scenarios that are used to answer the research questions is presented as well as the method of selecting these scenarios.

4.1 Research questions

30. The main research question “What are the effects of climate change and the new hydropower dam on salt intrusion in the Gambia river up to 2100?” will be answered by answering the research questions below. To answer these questions the 1-D SALNST model (see chapter 3) is used. Research questions I and II will be answered directly by the model output. Questions III, IV and V will be derived from the results and/or from a qualitative analysis of these results and the model.

- I. How does the salt intrusion length develop?
- II. How does the salt concentration develop?
- III. Can hyper salinity occur and under which circumstances?
- IV. What measures can be taken to mitigate salt intrusion and how effective are these measures?
- V. How will aqua- and agriculture in The Gambia be affected by the construction of the hydropower dam?

4.2 Required data and collection

31. Part 3 presented the theory on how the SALNST model used in this study calculates salt intrusion. The dispersion and salt balance equations, which calculate respectively the dispersion and salt concentration over the length of the river, are composed of the following parameters:

1. Salinity at the mouth of the river:	s_0	M/L^3
2. Gravitational constant:	g	L/t^2
3. Cross-sectional area of the river:	A	L^2
4. Cross-sectional area at the mouth of the river:	A_0	L^2
5. Cross-sectional area convergence length:	a	L
6. Width of the river:	B	L
7. Width convergence length:	b	L
8. Depth at the mouth of the river:	h_0	L
9. Tidal excursion at the mouth of the river:	E_0	L
10. Tidal period:	T	t

11. Van der Burgh's parameter:	K	-
12. Net precipitation:	P_n	L/t
13. River discharge:	Q_r	L ³ /t
14. Dispersion at the mouth of the river:	D_0	L ² /t
15. Salinity:	s	M/L ³
16. Dispersion:	D	L ² /t

32. The parameters can be roughly categorized into the following categories: known parameters (1 – 2), pre-determined parameters (3 – 11), measured and deducted parameters (12 – 13) and parameters to determine (14 – 16). Parameters of the first category are well-known constants, the ocean salinity (35 g/L) and gravitational constant (9.81 m/s²) and do not need further explanation. The pre-determined values were measured, deducted or optimized during a survey in 1971, led by Savenije. In personal communication with Savenije this data was obtained for this study. The measured and deducted parameters are described below. The values to determine consist of a parameter that follows from calibrating the model, while the dispersion and salt concentration over the length of the river result from solving the formulas for dispersion and the salt balance equation (see previous section).

4.2.1 Precipitation, evaporation and discharge

33. The measured and deducted parameters are the net precipitation which is calculated by subtracting evaporation from precipitation and river discharge which is predicted by another model. Evaporation needed for the net precipitation is estimated with Thornthwaite's method which depends on temperature (Thornthwaite, 1948). Temperature and precipitation are predicted by using a single GCM. The GCM, MIROC-ESM comes forth from a FAO study which can be found in **Error! Reference source not found.**Appendix A (FAO, 2020). This paragraph will summarize how the MIROC-ESM GCM was selected, how and why the potential evaporation is determined by Thornthwaite's method and how the model that predicts river discharge works.

GCM

34. To select a good GCM for predicting future precipitation and temperature, a comparison between five GCMs was made. The five selected GCMs have all been used in previous climate assessments performed by the FAO, and are part of the Coupled Model Intercomparison Project 5 (CMIP5), used in conducting analysis for the IPCC Fifth Assessment Report (AR5).⁸² These models are: the GFDL-ESM2M (Geophysical Fluid Dynamics Laboratory – Earth System Model 2M)(Dunne et al., 2012); the MIROC-ESM (Model for Interdisciplinary Research on Climate – Earth System Model) (Watanabe et al., 2011); the IPSL-CM5a-MR (Institut Pierre-Simon Laplace-Climate Model 5a-Mid-Resolution)(Dufresne et al., 2013); the NORESM (Norwegian Earth System Model 1-M)(Bentsen et al., 2013), and the HadGEM2-ES (Hadley Centre Global Environment Model ver.2-Earth System)(Martin et al., 2011).

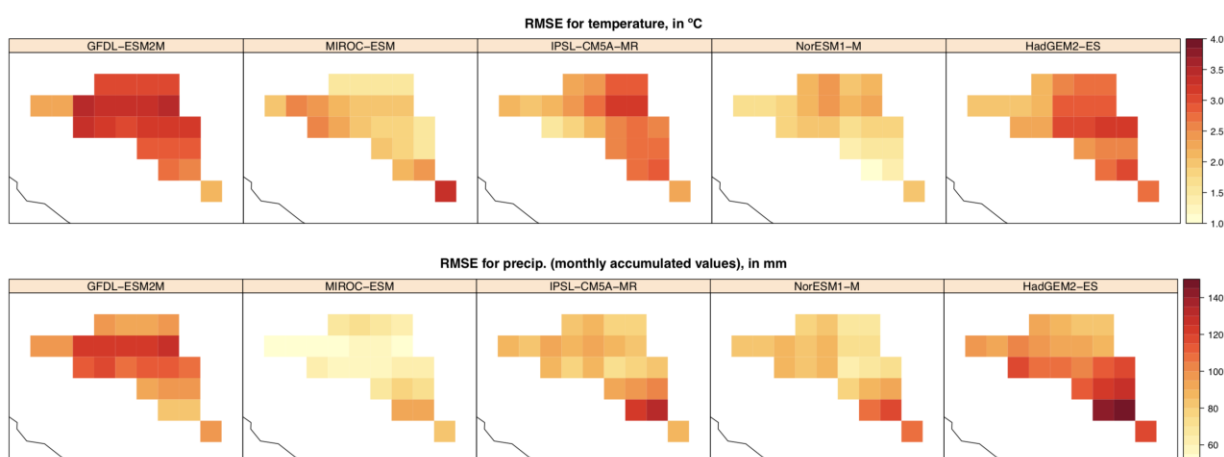
35. The best GCM was chosen by testing the capability of predicting historic precipitation and temperature from 1979 – 2018 and compare these to a historic dataset, the EWEMBI dataset. The MIROC-ESM GCM shows the smallest average Root Mean Squared Error (RMSE) when comparing the

⁸² For further details see the IPCC AR5 Chapter 9 "Evaluation of Climate Models" (https://www.ipcc.ch/site/assets/uploads/2018/02/WG1AR5_Chapter09_FINAL.pdf) and IPCC Data Distribution Center AR5 Reference snapshot http://www.ipcc-data.org/sim/gcm_monthly/AR5/Reference-Archive.html

precipitation and temperature to the EWEMBI dataset, this is visualized in Figure 6-6. This led to the selection of the MIROC-ESM GCM to predict future precipitation and temperature.

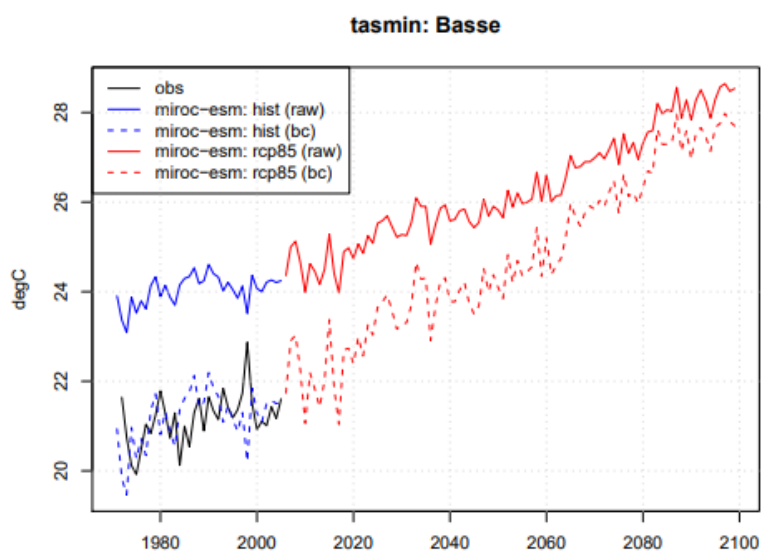
36. The output of the MIROC-ESM GCM was further improved through bias correction. This correction is based on the assumption that the predicted data has a systematic error, implying that the output can be corrected and improved. Figure 6-7 shows an example for the minimum temperature at Yundum with the raw model output (raw), the bias corrected output (bc) and observations. As can be seen, the bias corrected output fits much better to the observed data. This is due to a vertical shift in temperature and a change in the speed with which temperature rises.

Figure 6-6 GCM to EWEMBI Root Mean Square Error values (1979-2016) for temperature and precipitation across the Gambia River watershed (lighter colors denote smaller RMSEs)



Source: FAO analysis of EWEMBI dataset (FAO, 2020)

Figure 6-7: GCM raw output (raw), observations (obs) and bias corrected output (bc) for the minimum temperature in Basse (FAO, 2020)



Evaporation

37. Potential evaporation is estimated with Thornthwaite's method (Thornthwaite, 1948). This method gives a rough indication of the potential evaporation but is ideal in terms of required parameters. It only depends on temperature, days in the month and the averaged amount of daylight hours per month. The result is the monthly potential evaporation. Temperature is predicted by the MIROC-ESM GCM and the average amount of daylight hours per month are determined by using the NOAA Solar Calculator.

$$E_{pot} = 1.6 \left(\frac{L}{12} \right) \left(\frac{N}{30} \right) \left(\frac{10 \cdot Ta}{I} \right)^a$$

$$I = \sum \left(\frac{T_{ai}}{5} \right)^{1.514}$$

$$a = (6.75 \cdot 10^{-7}) \cdot I^3 - (7.71 \cdot 10^{-5}) \cdot I^2 + (1.792 \cdot 10^{-2}) \cdot I + 0.49239$$

Where:

Mean daily air temperature:	Ta	T
Number of days in the month:	N	-
Average daylight hours per month:	L	t
Heat index:	I	T
Mean air temperature for each month in the year:	Tai	T

Net precipitation

38. The net precipitation is calculated by subtracting evaporation from precipitation. Subtracting potential evaporation from precipitation would usually give an overestimate of the evaporation and therefore too low net precipitation. However, the evaporation is in the model also a calibration parameter and will be adjusted by multiplication of a factor (see paragraph 4.3). This justifies the use of potential evaporation in the determination of the net precipitation.

$$P_{net} = P - E_{pot}$$

4.2.2 River discharge

39. The Gambia river discharge has been recorded at the border of Senegal near Gouloumbou from 1970 until 2005 and for one and a half year starting July 2016 and ending December 2017. The data is not complete throughout the year, with most years lacking measurements in the dry season (December to June). The dataset was provided by Direction de la Gestion et de la Planification des ressources en Eau (DGPPE) through personal communication.

40. To predict river discharge for future scenarios a simple box model was developed and optimized based on the measured discharge and precipitation in Senegal ([Appendix B](#)). A monthly precipitation dataset for the wet season, from May to October, was purchased and made available for this study by the FAO. The dataset starting at January 1981 and ending at January 2017, contains the precipitation data for 6 locations; within The Gambia these are: Basse, Yundum, Janjanbur; within Senegal these are: Kedougou, Goudiry and Saraya. The precipitation data comes from ANACIM, the aviation and meteorology institute of Senegal. Several precipitation stations across Senegal are used to feed the model that ANACIM uses to extrapolate precipitation areas where there are no weather stations.

41. Geographically there is a distinct difference in precipitation. The north of the catchment receives less precipitation than the south of the catchment (see Figure 6-8). Furthermore, the east side of the catchment is more mountainous and functions as the driving force of the flow in the Gambia river. To create a trustworthy model for predicting river discharge it is important to take these features into account. Since the historical discharge was measured at Gouloumbou part of the catchment that receives rain goes not contribute to the river discharge at this point. Therefore, the catchment is split into two parts; a northern and southern part both lying in Senegal. From the several locations that the GCM predicted precipitation and temperature for two were chosen: Kedougou and Goudiry. Figure 6-9 shows a hypothetical split of the eastern side of the catchment, in which the discharge is partly generated by precipitation from Kedougou and partly by precipitation from Goudiry. In practice the model is optimized by calibrating and validating on the historical measurements, this results in a R-squared value of 86%. The actual contribution of each of the locations is determined by minimizing the error between the estimated discharge and the measured discharge with the `scipy.optimize.minimize` function in python.

42. The future predictions of river flow use the predicted precipitation and temperature data, generated by the MIROC-ESM GCM. For more details about the discharge model and its optimization [Appendix B](#).

Sea level rise and irrigational development

43. The sea level rise values that have been discussed in chapter 2 are split in yearly increments from 2006 to 2099 such that in 2099 the chosen sea level rise is reached. Furthermore, the average sea level rise from 1971 to now, which amounts to 0.16 m, is added.

44. Similarly, the development of irrigation surface which was discussed in chapter 2 is implemented. Table 6-2 Overview of increase in agricultural surface in the Gambia river catchment **Error! Reference source not found.** below shows the change in agricultural surface under irrigation for three scenarios.

Table 6-2 Overview of increase in agricultural surface in the Gambia river catchment

Scenario 1 (Current): no changes (i.e., no new land development beyond surface area currently under irrigation); data for The Gambia 2020 baseline from NRDS (2014); data for Senegal 2020 baseline based on a 2001 reference (see also Twente, 2005) to 250ha under production from 600 ha developed (FAO, 2001).																																																																																			
	A	B	Total																																																																																
2020	2300	250	2550	2021	2300	250	2550	2022	2300	250	2550	2023	2300	250	2550	2024	2300	250	2550	2025	2300	250	2550	2026	2300	250	2550	2027	2300	250	2550	2028	2300	250	2550	2029	2300	250	2550	2030	2300	250	2550	2031	2300	250	2550	2032	2300	250	2550	2033	2300	250	2550	2034	2300	250	2550	2035	2300	250	2550	2036	2300	250	2550	2037	2300	250	2550	2038	2300	250	2550	2039	2300	250	2550	2040	2300	250	2550
Scenario 2 (Expected): The Gambia has planned new land development between 2021-2024 (e.g., Islamic Development Bank, African Development Bank, financed Regional Rice Value Chain Development Project) gradually adding 2,685 ha; no further changes after 2024; Similarly, Senegal planned development based on assumption of bringing back into production the 350 ha of previous developed pump irrigation land that had been abandoned as referenced in FAO (2001) (see also Twente, 2005).																																																																																			
	A	B	Total																																																																																
2020	2300	250	2550	2021	2971	338	3309	2022	3643	425	4068	2023	4314	513	4826	2024	4985	600	5585	2025	4985	600	5585	2026	4985	600	5585	2027	4985	600	5585	2028	4985	600	5585	2029	4985	600	5585	2030	4985	600	5585	2031	4985	600	5585	2032	4985	600	5585	2033	4985	600	5585	2034	4985	600	5585	2035	4985	600	5585	2036	4985	600	5585	2037	4985	600	5585	2038	4985	600	5585	2039	4985	600	5585	2040	4985	600	5585
Scenario 3 (Maximum): Assumptions for The Gambia based on full development of irrigated potential 12,727 ha, based on maximum potential mentioned in NRDS (2014) up to 2024 (roughly 1/2 the 24,000ha targeted in the National Agricultural Investment Plan (2010); Assumption for Senegal based on future targets assumed in the 2005 Twente Study of 2,000 ha (roughly 1/2 of 4,100 potential irrigatable land referenced in FAO, 2001, and Twente, 2005).																																																																																			
	A	B	Total																																																																																
2020	2300	250	2550	2021	4325	542	4867	2022	6350	833	7183	2023	8375	1125	9500	2024	10400	1417	11817	2025	12425	1708	14133	2026	12727	2000	14727	2027	12727	2000	14727	2028	12727	2000	14727	2029	12727	2000	14727	2030	12727	2000	14727	2031	12727	2000	14727	2032	12727	2000	14727	2033	12727	2000	14727	2034	12727	2000	14727	2035	12727	2000	14727	2036	12727	2000	14727	2037	12727	2000	14727	2038	12727	2000	14727	2039	12727	2000	14727	2040	12727	2000	14727

Figure 6-8: A typical month in the rainy season (September 2019), retrieved from NASA: IMERG. The darker blue pixels show precipitation. It is clear that the northern part of the catchment receives less precipitation than the south side.

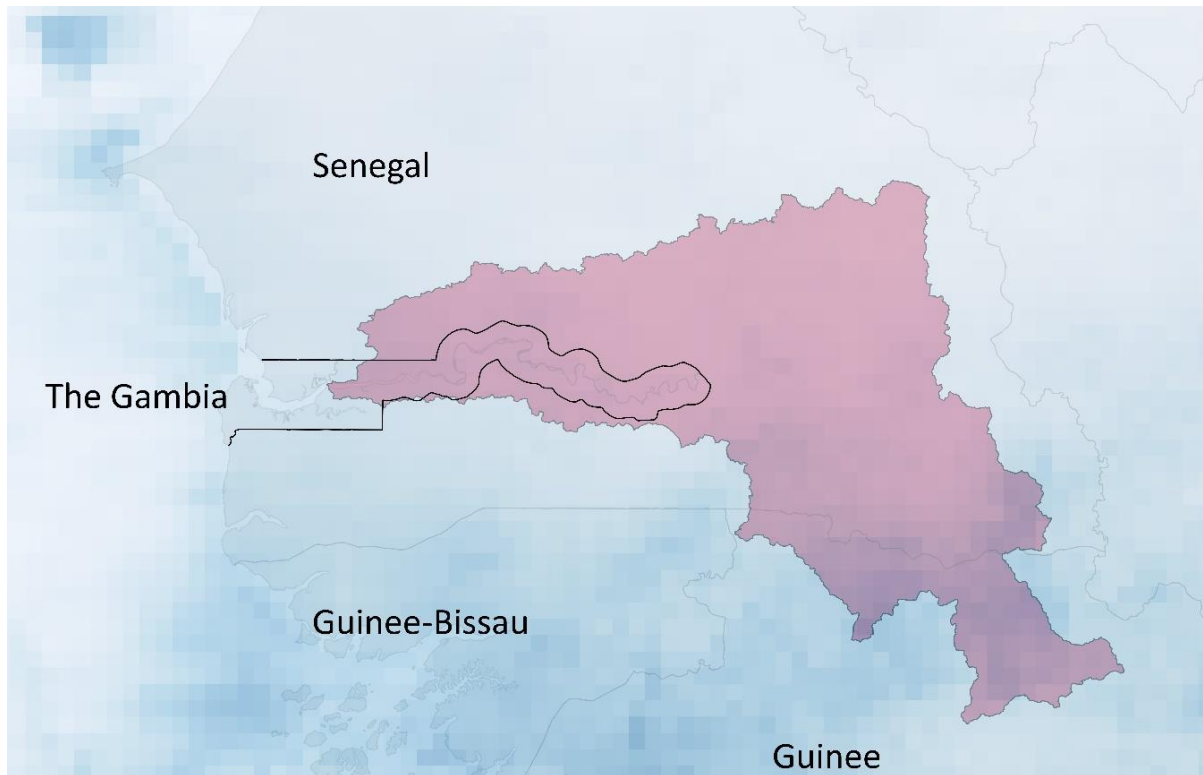
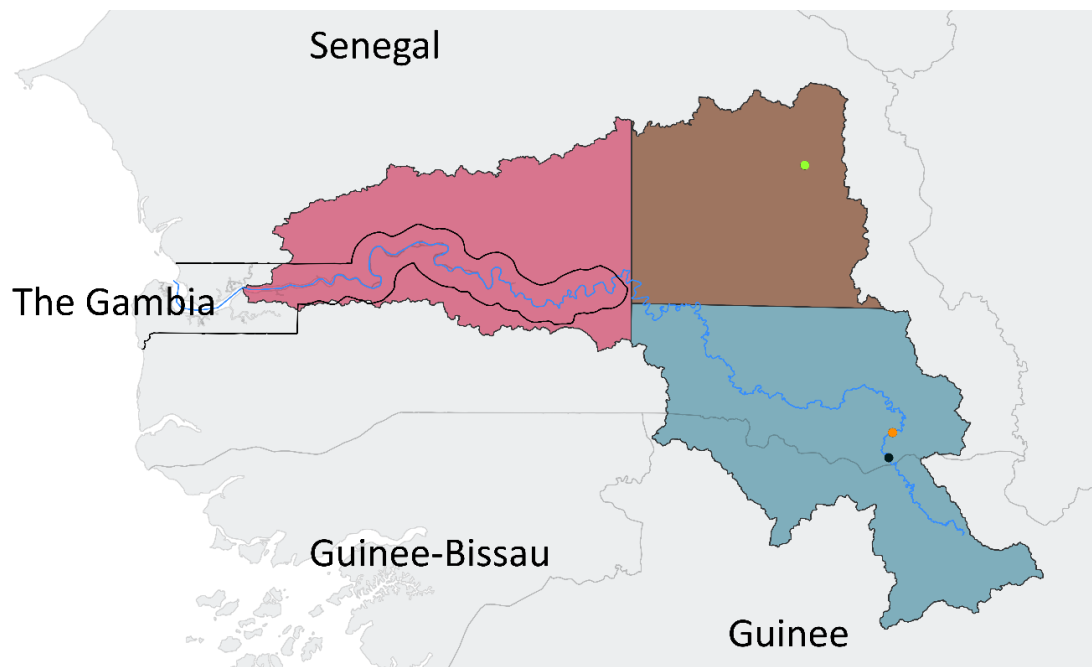


Figure 6-9: Hypothetical split of the catchment. The bright green dot shows Goudiry, the orange dot Kedougou and the black dot the location of the hydropower dam. In blue the Gambia river.



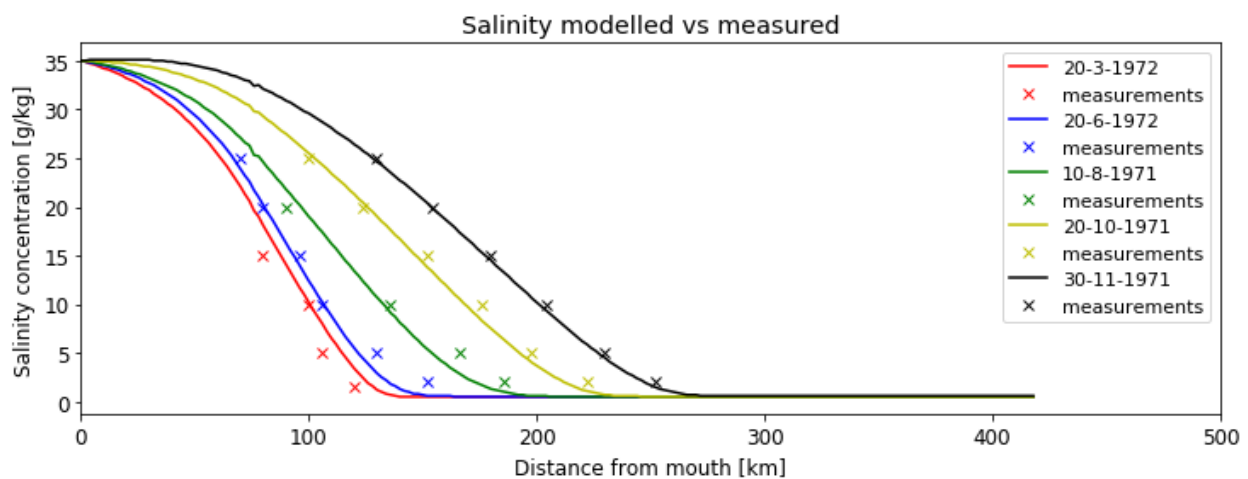
4.3 Calibration and validation of the model

45. The calibration of the model makes use of the accurate survey data from 1971. On a boat moving with high water slack they performed multiple measurements along the Gambia river multiple times. This measuring technique yields good salinity data because at high water slack the tidal inflow stocks ($Q_{\text{tidal}} = 0$) and therefore at this moment the salt intrusion is at its peak. Figure 6-10 shows the measurements as 'x' and the calibrated model as lines, close resemblance can be seen. Calibrating the model is done by changing two factors that scale the dispersion at the mouth (D_0) and evaporation: F_d and F_E , presented below. This is done manually because due to the steady and unsteady-state nature of the Gambia river a perfect fit is not possible.

$$F_d = 8.64$$

$$F_E = 2.5$$

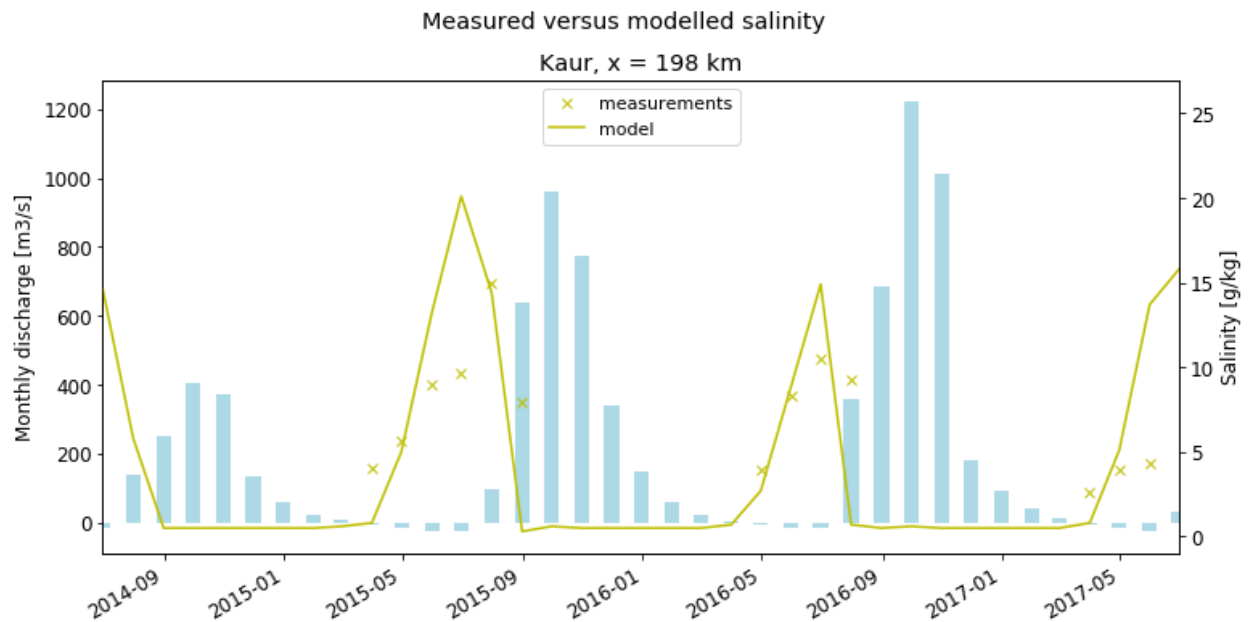
Figure 6-10: Model predictions for salt concentrations over distance, 'x' marks the measurements, the lines are the predictions of the model with the calibration settings mentioned above



The validation data however, makes use of salinity measurement systems (OTT Ecolog 500 & 800) installed along the Gambia river. According to the producer of the system these are accurate, trustworthy instruments that after installation are protected against vandalism, their batteries will last 10 years and it automatically sends data. However, in practice this is different. Within a year many of these instruments were reported to be broken, did not send data or needed spare parts that were not available. In the end six instruments measured salinities, however not continually. From these six datasets only four could be used of which the data is disputable. The recordings contain a salinity measured every 15 minutes. The maximum of these measurements should coincide with the calibrated model since the maximum salt intrusion occurs during high water slack. By taking the maximum of these measurements a small horizontal shift to the right takes place. The validation of predicted salt concentration 198 km from the mouth of the river can be seen in

46. Figure 6-11.

Figure 6-11: Validation of the model by comparison with measurements 198 km upstream of the mouth of the river. The salt concentrations from the measurements and model can be read from the y-axis on the right and are plotted respectively as 'x' and as a continuous line. The left y-axis shows the river discharge (blue bars).



4.4 Analysis of model output and selecting key features

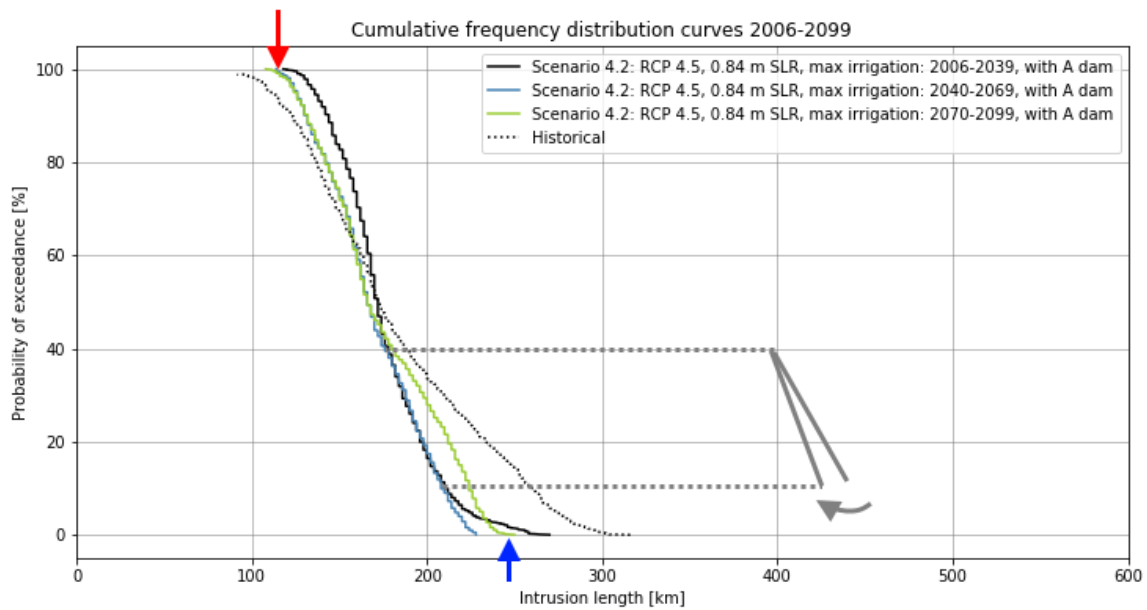
47. Each model run results in a lot of information. Graphical representation of this information gives a clear idea of the effects of certain parameters. Three graphs will be introduced and their key features explained. These key features will be used when discussing the results.

4.4.1 Cumulative frequency distribution curve

48. Starting with Figure 6-12, a cumulative frequency distribution curve (CFD curve). It shows on the y-axis the probability of exceedance or rarity of a certain intrusion length occurring, with 100% always occurring and 0% never occurring. The key features are the minimum and maximum probability of exceedance, these represent the minimum and maximum salt intrusion lengths that occur in the respective time period. In Figure 6-12 the minimum and maximum salt intrusion lengths are depicted by a blue and red arrow. It is important to realize that these intrusion lengths are determined based on a salt concentration of 1 g/L.

49. Another important key feature is the slope. A steep slope indicates little variation in salt intrusion length within the time period while a mild slope indicates stronger varying salt intrusion lengths. In Figure 6-12 the grey lines show how a steepening of the lower slope might look like. The upper slope is defined as the gradient between 90- and 60% probability of exceedance whereas the lower slope is defined as the gradient between 40- and 10% probability of exceedance, to exclude the influence of extremes.

Figure 6-12: Cumulative frequency distribution curve (CFD-curve) with key features indicated.



4.4.2 Median salt intrusion

The second important graph is the median seasonal salt intrusion (

50. Figure 6-13). This graph shows the monthly median salt intrusion length for the same time periods as the previous graph. The intrusion length in km is now represented by the y-axis and the months on the x-axis. The key features of this graph are respectively the peak during the dry season and dip during the wet season in the median salt intrusion length, visualized by the red and blue arrow. This is again for a salt concentration of 1 g/L. The magnitude of the difference between scenarios is a good indication for the expected shift in salt intrusion lengths because the median is the most occurring salt intrusion length. Furthermore, the median is less affected by extremes which makes it a good representative parameter.

In

51. Figure 6-13 a shift of the wet season dip is visible, marked by the grey arrow. This is another interesting key feature indicating a possible shift of the wet and dry season.

4.4.3 Salt concentration curve

52. The third graph that contains important information is a plot of all salt concentrations along the length of the estuary at 10-day intervals across the time period indicated. At the mouth of the estuary a constant salinity of 35 g/L is present. Depending on the scenario hypersaline events might occur. The key feature of this graph is the approximate range where hyper salinity occurs, and the magnitude of the hyper salinity (concentration). Figure 6-14 gives an example where the hyper saline region is marked in red and the maximum concentration in blue. In the final overview this graph has also been split into three time periods for easier comparison.

Figure 6-13: Example salt intrusion curve with key features indicated. The y-axis is the median salt intrusion length and the x-axis has the month in the year.

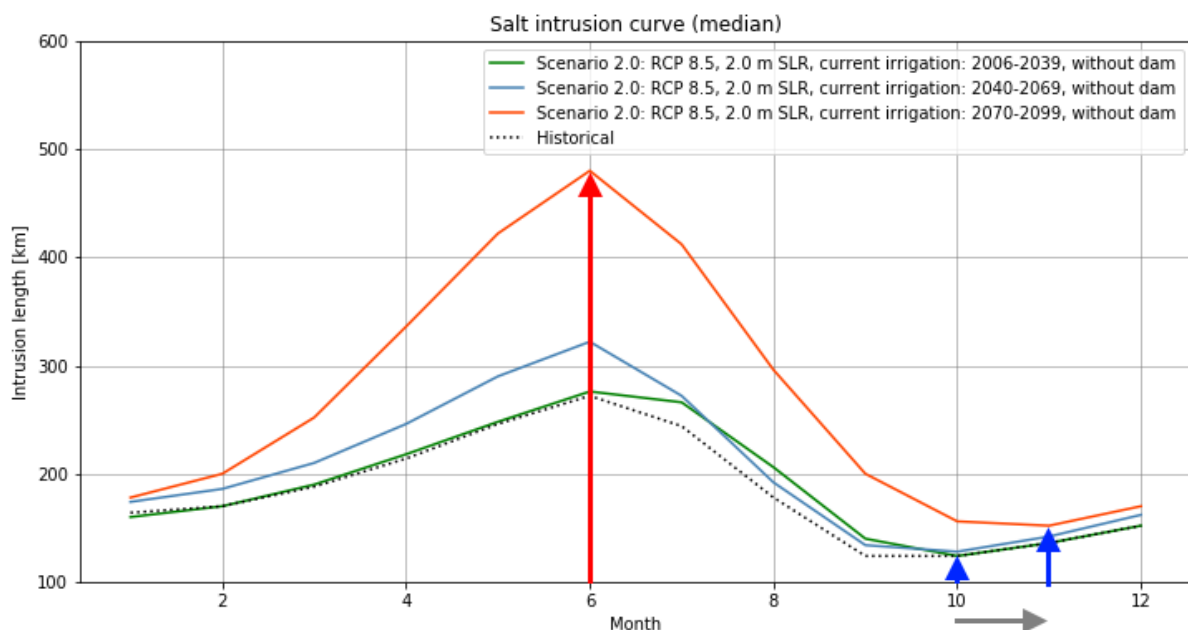
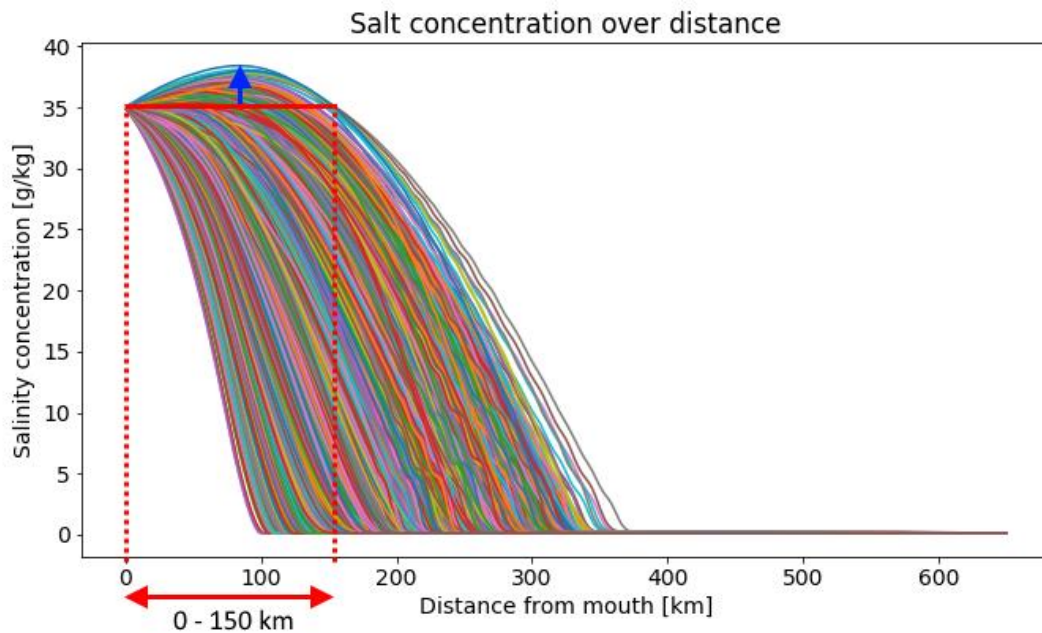


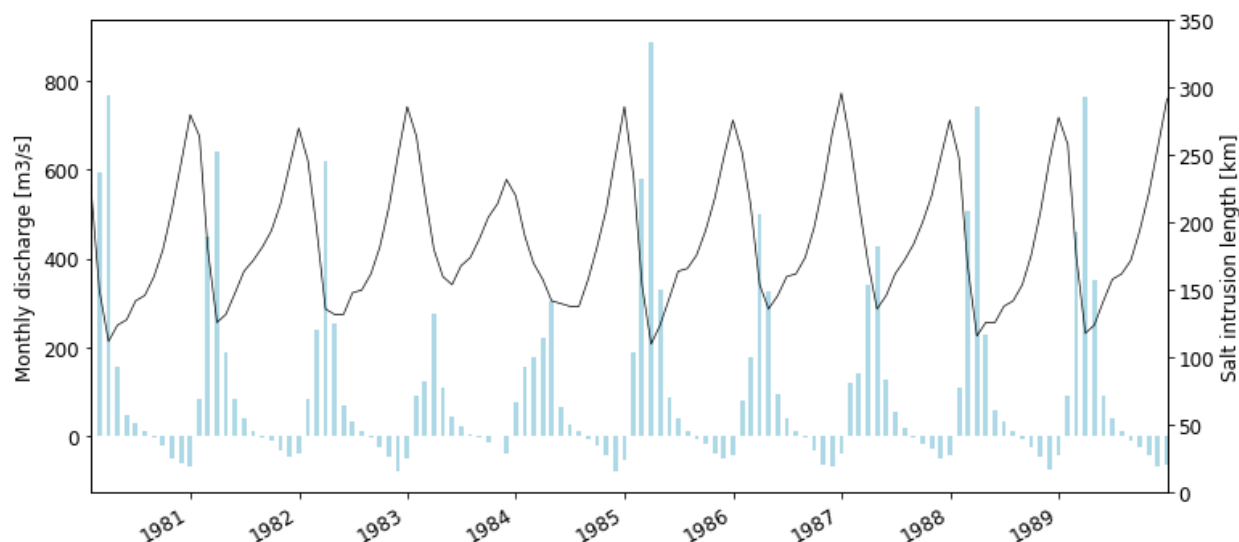
Figure 6-14: Example of the salt concentration curve with key features indicated. Each line represents the salt concentration over distance of a timestep in the model. All lines together give an impression of the hypersaline region that occurs during the modelled period.



4.4 Temporal distribution

53. The wet- and dry-season weather pattern has a strong effect on salt intrusion lengths and concentrations. During the dry season salt intrudes inland while in the wet season the salt front is pushed back. This is clearly represented in Figure 6-15. This year-to-year pattern with peaks during the dry season and dips during the wet season does not change during model runs. There can be vertical shifts in which wet season dips do not retreat as much and dry season peaks get higher but these are captured in the key features, such as minimum and maximum salt intrusion as well as the median salt intrusion curve mentioned before. The results however, will discuss date ranges which show the maximum and minimum salt intrusion lengths occurring in this period. It is imperative to realize that the presented results do not necessarily occur in the same year within the discussed time period.

Figure 6-15: Temporal distribution of salt intrusion. This graph shows the discharge and salt intrusion length (salt concentration of 1 g/L) for a small historic time range. The selection is interesting because it is well visible that 1984 had a relatively 'wet' dry season and a relatively 'dry' wet season.



4.5 Historical salt intrusion

54. The model predictions for historical salt intrusion are included in this report because they were the only reliable salt measures that have been taken in the Gambia river. These model results will be used as a baseline so that the results of the current model runs have a better baseline. It is however, absolutely wrong to base conclusions on the differences between these results due to the different datasets that have been used for the historical model results and the current model results.

Table 6-3 below gives an overview of the different datasets and their sources.

Figure 6-16 visualizes the historic and current model, the data applied to the models and certain transformations of the data undergoes. This displays how much change has occurred in the use of data.

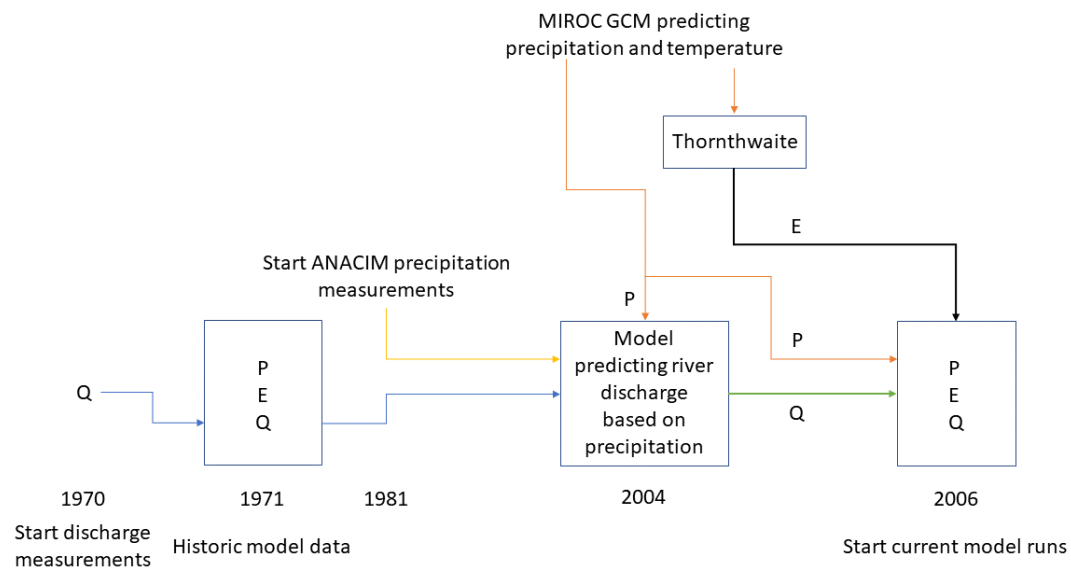
55. Figure 6-16 only shows the data that is used in both models, in the current model also sea level rise is taken into account which increases the gap between the results of the two models. Drawing conclusions based on comparison with the historic values is therefore absolutely wrong.

Table 6-3: Overview of the several datasets and their source, sorted by date range.

Data	Source	Comments	Date range
Historic salt measurements	Survey	Personal communication H.H.G. Savenije	1971
River geometry	Survey	Personal communication H.H.G. Savenije	1971
Historic river discharge		Personal communication Direction de la Gestion et de la Planification des ressources en Eau (DGPPE)	1970-2004 2016-2017
Precipitation for calibration of GCM	ANACIM	Dataset acquired by the FAO.	1981-2017
Current salt measurements		Personal communication Direction de la Gestion et de la Planification des ressources en Eau (DGPPE)	All within the period 2014-2018
Precipitation & Temperature	MIROC GCM		2006 - 2099
Evaporation	Thornthwaite	Based on temperatures from the MIROC GCM.	2006 - 2099
Freshwater discharge	Block model (see Appendix B)	Based on the precipitation from the MIROC GCM.	2006-2099

Figure 6-16: Flow chart of precipitation, evaporation and river discharge. The years mentioned at the bottom correspond to the date ranges in

Table 6-3. The colors visualize where data transforms.



4.6 Adjustments and simplifications of the model

56. There are a couple of differences between the theory and how the model applies the theory. These differences are treated in this paragraph together with an adjustment made in the calculations performed by the model.

57. The SALNST model is a numerical model. In combination with the dependency between the dispersion and salinity calculations this creates a loop in which errors are propagated and enhanced. This can be seen in the salt concentration plots (e.g., Figure 6-14). If salt intrusion lengths increase the error increases due to the extra numerical calculations and vice versa.

58. Furthermore, the model can account for unsteady-state dispersion but it does not detect when unsteady-state dispersion needs to be applied. Instead, it makes use of a combination of steady- and unsteady-state calculations where the steady-state calculations are used to kickstart the unsteady-state calculations.

59. The implementation of sea level rise is a simplification as well. The several values that are used for sea level rise are split in fractions that are added after each passing year. In addition, the expansion of the river evaporative surface due to sea level rise, which has been discussed in the section

60. *Additional geographical changes*, is a simplification as well.

61. An additional adjustment to the model has been made in its calculation. As has been presented in chapter 3 the salt balance equation to be solved is:

$$r_s \frac{\partial s}{\partial t} - q \frac{\partial s}{\partial x} - D \frac{\partial^2 s}{\partial x^2} + r_s \frac{P_n}{h_0} s = 0$$

Where:

$$q = (1 - K) \cdot \frac{Q_f + r_s B P_n b}{A} - \frac{D}{a} = (1 - K) \cdot \frac{Q}{A} - \frac{D}{a}$$

This can be rewritten to:

$$q = 1 \cdot \frac{Q_R}{A} - \frac{D}{a} - \frac{dD}{dx}$$

The model makes use of a dD/dx that is solely based on steady-state calculations. To account for the non-steady state calculations as well this has to be adjusted. This is implemented as follows. For better understanding of how the model calculates the salt intrusion consult Appendix D.

$$\frac{dD}{dx} = \frac{\left(\frac{dD_s}{dx} + C_{ns} \frac{dD_{ns}}{dx} \right)}{1 + C_{ns}} = \frac{\left(-K \cdot \frac{Q(x)}{A(x)} + C_{ns} D_{ns} K \cdot \frac{\Delta C(x)}{C(x) - C_r} \right)}{1 + C_{ns}}$$

Where:

Non steady state dispersion:

D_{ns}

Non steady state weight:

C_{ns}

4.7 Scenario overview

62. To answer all research questions numerous scenarios have been modelled. This paragraph treats the parameters used in these scenarios and presents an overview of the modelled scenarios.

4.7.1 Scenario parameters

63. Table 6-4 below, presents the parameters that are used in the scenarios. Sea level rise, representative concentration pathways for future weather and irrigation development have been treated. Dam operations will consist of two operational schemes, 'DO A' focusing on the flow scheme according to the environmental study in 2014 (OMVG) and 'DO B' focusing solely on power production, maximizing P while keeping it as constant as possible throughout the dry and wet season, see the formula below. More detailed information on how the reservoir is modelled and how the operational schemes have been created can be found in Appendix C.

$$P = \rho g \Delta h Q \eta$$

Where:

$$\Delta h = h_{\text{reservoir}} - h_{\text{turbine}}$$

Table 6-4: Model parameters and their values

Abbreviation	Parameters	1	2	3
SLR	Sea level rise	0 m	0.84 m	2 m
FW	Future weather	RCP 4.5	RCP 8.5	N/A
DO	Dam operations	A	B	N/A
ID	Irrigation development	Current	Expected	Max

4.7.2 Scenario overview

In

64. Table 6-5 the overview of all the modelled scenarios is presented. The goal of all these scenarios is to determine what salt intrusion lengths and concentrations can be expected in the years up to 2100, which parameter has the strongest contribution, if the estuary will or can turn hypersaline and what The Gambia can expect to change in the coming years. Several categories in the second column have been defined to show the purpose of the scenarios. H+Ref are the reference scenarios meant to compare other scenarios to, it functions as a 'baseline'. Reservoir filling, both SLRs and Ag dev are scenarios that identify the effect of the filling of the reservoir, the influence of sea level rise and agricultural development. Most of the scenarios are run for dam operational scheme A and B to identify what difference ecological flows versus solely power production has on the estuary. The output from each scenario is presented across three periods – near-, mid- and far-future (2006-2039, 2040-2069, and 2070-2099).

Table 6-5: Overview of all scenarios

Scenario ID:	Category:	Sea level rise:	Future weather:	Dam operations	Irrigation development:	Comment:
H	H+Ref	0 m	Historical	No dam	Current	
0.0	H+Ref	0 m	RCP 8.5	No dam	Current	
0.1	H+Ref	0 m	RCP 4.5	No dam	Current	
0.2	H+Ref	0 m	RCP 8.5	No dam	Expected	
1.0	Reservoir filling	0 m	RCP 8.5	Dam reservoir filling	Expected	2024
1.1	Reservoir filling	0 m	RCP 8.5	Dam reservoir filling	Expected	2024-2025
1.2	Reservoir filling	0 m	RCP 8.5	Dam reservoir filling	Expected	2024
1.3	Reservoir filling	0 m	RCP 8.5	Dam reservoir filling	Expected	2024-2025
2.0	2 m SLR	2 m	RCP 8.5	No dam	Current	
2.1	2 m SLR	2 m	RCP 8.5	A	Current	
2.2	2 m SLR	2 m	RCP 8.5	B	Current	
3.0	0.84 m SLR	0.84 m	RCP 4.5	No dam	Current	
3.1	0.84 m SLR	0.84 m	RCP 8.5	No dam	Current	
3.2	0.84 m SLR	0.84 m	RCP 4.5	A	Current	
3.3	0.84 m SLR	0.84 m	RCP 4.5	B	Current	
3.4	0.84 m SLR	0.84 m	RCP 8.5	A	Current	
3.5	0.84 m SLR	0.84 m	RCP 8.5	B	Current	
4.0	Ag dev	0.84 m	RCP 4.5	A	Expected	
4.1	Ag dev	0.84 m	RCP 4.5	B	Expected	
4.2	Ag dev	0.84 m	RCP 4.5	A	Max	
4.3	Ag dev	0.84 m	RCP 4.5	B	Max	
4.4	Ag dev	0.84 m	RCP 8.5	A	Expected	
4.5	Ag dev	0.84 m	RCP 8.5	B	Expected	
4.6	Ag dev	0.84 m	RCP 8.5	A	Max	
4.7	Ag dev	0.84 m	RCP 8.5	B	Max	
4.8	Ag dev	2 m	RCP 8.5	No dam	Expected	
4.9	Ag dev	2 m	RCP 8.5	No dam	Max	
4.10	Ag dev	2 m	RCP 8.5	A	Expected	
4.11	Ag dev	2 m	RCP 8.5	B	Expected	
4.12	Ag dev	2 m	RCP 8.5	A	Max	
4.13	Ag dev	2 m	RCP 8.5	B	Max	

Part 5 Results & Discussion

65. The analysis of results follows the modelled parameters (future weather, sea level rise, dam operations and irrigation development) and research questions. An analysis is performed for each parameter, split into sub-sections addressing the research questions. Figures illustrating the most relevant results are presented here for each parameter. These figures are used to illustrate processes and highlight some of the more significant possible outcomes or trends. A complete collection of the results from the analysis can be found in Appendix Y. The key features of the analysis, presented in previous chapters, are used here to organize the presentation of results, and are summarized in **Error! Reference source not found.** below. A summary of the most significant effects of the modelled parameters is presented after the discussion of the last model parameters. The chapter finishes with an expert interview on the morphological changes due to climate change and the hydropower dam.

66. Furthermore, it is important to keep in mind that to obtain these results numerous steps have been taken. These introduce uncertainties in e.g., projected precipitation, projected evaporation, freshwater discharge model, estimation of river expansion, use of several different datasets etc. Therefore, small differences in salt intrusion do not necessarily signify any change.

67. Finally, **it is imperative to understand** that the historical values are the baseline that is used to compare changes to. It is by all means wrong to compare with historical values due to the use of different data. This is explained in section 4.5 and visualized in figure 19.

Table 6-6 Overview and explanation of all key features.

Key Feature	Description
F1	The difference in salt intrusion length for the maximum probability of exceedance relative to the historical values. This value is the salt intrusion length that is always exceeded and can be considered the minimum salt intrusion length.
F2	Difference in salt intrusion length for the minimum probability of exceedance relative to the historical values. This can be considered the maximum salt intrusion length.
F3	The average gradient of the CFD-curve between 90- and 60 % probability of exceedance relative to the historical slope. The CFD-curve always has a negative gradient (see Figure 6-12) therefore, a negative value indicates steepening of the slope while a positive value indicates flattening of the slope. The gradient represents the variance of the more often occurring salt intrusion lengths. In combination with F1 this can show for example an increase in minimum salt intrusion length with a decreasing (steepening) slope, this indicates higher salt intrusion lengths with lower variance.
F4	The average gradient of the CFD-curve between 40- and 10 % probability of exceedance relative to the historic gradient. The gradient represents the variance of the less often occurring salt intrusion lengths.
F5	Difference in minimum median salt intrusion length of the scenario relative to the historical values. This gives an indication how salt intrusion lengths in the wet season evolve and gives a better indication for trends than solely the minimum intrusion lengths (F1) in combination with the upper slopes of the CFD-curve (F3).
F6	Difference in maximum median salt intrusion length of the scenario relative to the historical values.

F7	The month when the minimum median salt intrusion occurs. The moment on which the minimum salt intrusion occurs could shift due to climate change, lengthening or shortening the dry and wet season.
F8	The month when the maximum median salt intrusion occurs.
F9	The maximum occurring hypersaline region (of all timesteps in the model) for the selected scenario as measured from the coast until the point that the salt concentrations fall below ocean salinity concentrations.
F10	The maximum occurring salt concentration (of all timesteps in the model) for the selected scenario. This is an indicator for the level of hyper salinity.

5.1 Future weather

68. Future weather is the first model parameter that will be discussed. Starting with its effects on the minimum and maximum salt intrusion lengths and followed by the effect on probability of exceedance, effect on seasonality and effect on salt concentration. The scenarios and their results for this model parameter are presented in table X below. Four combinations have been made with model parameters, only changing the RCP used. To see the influence of future weather on salt intrusion the differences between RCP 4.5 and 8.5 are analyzed.

*Table 6-7: Model results for assessing the effects of future weather on salt intrusion lengths and salt concentrations.
Column 3 to 5 show all model parameters that are altered*

scenario ID	Period:	RCP	SLR	ID / DO	CFD-curve				Monthly median min/max				S-x curve	
					F1 [km]	F2 [km]	F3 [-]	F4 [-]	F5 [km]	F6 [km]	F7 [Mos]	F8 [Mos]	F9 [km]	F10 [g/L]
H	1971-2017	N/A	N/A	N/A	92	316	-0.74	-0.41	124	272	9	6	72	35.6
0.1	2006-2039	4.5	0.0	Cur	104	314	-0.94	-0.41	124	280	10	6	98	36.1
	2040-2069			/	96	308	-0.83	-0.39	112	278	10	6	92	36.0
	2070-2099			N/A	96	328	-0.78	-0.33	110	298	10	6	124	36.6
0.0	2006-2039	8.5	0.0	Cur	104	316	-0.88	-0.42	120	274	10	6	92	36.0
	2040-2069			/	92	336	-0.79	-0.37	110	282	10	6	128	36.8
	2070-2099			N/A	100	368	-0.87	-0.30	114	308	10	6	168	38.3
3.0	2006-2039	4.5	0.84	Cur	108	314	-0.94	-0.41	126	280	10	6	96	36.0
	2040-2069			/	100	308	-0.83	-0.41	116	278	10	6	90	35.9
	2070-2099			N/A	100	326	-0.78	-0.34	116	298	10	6	116	36.4
3.1	2006-2039	8.5	0.84	Cur	106	316	-0.84	-0.42	122	276	10	6	90	35.9
	2040-2069			/	96	336	-0.79	-0.38	114	284	10	6	122	36.6
	2070-2099			N/A	104	366	-0.82	-0.31	120	310	10	6	156	37.4
4.0	2006-2039	4.5	0.84	Exp	118	258	-1.25	-1.00	142	204	10	7	62	35.6
	2040-2069			/	112	222	-1.00	-0.94	128	204	10	6	56	35.5
	2070-2099			A	108	242	-0.98	-0.70	126	218	10	6	74	35.8
4.4	2006-2039	8.5	0.84	Exp	118	258	-1.07	-1.00	134	204	10	7	52	35.4
	2040-2069			/	108	244	-0.94	-0.88	124	206	10	6	76	35.9
	2070-2099			A	112	264	-1.14	-0.59	130	234	11	6	102	36.7
4.1	2006-2039	4.5	0.84	Exp	116	330	-1.00	-0.39	134	286	10	7	104	36.2
	2040-2069			/	108	324	-1.00	-0.36	122	266	10	6	88	35.9
	2070-2099			B	108	334	-0.98	-0.30	122	288	10	6	118	36.4
4.5	2006-2039	8.5	0.84	Exp	114	328	-1.07	-0.39	128	282	10	7	92	35.8
	2040-2069			/	106	342	-1.00	-0.30	120	264	10	6	128	36.7
	2070-2099			B	112	366	-1.05	-0.28	126	286	10	7	162	37.5

5.1.1 Future weather: Minimum and maximum salt intrusion lengths

69. Comparing the results of RCP 4.5 to the results of RCP 8.5 for the scenarios in Table 6-7, more or less the same pattern for all scenarios can be detected for the minimum salt intrusion length (F1). There is first a negligible decrease⁸³ in the first two periods for RCP 8.5 after which it increases negligibly in the third period⁸⁴. The maximum salt intrusion length (F2) shows a clear increase when RCP 8.5 is applied. In the first period the increase is negligible for all scenarios. In the second and third period for the scenarios without dam the difference between RCP 4.5 and RCP 8.5 is respectively 9% and 12%.

70. The scenarios with a dam implemented show a different course. For the ecological flow operated dam, DO A, the first period shows no difference between RCP 4.5 and RCP 8.5. The second and third period respectively increase with 10% and 9% for RCP 8.5 when comparing these to the same periods for RCP 4.5. For the power production focused operations, DO B, the first period shows a negligible decrease for RCP 8.5 compared to RCP 4.5. In the second and third period this is respectively 6% and 10%. This is an indication that the dam operations dampen the effect of future weather on maximum salt intrusion lengths.

5.1.2 Future weather: Effect on probability of exceedance

71. For the scenarios without dam the upper slopes of the CFD-curve (F3) the first two periods show a decrease in gradient for RCP 8.5 when comparing with RCP 4.5 this varies between -5% and -11%. This is an indication that for RCP 8.5 more variety in smaller salt intrusions lengths occur. The third period shows an increase between 6% and 12% which indicates less variety in smaller salt intrusion lengths. The lower slopes of the CFD-curve (F4) show the opposite. In the first period a negligible decrease in slope occurs after which the slope steepens between 6% and 8%.

72. For the scenarios with dam the upper slopes behave differently. For the ecologically operated dam, DO A, a relatively strong decrease of 14% can be seen while for the power production operated dam, DO B this is a steepening of 7% for RCP 8.5. The second period shows again a decrease of 14% for DO A for RCP 8.5 while for DO B no change is detected. In the third period for both lower slopes an increase in slope is detectable. This is respectively 15% and 7% for DO A and DO B. The upper slopes show a decreasing slope for the second and third period which varies between 6% and 16% for RCP 8.5 compared to RCP 4.5.

5.1.3 Future weather: Effect on seasonality

73. The effect of future weather on the median salt intrusion lengths (F5 and F6) is marginal. A small difference of 6% when comparing RCP 8.5 to RCP 4.5 in the first period for the ecologically operated dam. Similarly, only an increase of 7% is noticeable for the third period for the ecologically operated dam when comparing RCP 8.5 to RCP 4.5. The remainder of median wet or dry season peaks change negligible. Furthermore, there is no shift in the dry or wet season peak.

5.1.4 Future weather: Effect on salt concentration

74. The effect of the weather on the size of the hypersaline region (F9) and the maximum salt concentration (F10) is significant. For all scenarios in the first period RCP 8.5 shows a decrease in the

⁸³ With decrease of the gradient a flattening of the slope is meant. This is an indication of more variety of the respective salt intrusion lengths.

⁸⁴ Negligible is defined here as less than 5% in- or decrease between the reference and selected scenario.

size of the hypersaline region when compared to RCP 4.5. This is -6% for the scenarios without dam and varies between -12% and 16% for the scenarios with dam. In the second and third period a strong increase can be noticed for all scenarios regardless of the dam implementation which varies between 35% and 45%.

75. The only increase in salt concentration can be noticed when comparing RCP 8.5 to RCP 4.5 between scenarios 0.0 and 0.1. The remainder of the scenarios shows negligible change. This indicates a dampening effect of sea level rise on the increase of salt concentrations.

5.1.3 Future weather: Summary

76. Comparing RCP 8.5 to RCP 4.5 shows increases in maximum salt concentrations varying between 9% to 12%. Dampening effects of the hydropower dam on maximum salt intrusion lengths are visible. The variance of the smaller salt intrusion lengths is larger for RCP 8.5 in the first two periods before the gradient of the CFD-curve steepens. This is true for all scenarios except when DO B is implemented, then the lower slope of the CFD-curve continually steepens. The opposite is true for the variance of the larger salt intrusion lengths, this increases for all scenarios. This is an indication that RCP 8.5 leads to more variance in higher salt intrusion lengths. The median salt intrusion curve shows no significant changes and there is no change in seasonality between RCP 8.5 and RCP 4.5. The hypersaline region is strongly influenced by the type of weather. RCP 8.5 shows increases in the size of the hypersaline region of up to 45% when comparing to RCP 4.5. The salt concentration changes negligible except for the comparison between scenarios 0.0 and 0.1. This is an indication of a dampening effect of increasing sea level rise on future weather.

5.2 Sea level rise

77. Sea level rise is the second model parameter that will be discussed. Starting with its effects on the minimum and maximum salt intrusion lengths and followed by the effect on probability of exceedance, effect on seasonality and effect on salt concentration. The scenarios and their results for this model parameter are presented in Table 6-8 below.

Table 6-8: Model results for assessing the effects of sea level rise on salt intrusion lengths and concentrations. Column 3 and 4 show all model parameters that are altered⁸⁵.

scenario ID				CFD-curve				Monthly median min/max				S-x curve	
	Period:	SLR	FW	F1 [km]	F2 [km]	F3 [-]	F4 [-]	F5 [km]	F6 [km]	F7 [Mos]	F8 [Mos]	F9 [km]	F10 [g/L]
H	1971-2017	N/A	N/A	92	316	-0.74	-0.41	124	272	9	6	72	35.6
0.1	2006-2039	0	RCP 4.5	104	314	-0.94	-0.41	124	280	10	6	98	36.1
	2040-2069			96	308	-0.83	-0.39	112	278	10	6	92	36.0
	2070-2099			96	328	-0.78	-0.33	110	298	10	6	124	36.6
3.0	2006-2039	0.84	RCP 4.5	108	314	-0.94	-0.41	126	280	10	6	96	36.0
	2040-2069			100	308	-0.83	-0.41	116	278	10	6	90	35.9
	2070-2099			100	326	-0.78	-0.34	116	298	10	6	116	36.4
0.0	2006-2039	0	RCP 8.5	104	316	-0.88	-0.42	120	274	10	6	92	36.0
	2040-2069			92	336	-0.79	-0.37	110	282	10	6	128	36.8
	2070-2099			100	368	-0.87	-0.30	114	308	10	6	168	38.3
3.1	2006-2039	0.84	RCP 8.5	106	316	-0.84	-0.42	122	276	10	6	90	35.9
	2040-2069			96	336	-0.79	-0.38	114	284	10	6	122	36.6
	2070-2099			104	366	-0.82	-0.31	120	310	10	6	156	37.4
2.0	2006-2039	2.0	RCP 8.5	106	316	-0.84	-0.43	124	276	10	6	86	35.9
	2040-2069			98	452	-0.68	-0.27	128	322	10	6	240	37.7
	2070-2099			122	578	-0.57	-0.18	152	480	11	6	476	62.2

5.2.1 Sea level rise: Minimum and maximum salt intrusion lengths

78. The minimum salt intrusion length increases for all scenarios negligibly⁸⁶, with the exception of the last two periods of scenario 2.0 which show respectively 7% and 22% increase compared to the scenario without sea level rise. The same pattern repeats for the maximum salt intrusion length, negligible differences between a sea level rise of 0 and 0.84 m. However, scenario 2.0 shows an increase of respectively 35% and 57% when comparing to the 0 m sea level rise scenario. The comparison of **Error! Reference source not found.** show the huge differences of scenario 2.0 with scenario 3.1. It should be noted that the differences in maximum salt intrusion length decreased negligibly for both sea level rises of 0.84 m when comparing to their 0 m sea level rise equivalent. This could indicate a dampening effect of rising sea levels.

⁸⁵ The model parameters dam operations and irrigation development are kept constant on respectively 'no dam' and 'current irrigation'.

⁸⁶ Negligible is defined here as less than 5% in- or decrease between the reference and selected scenario.

Figure 6-17 CFD-curves for scenario 3.1 of which the values can be read from Table 6-8 above. On the vertical axis shows the probability of exceedance. At 100% the value is always exceeded: the minimum salt intrusion length. Slightly above 0% lies the maximum.

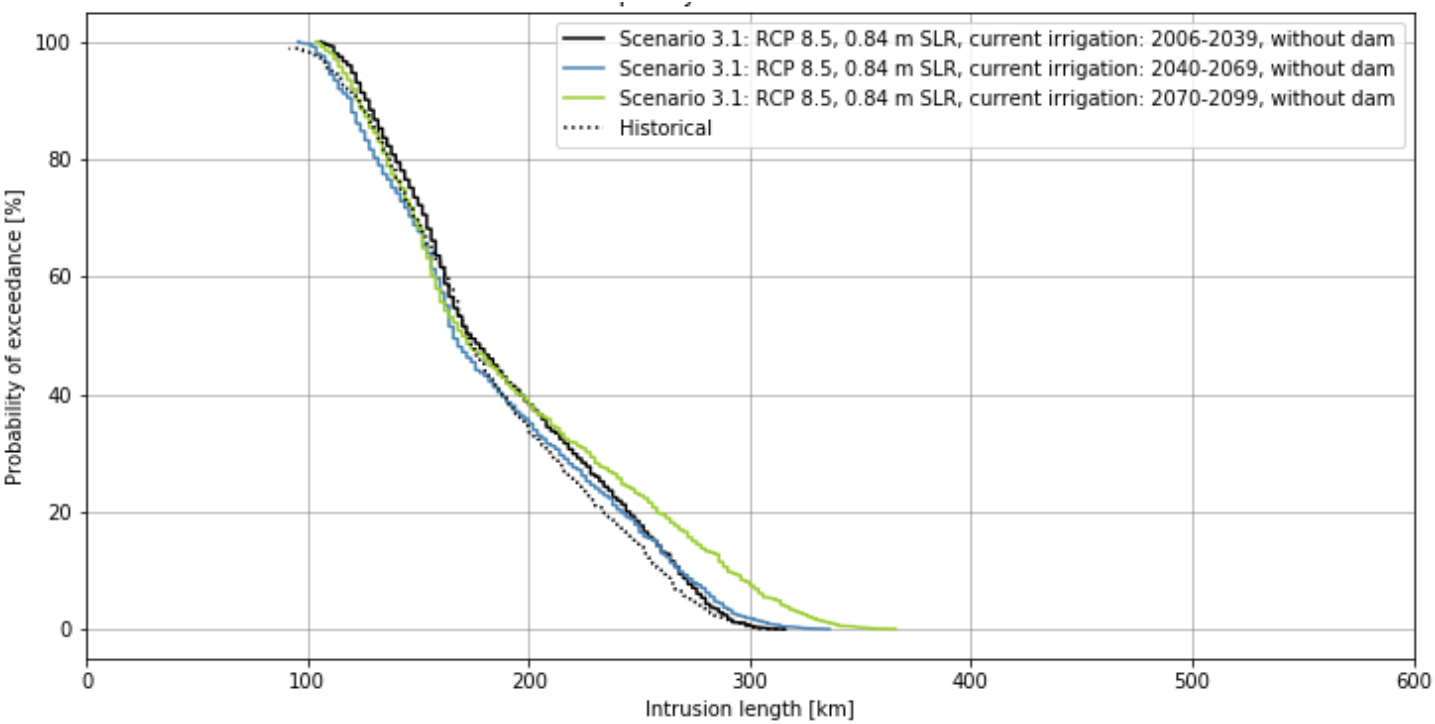
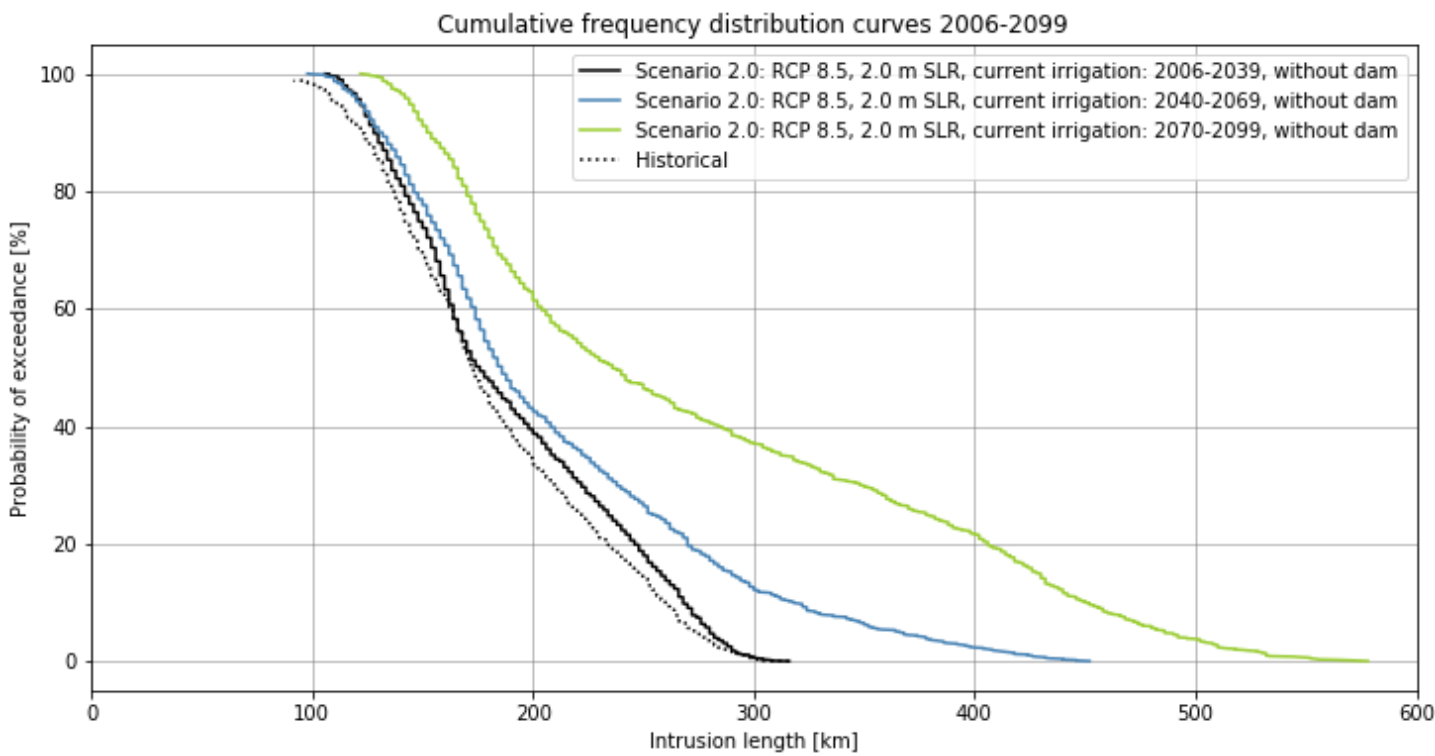


Figure 6-18: CFD-curves for scenario 2.0. When comparing with scenario 3.1 presented in the figure above, it can be seen that for the first period there are barely differences while the 2nd and 3rd period show large differences.



5.2.2 Sea level rise: Effect on probability of exceedance

79. Comparing both 0.84 m sea level rise scenarios with their 0 m sea level rise equivalents no significant differences can be spotted in either lower or upper slopes of their CFD-curves. For the 2.0 m sea level rise a significant decrease in both lower and upper slope can be detected of up to 41% in the third period when comparing to the 0 m equivalent. This can be seen well in Figure 6-18.

5.2.3 Sea level rise: Effect on seasonality

80. Looking at the wet season median dip (F5) an increase of 5% can be seen for both 0.84 m sea level rise scenarios when comparing with their 0 m sea level rise equivalents in the third period, the remaining periods show negligible change. It should be noted that although negligible the magnitude of the difference grows over time for the 0.84 m sea level rise scenarios. This indicates that rising sea levels cause a deeper inland salt front during the wet season. The dry season median peak (F6) is however not affected by the 0.84 m sea level rise scenarios. This is visualized in Figure 6-20.

81. The 2.0 m sea level rise shows again a much stronger response. In the second and third period the wet season median increases with respectively 16% and 33% when comparing to the 0 m sea level rise scenario. For the dry season median peak this is respectively 14% and 56%. Further more the wet season dip shifts with one month onto later in the year for the last period. This indicates a longer dry season which can be seen in Figure 6-21.

Figure 6-19: Monthly median salt intrusion curves for each time period for scenario 3.1 and reference scenario 0.0. It can be seen that the differences between scenario 3.1 and the reference scenario are very small.

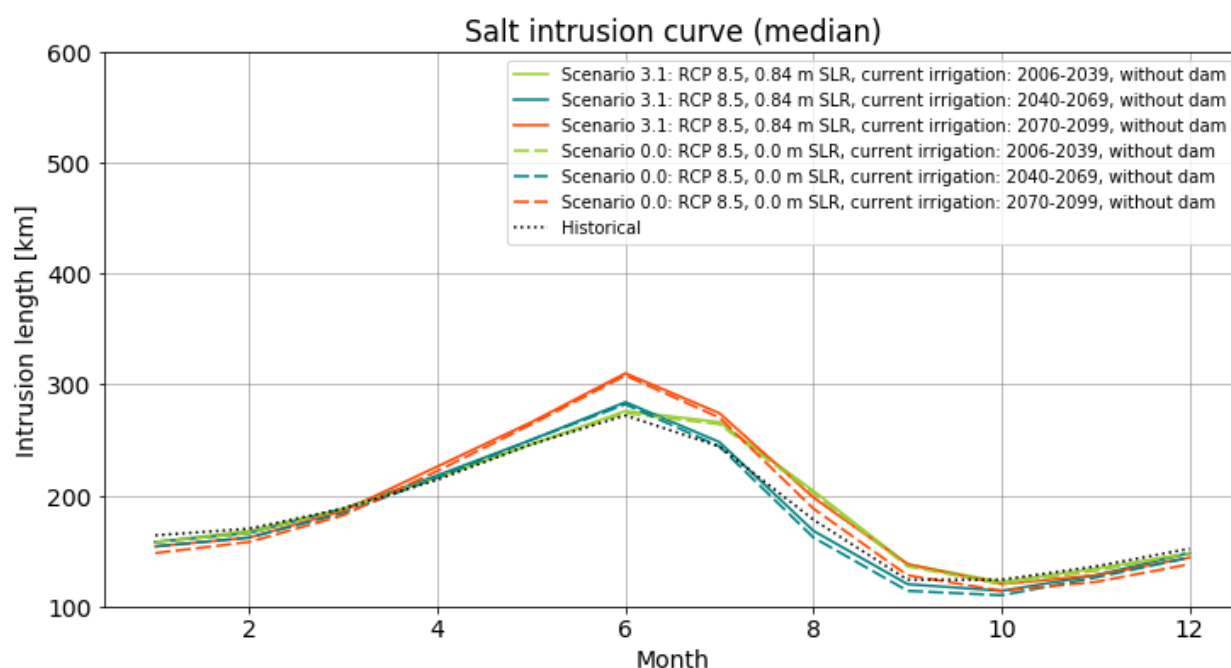
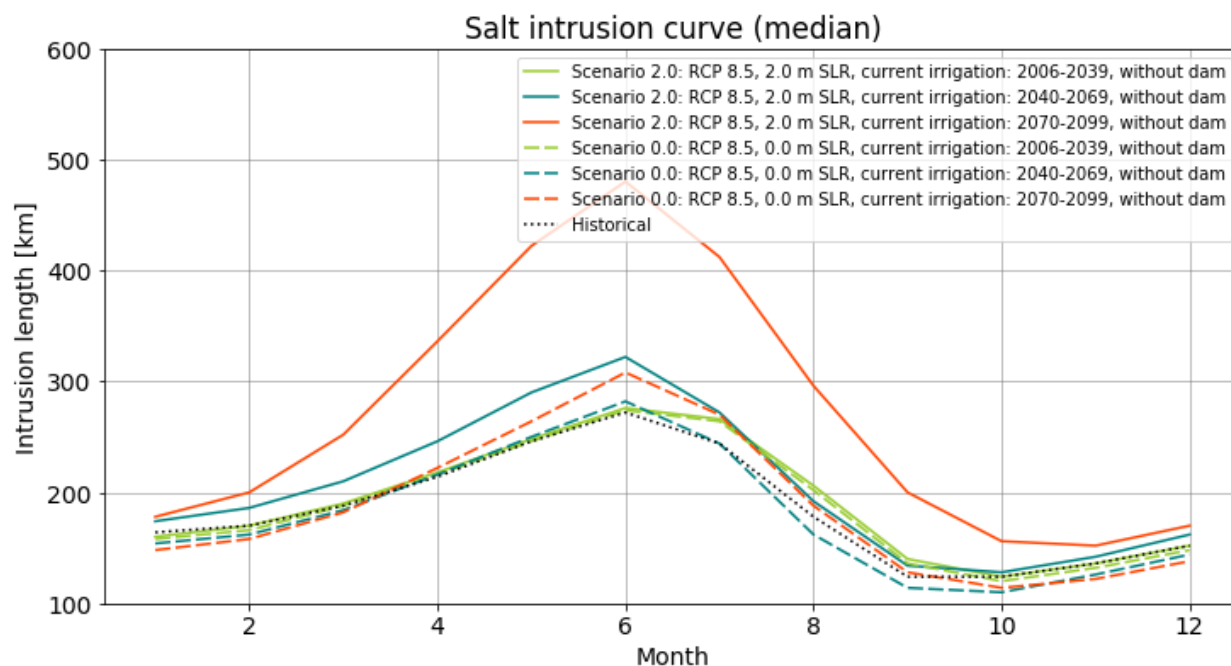


Figure 6-20: Monthly median salt intrusion curves for scenario 2.0 with reference scenario 0.0. Comparing this figure with the figure above; it can be seen that the first period shows more or less the same differences while the second and third period show large differences with the reference scenario.

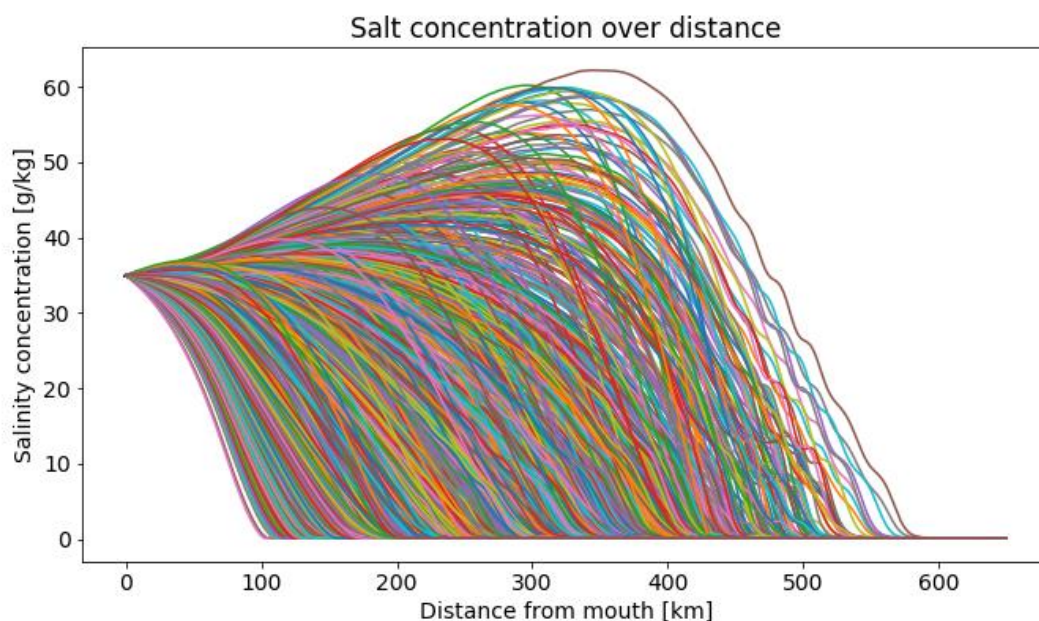


5.2.4 Sea level rise: Effect on salt concentration

82. Comparing the hypersaline region and salt concentrations, respectively F9 and F10, between the 0.84m sea level rise scenarios and the respective 0 m sea level rise equivalents, show remarkable results. The size of the hypersaline region decreases slightly, up to 7% in the third period. This effect is slightly stronger for the scenario that also applies RCP 8.5 which confirms the somewhat dampening effect of sea level rise on salt intrusion. The maximum salt concentrations decrease negligibly.

83. 2.0 m sea level rise shows a decrease in the size of the hypersaline region of 7% in the first period. The second and third period however, show an increase of respectively 88% and 183% in the size of the hypersaline area. More than doubling the size of the hypersaline area of the 0 m equivalent in the third period. The maximum salt concentration only increases significantly in the third period with 62%, coming close to double the ocean salinity.

Figure 6-21: Salt concentration plot for scenario 2.0. Each line is a timestep (10 day period) and gives a salinity profile of the Gambia river.



5.2.5 Sea level rise: Summary

84. Sea level rise has little impact on minimum and maximum salt intrusion lengths and the variance of salt intrusion lengths. In addition, no significant impact on the dry season median peak and wet season median dip can be noticed. A 0.84 m increase in sea level does however show a dampening impact on the hypersaline region, reducing it slightly when compared to the 0 m sea level rise equivalents. It has no impact on maximum salt concentrations.

85. The 2.0 m sea level rise shows different results. There are strong increases in minimum and maximum intrusion lengths and the variance of salt intrusion lengths increase significantly, indicating less predictability of salt intrusion lengths in the estuary. Furthermore, the increase in both wet season and dry season median peaks shows an overall shift of salt intruding further inland. The hypersaline region grows significantly compared to the 0 m sea level rise equivalent from 168 to 476 km. The maximum salt concentration also increases with 62% coming close to double ocean salinity.

5.3 Reservoir filling

86. The filling of the reservoir is the third item that will be discussed, it is not a model parameter but a separate model run to see what effect the construction of the dam has on salt intrusion. Starting with its effects on the minimum and maximum salt intrusion lengths and followed by the effect on probability of exceedance and monthly median these scenarios have not the full range of data as seen in the other scenarios. The difference between the two scenarios is the time the reservoir behind the dam requires to be filled. Scenario 1.0 assumes this takes 1 year and scenario 1.1 assumes this will take 2 years. The results of these scenarios can be found in the table below.

Table 6-9: Model results for assessing the effects of reservoir filling on salt intrusion lengths⁸⁷

Scenario ID:	Period:	ID	CFD-curve				Monthly median	
			F1 [km]	F2 [km]	F3 [-]	F4 [-]	F5 [km]	F6 [km]
H	1971-2017	N/A	92	316	- 0.41	- 0.74	124	272
0.0	2006-2039	Current	104	316	- 0.42	- 0.88	120	274
1.0	2006-2039 [2024]	Expected	104	314	- 0.42	- 0.92	132	295
1.1	2006-2039 [2024-2025]	Expected	104	324	- 0.41	- 0.92	132	295

5.3.1 Reservoir filling: Minimum and maximum salt intrusion lengths

87. There is no difference when comparing both scenarios with the minimum salt intrusion lengths to the reference scenario. The maximum intrusion length however shows an increase for the case in which the filling of the reservoir takes two years, while the single year scenario shows a decrease. The increase and decrease in both scenarios are negligibly small.

5.3.2 Reservoir filling: Effect on probability of exceedance

88. Similarly, the change in both the upper slope that indicates the variety of the more common salt intrusion lengths as well as the lower slopes which indicates the variety of the less common salt intrusion lengths is negligibly small for both scenarios.

5.3.3 Reservoir filling: Effect on seasonality

89. The monthly median salt intrusion peaks change as much for the single year filling as for the two-year filling scenario. The dry season peak increases more indicating a shift to deeper inland salt intrusion lengths during the filling of the reservoir, independent on the duration. The comparison can be seen in Figure 6-22. This indicates a longer period with high salt intrusion lengths for the scenario in which the dam fills for two consecutive years.

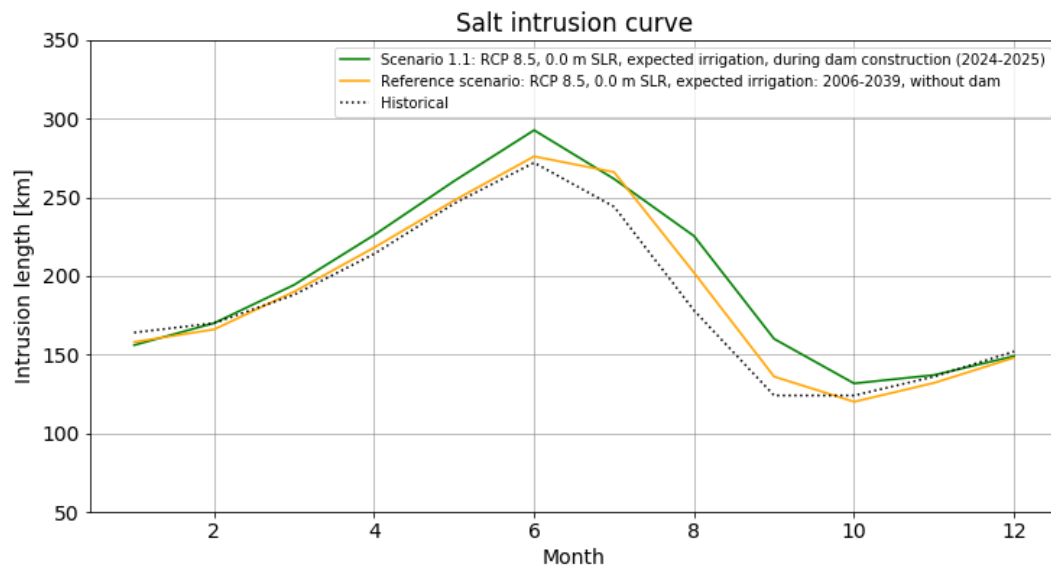
5.3.4 Reservoir filling: Summary

90. The filling of the reservoir has a small impact. Compared to the reference scenario there is a shift in maximum intrusion length. The more common salt intrusion lengths do not change their variance but the less common salt intrusion lengths do, which indicates a less predictable salt intrusion

⁸⁷ Future weather and sea level rise are constant and respectively RCP 8.5 and 0.0 m sea level rise.

pattern for less likely salt intrusion lengths. Furthermore, an increase of the monthly median dry season peak indicates more often occurring deeper inland salt intrusion lengths.

Figure 6-22: Monthly median salt intrusion curve for the 2 year filling scenario compared to the reference scenario.



5.4 Dam operations

91. The dam operational schemes are the third model parameter that will be discussed. Starting with its effects on the minimum and maximum salt intrusion lengths and followed by the effect on probability of exceedance, effect on seasonality and effect on salt concentration. The scenarios and their results for this model parameter are presented in Table 6-10 below. Scenarios 3.0 and 3.1 will be used as reference scenarios since these are the scenarios where no dam has been implemented.

Table 6-10: Model results for assessing the effects of dam operations on salt intrusion lengths and salt concentrations⁸⁸.

scenario ID	Period:	FW	DO	CFD-curve				Monthly median min/max				S-x curve	
				F1 [km]	F2 [km]	F3 [-]	F4 [-]	F5 [km]	F6 [km]	F7 [Mos]	F8 [Mos]	F9 [km]	F10 [g/L]
H	1971-2017	N/A	N/A	92	316	-0.74	-0.41	124	272	9	6	72	35.6
3.0	2006-2039	RCP 4.5	No dam	108	314	-0.94	-0.41	126	280	10	6	96	36.0
	2040-2069			100	308	-0.83	-0.41	116	278	10	6	90	35.9
	2070-2099			100	326	-0.78	-0.34	116	298	10	6	116	36.4
3.2	2006-2039	RCP 4.5	A	118	258	-1.25	-1.00	140	202	11	7	60	35.6
	2040-2069			112	220	-1.00	-1.00	128	202	10	6	54	35.5
	2070-2099			108	242	-0.98	-0.74	126	216	10	6	74	35.8
3.3	2006-2039	RCP 4.5	B	116	322	-1.00	-0.39	134	284	10	7	100	36.1
	2040-2069			108	316	-1.00	-0.37	122	264	10	6	86	35.8
	2070-2099			108	328	-1.05	-0.30	122	288	10	6	114	36.4
3.1	2006-2039	RCP 8.5	No dam	106	316	-0.84	-0.42	122	276	10	6	90	35.9
	2040-2069			96	336	-0.79	-0.38	114	284	10	6	122	36.6
	2070-2099			104	366	-0.82	-0.31	120	310	10	6	156	37.4
3.4	2006-2039	RCP 8.5	A	118	258	-1.07	-1.00	134	202	10	7	52	35.4
	2040-2069			108	242	-0.94	-0.94	124	204	10	6	74	35.9
	2070-2099			112	262	-1.05	-0.59	130	232	11	6	102	36.6
3.5	2006-2039	RCP 8.5	B	114	322	-1.07	-0.39	128	282	10	7	88	35.7
	2040-2069			106	338	-1.07	-0.31	120	262	10	6	124	36.7
	2070-2099			112	360	-1.05	-0.28	126	282	10	7	158	37.4

5.4.1 Dam operations: Minimum and maximum salt intrusion lengths

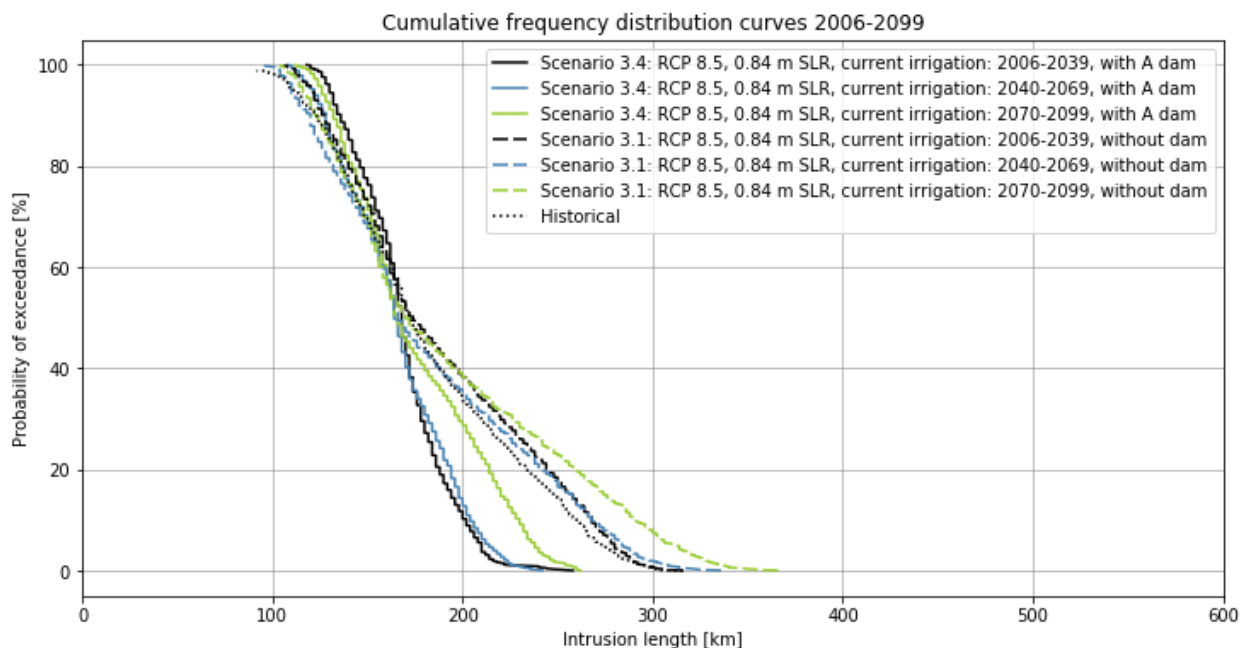
92. Table 6-10 shows scenarios with several possible operational schemes for the hydropower dam and both RCPs. In the table above 'A' and 'B' respectively stand for the 'ecology focused operations' and 'power production focused operations'.

93. When comparing the ecology focused operations, DO A, with the reference scenarios it can be seen that the minimum salt intrusion lengths increase significantly ranging between 8% and 13%.

⁸⁸ Sea level rise and irrigation development are constant and respectively 0.84 m sea level rise and 'current' irrigation development.

However, maximum salt concentrations decrease significantly for these operations ranging between -18% and -29%. When comparing the power production focused operations, DO B, with the reference scenarios a different pattern is visible. Again an increase in minimum salt intrusion lengths of the same magnitude as for DO A can be seen. However, the maximum salt intrusion lengths do not decrease but increase negligibly.

Figure 6-23: CFD-curves for scenario 3.4 and reference scenario 3.1. The increase in minimum salt intrusion length can be seen as well as the decrease in maximum salt intrusion length. The steepening in the slopes is visible as well, indicating a trend of more stabilized salt intrusion lengths.



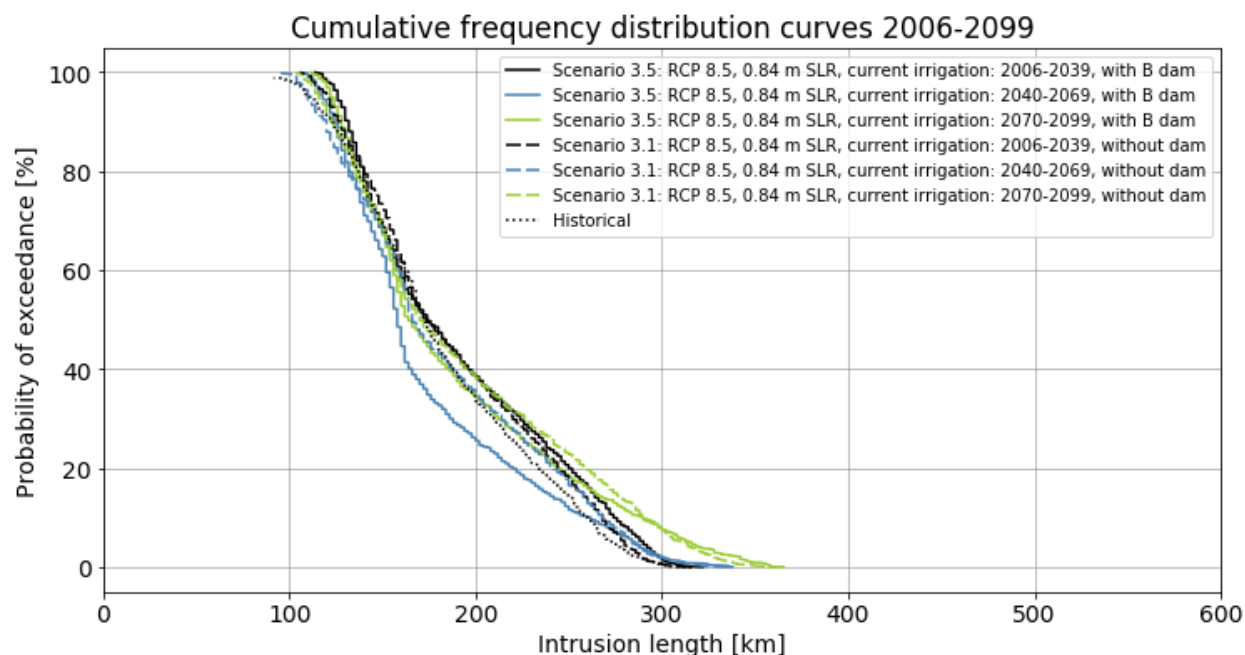
5.4.2 Dam operations: Effect on probability of exceedance

94. The comparison of the ecological operations, DO A, show a strong steepening of the gradient of the upper CFD-curve (F3) for DO A compared to the reference scenarios. The increase in slope ranges between 19% and 33%. The increase in the lower CFD-curve is even more substantial which ranges between 88% and 150%. Figure 6-23 visualizes these changes in slope for scenario 3.4 compared to scenario 3.1. The increase in slope of both the upper and lower part of the CFD-curve indicates more predictable salt intrusion lengths with less variation.

95. When doing the same comparison for the power production focused operations, DO B, a similar increase in upper slope can be detected, ranging between 7% and 36%. The lower slope however, decreases between 5 and 17%. This indicates less predictable higher salt intrusion lengths. This is visualized in Figure 6-24.

96. Comparing Figure 6-23 and Figure 6-24 gives an impression of the differences between the implemented dam operations and the range between dam operations can influence the degree of salt intrusion.

Figure 6-24: CFD-curves for scenario 3.3. The steepening in the upper slopes and afterwards the flattening of the lower slopes can be seen. This indicates less variety in small salt intrusion lengths while the larger salt intrusion lengths show more variety.



5.4.3 Dam operations: Effect on seasonality

97. Ecological operations can cause a shift in the wet season median peak towards later in the year. This is not the case for power production focused operations. Both dam operations cause during some periods a shift in the dry season peak towards later in the year as well. This can lead for DO A, to an decrease of the dry season while for DO B this can lead to an increase.

98. Comparing Figure 6-25 and Figure 6-26 shows the difference between the two different operating schemes. The prolonged dry season (buildup of salt) can be noticed for DO B whereas for DO A only a shift occurs.

Figure 6-25: Monthly median salt intrusion for scenario 3.5 compared to the reference scenario 3.1. In this case a shift of dry and wet season peaks is visible for the first and third period

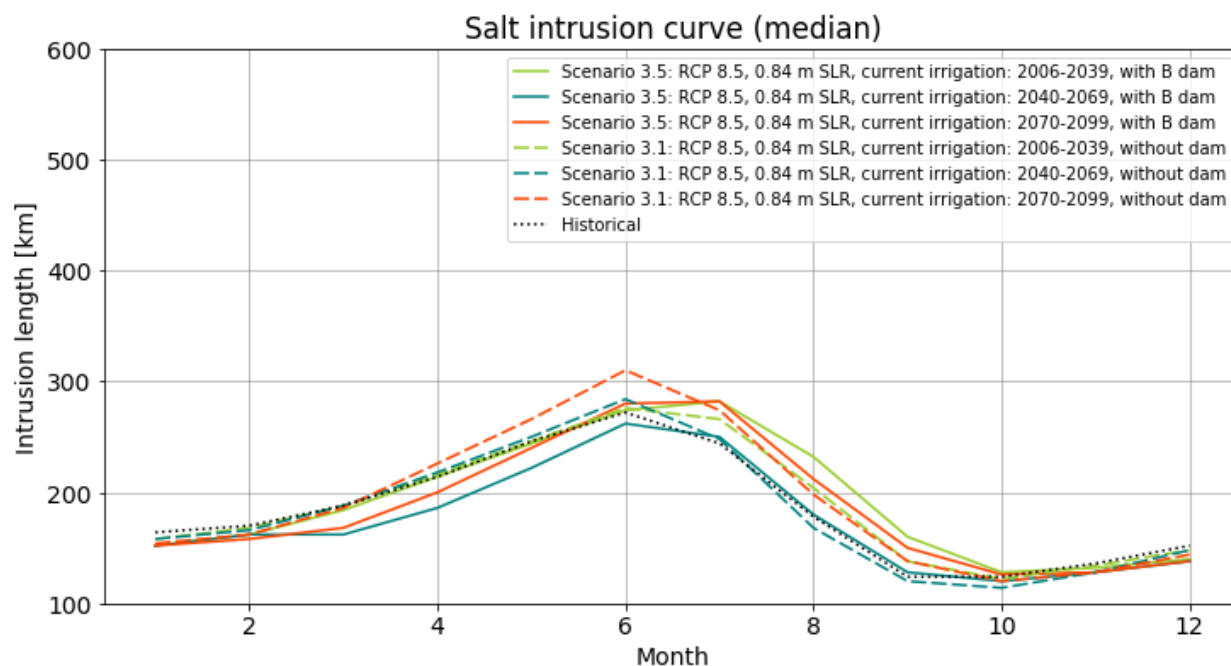
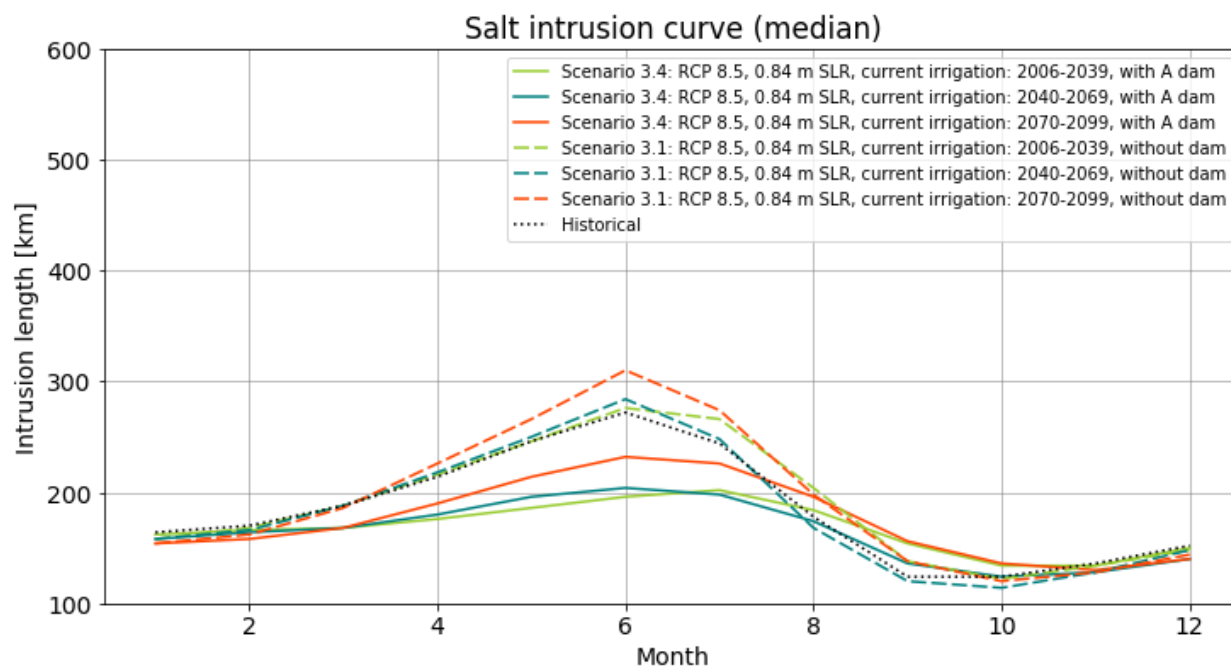


Figure 6-26: Monthly median for scenario 3.4 compared to the reference scenario 3.1. A reduction in dry season median and shift in seasonality are well visible.



5.4.4 Dam operations: Effect on salt concentration

99. The ecological operated dam has significant influence on the size of the hypersaline region. Reductions between 35% and 42% compared to the scenarios without dam can be seen. The power production focused operations show negligible differences and no trend. For both ways of operating the dam the maximum salt concentration is negligibly impacted.

5.4.5 Dam operations: Summary

100. Both ways of operating the dam are created to be extremes this is reflected in their impact. This is visualized in the figures above.

101. The ecological dam operations show an increase in minimum salt intrusion length of up to 13% compared to the situation without dam. The maximum salt intrusion length decreases significantly, up to 29%. This leads to a more stabilized flow which is represented by the steepening of both slopes of the CFD-curve. The monthly median peaks continue with this pattern, slightly increasing the peak during the wet season and decreasing the peak strongly during the dry season. Further more a strong impact on the size of the hypersaline region can be noticed for these dam operations. However, no significant change in salt concentrations can be noticed.

102. The power production focused operations show a totally different impact. The minimum salt intrusion lengths still increase up to 10% but no reduction of the maximum salt intrusion length can be seen. The lower slope of the CFD-curve flattens which indicates more variation for the rarer salt intrusion lengths. Furthermore, no significant changes in the wet and dry-season peaks can be noticed. The size of the hypersaline region changes negligibly as well as the maximum salt concentrations.

5.5 Irrigation development

103. Irrigation development is the final model parameter that will be discussed. Starting with its effects on the minimum and maximum salt intrusion lengths and followed by the effect on probability of exceedance, effect on seasonality and effect on salt concentration. The scenarios and their results for this model parameter are presented in Table 6-11 below. Scenarios 3.2 and 3.4 will be used as reference scenarios since these have the current level of irrigated surface.

Table 6-11: Model results for assessing the effects of irrigation development on salt intrusion lengths and salt concentrations⁸⁹.

scenario ID				CFD-curve				Monthly median min/max				S-x curve	
	Period:	FW	ID	F1 [km]	F2 [km]	F3 [-]	F4 [-]	F5 [km]	F6 [km]	F7 [Mos]	F8 [Mos]	F9 [km]	F10 [g/L]
H	1971-2017	N/A	Current	92	316	-0.74	-0.41	124	272	9	6	72	35.6
3.2	2006-2039	RCP 4.5	Current	118	258	-1.25	-1.00	140	202	11	7	60	35.6
	2040-2069			112	220	-1.00	-1.00	128	202	10	6	54	35.5
	2070-2099			108	242	-0.98	-0.74	126	216	10	6	74	35.8
4.0	2006-2039	RCP 4.5	Expected	118	258	-1.25	-1.00	142	204	10	7	62	35.6
	2040-2069			112	222	-1.00	-0.94	128	204	10	6	56	35.5
	2070-2099			108	242	-0.98	-0.70	126	218	10	6	74	35.8
4.2	2006-2039	RCP 4.5	Max	118	270	-1.25	-0.94	142	208	11	7	66	35.7
	2040-2069			114	228	-1.00	-0.94	128	210	10	6	60	35.5
	2070-2099			108	250	-1.05	-0.67	126	226	10	6	78	35.9
3.4	2006-2039	RCP 8.5	Current	118	258	-1.07	-1.00	134	202	10	7	52	35.4
	2040-2069			108	242	-0.94	-0.94	124	204	10	6	74	35.9
	2070-2099			112	262	-1.05	-0.59	130	232	11	6	102	36.6
4.4	2006-2039	RCP 8.5	Expected	118	258	-1.07	-1.00	134	204	10	7	52	35.4
	2040-2069			108	244	-0.94	-0.88	124	206	10	6	76	35.9
	2070-2099			112	264	-1.14	-0.59	130	234	11	6	102	36.7
4.6	2006-2039	RCP 8.5	Max	120	258	-1.07	-0.88	136	208	10	7	56	35.5
	2040-2069			110	250	-0.94	-0.79	124	212	10	6	80	36.0
	2070-2099			112	272	-1.05	-0.57	132	242	11	6	108	36.8

5.5.1 Irrigation development: Minimum and maximum salt intrusion lengths

104. Table 6-11 shows six scenarios. These are chosen such that the three agricultural development irrigation areas (current irrigated surface, expected irrigated surface and maximum irrigated surface) are applied. The remaining parameters are kept constant, with a sea level rise of 0.84 m and ecological dam operations, DO A.

105. Comparing the minimum salt intrusion lengths of the expected and maximum irrigated surfaces with the current irrigated surface shows negligible changes. For the expected irrigated surface scenarios, no change is noticeable while for the maximum irrigated surface scenarios there is a negligibly small increase.

⁸⁹ Sea level rise and dam operations are constant and respectively 0.84 m sea level rise and ecological flow, DO A. Furthermore, the first row 'scenario ID: H' shows historic values while all other rows show the difference compared to the historic scenario.

106. The maximum salt intrusion lengths do show some differences between the selected scenarios. The expected irrigated surface now has negligibly small increases while the maximum irrigated surface shows a bigger increase.

5.5.2 Irrigation development: Effect on probability of exceedance

107. Comparing the reference scenarios (3.2 and 3.4) with all other scenarios presented in Table 6-11 it becomes clear the upper slopes (F3) show no change or a very small steepening (scenario 4.2, p3 and scenario 4.4, p3 show an increase of respectively 7% and 8%).

108. The lower slopes (F4) show a more significant change. The slopes for the expected irrigated surface flatten slightly, ranging between 5% and 6%. This indicates more variation in less common salt intrusions. The slopes for the maximum irrigated surface flatten slightly more, especially for RCP 8.5 ranging up to 16%. All variations in the lower slopes point towards a slightly flattening of the lower slope with increasing irrigated surface. Figure 6-27 shows the different CFD-curves for current irrigated surface and the maximum increase in irrigated surface.

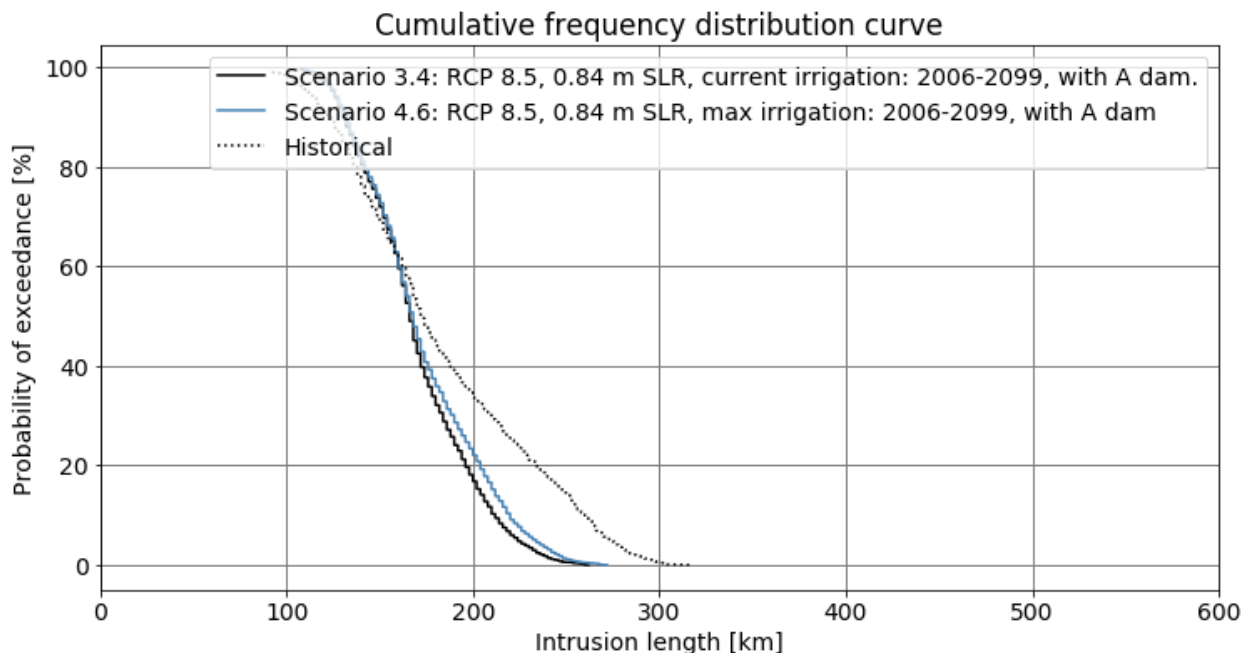
5.5.3 Irrigation development: Effect on seasonality

109. Both dry and wet season peaks vary negligibly due to the change in irrigated surface. Furthermore, no shift in seasonality due to the increase in irrigated surface can be noticed.

5.5.4 Irrigation development: Effect on salt concentration

110. There is no effect on salt concentrations noticeable due to an increase in irrigation surfaces.

Figure 6-27: Scenario 3.4 which is used as reference scenario to see the influence of change in irrigated area. Scenario 4.6, which has the maximum irrigated area applied shows no change in small salt intrusion lengths but does affect larger salt intrusion lengths.



5.5.5 Irrigation development: Summary

111. Irrigation development does not have an effect on minimum or maximum salt intrusion length. Furthermore, the size of the hypersaline region and salt concentrations within do not depend on the irrigation surface. There is however an increase in the monthly median peak for the dry season

when the maximum irrigated surface is implemented. This also shows in the variety of less common salt intrusion lengths which slightly flattens for scenario 4.6 (see Figure 6-27).

5.6 Simplified summary of model parameter influence

112. The future weather is discussed by comparing weather scenarios for RCP 8.5 with RCP 4.5. Salt intrusion lengths are only slightly impacted by the difference in future weather. The salt intrudes further for RCP 8.5 but the difference between RCP 8.5 and RCP 4.5 is not large. The length between the river mouth and the salt front shows an increase in variability for RCP 8.5. This means that it becomes less predictable how deep the salt intrudes inland. The hypersaline region, the area with salt concentrations above ocean salinity, grows significantly for RCP 8.5 when comparing with RCP 4.5. This shows a strong impact of future weather. Furthermore, the weather varies, this is also imposed onto the salt intrusion lengths.

113. Sea level rise has a moderate impact when the river stays within its banks. It dampens the effects of more extreme weather (RCP 8.5) and stabilizes larger salt intrusion lengths. The average salt intrusion length shifts inland with increasing sea level rise. Remarkably, a rising sea level decreases the size of the hypersaline region and salt concentrations, albeit only by a little.

114. Considering the 2.0 m sea level rise scenario a different image of the effect of sea level rise is sketched. The river is forced outside of its banks, this leads to freshwater being depleted quickly by evaporation which results in a hypersaline estuary during the dry season (duration ~ 6 months). The salt intrudes far inland, the hypersaline region grows strongly (183%) and the maximum salt concentration within the estuary reaches almost double ocean salinities.

115. The filling of the reservoir has a small impact which is only noticeable in the median salt intrusion during the dry season. This increases to some extent and is slightly stronger in case that the filling will take two years.

116. The dam operations show large differences in their impact. One being a strong reductor of extreme salt intrusion lengths (ecological flow, DO A), the other increasing them slightly (power production focused, DO B). The ecologically operated dam shows a strongly stabilized estuary in terms of salt intrusion. This makes it easy to predict between what ranges the salt front will be. Furthermore, it has strong decreasing effects on the size of the hypersaline region, almost halving it. The power production focused operations show larger similarities with the reference scenarios. It improves the predictability of the salt intrusion length but at the cost of the average salt front being deeper inland. Neither of the dam operations has significant influence on the salt concentrations.

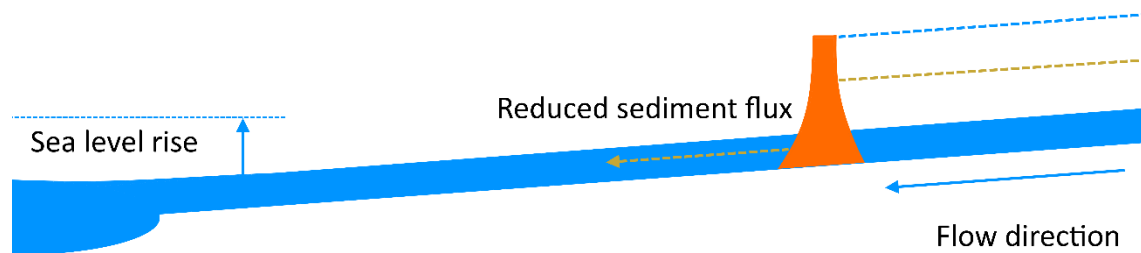
117. Irrigation development has negligible effects allover. The maximum use of irrigation shifts the occurrence of rarer salt intrusion lengths slightly.

5.7 Discussion of non-model results

5.7.1 Morphological effects due to dam and sea level rise

118. The hydropower dam will trap sediment which lead to a decrease in sediment supply downstream of the dam. This change in sediment supply will affect the river morphology which influences salt intrusion. Besides the dam the rising sea level also affects river morphology. Respectively the hydropower dam and sea level rise can be seen as an upper and lower boundary (see Figure 6-28).

Figure 6-28: Simplified visualization of sea level rise and sediment build up due to the hydropower dam



119. It is important to note that the Gambia river is an alluvial river along the entire length of the river. This implies that the river can adjust its slope as well as its width. Secondly, a variable flow (dry and wet season flow) with an averaged sediment flux is present. The hydropower dam will attenuate the wet season flows and increases the current dry season flows. Since sediment flux is non-linearly related to the flow per meter width the total downstream directed sediment flux presumably will change.

Expert interview

120. To get an impression of the possible effects on river morphology due to the hydropower dam and sea level rise an interview was conducted with professor C.J. Sloff, an expert on sedimentation processes and sediment management in reservoirs. The interview started with the preliminary statement that it is very hard to say what will happen and that the following possibilities might not happen. As previously described the hydropower dam and sea level rise pose two boundaries which affect the river and estuary.

121. The hydropower dam can be operated in several ways. This study treats two of them (ecological flow & power production) but there is another possibility within the power production category: peaking. Peaking is applied in water scarce regions and it is based on the expected power usage. During the day when power usage peaks energy is produced while during the night, when there is barely any power usage water is saved. If such an operating strategy is applied this creates oscillations in water level between day and night, high and low water. These oscillations cause increased bank erosion compared to when there is a normal, relatively constant flow. The oscillations are strongest near the dam and dampen over distance, however their effect on bank erosion should not be underestimated. Bank erosion is also dependent on the composition and strength of the river banks. If the bank erodes the river widens, this leads to a decrease of depth which can alter the river's characteristics.

122. Another effect of the hydropower dam is a change in the amount of sediment that is let through. This depends on the type of sediment that is present in the river and the dam and its reservoir's characteristics; how high is the dam; what discharge is let through; what is the size of the

reservoir etc. What usually happens is that the heaviest particles such as gravel and sand sink to the bottom of the reservoir. Lighter particles such as clay and silt partially pass through the dam. The amount of sediment that passes through the dam is important for the change in morphology. Just after construction of the hydropower dam the transport capacity of the river is the same as before. If there is a strong sediment reduction this sediment is supplied from the riverbed. However, the riverbed is often covered with larger pieces of sediment, which cannot be transported with such flow. This causes that only the fine sediment entrapped in the riverbed is taken. This leads to a downward migrating wave where the fine sediments are removed from the bed. Due to gravel and sand being trapped in the reservoir the ratio of sediments changes from partially coarse and partially fine to a majority of fine particles. This causes the river to become muddier, especially in the saline parts of the river and in the estuary. Clay interacts with salt, which creates larger flakes that sediment faster than single clay particles. A strong increase in mud (clay and silts) is to be expected in the downstream regions. In the long term, the slope of the river adjusts to the new sediment load. This is a very slow process. The larger particles at the bottom of the river are not easily transported and protect the underlying sediments. Furthermore, the hydropower dam changes the flow pattern, attenuating the minimum and maximum flows. Since the transportation capacity is non-linearly dependent on the flow it is possible the total sediment flux decreases even though the minimum flows increase. If the river becomes wider due to bank erosion it becomes less deep. This can form a new equilibrium based on sediment supply but leads to another threat. Vegetation can grow on parts it could not before. If then a highwater event occurs (e.g. upstream storm and lots of water spilled over/through the hydro power dam) the river has higher friction and lower transport capacity which increases the chance on flooding.

123. On the downstream end of the river sea level increases depth. The tidal influence increases which increase the amount of water flowing in and out of the estuary. If the sediment supply from upstream is large enough, the river bed can grow with the sea level rise. Coastal erosion due to the reduced sand supply should be expected and due to the attenuation of the hydrograph. However, the erosion or sedimentation in the coastal region is very complex and hard to predict.

124. Apart from the clear positive effects of a hydropower dam there are always unexpected negative consequences. The effects of a change in sediment supply are often underestimated or overlooked. However, unbalancing the system has clear negative effects for the population. Care has to be taken for them so that they can cope with the change. Besides the morphological changes also ecological and environmental changes should be expected.

5.7.2 Effects of sea level rise and salination on vegetation

125. Fent et al. (2019) confirmed a net increase in mangrove tree cover nationally between 1988 and 2018 after a period of drought in the 1970s and 80s. It shows the sensitivity of mangroves to lack of freshwater and partially the effort that is made in conserving and increasing these areas. Earlier studies confirmed a severe decrease of mangroves (e.g. Carney et al., 2014) caused by these droughts. The mangroves have a double function, on one side they are the nursery of many fish and other species and on the other side they protect coastal regions by reducing their vulnerability (Guannel et al., 2016). However, Ellison already showed in 1993 that the now thriving mangrove forests will retreat with increased sea level rise. Similarly, Naidoo et al. showed with their research in 2011 that hypersaline environments are detrimental for mangroves. Under certain scenarios either one or both

of these negative impacts will increase the stress on the mangrove forests present in The Gambia. The expected reduction of mangrove forests increases the sensitivity to a reduced sediment flux.

Part 6 – Limitations

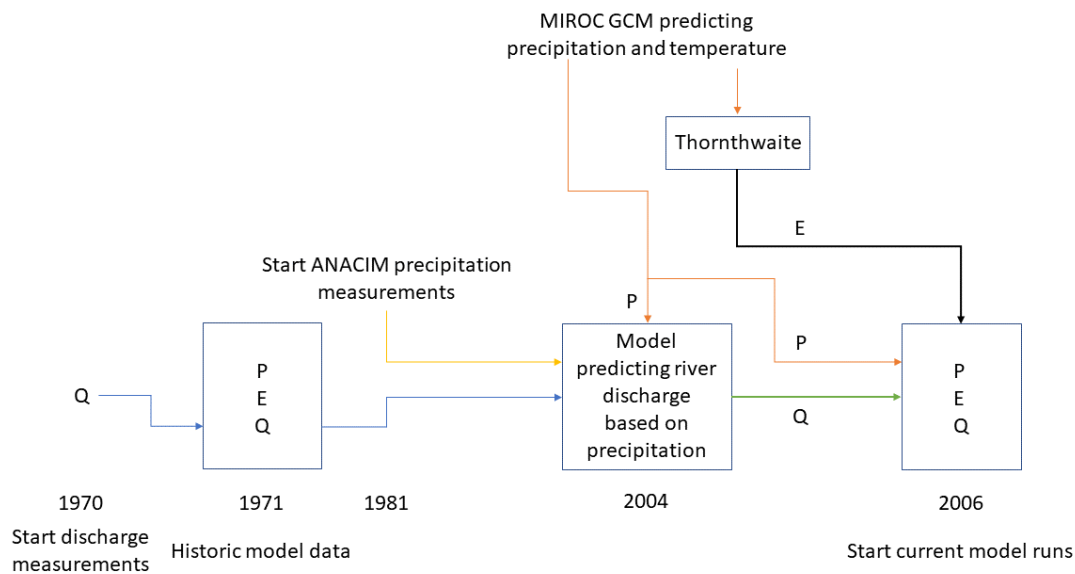
126. This section will discuss limitations of this study. First the data and quality of model output will be discussed after which several other limitations will be discussed.

6.1 Different data sources and salt intrusion error

127. The acquired data to model the salt intrusion of the Gambia river consists of many separate sources. Because these sources are often not linked the quality of the model results can be questioned. The model is for example calibrated on historic data, the quality of some of this data is unknown (e.g., river discharge). To estimate what the quality of the model output is, an error analysis should have been performed. This has not been done, limiting the knowledge of the model output quality. Keeping in mind the limitations of the data that has been used in the model lead to a sounder understanding of the quality of the model output. Figure 6-29 below is presented again and contains the overview of data that shows how the historic and current model differ.

Figure 6-29: Flow chart of precipitation, evaporation and river discharge. The years mentioned at the bottom correspond to the date ranges in

Table 6-3. The colors visualize where data transforms



6.2 Evaporation and calibration

128. During data collection an unexpected error in the generated evaporation values was discovered. This was due to applying Hargreaves formula for evaporation, which is dependent on minimum and maximum temperature. Because the rate of change of the minimum and maximum temperature differed, with minimum temperature raising faster than maximum, the evaporation decreased over time, even as the temperatures rose. Therefore, another method to estimate evaporation was applied which would only require the average monthly temperature data: Thornthwaite. Even though this method does not have this particular weakness the method was not developed for (projected) time series analysis. The respective average monthly temperature of RCP 4.5 and 8.5 rose between 2.1 and 3.9 degrees between 2006 and 2099, and the average monthly evaporation rose respectively with 112 and 228 mm. Since the precipitation does not vary significantly between the start and end of the modelling period this increase in evaporation has a relatively high impact. Secondly, the open water evaporation applied on the reservoir is a percentage of this evaporation estimate. It is important to realize that Thornthwaite estimates the potential evaporation, the model is amongst others calibrated by adjusting the evaporation which validates the use of potential evaporation.

129. For the scenarios in which the threshold value for sea level rise is exceeded and the river bursts its banks this evaporation might no longer be correct. The calibration adjusted the evaporation such that the best fit on measurements was accounted for. Previously the model had a constant river surface, allowing for the evaporation to be used as calibration parameter. Due to the expansion of the river and therefore the evaporative surface this scaling could lead to an overestimation of the extra evaporated water. During all model runs the parameters that change between scenarios are only the hydrological parameters, influenced by future weather, water extraction etc. However, due to sea level rise the hydraulic parameters in the model also change. Once the threshold value is exceeded and the evaporative surface is significantly increased one can question if the calibration is still correct for this situation and not an overestimation.

6.3 Numerical nature

130. Another limitation that has a strong impact on the precision of the model results is the numerical nature of the model. This leads to increasingly large errors for large intrusion lengths, in which the model has to calculate more steps. Resulting are oscillations that become larger for large salt intrusion lengths, as can be seen in Figure 6-21. The errors caused by the numerical calculations still allow trends to be detected but for more precise estimates these numerical errors should be solved. Instead of solving the numerical nature of the model an error analysis could also be performed, giving an accurate idea within what range the predicted salt concentrations are.

6.4 Temporal analysis

131. This study has not looked deeply in the temporal dimensions of salt intrusion. The duration with which the dry season salt peaks increase in certain scenarios or decrease in others has not been looked at. This is however, a possible important feature. Furthermore, the chosen date ranges show often a sudden increase in the third period. A more in-depth analysis of the temporal feature could give the answer. Depending on the need of knowing what to expect and when to expect it this analysis could be of great value.

6.5 Dam operations

132. Scenario 'DO A' derived from the environmental study (OMVG, 2014) has unclear relations between water levels in the reservoir and the discharge. These relations could not be verified but have been used nonetheless. Furthermore, the reservoir that will be created once the dam is constructed is based on simple relations of the volume of a frustrum of a cone. This assumption was made for modelling the reservoir. All calculated parameters that came from this assumption exactly matched the reservoir presented in the study of the OMVG (2014). This is an indication that the expected characteristics of the reservoir and therefore the water level – discharge relations have not yet been determined accurately.

Scenario 'DO B' optimized the power production only for a single scenario and not for each. This leads to sub-optimal performance of the scenarios which implement DO B for some of the. This sub-optimal performance is enlarged by the larger difference in evaporation between RCP 4.5 and RCP 8.5. Secondly, scenario 'DO B' assumes a constant flow for respectively the dry and wet season. The expert interview indicates another possible operating scheme that aims to produce power when it is needed. This has not been modelled.

Part 7 – Conclusions

133. The presentation of conclusions from this study are organized around the research questions, which are presented below. To answer these questions the key features and results discussed in part 5 are summarized. All modelled parameters (sea level rise, dam operations, irrigated area, future weather) and time periods are included to provide an as complete as possible conclusion.

- I. How does the salt intrusion length develop?
- II. How does the salt concentration develop?
- III. Can hyper salinity occur and under which circumstances?
- IV. What measures can be taken to mitigate salt intrusion and how effective are these measures?
- V. How will aqua- and agriculture in The Gambia be affected by the construction of the hydropower dam?

7.1 How do the salt intrusion length and concentration develop?

134. The modelled salt intrusion length and concentration are influenced by future weather, sea level rise, dam operations and irrigation development. The first two will be discussed first and can be considered climate change related, while the latter two can be considered short-term anthropogenic changes.

7.1.1 Climate change related development of salt intrusion length and concentration

Future weather

135. Future weather has a significant impact on salt intrusion lengths as can be seen when comparing RCP 4.5 with RCP 8.5. The maximum salt intrusion length shows increases of up to 12% between RCP 8.5 and RCP 4.5. Furthermore, a strong increase in the size of the hypersaline region, up to 45%, can be seen. Future weather does not show a significant impact on salt concentrations.

Sea level rise

136. Sea level rise has a limited influence on salt intrusion until the river is forced outside of its boundaries. Below the expansion threshold increases in sea level show increases in the wet season median peak around 5%. Remarkably the increase in sea level rise has a decreasing effect on the size of the hypersaline region.

137. When the river is forced outside of its boundaries however, the evaporative surface area of the river expands dramatically, leading to high levels of freshwater removal due to evaporation. This results in a strong increase in salt intrusion lengths and a strongly hypersaline river with hypersaline concentrations coming close to double ocean salinity for large extents of time (~ 6 months).

7.1.2 Short-term anthropogenic change related development of salt intrusion length and concentration

Reservoir filling

138. The reservoir filling scenarios have a small impact on the wet and dry season median peaks, which increases respectively with 10% and 8%

Dam operations

139. Dam operations have a significant impact on the salt intrusion lengths of the river. The difference between the two extreme dam operation scenarios (ecology focused flow and power

production focused flow) is large. Ecology focused flow shows a strong reducing effect on maximum salt intrusion lengths, up to 29%. This leads to a more stabilized salt intrusion pattern, where the salt front is contained in a smaller range than the case without dam. Furthermore, the hypersaline region is strongly decreased, up to 42% compared to the scenario without dam.

140. Power production focused operations shows salt intrusion lengths that are closer to the scenarios without dam. This also leads to a smaller range in which the salt front moves. However, where the ecology focused operations show to strongly reduce the maximum salt intrusion length and the size of the hypersaline region the power production focused operations do not. Both ways of operating the dam result in a negligible decrease of salt concentrations.

Irrigation development

141. Somewhat surprisingly the development of irrigation surface does not result in significant impact. Even when maximum irrigated surface is applied this does not lead to significantly different salt intrusion levels. Similarly, the salt concentration levels are barely affected. This is due to the relatively small amount of water extracted necessary for the increased irrigational area.

7.2 Hyper salinity

142. Periods of hyper salinity are found in all scenarios, occurring in the dry season where a point is reached when the freshwater flow is depleted and evaporative losses lead to a buildup of salt in the remaining river volume. This can be close to the river mouth or deep inland depending on climate change and short-term anthropogenic combinations. Severe hyper salinity (> 40 g/L) only occurs in the 2.0-meter sea level rise scenario.

7.3 Measures to mitigate salt intrusion

143. Depending on the freedom to adjust dam operation, and how sea level rise and the weather develop, the dam operations could be used to limit salt intrusion lengths as well as hyper salinity. The difference between the two modelled ways of operating the dam illustrate the extent to which salt intrusion lengths can be pushed back through changes in the dam discharge rate.

144. Occasionally supplying the river with fresh sediment that has settled in the reservoir behind the dam could potentially help limit the increase in salt intrusion lengths due to morphological changes. However, this issue was not included in the present study. Therefore, the effect of the reduced sediment supply on salt intrusion lengths and the potential effectiveness of this strategy are unknown.

145. Limiting the expansion of the river would make sure that severe hyper salinity and long salt intrusion lengths cannot occur. Comparing the scenarios with 2.0 m sea level rise and those with more moderate sea level rise shows the importance of efforts aimed at preventing future emissions of greenhouse gasses.

7.4 Influence of dam operations on agri- and aquaculture

146. The construction of the dam shows higher salt intrusion lengths and more occurring higher salt intrusion lengths. These increases are not significant enough to harm agri- and aquaculture. The operation of the dam does not pose a threat to agriculture. Furthermore, the stabilizing effect of the dam on salt intrusion levels leads to less varying salt intrusion lengths and concentrations which would create a better environment for aquaculture. The magnitude of the shift in seasonality mentioned

before can increase when the hydropower dam is solely operated to produce power. This could have implications for agri- and aquaculture.

7.5 Issues for policy makers

147. The salt intrusion length and salt concentrations in the Gambia river will be heavily affected by climate change. Effort should be made to convince all stakeholders and financiers of the dam to leave some room in dam operations. This enables to use the strong effects the dam operation has in decreasing salt concentrations and salt intrusion lengths in periods of need.

148. Banjul lies at the mouth of the Gambia river. The elevation of the city is only slightly more than that of sea level and if sea level rise continues as predicted in the worst-case scenario used in this study (2.0-meter sea level rise) large parts of Banjul will eventually flood. Flooding and other water related problems in Banjul will likely occur before hyper salinity reaches unacceptable levels in the estuary. If Banjul is to be protected this would require substantial financial means. This leads to the question that if financial resources are used to protect Banjul will there be enough to protect the estuary, by for example limiting the expansion of the river due to sea level rise, as well?

Conclusions

149. Sea level rise, combined with insufficient sedimentation, decreased rainfall, increased evaporation and offtake of water for irrigation will lead to more saltwater entering the Gambia River estuary, and advancing further upriver. The construction of the dam at Sambangalou will have additional impacts on the river's hydrologic functioning by altering the stream flow timing and volume in wet and dry periods. Combined, these changes will have both spatial and temporal dimensions that may have serious implications for different species in the fisheries depending on their lifecycle and seasonal use of estuary, as well as their relative mobility. While the report focuses on the upper extent of the saline front during the dry season (above KP 170), there will also be changes to the front during both the rainy and dry seasons, as the dam release schedule will reduce the rainy season streamflow and increase the flow during the dry. A decrease in volume, and delay, in wet season flooding will tend to increase opportunities for marine species within estuary. Estuary species whose spawning is linked to the wet season conditions (retreat of saline front and decreased salinity) may be geographically impacted as the duration and intensity of the wet season flooding decreases. In contrast, species whose spawning is tied to the increased salinity of the dry season (further advance of the saline front and higher salinity levels), will find geographic advantage. There will likely be geographically progressive impacts to the species composition of mangroves and associated foodchains as well. Although not mentioned in the report, the acute reduction in streamflow (planned over two rainy seasons) while the dam's reservoir is filled, may have an important impact on biodiversity throughout freshwater portion of the river. Sea level rise will affect ecologies under tidal influence along the river's length, effectively drowning out those located on the deep-water margin.

References

- Abdi Aris, N. (2012). *Modeling of Salt Water Intrusions Into Langat River Estuary, Malaysia* (Doctoral dissertation, Universiti Putra Malaysia).
- Amuzu, J., Jallow, B. P., Kabo-Bah, A. T., & Yaffa, S. (2018). The climate change vulnerability and risk management matrix for the coastal zone of the Gambia. *Hydrology*, 5(1), 14.
- Bamber, J. L., Oppenheimer, M., Kopp, R. E., Aspinall, W. P., & Cooke, R. M. (2019). Ice sheet contributions to future sea-level rise from structured expert judgment. *Proceedings of the National Academy of Sciences*, 116(23), 11195-11200.
- Bentsen, M., et al. 2013. The Norwegian Earth System Model, NorESM1-M – Part 1: Description and basic evaluation of the physical climate, *Geosci. Model Dev.*, 6, 687-720.
- Vd Burgh, P. (1972). Ontwikkeling van een methode voor het voorspellen van zoutverdelingen in estuaria, kanalen en zeeën.
- Cai, H., Savenije, H. H. G., & Jiang, C. (2014). Analytical approach for predicting fresh water discharge in an estuary based on tidal water level observations. *Hydrology and Earth System Sciences*, 18(10), 4153.
- Cai, H., Savenije, H. H.G., Zuo, S., Jiang, C., & Chua, V. P. (2015). A predictive model for salt intrusion in estuaries applied to the Yangtze estuary. *Journal of Hydrology*, 529, 1336-1349.
- Carney, J., Gillespie, T. W., & Rosomoff, R. (2014). Assessing forest change in a priority West African mangrove ecosystem: 1986–2010. *Geoforum*, 53, 126-135.
- Central Intelligence Agency. 2020. The Gambia. In *The world factbook*. Retrieved from <https://www.cia.gov/library/publications/the-world-factbook/geos/ga.html>
- Chen, C., Huang, H., Beardsley, R. C., Liu, H., Xu, Q., & Cowles, G. (2007). A finite volume numerical approach for coastal ocean circulation studies: Comparisons with finite difference models. *Journal of Geophysical Research: Oceans*, 112(C3).
- Chen, W. B., Liu, W. C., & Hsu, M. H. (2015). Modeling assessment of a saltwater intrusion and a transport time scale response to sea-level rise in a tidal estuary. *Environmental Fluid Mechanics*, 15(3), 491-514.
- Davies, G., & Woodroffe, C. D. (2010). Tidal estuary width convergence: Theory and form in North Australian estuaries. *Earth Surface Processes and Landforms: The Journal of the British Geomorphological Research Group*, 35(7), 737-749.
- DMCI [Development Management Consultants International] (2014). *National Rice Development Strategy* (NRDS) – The Gambia. IFAD-sponsored national agricultural land and water management development project (NEMA) of the Ministry of Agriculture.
- Dufresne, J., et al. 2013. Climate change projections using the IPSL-CM5 Earth System Model: from CMIP3 to CMIP5. *Clim Dyn* 40, 2123–2165.
- Dunne, J.P., et al. 2012. GFDL's ESM2 global coupled climate–carbon Earth System Models. Part I: Physical formulation and baseline simulation characteristics. *Journal of Climate* 25:6646–6665.
- Economic Community of West African States (ECOWAS, 2020). <https://www.ecowas.int/about-ecowas/vision-2020/>

ECOWAPP (2020), <http://pipes.ecowapp.org/en/project/implementation/128-mw-sambangalou-hydropower-plant>

Ellison, J. C. (1993). Mangrove retreat with rising sea-level, Bermuda. *Estuarine, Coastal and Shelf Science*, 37(1), 75-87.

Ettritch, G., Hardy, A., Bojang, L., Cross, D., Bunting, P., & Brewer, P. (2018). Enhancing digital elevation models for hydraulic modelling using flood frequency detection. *Remote sensing of environment*, 217, 506-522.

Fent, A., Bardou, R., Carney, J., & Cavanaugh, K. (2019). Transborder political ecology of mangroves in Senegal and The Gambia. *Global Environmental Change*, 54, 214-226.

Gay, P. S., & O'Donnell, J. (2007). A simple advection-dispersion model for the salt distribution in linearly tapered estuaries. *Journal of Geophysical Research: Oceans*, 112(C7).

Gisen, J. I. A., Savenije, H. H., Nijzink, R. C., & Abd. Wahab, A. K. (2015a). Testing a 1-D analytical salt intrusion model and its predictive equations in Malaysian estuaries. *Hydrological Sciences Journal*, 60(1), 156-172.

Gisen, J. I. A., Savenije, H. H. G., & Nijzink, R. C. (2015b). Revised predictive equations for salt intrusion modelling in estuaries. *Hydrology & Earth System Sciences Discussions*, 12(1).

Guannel, G., Arkema, K., Ruggiero, P., & Verutes, G. (2016). The power of three: coral reefs, seagrasses and mangroves protect coastal regions and increase their resilience. *PloS one*, 11(7), e0158094.

Haddout, S., Maslouhi, A., Baimik, I., Igouzal, M., & Marah, H. (2019). Two-dimensional modeling of the vertical circulation of salt intrusion in the Sebou estuary under different hydrological conditions. *ISH Journal of Hydraulic Engineering*, 25(2), 170-187.

IPCC (Intergovernmental Panel on Climate Change). 2019a. The Ocean and Cryosphere in a Changing Climate. Summary for Policy Makers. In: Special Report on the Ocean and Cryosphere in a Changing Climate [H.-O. Pörtner, et al. (eds.)]. Geneva, Switzerland: IPCC.

IPCC, 2019: Summary for Policymakers. In: IPCC Special Report on the Ocean and Cryosphere in a Changing Climate [H.-O. Pörtner, D.C. Roberts, V. Masson-Delmotte, P. Zhai, M. Tignor, E. Poloczanska, K. Mintenbeck, A. Alegría, M. Nicolai, A. Okem, J. Petzold, B. Rama, N.M. Weyer (eds.)]. In press.

Kuang, C., Huang, J., Chen, S., & Liu, S. (2012). A saltwater intrusion model based on semi-implicit Eulerian-Lagrangian finite-volume method. *Journal of Tongji University. Natural Science*, 40(1), 38-44.

Kurup, R. G., Hamilton, D. P., & Phillips, R. L. (2000). Comparison of two 2-dimensional, laterally averaged hydrodynamic model applications to the Swan River Estuary. *Mathematics and Computers in Simulation*, 51(6), 627-638.

Lewis, R. E., & Uncles, R. J. (2003). Factors affecting longitudinal dispersion in estuaries of different scale. *Ocean Dynamics*, 53(3), 197-207.

Martin, G.M., et al. 2011. The HadGEM2 family of Met Office Unified Model climate configurations, *Geosci. Model Dev.*, 4, 723–757.

Naidoo, G., Hiralal, O., & Naidoo, Y. (2011). Hypersalinity effects on leaf ultrastructure and physiology in the mangrove *Avicennia marina*. *Flora-Morphology, Distribution, Functional Ecology of Plants*, 206(9), 814-820.

- Nauels, A., Gütschow, J., Mengel, M., Meinshausen, M., Clark, P. U., & Schleussner, C. F. (2019). Attributing long-term sea-level rise to Paris Agreement emission pledges. *Proceedings of the National Academy of Sciences*, 116(47), 23487-23492.
- NOAA (National Oceanic and Atmospheric Administration). 2017. Global and Regional Sea Level Rise Scenarios for the United States. NOAA Technical Report NOS CO-OPS 083. Silver Springs (MD): NOAA.
- Organisation de développement du bassin du fleuve Gambie (2014). Étude d'impact environmental et social (EIES) de l'aménagement hydroélectrique de Sambangalou et de l'interconnexion.
- Van Os, A. G., & Abraham, G. (1990). Density Currents and Salt Intrusion. Delft Hydraulics. *International Institute for Hydraulic and Environmental Engineering, Lecture Notes*.
- Parsa, J., & Etemad-Shahidi, A. (2011). An empirical model for salinity intrusion in alluvial estuaries. *Ocean Dynamics*, 61(10), 1619-1628.
- Pillsbury, G. B. (1956). Tidal hydraulics (Vol. 34). *Corps of Engineers, US Army*.
- Pour, O.D.N.U. (2007). *Caracterisation des systems de production Agricole au Senegal*.
- Sarr, B. (2012). Present and future climate change in the semi-arid region of West Africa: a crucial input for practical adaptation in agriculture. *Atmospheric Science Letters*, 13(2), 108-112.
- Savenije, H.H.G. (1986). A one-dimensional model for salinity intrusion in alluvial estuaries. *Journal of Hydrology*, 85(1-2), 87-109.
- Savenije, H. H. (1989). Salt intrusion model for high-water slack, low-water slack, and mean tide on spread sheet. *Journal of Hydrology*, 107(1-4), 9-18.
- Savenije, H.H.G. (1992). Rapid assessment technique for salt intrusion in alluvial estuaries.
- Savenije, H. H., & Pagès, J. (1992). Hypersalinity: a dramatic change in the hydrology of Sahelian estuaries. *Journal of Hydrology*, 135(1-4), 157-174.
- Savenije, H. H. (1993). Predictive model for salt intrusion in estuaries. *Journal of Hydrology*, 148(1-4), 203-218.
- Savenije, H.H.G., (2005). *Salinity and tides in alluvial estuaries*. Gulf Professional Publishing.
- Savenije, H.H.G., (2012). *Salinity and Tides in Alluvial Estuaries*, second ed.
- Shaha, D. C., & Cho, Y. K. (2009). Comparison of empirical models with intensively observed data for prediction of salt intrusion in the Sumjin River estuary, Korea. *Hydrology & Earth System Sciences*, 13(6).
- Sivapalan, M. (2003). Process complexity at hillslope scale, process simplicity at watershed scale: Is there a connection? *EAEJA*, 7973.
- Symonds, A. M., Vijverberg, T., Post, S., van der Spek, B. J., Henrotte, J., & Sokolewicz, M. (2016). Comparison between Mike 21 FM, Delft3D and Delft3D FM flow models of western port bay, Australia. *COASTAL ENGINEERING*, 2.
- Thorntwaite, C. W. (1948). An approach toward a rational classification of climate. *Geographical review*, 38(1), 55-94.

- Verkerk, M. P., & van Rens, C. P. M. (2005). *Saline intrusion in Gambia River after dam construction. Solutions to control saline intrusion while accounting for irrigation development and climate change*. University of Twente, The Netherlands, Enschede.
- Watanabe, S., et al. 2011. MIROC-ESM 2010: Model description and basic results of CMIP5-20c3m experiments. *Geoscientific Model Development* 4(4):845-872.
- White, E. D., Messina, F., Moss, L., & Meselhe, E. (2018). Salinity and marine mammal dynamics in Barataria Basin: Historic patterns and modeled diversion scenarios. *Water*, 10(8), 1015.
- Zhang, Z. (2019). *A theoretical basis for salinity intrusion in estuaries* (Doctoral dissertation, Delft University of Technology).

Appendix A Discharge model

For each region in the catchment area (Kedougou and Goudiry), the model approaches the contribution to river flow as follows. When it rains, a certain threshold volume of water needs to be exceeded before the precipitation is contributing to the flow in the river. Depending on the amount of water intercepted by leaves, types of vegetation, types of soil, moisture content in the soil etc. several flows to the river arise. These flows have again a clear distinction. Subsurface flows and groundwater flows are much slower than overland flow but continue for a longer time. To mimic all these hydrological effects and account for the several timescales the model works with a threshold volume that incorporates all resistances before the precipitation reaches the river. Furthermore, multiple timesteps are applied to ensure that groundwater flows are represented well.

The `scipy.optimize.minimize` function is used to optimize the factors that determine the contribution for each timestep for each region by minimizing the error. The error is the difference between the predicted amount of flow and the measured flow in Gouloumbou. For each timestep and for each region a c is given by the optimization. Since negative flow cannot occur the first negative c determines the number of months that contribute to river flow. This is four months.

$$Error = \sum c_{ij} \cdot P_{ij} - m$$

Where:

Weight per timestep:

c

-

Precipitation:

P

L/T

Time:

I

T

Region:

j

-

Measurement of flow:

m

L^3/T

Another complication is the hydropower dam. Part of the generated flow around Kedougou contributes to filling the reservoir behind it and part of it directly feeds into the Gambia river. In personal contact with the FAO it has been shared that half of the flow measured in Gouloumbou is generated in the region which feeds into the reservoir of the hydropower dam. To determine the ideal ratio between the areas around Kedougou and the threshold values for the two regions, an iterative process in excel that maximizes the R squared value between the measured and predicted flow follows. This process consists of interchangeably changing the threshold values for each region or changing the ratio of contribution, this is done manually. The reason for doing this labor-intensive job manually is simply because perfect solutions are not necessarily the most realistic. Equifinality, the possibility of having multiple best scenarios with different parameter combinations, occurs when having more parameters to optimize than measurements to verify with. The optimization leads to the results presented in **Error! Reference source not found.** which meet the flow requirements. The model achieves an R squared value of 86%. The prediction of flow is based on precipitation of previous months and is calculated by following formula 1. The separation of the flow near Kedougou is calculated with formula 2.

$$Q = \sum (P - T)_{t_i, r_j} \cdot C_{t_i, r_j} \quad 1$$

$$Q_{river} = (\sum (P - T)_{t_i} \cdot C_{t_i}) \cdot \alpha \quad 2$$

Where:

Discharge

Q

L^3/T

Threshold volume

T

L/T

Ratio of flow generated near Kedougou contributing directly to riverflow

α

-

Table 6-12 Results of discharge model optimization

Threshold value Kedougou	60 mm/month
Threshold value Goudiry	55 mm/month
α	26 %

Appendix B Hydropower dam operational schemes

Two operational schemes for the hydropower dam have been created. The limited information about the dam lead to some assumptions. This Annex will start with how the reservoir has been modelled and the assumptions made for it. Afterwards both operational schemes are explained in detail. **Error! Reference source not found.** c containing dam and reservoir characteristics is presented here again as Table 6-13.

Table 6-13: Dam and reservoir characteristics.

Characteristics	Minimum	Maximum
Water level inside reservoir	188 m	200 m
Surface area reservoir	110 km ²	181 km ²
Volume reservoir	2.1 billion m ³	3.8 billion m ³
Useful capacity	-	1.7 billion m ³
Turbine discharge	0 m ³ /s	200 m ³ /s
Turbine height	75 m	

Reservoir modelling

To know the water level inside the reservoir a relation between the volume and water level needs to be established. The first assumption is that the volume takes the shape of a frustum of a cone between the minimum and maximum water level. Below the minimum water level, a simple cone shape determines the water level to volume relation see Figure 6-30. The volume present in the reservoir is calculated via a volume balance according to:

$$V_1 = V_0 + (Q_{in} - Q_{out}) \cdot t - E \cdot A \cdot t$$

Where:

Volume:	V	L ³
Discharge:	Q	L ³ /t
Timestep:	t	t
Evaporation:	E	L/t
Surface area:	A	L ²

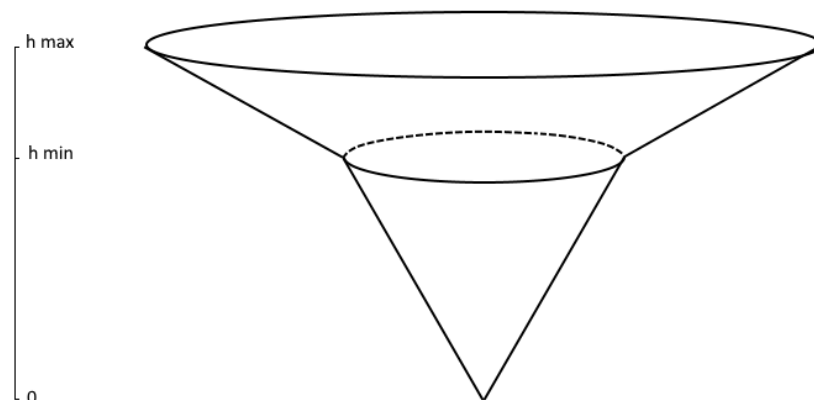


Figure 6-30: Simple approximation of the reservoir shape.

A frustum of a cone has the following relationship to between the volume and height.

$$V = \frac{1}{3}\pi h(r_{max}^2 + r_{max}r_{min} + r_{min}^2) \quad 3$$

Where:

Water level:	h	L
Radius:	r	L

If here the minimum radius is set equal to zero the volume of a cone is calculated. If r_{max} is subsequently calculated from the minimum operational surface area of the reservoir, this can be rewritten to read:

$$V - V_{min} < 0 \begin{cases} h = \frac{3 \cdot V}{\pi \cdot r_{min}^2} \\ r = \frac{r_{min}}{h_{min}} \cdot h \end{cases}$$

For the upper part of the reservoir first formula 3 is rewritten such that:

$$V = \frac{h}{F_1}$$

With:

$$F_1 = \frac{3}{\pi(r_{max}^2 \cdot r_{max} r_{min} \cdot r_{min}^2)}$$

The height of the water level in the reservoir behaves as follows:

$$h_t = \Delta h + h_{t-1} = (V_t - V_{t-1}) \cdot F_1 + h_{t-1}$$

The radius that determines the surface area is calculated similarly:

$$r_t = \Delta r + r_{t-1} = (h_t - h_{t-1}) \cdot F_2 + r_{t-1}$$

With:

$$F_2 = \frac{r_{max} - r_{min}}{h_{max} - h_{min}}$$

$$V - V_{min} \geq 0 \begin{cases} h = (V - V_0) \cdot F_1 + h_{min} \\ r = (h - h_{min}) \cdot F_2 + r_{min} \end{cases}$$

Finally, the surface area is calculated for a circle. This results in the same characteristics as in Table 6-13.

Dam operational scheme A: ecology focused flow

Dam operational scheme A, ecology focused flow, is based on the environmental study (OMVG, 2014). In this study a basic flow scheme is shown, presented in Table 6-14. The table contents are open for interpretation, it is not clear when certain discharge turbines are exactly reached. Therefore, the percentages in the annual distribution of production flows have been applied to the water level in the reservoir, which results in increasing discharge when the reservoir level increases. The relations between discharge and reservoir level are presented below in Table 6-15.

Table 6-14: Translated table from the OMVG study in 2014 with approximate flow characteristics through the hydropower dam.

Discharge Turbine	Annual distribution of production flows	Comments
200 m ³ /s	8% of the time	Continuously during the wet months of periods of high inputs (such as the years 1954 – 1978 and 1994-2001)
Intermediate flow rates between: 64 and 200 m ³ /s	8% of the time	
Flow rates close to 60 m ³ /s (between 54 and 64 m ³ /s)	80% of the time	Continuous supply of guaranteed power, with fluctuations around this average value according to the requirements of the network in certain years, and according to the filling state of the reservoir at the end of the rainy season.

Flow rates between 60 m ³ /s and almost zero	4% of the time	In episodes of extreme drought
---	----------------	--------------------------------

Table 6-15: Relations between water elevation in the reservoir and discharge through the turbines.

Water level reservoir	Discharge [m ³ /s]
$h \geq h_{max} - 0.08 \cdot \Delta h$	200
$h \geq h_{max} - 0.16 \cdot \Delta h$	$141.6664984 \cdot h - 27997.3$
$h \geq h_{max} - 0.96 \cdot \Delta h$	$1.041664898 \cdot h - 142.333$
$h \geq h_{max} - 1.00 \cdot \Delta h$	$112.5 \cdot h - 21150$
$h < h_{min}$	0

It should be noted that in the case of a water level higher than h_{max} the water will be spilled on top of the discharge of 200 m³/s.

Dam operational scheme B: power production focused

The power production focused flow scheme is based on the maximization of power production (power term in the formula below). It should be noted that this operational scheme is created for a single scenario in which it was optimized and used on all scenarios that were run with this type of operations. A lower boundary was set by the FAO for ecological minimum flow. This implies that the flow is not allowed to be less than the minimum flow of 18 m³/s (OMVG, 2014). Furthermore, the goal is to produce power as constant as possible which increases the reliability of the power grid. To do this the power production is split with the wet and dry season. During the dry season the reservoir slowly drains with a constant discharge while during the wet season the reservoir is filled again.

$$Q_t = \frac{Power}{\rho \cdot g \cdot \Delta h \cdot \eta}$$

Where:

Discharge through the turbine:

Q_t L³/T

Power of the turbine:

Power Watt

Distance between reservoir water level and turbine

Δh

L

Efficiency:

η

-

The maximization of power production has been done manually, which does not guarantee the perfect discharge settings. Nonetheless, the difference between the two different operational schemes show a significant change. The final results for power focused operations lead to the following turbine powers. During the wet season turbines can operate on average with 100 MW while during the wet season turbines operate at 30 MW. It should be noted that the minimum flow condition of 18 m³/s is always met except for some scenarios in which the reservoir water level reduces too fast (e.g. due to evaporation). In such a moment the reservoir stops flow to retain water. This is because the power production was maximized without some safety factor to ensure such situations do not occur.

A rough estimate of the yearly produced power with these settings would be around 460 GWh, which is higher than the estimates in the environmental flow study.

Dry season: $Power \cdot time \approx 30 \cdot 8 \cdot 30 \cdot 24 = 172.8 \text{ GWh}$

Wet season: $Power \cdot time \approx 100 \cdot 4 \cdot 30 \cdot 24 = 288 \text{ GWh}$

It is important to realize that the above settings were chosen to show another extreme. For power production a smaller power production ensures that water will always flow according to minimum flow requirements.

Appendix C Model scenarios

Scenario ID:	Category:	Sea level rise:	Future weather:	Dam operations	Irrigation development:	Comment:
H	H+Ref	0 m	Historical	No dam	Current	
0.0	H+Ref	0 m	RCP 8.5	No dam	Current	
0.1	H+Ref	0 m	RCP 4.5	No dam	Current	
0.2	H+Ref	0 m	RCP 8.5	No dam	Expected	
1.0	Reservoir filling	0 m	RCP 8.5	Dam reservoir filling	Expected	2024
1.1	Reservoir filling	0 m	RCP 8.5	Dam reservoir filling	Expected	2024-2025
1.2	Reservoir filling	0 m	RCP 8.5	Dam reservoir filling	Expected	2024
1.3	Reservoir filling	0 m	RCP 8.5	Dam reservoir filling	Expected	2024-2025
2.0	2 m SLR	2 m	RCP 8.5	No dam	Current	
2.1	2 m SLR	2 m	RCP 8.5	A	Current	
2.2	2 m SLR	2 m	RCP 8.5	B	Current	
3.0	0.84 m SLR	0.84 m	RCP 4.5	No dam	Current	
3.1	0.84 m SLR	0.84 m	RCP 8.5	No dam	Current	
3.2	0.84 m SLR	0.84 m	RCP 4.5	A	Current	
3.3	0.84 m SLR	0.84 m	RCP 4.5	B	Current	
3.4	0.84 m SLR	0.84 m	RCP 8.5	A	Current	
3.5	0.84 m SLR	0.84 m	RCP 8.5	B	Current	
4.0	Ag dev	0.84 m	RCP 4.5	A	Expected	
4.1	Ag dev	0.84 m	RCP 4.5	B	Expected	
4.2	Ag dev	0.84 m	RCP 4.5	A	Max	
4.3	Ag dev	0.84 m	RCP 4.5	B	Max	
4.4	Ag dev	0.84 m	RCP 8.5	A	Expected	
4.5	Ag dev	0.84 m	RCP 8.5	B	Expected	
4.6	Ag dev	0.84 m	RCP 8.5	A	Max	
4.7	Ag dev	0.84 m	RCP 8.5	B	Max	
4.8	Ag dev	2 m	RCP 8.5	No dam	Expected	
4.9	Ag dev	2 m	RCP 8.5	No dam	Max	
4.10	Ag dev	2 m	RCP 8.5	A	Expected	
4.11	Ag dev	2 m	RCP 8.5	B	Expected	
4.12	Ag dev	2 m	RCP 8.5	A	Max	
4.13	Ag dev	2 m	RCP 8.5	B	Max	

Appendix D Model results

Table 6-16: Overview of all model results

scenario ID						CFD-curve				Monthly median min/max				S-x curve	
	Period:	SLR	FW	DO	ID	F1 [km]	F2 [km]	F3 [-]	F4 [-]	F5 [km]	F6 [km]	F7 [Mos]	F8 [Mos]	F9 [km]	F10 [g/L]
H	1971-2017	0	N/A	N/A	Current	92	316	-0.74	-0.41	124	272	9	6	72	35.6
0.0	2006-2039	0	RCP 8.5	No dam	Current	104	316	-0.88	-0.42	120	274	10	6	92	36.0
	2040-2069					92	336	-0.79	-0.37	110	282	10	6	128	36.8
	2070-2099					100	368	-0.87	-0.30	114	308	10	6	168	38.3
0.1	2006-2039	0	RCP 4.5	No dam	Current	104	314	-0.94	-0.41	124	280	10	6	98	36.1
	2040-2069					96	308	-0.83	-0.39	112	278	10	6	92	36.0
	2070-2099					96	328	-0.78	-0.33	110	298	10	6	124	36.6
2.0	2006-2039	2.0	RCP 8.5	No dam	Current	106	316	-0.84	-0.43	124	276	10	6	86	35.9
	2040-2069					98	452	-0.68	-0.27	128	322	10	6	240	37.7
	2070-2099					122	578	-0.57	-0.18	152	480	11	6	476	62.2
2.1	2006-2039	2.0	RCP 8.5	A	Current	120	258	-1.07	-1.00	136	206	10	7	50	35.4
	2040-2069					114	344	-1.00	-0.50	138	238	10	6	140	36.4
	2070-2099					134	430	-0.57	-0.22	164	404	11	6	394	54.9
2.2	2006-2039	2.0	RCP 8.5	B	Current	114	322	-1.16	-0.39	130	282	10	7	86	35.7
	2040-2069					110	454	-1.07	-0.30	134	278	10	7	254	37.8
	2070-2099					134	572	-0.67	-0.17	158	452	11	6	468	59.5
3.0	2006-2039	0.84	RCP 4.5	No dam	Current	108	314	-0.94	-0.41	126	280	10	6	96	36.0
	2040-2069					100	308	-0.83	-0.41	116	278	10	6	90	35.9
	2070-2099					100	326	-0.78	-0.34	116	298	10	6	116	36.4
3.1	2006-2039	0.84	RCP 8.5	No dam	Current	106	316	-0.84	-0.42	122	276	10	6	90	35.9
	2040-2069					96	336	-0.79	-0.38	114	284	10	6	122	36.6
	2070-2099					104	366	-0.82	-0.31	120	310	10	6	156	37.4
3.2	2006-2039	0.84	RCP 4.5	A	Current	118	258	-1.25	-1.00	140	202	11	7	60	35.6
	2040-2069					112	220	-1.00	-1.00	128	202	10	6	54	35.5
	2070-2099					108	242	-0.98	-0.74	126	216	10	6	74	35.8
3.3	2006-2039	0.84	RCP 4.5	B	Current	116	322	-1.00	-0.39	134	284	10	7	100	36.1
	2040-2069					108	316	-1.00	-0.37	122	264	10	6	86	35.8
	2070-2099					108	328	-1.05	-0.30	122	288	10	6	114	36.4
3.4	2006-2039	0.84	RCP 8.5	A	Current	118	258	-1.07	-1.00	134	202	10	7	52	35.4
	2040-2069					108	242	-0.94	-0.94	124	204	10	6	74	35.9
	2070-2099					112	262	-1.05	-0.59	130	232	11	6	102	36.6
3.5	2006-2039	0.84	RCP 8.5	B	Current	114	322	-1.07	-0.39	128	282	10	7	88	35.7
	2040-2069					106	338	-1.07	-0.31	120	262	10	6	124	36.7
	2070-2099					112	360	-1.05	-0.28	126	282	10	7	158	37.4
4.0	2006-2039	0.84	RCP 4.5	A	Expected	118	258	-1.25	-1.00	142	204	10	7	62	35.6
	2040-2069					112	222	-1.00	-0.94	128	204	10	6	56	35.5
	2070-2099					108	242	-0.98	-0.70	126	218	10	6	74	35.8
4.1	2006-2039	0.84	RCP 4.5	B	Expected	116	330	-1.00	-0.39	134	286	10	7	104	36.2
	2040-2069					108	324	-1.00	-0.36	122	266	10	6	88	35.9

	2070-2099					108	334	-0.98	-0.30	122	288	10	6	118	36.4
4.2	2006-2039	0.84	RCP 4.5	A	Max	118	270	-1.25	-0.94	142	208	11	7	66	35.7
	2040-2069					114	228	-1.00	-0.94	128	210	10	6	60	35.5
	2070-2099					108	250	-1.05	-0.67	126	226	10	6	78	35.9
4.3	2006-2039	0.84	RCP 4.5	B	Max	116	354	-0.94	-0.37	134	294	11	7	114	36.3
	2040-2069					108	352	-1.00	-0.33	124	278	10	6	100	36.1
	2070-2099					108	350	-0.98	-0.27	122	300	10	6	124	36.5
4.4	2006-2039	0.84	RCP 8.5	A	Expected	118	258	-1.07	-1.00	134	204	10	7	52	35.4
	2040-2069					108	244	-0.94	-0.88	124	206	10	6	76	35.9
	2070-2099					112	264	-1.14	-0.59	130	234	11	6	102	36.7
4.5	2006-2039	0.84	RCP 8.5	B	Expected	114	328	-1.07	-0.39	128	282	10	7	92	35.8
	2040-2069					106	342	-1.00	-0.30	120	264	10	6	128	36.7
	2070-2099					112	366	-1.05	-0.28	126	286	10	7	162	37.5
4.6	2006-2039	0.84	RCP 8.5	A	Max	120	258	-1.07	-0.88	136	208	10	7	56	35.5
	2040-2069					110	250	-0.94	-0.79	124	212	10	6	80	36.0
	2070-2099					112	272	-1.05	-0.57	132	242	11	6	108	36.8
4.7	2006-2039	0.84	RCP 8.5	B	Max	114	352	-1.00	-0.37	128	284	10	7	104	35.9
	2040-2069					106	360	-1.00	-0.28	120	274	10	6	138	36.9
	2070-2099					112	388	-0.98	-0.26	128	296	10	7	176	37.7
4.8	2006-2039	2.0	RCP 8.5	No dam	Expected	106	320	-0.84	-0.42	124	278	10	6	90	35.9
	2040-2069					98	456	-0.71	-0.27	128	326	10	6	242	37.7
	2070-2099					122	584	-0.55	-0.17	152	486	11	6	480	62.8
4.9	2006-2039	2.0	RCP 8.5	No dam	Max	106	342	-0.88	-0.41	124	280	10	6	98	35.9
	2040-2069					98	474	-0.71	-0.25	128	344	10	6	266	38.1
	2070-2099					122	602	-0.53	-0.17	154	504	11	6	496	64.5
4.10	2006-2039	2.0	RCP 8.5	A	Expected	120	258	-1.07	-1.00	136	206	10	7	52	35.4
	2040-2069					114	346	-0.94	-0.48	138	240	10	6	144	36.4
	2070-2099					134	430	-0.59	-0.22	164	406	11	6	394	55.2
4.11	2006-2039	2.0	RCP 8.5	B	Expected	116	328	-1.07	-0.39	130	282	10	7	88	35.7
	2040-2069					110	460	-1.00	-0.29	134	280	10	6	262	38.0
	2070-2099					134	578	-0.70	-0.17	158	454	11	6	474	60.0
4.12	2006-2039	2.0	RCP 8.5	A	Max	122	258	-1.07	-0.88	110	208	10	7	54	35.4
	2040-2069					114	354	-0.94	-0.45	140	244	10	6	154	36.6
	2070-2099					134	438	-0.55	-0.22	166	412	11	6	396	56.0
4.13	2006-2039	2.0	RCP 8.5	B	Max	116	352	-1.00	-0.38	132	284	10	7	100	35.9
	2040-2069					110	484	-0.94	-0.26	136	294	10	6	294	38.5
	2070-2099					134	596	-0.64	-0.16	158	468	11	6	486	61.5

Chapter 7 BIOLOGICAL IMPACTS of CLIMATE CHANGE on THE GAMBIAN FISHERIES

Observed Impacts of Climate Change on the Freshwater and Marine Environments of The Gambia and Forecast of Future Changes

1. **A growing body of evidence is bringing greater clarity to the direction and rate of change in key climate change drivers affecting The Gambia fisheries** (as summarised in Table 7-1). Some of the most notable trends include the average **increase in sea temperature** of approximately 0.9 °C (0-200 m depth) in total warming from 1980 to 2010 within the Canary Current Large Marine Ecosystem (CCLME) (Vélez-Belchí et al., 2015). Considerable variation exists in the rate of warming across the CCLME however, with increases of up to 0.65 - 0.9 °C per decade (i.e. 2-3 times faster warming) observed in certain locations (ibid). Based on IPCC projections of temperature increases it is expected that waters within the CCLME will experience further temperature increases of up to 1.4–1.9 °C per decade by 2100 (IPCC, 2019). Temperature increases directly affect other critical water quality parameters, reducing dissolved oxygen levels and raising salinity.
2. **Another important environmental change brought by climate change is sea level rise.** Sea levels in the southern portion of the CCLME rose by approximately 4.5 mm per year during the period 1992-2013 (Pérez-Gómez et al., 2015), a rate that is expected to accelerate with sea levels ultimately rising by 0.84 to 2.0 m by 2100 (IPCC, 2019; NOAA, 2017; Bamber et al., 2019). A 1 m rise in sea level is projected to submerge 61 percent of the country's mangroves (Jaiteh and Sarr, 2011). Recent findings indicate that melting of the Greenland ice sheet may have crossed a point of no return (or "tipping point"), entering into a phase of self-sustained melting that will continue independent of efforts to limit global temperature increases (King et al., 2020). The volume of water contained in the Greenland ice sheet has the potential of causing sea levels to rise by 7.4 m (WCRP, 2018); capable of inundating vast portions of the country. Other predicted impacts of climate change in The Gambian marine environment include increases in ocean acidification and the incidence of extreme events (see Table 7-1).
3. **Clear trends, however, have not been identified for all the environmental impacts of climate change.** Uncertainty remains, for example, regarding the predicted trend in upwelling productivity. The lack of observational data in Gambian waters and the highly heterogeneous nature of the CCLME precludes the making of specific predictions (Vélez-Belchí et al., 2015). Productivity has shown a slight decrease in the southern portion off the Gambian coast from 1998 to 2014 (Demarcq and Benazzouz, 2015). These observed changes in productivity are likely associated with increases in SST leading to higher thermal stratification, with productivity expected to decline by a further 7-16 % by 2081-2100 (IPCC, 2019a) despite an increase in the speed of favorable winds associated with upwelling, predicted by some models for the central and northern CCLME (Lachkar and Gruber, 2013). Any change in productivity of the upwelling in the CCLME would have immense impact on the future stocks of small and large pelagic species.
4. **In terms of the freshwater environment within the Gambia River, marked increases in air temperature (as a proxy for water temperature) are also predicted.** Even with forecast future temperatures within the watershed at the lower end of those predicted globally (1.5 – 2.25 °C locally versus 2.3 – 4.7 °C globally) (Sherwood et al., 2020) (see Chapter 5), the anticipated increases in

minimum and maximum water temperatures will begin to have negative effects on the productivity of the mangrove and, more selectively, individual aquatic species. An increase in moisture loss through

Table 7-1 Overview of observed and forecast trends in key climate change stressors in the freshwater and marine environments of The Gambia

Attribute	Trends	Comments
Freshwater		
Air temperature (proxy for water temp.)	Expected increase in the average temperature of 0.05–0.1 °C per year from 2011–2099, with predicted average high temperatures in the rainy season rising from 31.3 °C to 34.6 °C from 2011–2099; and average low temperatures in the dry season rising from 25.4 °C to 32.4 °C (min-max) from 2011–2099.	Temperatures averaged across output from the five GCMs for the rainy season (May–October) and dry season (November–April); minimum temperatures are projected to rise nearly twice as fast as maximum temperatures. See Chapter 2 “Climate Trend Analysis and Projected Climate Change in the Gambia River Watershed” for details.
Floods/droughts	Likely modest declines in precipitation in the Gambia River basin in the future; moderate agreement among the five earth system models used in the analysis. Potential shifting in the seasonality (timing and length) of the natural annual flood/recession cycle, within a context of declining overall streamflow, may have greater effect on niches and species.	See Chapter 3 “Climate Trend Analysis and Projected Climate Change in the Gambia River Watershed” for details.
Freshwater flow	The Gambia River basin future streamflow will likely decline by 4.5 % (Roudier et al., 2014). Projections for 2070–2090 suggests that with the dam in operation the discharge for the rainy season will be 100–480m ³ /s (below and later than natural discharge) and for the dry season 50–100 m ³ /s (above and shorter than natural discharge). The influence of the dam release on river flow, volume and timing, will serve to further accentuate the anticipated shifting in natural flood/recession cycle.	The higher flowrate during the dry season will keep the salinity front further downstream, affecting the geographic extent of marine species habitat during this period, while allowing saline intrusion to advance further upstream during the rainy season. See Chapter 3 “Climate Trend Analysis and Projected Climate Change in the Gambia River Watershed” for details.
Salinity intrusion	Salinity intrusion in the Gambia River: 176–243KP upstream with a maximum of 309 KP if stoppage of dam for 2.5 months.	See Chapter 6 ‘Saline Intrusion in the Gambia River After Dam Construction’ for details.
Marine		
Sea level	Sea level has increased by approximately 4.5 mm per year during 1992–2013 in the southern portion of the CCLME (Pérez-Gómez et al., 2015), but is predicted to accelerate in the period up to 2050. Sea level rise (SLR) of 0.84–2.0 m is predicted by 2100; potentially increasing to 15 mm/year.	The predicted .84 - 2 m of SLR by 2100 would allow sea water to enter much of the length of the Gambia River within the country and inundate most parts of the capital city; 1 m of SLR would cover 61 percent of the mangroves, as well as potentially contributing to hypoxia conditions within estuary. See Chapter 6 “Salinity intrusion” for details.
Extreme events	Marine heatwaves (MHWs) and incidence of harmful algal blooms (HABs) are likely to increase. Frequency of MHW have doubled since 1982; an increase in the	See Chapter 4 ‘Climate Change and the Oceanic Environment’

	frequency of 50 times and intensity by 10 times is predicted by 2100. HAB are associated with rising SST and are expected to increase.	
Temperature	Upper ocean temperatures (0-200 m depth) in the CCLME have increased by ~ 0.28 °C per decade during 1982-2013 (Vélez-Belchí et al., 2015), or 0.9 °C of total warming. Some areas within the CCLME have warmed at 0.65 °C per decade. IPCC predicts an increase of 1.4–1.9 °C per decade by 2100 for the CCLME.	Higher warming rates (up to 0.9°C per decade) observed in locations with greater downwelling during the summer months. See Chapter 4 'Climate Change and the Oceanic Environment'.
Circulation, mixing and productivity	Possible slight decrease in productivity in the southern portion off the Gambian coast from 1998 to 2014 (Demarcq and Benazzouz, 2015). Increase in SST leading to higher stratification by 12-30% within the continental shelf and less mixing of surface and deeper waters. Net primary productivity (NPP) is predicted to decline by 7-16 % during 2081-2100 due to increased stratification (IPCC, 2019a), thus precluding a doubling of NPP in response to a doubling of upwelling induced by increasing wind speed predicted by some models for the central and northern CCLME (Lachkar and Gruber, 2013).	There has been an increase in speed of winds that are considered favourable to upwelling in the CCLME (Benazzouz et al., 2015), however, this has not resulted in any actual increase in upwelling activity associated with these winds.
Acidification	A decline in pH of -0.0013 to -0.0025 per year within the CCLME since 1994 (Canary Islands), roughly double the global rate of ocean acidification. Ocean pH levels are projected to continue to decline by an estimated 0.3 – 0.4 units under RCP 8.5 by the end of the century.	See Chapter 4 'Climate Change and the Oceanic Environment'
Deoxygenation	The oxygen minimum zone (OMZ) in the CCLME is the least hypoxic OMZ globally, but the rate of decline in dissolved oxygen levels is twice as fast (Pelegri and Peña-Izquierdo, 2015b; Stramma et al., 2008). 50% O ₂ reduction is predicted to 1000 m depth, and 98% reduction below this.	See Chapter 4 'Climate Change and the Oceanic Environment'
Salinity	Measurements in the CCLME show both an increase in temperatures of the surface layer, and a corresponding increase in salinity of 0.03 +/- 0.023 per decade (Vélez-Belchí et al., 2015). Due to the relationship between SST, water density and salinity, it is expected that salinity in the upper oceans will continue to rise as waters warm.	

evaporation, due to rising temperatures, and moderate declines in precipitation in the Gambia River basin, will likely result in a decline in stream flow of 4.5 percent (Roudier et al., 2014). When combined with the expansion of irrigation and dam construction, a potential shift in the seasonality (timing and length) of the annual flood/recession cycle and overall river flow (see chapter 6) is likely in the years ahead, with unknown impacts on overall ecologies, species assemblages and individual species. Overall, salinity intrusion is expected to become more pronounced due to both changes in river flow and sea level rise.

5. A summary of observed and future trends in climate change impacts on the freshwater and marine environments of The Gambia are presented in Table 7-1, based on the detailed assessment contained in earlier chapters in this proposal.

Climate Vulnerability Assessment: Methods

6. **The vulnerability assessment (VA) framework used in this analysis is adapted from Cochrane et al. (2019), and it is consistent with the VA framework of the Intergovernmental Panel on Climate Change (IPCC).** This framework has been successfully applied in other African fisheries, such as Madagascar and the Benguela Current (Cochrane et al., 2019; 2020b). Within the framework, vulnerability is defined as the degree to which a system (or a species) is susceptible to or unable to cope with the adverse effects of climate change stressors as a function of their exposure (nature and degree to which a system or species is exposed to significant climatic variations), sensitivity (the degree to which a system or species responds, either adversely or beneficially, to climate related stimuli), and adaptive capacity (the ability to adjust to potential damage, to take advantage of opportunities, or to respond to consequences) (e.g., Marshall et al., 2009, 2013; Sowman and Raemaekers, 2018).

7. **The VA framework has four components:** exposure to climate drivers (modified here to also include an assessment of species sensitivity), ecological resilience, social-economic resilience and national economy and governance. The ecological and social-economic resilience elements evaluate the exposure and sensitivity of a fishery as a whole, or specific sub-groups of stakeholders within the fishery, while the National Economy and Governance components are defined at the national level to represent the role that a strong economy and effective governance system can have in supporting adaptation.

8. **In this analysis, the VA framework is adapted and used here in carrying out an expanded species-level assessment of the exposure and sensitivity to climate change drivers (first component of the VA framework) for key species in The Gambia freshwater and marine environments.** The steps in carrying out the assessment are the following:

9. **Selection of key species in The Gambia:** The focus of the assessment is on freshwater and marine fish and invertebrate species of ecological and economic importance in The Gambia. The assessment includes target species of the main fisheries in the country, but also species of potential importance for the aquaculture production. Information on landings from the commercial and artisanal fisheries were used to determine key species representative from the different fishery habitats in The Gambia, e.g., oceanic, coastal, estuarine/brackish, and freshwater. Several species included in the assessment occupy different habitats at different stages of their lifecycle (see Table 7-3), for instance, the use of estuarine habitats by marine species for reproduction and subsequent early stages of larval growth. The final list of species included in this analysis was vetted and selected based on consultations with local fisheries experts (as presented in Table 7-3).

10. **Species information – habitats:** The selected species grouped, based on expert opinion, according to the dominant fishery habitat they occupy as follows:

- **Freshwater:** Corresponding to the upper reaches of The Gambia River that are permanently freshwater. This habitat generally starts above KP 254 (310 km in extremely dry periods) upstream from the river mouth, depending on the seasonal flow in The Gambia River, to the Senegal border at KP 460.
- **Brackish:** Middle reaches of The Gambia River, representing the interaction between freshwater and marine waters with salinities ranging from 1-34 ppt. This habitat starts at approximately 64 KP to the upper extent of the saline front, around 254 KP.
- **Estuary:** Lower reaches of The Gambia River, with permanent ocean water and salinities of 35 ppt. This habitat starts at the mouth of The Gambia River (0 KP) to around 64 KP.
- **Coastal:** Characterized by ocean salinities of 35 ppt, extending from the coastline to the edge of the continental shelf approximately 70 km offshore.
- **Oceanic/marine:** Characterized by salinities of 35 ppt, extending from the edge of the continental shelf 70 km offshore to the limit of the economic exclusion zone at 370 km from shore.

11. **Selection of climate variables to include as exposure factors:** The climate drivers that could have an impact on the species were selected based on a literature review and in consultations with local experts. For each of the climate drivers information was gathered on both observed and predicted trends, and their known or expected impact on the selected species. Key drivers impacting both freshwater and marine environments were included to cover the diversity of habitats in The Gambia since many species used different habitats through their life stages. **A final list of eight climate drivers were retained**, including: sea level rise, extreme events⁹⁰ (i.e., marine heatwaves), sea/land surface temperature, ocean circulation (e.g., upwelling driven plankton productivity⁹¹), precipitation, ocean acidification, ocean deoxygenation and salinity. The influence of these eight drivers on species from coastal and marine habitats was evaluated. For freshwater habitats, the influence of SLR, extreme events (e.g. salinity intrusion or hypersalinity), air temperature, salinity and precipitation was evaluated. Air temperature was used as a proxy for water temperature in freshwater habitats since most climate models do not adequately resolve temperature in freshwater and estuarine environments. Acidification and deoxygenation trends for The Gambia River were not available since most climate models do not resolve these variables for freshwater environments. The rationale for the selection of climate drivers can be found in Table 7-1. The influence of each climate driver on a species was assumed to be equal with regards to critical thresholds.

12. **Biological information on species' sensitivity – environmental tolerances:** The literature review and discussions with national stakeholders indicate that at this stage no other studies have evaluated the sensitivity of Gambian species to climate change using trait-based or other vulnerability approaches. In the present analysis, sensitivity is estimated using information of species-specific environmental tolerances and is combined with the exposure assessments to provide an indication of the capacity of a species to respond to environmental change. For instance, if the projected change in temperature is expected to exceed a species thermal tolerance, then the species is considered highly vulnerable to climate change.

⁹⁰ An extreme weather event is an event that is rare at a particular place and time of year. Definitions of rare vary, but an extreme weather event would normally be as rare as or rarer than the 10th or 90th percentile of a probability density function estimated from observations (IPCC, 2014).

⁹¹ Ocean productivity refers to the production of organic matter by phytoplankton (Sigman and Hain, 2012)

13. **Reports and peer-reviewed literature were used to compile information on species' environmental tolerances.** For some species, only limited information on their specific tolerances and environmental thresholds was available. Based on the limited available of information on some species, it was decided that:

- 1) If information is not available for a given species in Gambian waters, information for that species (or genus) in another geographical area is used.
- 2) If no information was available for a given species in other geographical areas, estimates of species preferences (or environmental envelopes) from the Aquamaps tool (Kaschner et al., 2019) are used. The environmental preferences are derived from large sets of occurrence data available from collection databases (Kesner-Reyes et al., 2016).

14. **Gathering information on climate projections:** Information on climate drivers was obtained from the analysis carried out in preparation of this proposal and the available scientific literature. Detailed information on climate change projections can be found in Chapters 3-6 in this study. Climate projections of changes to precipitation and temperature are based on the analysis of the global circulation models used in the Intergovernmental Panel on Climate Change Assessment Report 5 (IPCC AR5) under the Representative Concentration Pathway 8.5. Changes in exposure were estimated using a straight-line trend extension of the projected changes through the end of the century (2070-2099) as presented in Chapter 3. These projected changes in precipitation and temperature, along with other data, were further analyzed in the SALNST model to assess the extent of saltwater intrusion into the Gambia River and likelihood of the river becoming hypersaline (Chapter 6). Additional, detailed information on the climate change impacts on each of environmental segments of the fisheries – marine, estuarine, freshwater – were drawn from the literature (Chapters 4 and 5).

15. **Scoring vulnerability to individual climate drivers:** Information on species sensitivity (environmental tolerances) and exposure to climate drivers were used to estimate vulnerability. The direction of a species response to changing climate was scored as either positive, negative, neutral or uncertain. Climate drivers were scored on a scale ranging from -2 (high negative impact) to +2 (high positive impact). Scores were assigned based on the combination of the projected change in a climate driver and the species tolerance. For instance, if sea temperature is expected to increase above the upper limit of the thermal tolerance/preference of a species then, their vulnerability will be scored as highly negative (-2). If a species was not exposed to a given factor, e.g., black hake is not exposed to changes in freshwater temperature because they are marine species living in deeper oceanic waters, then this attribute was not scored. Vulnerability scores were then reviewed by local experts.

16. **Overall climate vulnerability rating:** Based on the available information, the overall species vulnerability (i.e., representing the combined effect of two or more climate drivers) was scored on a scale from -2 (high vulnerability) to +2 (high resilience). The overall vulnerability was estimated using an established logic rule (Hare et al., 2016, Cochrane et al. 2019). The scoring criteria assumes that a small number of elements (i.e., climate drivers) showing high vulnerability (or high resilience) will have a strong influence on overall vulnerability or resilience of the species (see

17. Table 7-2). All scores were assumed to have an equal weighting when determining the overall vulnerability but, in effect, the logic rules give a higher weighting to the more extreme negative values or critical climate stressors.

Table 7-2 Logic rules used to derive the overall climate vulnerability score (adapted from Cochrane et al. 2019)

Category	Composite score	Logic rule
<i>If two or three climate stressors are assessed</i>		
High vulnerability	-2	If at least 1 stressor = -2
Moderate vulnerability	-1	If all stressors >-2 and at least 1 = -1
Neutral	0	If all stressors >-1 and at least 2 = 0
Moderate resilience	+1	If all stressors >-1 and at least 2 = +1
High resilience	+2	If all stressors >-1 and at least 2 = +2
<i>If four climate stressors or more are assessed</i>		
High vulnerability	-2	If at least 2 stressors = -2
Moderate vulnerability	-1	If less than 2 stressors = -2 and at least two stressors \leq -1
Neutral	0	If less than 2 stressors = -1 and the mean of the rest \leq 0.5
Moderate resilience	1	If less than 2 stressors = -1 and the mean of the rest \geq 0.5 and less than 1.5
High resilience	2	If less than 2 stressors = -1 and the mean of the rest \geq 1.5

Vulnerability of Key Species to the Likely Impacts of Climate Change

18. Twenty-eight aquatic species of ecological and economic importance were selected for inclusion in the analysis (see Table 7-3). The selected species include invertebrates and fish species, inhabiting the full range of ecosystems found in The Gambia, from freshwater to marine habitats. As shown in the Table, several species occupy different habitats through their life cycle. The selected species have a wide distributional range and are not restricted to The Gambian waters.

19. The adapted assessment framework accounts for the major climate drivers that, individually and jointly, impact the freshwater and marine environments and potentially impact the selected species. The overall vulnerability of a species combines the climate exposure and a species-specific sensitivity to climate drivers. Our assessment found that the overall climate vulnerability ranges from highly resilient to highly vulnerable. Nine species were found to be highly vulnerable to climate drivers suggesting these species are more at risk of the potential impacts of climate change. These species include the pink shrimp (*Penaeus notialis*), giant tiger shrimp (*P. monodon*), striped shrimp (*P. kerathurus*), deep-water shrimp (*P. longirostris*), Guinean shrimp (*Parapenaeopsis atlantica*), tuna species (*Thunnus* spp.), octopus (*Octopus vulgaris*) and African giant cuttlefish (*Sepia hierredda*). The giant tiger and striped shrimp were found to be highly vulnerable in both the estuarine and coastal environments because of sea temperature and extreme events such as floods and droughts, while the Guinean and pink shrimps (juveniles) were scored as moderately vulnerable in the estuarine environment, due to climate factors such as ocean acidification and circulation. While tolerance to environmental drivers are species-specific, all shrimp species were found to be vulnerable to acidification and changes in ocean circulation (e.g., thermal stratification affecting larval dispersal and survival). Marine invertebrates, such as molluscs and crustaceans, are generally among the most sensitive to the effects of ocean acidification (Kroeker et al., 2013).

20. Nine species scored moderately vulnerable, these include mackerel (*Scomber colias*), horse mackerel (*Trachurus* spp.), sea breams (*Dentex* spp.), grouper (*Epinephelus aeneus*), snappers (*Lutjanus* spp), hake (*Merluccius* spp.), West African mangrove oyster (*Crassostrea gasar/tulipa*), tilapia (*Oreochromis niloticus*) and the African arowana (*Heterotis niloticus*). The moderate vulnerability of these coastal and marine species was mainly attributed to the negative impacts of warming sea

temperature and changes in upwelling (Table 6). While SLR and changes in precipitation were the drivers explaining the moderate vulnerability of tilapia and the West African mangrove oyster.

21. Eight species were found to have a neutral climate vulnerability, including both pelagic and demersal species such as round sardinella (*Sardinella aurita*), flat sardinella (*S. maderensis*), flase scad (*Caranx rhoncus*), blue spotted sea bream (*Sparus caeruleostictus*), red pandora (*Pagellus bellottii*), croackers (*Pseudolithus* spp.), bonga shad (*Ethmalosa fimbriata*), and marine catfish (*Arius* spp). A commonality among these species is their broader thermal preferences explaining the neutral score to increased sea temperature. There is some evidence of higher recruitment of flat sardinella in waters with low chlorophyll (Chl-a) values associated with phytoplankton concentrations (Diankha et al., 2018), suggesting that the predicted reduction in upwelling productivity may not negatively affect the flat sardinella. As for the majority of species selected, information on acidification and deoxygenation effects were not available, thus, it is important to note that if information were to become available indicating either negative or positive impacts of these drivers, the vulnerability of these species should be revised.

22. The sole (red and black sole: *Cynoglossus senegalensis*/ *Dagetichthys cadenati*) was found to be moderately resilient to the climate drivers analyzed here. While increases in sea temperature are expected to have negative effects on this species, its broad salinity tolerance ranging from 0-38 psu (Panfili et al., 2006) contributes to their resilience to both predicted salinity increases and decreased precipitation. The African catfish (*Clarias* spp.) and the kosso (*Synodontis schall*) were scored as highly resilient to the impacts of climate change. The African catfish is quite resilient to temperature changes and tolerate water temperatures of up to 35 °C (Van Vliet et al. 2013).

23. Overall, the analysis highlights that there are several information gaps regarding the environmental tolerances of the selected species. Generally, more information was available for freshwater and invertebrate species when compared to coastal and pelagic species. As mentioned above, information on species responses to acidification, deoxygenation and extreme events were not available for most species. This underlines important knowledge gaps and efforts should be made to address these gaps to obtain a more informed assessment of species likely response to climate change stressors.

24. Some of the species most at risk to the effects of climate change are important, high-value target fisheries (e.g. shrimps, octopus, cuttlefish). This finding underlines the critical importance in managing these stocks in a sustainable manner as a means of extending their resilience to climate change stressors. Detailed information on the exposure and sensitivity of these species can be found in Appendix 1 of this chapter.

Table 7-3 List of key species of ecological and economic importance in The Gambia and their habitat preference according to their life cycle and seasonal variations.

All year presence in a habitat is marked in orange, periodic presence is marked in light cream with the respective month and relative activity indicated. Potential aquaculture species are also indicated. Seasonality: Rain/Hot: rainy and hot season (May to October); Dry/Cold: dry and cold season with harmattan winds (November to April); Y: yearly. Additional notes within columns refer to specific events occurring in given months (e.g., M6, indicates an event occurring in June).

Common name	Scientific name	Distance from shore/mouth	3 7 0 k m		7 0 k m		K P 0		K P 6 4		K P 2 5 4	K P 3 7 0		K P 4 5 0	
		Ecology		Oceanic		Coastal		Estuary		Brackish			Freshwater		Aquaculture
		Salinity		35ppt		35ppt		35ppt		1-34ppt			<1ppt		
		Seasonality													
Tuna	<i>Thunnus sp.</i>	Y													
Round sardinella	<i>Sardinella aurita</i>	Rain/Hot		M6: spawning M9: migrating north		Juveniles									
		Dry/Cold		M4: arriving from Cabo verde		Juveniles									
Flat sardinella	<i>Sardinella maderensis</i>	Rain/Hot				M6: living to Joal M7-M9: breeding									
		Dry/Cold				M3: arriving		Immature juveniles							

[illegible]

		Dry/Cold				M11& M3: spawning peak		M2-M5: spawning / larvae		M1: migration upstream M5: larvae						
Solefish	<i>Cynoglossus senegalensis</i> <i>Synaptura cadenati</i>	Y														
Catfish	<i>Arius spp.</i>	Y														
False scad	<i>Caranx rhonchus</i>	Y						M4-M7: spawning shallow water								
Tilapia	<i>Oreochromis niloticus</i>	Y														
African catfish	<i>Clarias gariepinus/anguillaris</i>	Y														
Catfish/ Kosso	<i>Synodontis spp.</i>	Rain/Hot Dry/Cold														
African arowana/ fantango	<i>Heterotis niloticus</i>	Y														
Octopus	<i>Octopus vulgaris</i>	Y														

African giant cuttlefish	<i>Sepia officinalis hierredda</i>	Y													
Guinean shrimp	<i>Parapenaeopsis atlantica</i>	Y				Spawning and larvae marine		Juvenile migrating downstream							
Giant tiger shrimp	<i>Penaeus monodon</i>	Y				Spawning and larvae marine		Juvenile migrating downstream							
Striped shrimp	<i>Penaeus kerathurus</i>	Y				Spawning and larvae marine		Juvenile migrating downstream							
deep-water shrimp	<i>Parapenaeus longirostris</i>	Y													
Pink shrimp	<i>Penaeus notialis</i>	Rain/Hot						M8-M11: juvenile migrating downstream							
		Dry/Cold				M12-M3: Spawning & larvae marine		M1-M8: postlarvae		M1-M5: migration upstream					
West African mangrove oyster	<i>Crassostrea gasar/tulipa</i>	Rain/Hot				Where Mangrove									
		Dry/Cold				Where Mangrove		Pelagic larvae		M4-M7 colonization					

Table 7-4 Summary of the vulnerability assessment of ecological resilience for species of economic importance to The Gambia fisheries sectors.

Red (−2): high negative impact; orange (−1): moderate negative impact; peach (0): neutral impact; green (+1): moderate positive impact; blue (+2): high positive impact; grey: Not applicable and U: uncertain. Species highlighted in bold correspond to those that use more than one habitat through their life stages. All species listed on the coastal habitat are also found on estuarine habitats.

Area	Species	Climate drivers								Overall score
		1.1	1.2	1.3	1.4	1.5	1.6	1.7	1.8	
		SLR	Extreme events	Temperature	Ocean circulation	Acidification	Deoxygenation	Precipitation	Salinity	
Oceanic	Tuna <i>Thunnus</i> spp.	+1	-2	-2	-2	-2	-2	+2	0	-2
	Deep-water rose shrimp <i>P. longirostris</i>	+1	+2	+2	-2	-2	+1	+2	+2	-2
Oceanic & Coastal	Round sardinella <i>Sardinella aurita</i>	0	U	-1	0	U	U	+1	0	0
	Flat sardinella <i>Sardinella maderensis</i>	0	U	0	0	U	U	-1	0	0
	Mackerel <i>Scomber colias</i>	0	U	-1	-1	U	U	U	0	-1
	Atlantic horse mackerel <i>Trachurus</i> spp.	0	U	-1	-1	U	U	U	0	-1
	Hake <i>Merluccius</i> spp.	0	U	-1	-1	U	U	U	0	-1
	Blue spotted seabream <i>Sparus caeruleostictus</i>	0	U	-1	0	U	U	U	0	0
	Sea breams <i>Dentex</i> spp.	0	U	-1	-1	U	U	U	0	-1
	Groupers <i>Epinephelus aeneus</i>	0	U	-1	-1	-1	U	U	0	-1
	Octopus <i>Octopus vulgaris</i>	0	+2	-2	-2	-2	-1	-2	0	-2

	Cuttlefish <i>Sepia officinalis hierredda</i>	+2	U	-1	-2	-2	+2	-1	+2	-2
	Red pandora <i>Pagellus bellottii</i>	0	U	0	-1	U	U	U	0	0
	Croakers <i>Pseudolithus</i> spp.	0	U	0		U	U	+1	0	0
Coastal	Bonga shad <i>Ethmalosa fimbriata</i>	0	U	0	-1	U	U	0	0	0
	False scad <i>Caranx rhonchus</i>	0	U	0	-1	U	U	U	0	0
	Snappers <i>Lutjanus</i> spp.	0	U	0	-1	U	U	-1	0	-1
	Solefish <i>Cynoglossus senegalensis/ Dagetichthys cadenati</i>	0	U	-1	U	U	U	+1	+2	+1
	Catfish <i>Arius</i> spp.	0	U	0	0	U	U	-1	0	0
	Guinean shrimp <i>P. atlantica</i>	+1	+2	-2	-2	-2	+1	+2	+2	-2
	Pink shrimp <i>P. notialis</i>	+1	+2	-2	-2	-2	+1		+2	-2
	Striped shrimp <i>P. kerathurus</i>	+1	-2	-2	-2	U	U	+2	+2	-2
	Giant tiger shrimp <i>P. monodon</i>	-2	-2	-2	-2	-2	U	+2	-2	-2
Estuarine	West African mangrove oyster <i>Crassostrea gasar/tulipa</i>	-1	-2	U	U	U	U	-1	-1	-1
	Guinean shrimp <i>P. atlantica</i>	+2	+2	-2				+2	-1	-1
	Pink shrimp <i>P. notialis</i>	+1	+2	-2					-1	-1
	Striped shrimp <i>P. kerathurus</i>	+1	-2	-2				+2	-1	-2

	Giant tiger shrimp <i>P. monodon</i>	-2	-2	-2				+2	-2	-2
	West African mangrove oyster <i>Crassostrea gasar/tulipa</i>	-1	-2	U				-1	-1	-1
Brackish & Freshwater	African catfish <i>Clarias gariepinus/anguillaris</i>	U	+2	+2				+2	-1	+2
	African arowana fatango <i>Heterotis niloticus</i>	U	-2	-1				0	U	-1
	Nile tilapia <i>O. niloticus</i>	-1	+2	+1				U	-1	-1
	Catfish/kosso <i>Synodontis schall</i>	U	+2	U				+2	U	+2
Aquaculture	West African mangrove oyster <i>Crassostrea gasar/tulipa</i>	-1	-2	U				-1	-1	-1
	Pink shrimp <i>P. notialis</i>	+1	+2	-2				U	-1	-1
	Striped shrimp <i>P. kerathurus</i>	+1	-2	-2				+2	-1	-2
	Giant tiger shrimp <i>P. monodon</i>	-2	-2	-2				+2	-2	-2
	Nile tilapia <i>O. niloticus</i>	-1	+2	+1				U	-1	-1
	African catfish <i>Clarias gariepinus/anguillaris</i>	U	+2	+2				+2	-1	+2
	African arowana fatango <i>Heterotis niloticus</i>	U	-2	-1				0	U	-1

Vulnerability to Climate Change of Different Segments (habitats) of The Gambia Fisheries and Aquaculture

25. As mentioned above, several species included in the climate vulnerability assessment occur in different habitats through their life stages or are simultaneously found in different habitats (see Table 7-3). While this suggests that these species have broad environmental tolerances, as they are able to occupy different habitats, it also indicates that they are likely to encounter exposure to additional stressors in the habitats they occupy at different points in their lifecycle. The number of species analyzed here under each habitat varies, for instance only two ‘strictly’ oceanic species were included in the assessment with the remainder found in other habitats.

26. **Overall, the highest number of highly vulnerable species were found on the coastal and estuarine environments, e.g., particularly shrimp species.** These species were highly vulnerable to the effects of warming, ocean acidification and changes in thermal stratification affecting larval survival and dispersal. The West African mangrove oyster and the snappers scored as moderately vulnerable in the coastal habitats. The vulnerability of snappers is a result of changes in ocean circulation and precipitation. For instance, while *Lutjanus goreensis* spawns throughout the year, a peak in the breeding season has been observed during the heavy rains (May to September) in Nigeria (Fakoya and Anetekha, 2019), thus, it is expected that a decline in precipitation or disruption in streamflow due to the dam release schedule during this period would negatively affect snappers’ breeding and spawning rhythm. The response of snappers to SLR, salinity and temperature were scored as neutral since these species have been found to spawn year-round, with peaks in spawning during warm water temperatures (Thresher, 1984), and an exhibited tolerance to a broad range of salinities.

27. In the coastal habitat, bonga shad, marine catfish and solefish scored a neutral vulnerability or moderate resilience to climate change impacts. Bonga shad, the most important target of the artisanal fisheries in terms of landings in The Gambia, has been found to withstand a wide range of environmental conditions and can spawn even under moderately hypersaline conditions (Panfili et al., 2004). This species scored a moderate vulnerability to the likely decrease in upwelling productivity, since a peak in fecundity of Bonga shad has been associated with periods of high upwelling intensities (Baldé et al., 2019). While these authors reported that fecundity peaked at an SST of 25 °C during the period 2004-2012, the species has been found to spawn in temperatures as high as 30.2 °C (Albaret and Gerlotto, 1976; Döring et al., 2017). While this species is considered resilient to environmental changes, strong declines in upwelling productivity due to climate change could negatively affect their fecundity and abundance.

28. In the oceanic and coastal habitats, octopus and the African giant cuttlefish scored the highest vulnerability. Climate drivers such as temperature, acidification and ocean circulation explained octopus vulnerability. The mortality rates of *O. vulgaris* increase at temperatures higher than 25 °C (Giménez & García, 2002; Repolho et al. 2014). Moreover, decreases in pH have negative effects on oxygen affinity reducing metabolism and consequently growth and reproduction of this species (Pecl & Jackson, 2008). Similarly, premature hatching of African giant cuttlefish eggs and lower survival rates have been recorded at pH lower than 7.5 (Bloor, 2016). The medium vulnerability of mackerel, hake, horse mackerel, white grouper and sea breams is attributed to the impacts of warming and decreases in upwelling productivity. The white grouper undertakes a seasonal migration from Mauritania to Senegal related to the onset of

productivity in Senegalese waters and decreased productivity in Mauritania (Cury and Roy, 1988). The expected decrease in upwelling productivity and possibly timing of the upwelling season is likely to have negative impacts in the phenology and biomass of white grouper. The decrease in productivity is also likely to result in negative impacts for planktivore species such as mackerel, horse mackerel and sea breams, which feed on zooplankton through their life stages. While flat and round sardinella, false scad, red pandora and groupers scored a neutral vulnerability, drivers such as upwelling productivity, temperature and precipitation are likely to have negative impacts on their abundance and resilience (Table 6). For instance, a seasonal inshore migration of red pandora (up to 18 m depth) has been observed in Ghanaian waters during the upwelling months (Amponsah et al., 2016), and spawning also takes place during the upwelling season (Jun- Sep) (Asabere-Ameyaw, 2000). Productivity changes are thus likely to affect the phenology and spawning of this species.

29. The species included in the estuarine habitats scored moderate to high vulnerability, with shrimp species also scoring high vulnerability in the coastal environments. The vulnerability of several estuarine species is further exacerbated by their dependency on mangrove habitats (see Table 7-5), since mangroves play a key role in their reproduction, feeding and protection. Recent studies suggest that mangrove cover has declined by nearly 50 percent from the early 1980s to 2009-2010 (Government, 2010), and the onset of the 1968-1974 Sahelian drought led to a major dieback of mangrove habitat in the Gambia watershed (Mangrove chapter). There is uncertainty regarding the additive response of mangroves to SLR and salinity changes in the river, either resulting in vertical adaptation, horizontal movement shoreward, retreat further upstream or in die-off of roots and degradation of mangroves forests. In the Gambia River, vertical adaptation of mangroves in response to SLR may not be possible due to the decrease in river flow and static or reduced sediment transport, combined with salinity and temperature stress. Species such as bonga shad, solefish, cassava fish, Nile tilapia and mangrove oyster have a strong dependency on mangrove forests. Nile tilapia is restricted to estuaries, while the bonga shad and solefish are both estuarine of marine origin spending most of their life cycle within The Gambia estuary (Louca et al., 2009) and usually representing large fish aggregations all year around. Cassava fish is a marine-estuarine species and utilizes the mangrove systems as nursery grounds. Thus, a further decrease in mangrove cover could strongly decrease the population of the Cassava fish.

Table 7-5 List of species associated to mangrove systems in The Gambia, and threatened through habitat change/loss

Species	Mangroves play a specific role in reproduction	Mangroves play a specific protection role at some stage in the life cycle	Mangroves play a specific role in the food web of the species
Flat sardinella (<i>Sardinella maderensis</i>)		X	
Bonga shad (<i>Ethmalosa fimbriata</i>)	X	X	X
Solefish (<i>Cynoglossus</i> spp.)	X	X	X
Marine catfishes (<i>Arius</i> spp)		X	X

Groupers (<i>Epinephelus aeneus</i>)		X	
Cassava fish (<i>Pseudolithus spp.</i>)	X	X	X
Nile tilapia (<i>O. niloticus</i>)	X	X	X
Guinean shrimp (<i>Parapenaeopsis atlantica</i>)		X	
Pink shrimp (<i>Penaeus notialis</i>)		X	
Striped shrimp (<i>Penaeus kerathurus</i>)		X	
Giant tiger shrimp (<i>Penaeus monodon</i>)		X	
West African mangrove oyster (<i>Crassostrea gasar/tulipa</i>)	X	X	X

30. The African arowana scored a medium vulnerability from the brackish and freshwater systems, explained by their high sensitivity to extreme events specifically droughts, which will reduce the available habitat for this species since it inhabits permanent pools, deep swamps and flooded forests with slow current and dense vegetation. Information was available to score the impacts of temperature, precipitation and extreme events for this species, but information on the other stressors was not available. As mentioned above, African catfish and kosso scored a high resilience mostly due to their resilience to changes in precipitation and floods/droughts combined with a broad thermal tolerance in the case of the African catfish.

31. All species living in the saline influenced segments of estuary are vulnerable to extreme hypersaline conditions. When the Casamance river turned hypersaline in the 1980s, Surveys found no fish in areas of the river with salinity content above 83 ppt (DeGeorge and Reilly, 2007), even the most saline tolerant at salinities above 90 ppt (Savenije and Pagès, 1992). The pink shrimp population collapsed, oysters moved seaward, with over 60 km of Rhizophora mangrove eradicated (Savenije and Pagès, 1992). In the Gambia River, of the more than 30 species whose lifecycle depends directly or indirectly on the estuary environment, including a majority of those species in the coastal fishery, it is estimated that the catch would be reduced to four to six species should the river begin to cycle through periods of hypersaline conditions (DeGeorge and Reilly, 2007).

32. The vulnerability of aquaculture target species agreed with the vulnerability in the species' natural environments, it is important to note that while many environmental conditions can be controlled in aquaculture systems to represent the optimal conditions for a species, the negative impacts of climate change can be reduced, but it may not be possible to mitigate them in a cost effective manner.

33. It is recognized that there is uncertainty in the forecast of climate impacts for The Gambia. The uncertainty in the future pace and extent of weather trends, combined with a lack of available information on the potential impacts of climate change drivers on important resources in the country (such as water and forest cover), does not allow precise predictions to be made as to the timing and degree of climate change related impacts. Despite the uncertainty and gaps in information, changes in sea level, sea temperature, salinity and decreases in primary productivity have already been observed in The Gambian

riverine and the associated marine environment (see table Table 7-1) and the impacts on some important target species have also been recorded in the available literature reviewed for the present vulnerability assessment.

Figure 7-1 Visual summary of the climate change vulnerability assessment for the main Gambian fish species⁹²



⁹² In this figure, the two categories “moderately resilient” and “highly resilient” have been combined into a single category “resilient”, coloured in green.

References

- Albaret, J.J., Simier, M., Darboe, F.S. et al. 2004. Fish Diversity and Distribution in the Gambia Estuary, West Africa, in Relation to Environmental Variables. *Aquatic Living Resources* Vol. 17(1): 35-46. doi:10.1051/alr:200400.
- Albaret, J. J. and F. Gerlotto. 1976. Biologie de l’Ethmalose (*Ethmalosa fimbriata* Bowdich) en Côte D’Ivoire. I.- Description de la reproduction et des premiers stades larvaires. *Doc. Sci. Cent. Rech. Océanographiques* 7, 113–133.
- Amponsah, S. K., Ofori-Danson, P. K., Nunoo, F. K. and G.A. Ameyaw 2016. Aspects of population dynamics of Red Pandora, *Pagellus bellottii* (Steindachner, 1882) from the coastal waters of Ghana. *J. Scientific Innov. Res.* 5, 215–224.
- Amuzu, J. 2018. The Socio-economic Impact of Climate Change on Marine and Freshwater Fisheries Resources in the Coastal Zone of the Gambia. *Natural Resources and Conservation* 6(1): 1-12, 2018. doi:10.13189/nrc.2018.060101
- Arístegui, J., Álvarez-Salgado, X. A. Barton, E. D., Figueiras, F. G., Hernández-León, S., Roy, C. and A.M.P. Santos. 2006. “Oceanography and fisheries of the Canary Current/Iberian region of the Eastern North Atlantic (18a, E)” in *The Sea: The Global Coastal Ocean: Interdisciplinary Regional Studies and Syntheses, Vol. 14B.*, eds. A.R. Robinson and K. H. Brink (Harvard University Press), 877–931.
- Asabere-Ameyaw, A. 2000. Aspects of the reproductive biology of the red Pandora *Pagellus bellotti* (Pisces: Sparidae) in Ghana. *J. Ghana Sci. Assoc.* 2, 23–30.
- Bah, O., Kone, T., Yaffa, S., Ndiaye, M. and S. Sane. 2019. Water quality parameters and fisheries in central river region of the Gambia: Differences between wet and dry seasons. *Int. J. Fish. Aquat. Stud.* 7, 285–295.
- Baldé, B. S., Döring, J., Ekau, W., Diouf, M., and P. Brehmer. 2019. Bonga shad (*Ethmalosa fimbriata*) spawning tactics in an upwelling environment. *Fish. Oceanogr.* 28, 686–697. doi:10.1111/fog.12451.
- Bamber, J.L., M. Oppenheimer, R.E. Kopp, W.P. Aspinall and R.M. Cooke. 2019. Ice Sheet Contributions to Future Sea-Level Rise from Structured Expert Judgement. *Proceedings of National Academy of Sciences* Vol. 116(23):11195-11200.
- Barange, M., Merino, G., Blanchard, J.L., Scholtens, J., Harle, J., Allison, E.H. et al. 2014. Impacts of climate change on marine ecosystem production in societies dependent on fisheries. *Nature Climate Change* 4: 211–216.
- Belhabid, D., Mendy, A., Subah, Y. et al. 2016. Fisheries catch under-reporting in The Gambia, Liberia and Namibia and the three large marine ecosystems which they represent. *Environmental Development* 17: 157–174. doi:10.1016/j.envdev.2015.08.004
- Bell, J.D., Johnson, J.E. and A.J. Hobday. 2011a. Vulnerability of tropical Pacific fisheries and aquaculture to climate change. Noumea, New Caledonia, Secretariat of the Pacific Community. 925pp.
- Bell, J.D., Johnson, J.E., Ganachaud, A.S., Gehrke, P.C., Hobday, A.J., Hoegh-Guldberg, O., Le Borgne, R., Lehodey, P., Lough, J.M., Pickering, T., Pratchett, M.S. and M. Waycott. 2011b. Vulnerability of Tropical Pacific Fisheries and Aquaculture to Climate Change: Summary for Pacific Island Countries and Territories. Secretariat of the Pacific Community, Noumea, New Caledonia.

- Benazzouz, A., Demarcq, H. and G. González-Nuevo. 2015. "Recent changes and trends of the upwelling intensity in the Canary Current Large Marine Ecosystem," in *Oceanographic and biological features in the Canary Current Large Marine Ecosystem. IOC Technical Series, No. 115*, 321–330.
- Biagini, B., Bierbaum, R., Stults, M., Dobardzic, S. and S.M. McNeeley. 2014. A typology of adaptation actions: A global look at climate adaptation actions financed through the Global Environment Facility. *Global Environmental Change* 25 (2014) 97–108. doi:10.1016/j.gloenvcha.2014.01.003
- Bloor, I.S.M. 2016. The Current and changing role of physico-chemical factors and cues in the embryonic and early life stage development of the common cuttlefish (*sepia Officinalis*). *Vie Et Milieu - Life And Environment* 66 (1): 81-95
- Cheung, W. W. L. and M.A. Oyinlola. 2018. Vulnerability of flatfish and their fisheries to climate change. *J. Sea Res.* 140, 1–10. doi:https://doi.org/10.1016/j.seares.2018.06.006.
- Cheung, W., Bruggeman, J., and M. Butenschön. 2018. "Projected changes in global and national potential marine fisheries catch under climate change scenarios in the twenty-first century," in *Impacts of climate change on fisheries and aquaculture Synthesis of current knowledge, adaptation and mitigation options. FAO Fisheries and Aquaculture technical paper 627.*, eds. M. Barange, T. Bahri, M. Beveridge, K. Cochrane, S. Funge-Smith, and F. Poulain, 63–85.
- Cochrane, K.L., Rakotondrazafy, H., Aswani, S. et al. 2019. Tools to Enrich Vulnerability Assessment and Adaptation Planning for Coastal Communities in Data-Poor Regions: Application to a Case Study in Madagascar. *Frontiers in Marine Science* 5:505. doi: 10.3389/fmars.2018.00505
- Cochrane, K., Iitembu, J., Ortega-Cisneros, K., Santos, C. and W.H.H. Sauer. 2020. Application of a general methodology to understand vulnerability and adaptability of the small pelagic fisheries in the Benguela countries. Prepared for the Benguela Current Commission (BCC) and Food and Agricultural Organisation (FAO). April 2020.
- Cury, P. and C. Roy. 1988. Migration saisonnière du thiof (*Epinephelus aeneus*) au Sénégal: influence des upwellings sénégalais et mauritanien. *Oceanol. Acta* 11, 25–36.
- Dapilah, F., Nielsen, J.Ø. and C. Friis. 2020. The role of social networks in building adaptive capacity and resilience to climate change: a case study from northern Ghana, *Climate and Development*, 12:1, 42-56, doi:10.1080/17565529.2019.1596063
- Darboe, F.S. 2002. Fish species abundance and distribution in The Gambia Estuary. The United Nations University. Fisheries Training Program. Final Report. 40pp.
- Davies, S., Sheridan, S., Hjort, A. and H. Boyer. 2014. Gap analysis of national and regional fisheries and aquaculture priorities and initiatives in Western and Central Africa in respect to climate change and disasters. *FAO Fisheries and Aquaculture Circular No. 1094*. Rome, FAO. 107 pp.
- DeAlteris, J., Cessay, S. and A. Jallow. 2012. The Gambian Sole Stock Assessment: Final Report. Gambia-Senegal Sustainable Fisheries Project (USAID/Ba Nafaa). Coastal Resources Center, University of Rhode Island, 21pp.
- Demarcq, H., and A. Benazzouz. 2015. "Trends in primary production," in *Oceanographic and biological features in the Canary Current Large Marine Ecosystem. IOC-UNESCO, Paris. IOC Technical Series, No. 115*, eds. L. Valdés and I. Déniz-González, 331-341.

Dia Ibrahima, M. 2012. Vulnerability Assessment of Central Coast Senegal (Saloum) and The Gambia Marine Coast and Estuary to Climate Change Induced Effects. Coastal Resources Center and WWF-WAMPO, University of Rhode Island.

Diankha, O., Ba, A., Brehmer, P., Brochier, T., Sow, B. A., Thiaw, M., et al. 2018. Contrasted optimal environmental windows for both sardinella species in Senegalese waters. *Fish. Oceanogr.* 27, 351–365. doi:10.1111/fog.12257.

Ding, Q., Chen, X., Hilborn, R. and Y. Chen. 2017. Vulnerability to impacts of climate change on marine fisheries and food security. *Marine Policy* 83 (2017) 55–61. doi:10.1016/j.marpol.2017.05.011

DoF (Department of Fisheries). 2015. The Common Marine and Inland Fish Species in The Gambia.

Döring, J., Tiedemann, M., Stäbler, M., Sloterdijk, H., and W. Ekau. 2017. *Ethmalosa fimbriata* (Bowdich 1825), a Clupeid Fish That Exhibits Elevated Batch Fecundity in Hypersaline Waters. *Fishes* 2. doi:10.3390/fishes2030013.

FAO. 2007. Fishery country profile: The Gambia. Available at: http://www.fao.org/fishery/docs/DOCUMENT/fcp/en/FI_CP_GM.pdf. Accessed 15 March 2020

FAO. 2016a. Fishery Committee for the Eastern Central Atlantic, Report of the seventh session of the Scientific Sub- Committee, Tenerife, Spain, 14–16 October 2015 / FAO Fisheries and Aquaculture Report. No. 1128. Rome, Italy.

FAO. 2016b. Aquaculture insurance in Viet Nam: Experiences from the pilot programme. FAO Fisheries and Aquaculture Circular No. 1133, Rome, FAO.

FAO. 2018. Report of the FAO/CECAF Working Group on the Assessment of Demersal Resources – Subgroup North. Tenerife, Spain, from 6 to 15 June 2017/Rapport du Groupe de travail FAO/COPACE sur l'évaluation des ressources démersales – Sous- groupe Nord. Tenerife, Espagne, du 6 au 15 juin 2017. CECAF/ECAF Series/COPACE/PACE Séries. No. 18/78. Rome, FAO.

FAO. 2019. Report of the FAO Working Group on the Assessment of Small Pelagic Fish off Northwest Africa. Banjul, the Gambia, 26 June–1 July 2018. FAO Fisheries and Aquaculture Report, No. R1247. Rome, FAO.

FAO. 2020. FAO Fisheries and Aquaculture Draft Report: Review, Assessment and gap analysis of The Gambia fisheries and aquaculture sector. Fisheries, Environment (-climate change) issues and options to improve. 55pp.

Faye, S., Lazar, A., Sow, B.A. and A.T. Gaye. 2015. A model study of the seasonality of sea surface temperature and circulation in the Atlantic North-eastern Tropical Upwelling System. *Frontier in Physics* 3:76. doi: 10.3389/fphy.2015.0007.

Fakoya, K. A., and M.A. Anetekha. 2019. Macroscopic gonad staging and reproductive seasonality in the Gorean snapper, *Lutjanus goreensis* a gonochoristic West African Lutjanid. *West African J. Appl. Ecol.* 27, 1–22.

Fernández-Peralta, L. and A. Sidibé. 2015. Demersal fish in the Canary Current Large Marine Ecosystem. In: *Oceanographic and biological features in the Canary Current Large Marine Ecosystem*. Valdés L, Déniz-González I. (eds). Paris, IOC-UNESCO, IOC Technical Series, No. 115, pp. 215–229. URL: <http://hdl.handle.net/1834/9190>.

GEF/UNDP. 2018. Climate change adaptation in Africa: UNDP Synthesis of experiences and recommendations. Bangkok, United Nations Development Programme. 98pp.

Giménez, F.A., and B.G. García. 2002. Growth and food intake models in *Octopus vulgaris* Cuvier (1797): influence of body weight, temperature, sex and diet. *Aquaculture International* 10: 361–377

Government of The Gambia. 2010. National Forest Assessment 2008-2010 – The Gambia.

Gross, J.E., Woodley, S., Welling, L.A. and J.E.M. Watson (Eds.). 2016. Adapting to Climate Change: Guidance for protected area managers and planners. Best Practice Protected Area Guidelines Series No. 24, Gland, Switzerland, IUCN. 129 pp. doi:10.2305/IUCN.CH.2017.PAG.24.en

Guilliard, J., Albaret, J.J., Simier, M. and I. Sow. 2004. Spatio-temporal Variability of Fish Assemblages in the Gambia Estuary (West Africa) Observed by Two Vertical Hydroacoustic Methods: Moored and mobile sampling. *Aquatic Living Resources* Vol. 17(1): 47-55.

Hare, J. A., Morrison, W. E., Nelson, M. W., Stachura, M. M., Teeters, E. J., Griffis, R. B., et al. (2016). A Vulnerability Assessment of Fish and Invertebrates to Climate Change on the Northeast U.S. Continental Shelf. *PLoS One* 11, e0146756. doi:10.1371/journal.pone.0146756.

Horemans, B., Ajayi, T. and J. Galléne. 1996. Sector Review of the Artisanal Marine Fisheries in The Gambia. IDAF/WP/80. Cotonou, Benin: Programme for the Integrated Development of Artisanal Fisheries in West Africa.

ICCAT. 2019. Report of the 2019 ICCAT Yellowfin Tuna Stock Assessment Meeting. Grand Bassam, Cote d'Ivoire 8 – 16 July 2019.

IPCC. 2014. Climate Change 2014: Synthesis Report. Contribution of Working Groups I, II and III to the Fifth Assessment Report of the Intergovernmental Panel on Climate Change [Core Writing Team, R.K. Pachauri and L.A. Meyer (eds.)]. IPCC, Geneva, Switzerland, 151 pp.

IPCC. 2019: IPCC Special Report on the Ocean and Cryosphere in a Changing Climate [H.-O. Pörtner, D.C. Roberts, V. Masson-Delmotte, P. Zhai, M. Tignor, E. Poloczanska, K. Mintenbeck, A. Alegría, M. Nicolai, A. Okem, J. Petzold, B. Rama, N.M. Weyer (eds.)].

Johnson, J., Bell, J. and C. De Young. 2013. Priority adaptations to climate change for Pacific fisheries and aquaculture: reducing risks and capitalizing on opportunities. FAO/Secretariat of the Pacific Community Workshop, 5–8 June 2012, Noumea, New Caledonia. FAO Fisheries and Aquaculture Proceedings No. 28. Rome, FAO. 109 pp.

Kaschner, K., Kesner-Reyes, K., Garilao, C., Rius-Barile, J. et al. 2019. AquaMaps: Predicted range maps for aquatic species. World wide web electronic publication, www.aquamaps.org, version 10/2019.

Kaufmann, D., Kraay, A. and M. Mastruzzi. 2010. The worldwide governance indicators: methodology and analytical issues. Policy Research Working Paper Series 5430, The World Bank. www.govindicators.org

Kesner-Reyes, K., Kaschner, K., Kullander, S., Garilao, C., Barile, J., and R. Froese. 2016. AquaMaps: algorithm and data sources for aquatic organisms. In: Froese, R. and D. Pauly (editors). 2012. FishBase. World Wide Web electronic publication. www.fishbase.org, version (04/2012).

King, M.D., Howat, I.M., Candela, S.G. et al. 2020. Dynamic Ice Loss from the Greenland Ice Sheet Driven by Sustained Glacier Retreat. *Nature Communications Earth and Environment* 1, 1 (2020). doi:10.1038/s43247-020-0001-2.

- Kroeker, K. J., Kordas, R. L., Crim, R., Hendriks, I. E., Ramajo, L., Singh, G. S., et al. 2013. Impacts of ocean acidification on marine organisms: quantifying sensitivities and interaction with warming. *Glob. Chang. Biol.* 19, 1884–1896. doi:10.1111/gcb.12179.
- Lachkar, Z., and N. Gruber. 2013. Response of biological production and air–sea CO₂ fluxes to upwelling intensification in the California and Canary Current Systems. *J. Mar. Syst.* 109–110, 149–160. doi:<https://doi.org/10.1016/j.jmarsys.2012.04.003>.
- Lam, V.W.Y., Cheung, W.W.L., Swartz, W. and U.R. Sumaila. 2012. Climate change impacts on fisheries in West Africa: implications for economic, food and nutritional security. *African Journal of Marine Science* 34(1): 103–117. doi:10.2989/1814232X.2012.673294
- Louca, V., Lindsay, S.W., Majambere, S. and M.C. Lucas. 2009. Fish community characteristics of the lower Gambia River floodplains: a study in the last major undisturbed West African river. *Freshwater Biology*: 254–271. doi:10.1111/j.1365-2427.2008.02105.x
- Marshall, N.A., Marshall, P.A., Tamelander, J., Obura, D., Malleret-King, D. and J.E. Cinner. 2009. A Framework for Social Adaptation to Climate Change; Sustaining Tropical Coastal Communities and Industries. Gland, Switzerland.
- Marshall, N. A., Tobin, R. C., Marshall, P. A., Gooch, M., and A.J. Hobday. 2013. Social Vulnerability of Marine Resource Users to Extreme Weather Events. *Ecosystems* 16, 797–809. doi:10.1007/s10021-013-9651-6.
- Mendy, A.N. 2004. A Trophic Model of the Gambian Continental Shelf System in 1986. In: Palomares, M. and D. Pauly (Eds.). *Trophic Models of Northwest African Ecosystems: Models and Fisheries Impacts*. Fisheries Centre Research Reports, 81–94.
- Moore, A.B.M., Séret, B., and R. Armstrong. 2019. Risks to biodiversity and coastal livelihoods from artisanal elasmobranch fisheries in a Least Developed Country: The Gambia (West Africa). *Biodiversity and Conservation*. doi:10.1007/s10531-019-01732-9
- Muchuru, S. and G. Nhamo. 2018. Climate change adaptation and the African fisheries: evidence from the UNFCCC National Communications. *Environ Dev Sustain* 20:1687–1705 <https://doi.org/10.1007/s10668-017-9960-6>
- NAPA. 2007. The Gambia National Adaptation Programme of Action (NAPA) on Climate Change. Government of the Gambia, Banjul.
- NOAA (National Oceanic and Atmospheric Administration). 2017. Global and Regional Sea Level Rise Scenarios for the United States. NOAA Technical Report NOS CO-OPS 083. Silver Springs (MD): NOAA.
- Njie, E. 2016. Review of the Fisheries Sector, The Gambia. Banjul: Food and Agriculture Organization of the United Nations. 30pp.
- Nijie, M. and O. Drammeh. 2011. Value Chain of the Artisanal Oyster Harvesting Fishery of The Gambia. Gambia-Senegal Sustainable Fisheries Program (Ba Nafaa). Narrangansett, Rhode Island: Coastal Resources Center, University of Rhode Island. 74pp.
- Panfili, J., Durand, J.D., Mbow A. et al. 2014. Influence of salinity on life history traits of the bonga shad *Ethmalosa fimbriata* (Pisces, Clupeidae): comparison between the Gambia and Saloum estuaries. *Marine Ecology Progress Series* 270: 241–257. doi:10.3354/meps270241

- Pecl, G.T. and G.B. Jackson. 2008. The potential impacts of climate change on inshore squid: biology, ecology and fisheries. Review in Fish Biology and Fisheries 18:373–385. doi:10.1007/s11160-007-9077-3
- Pelegrí, J. L., and J. Peña-Izquierdo. 2015. “Eastern Boundary Currents off North-West Africa,” in *Oceanographic and biological features in the Canary Current Large Marine Ecosystem. IOC-UNESCO, Paris. IOC Technical Series, No. 115*, 81–92.
- Pérez-Gómez, B., Álvarez-Fanjul, E., Marcos, M., Puyol, B., and M. García. 2015. “Sea level variability and trends in the Canary Current Large Marine Ecosystem,” in *Oceanographic and biological features in the Canary Current Large Marine Ecosystem. IOC Technical Series, No. 115*, 309–320.
- Poulain, F., Himes-Cornell, A. and C. Shelton. 2018. Methods and tools for climate change adaptation in fisheries and aquaculture. In: Barange, M., Bahri, T., Beveridge, M.C.M., Cochrane, K.L., Funge-Smith, S. & Poulain, F., eds. Impacts of climate change on fisheries and aquaculture: synthesis of current knowledge, adaptation and mitigation options. FAO Fisheries and Aquaculture Technical Paper No. 627. Rome, FAO. 628 pp
- Ragusa, G. 2014. Overview of the Fisheries Sector in The Gambia. Fisheries and Aquaculture Journal 5(3). doi:10.4172/2150-3508.1000107
- Repolho, T., Baptista, M., Pimentel, M.S. et al. 2014. Developmental and physiological challenges of octopus (*Octopus vulgaris*) early life stages under ocean warming. Journal of Comparative Physiology B (2014) 184:55–64. doi:10.1007/s00360-013-0783-
- Roudier, P., Ducharne, A., and L. Feyen. 2014. Climate change impacts on runoff in West Africa: a review. *Hydrol. Earth Syst. Sci.* 18, 2789–2801. doi:10.5194/hess-18-2789-2014
- Sherwood et al., 2020. An Assessment of Earth’s Climate Sensitivity Using Multiple Lines of Evidence. Review of Geophysics doi: 10.1029/2019RG000678
- Sigman, D. M., and M.P. Hain. 2012. The Biological Productivity of the Ocean. *Nat. Educ. Knowl.* 3, 21.
- Sowe, A. 2017. Socioeconomic Study of the Fisheries Sector, The Gambia. Banjul, Food and Agriculture Organization of the United Nations. 49pp
- Sowman, M., and S. Raemaekers. 2018. Socio-ecological vulnerability assessment in coastal communities in the BCLME region. *J. Mar. Syst.* doi:https://doi.org/10.1016/j.jmarsys.2018.01.013.
- Stramma, L., Brandt, P., Schafstall, J., Schott, F., Fischer, J., and A. Körtzinger. 2008. Oxygen minimum zone in the North Atlantic south and east of the Cape Verde Islands. *J. Geophys. Res. Ocean.* 113. doi:10.1029/2007JC004369.
- Stramma, L., Prince, E. D., Schmidtko, S., Luo, J., Hoolihan, J. P., Visbeck, M., et al. 2012. Expansion of oxygen minimum zones may reduce available habitat for tropical pelagic fishes. *Nat. Clim. Chang.* 2, 33–37. doi:10.1038/nclimate1304.
- Sylla, A., Mignot, J., Capet, X. and A.T. Gaye. 2019. Weakening of the Senegalo–Mauritanian upwelling system under climate change. *Climate Dynamics* 53:4447–4473. doi:10.1007/s00382-019-04797-y
- Tobey, J., Castro, K., Lee, V. et al. 2009. An Overview of Marine Fisheries in The Gambia and Preliminary Governance Baseline. Gambia-Senegal Sustainable Fisheries Program (Ba Nafaa). Narrangansett, Rhode Island: Coastal Resources Center, University of Rhode Island.

Thresher, R.E. 1984. Reproduction in reef fishes. T.F.H. Publication. Inc. Ltd Neptune City, New Jersey, USA.

Twinomuhangi ,R. and G.O. Ouma. 2015. “Strengthening of the Gambia’s Climate Change Early Warning Systems”. Final Report. UNEP/GEF. 125pp.

UNCTAD (United Nations Conference on Trade and Development Enhanced Integrated Framework). 2014. The Fisheries Sector in The Gambia: Trade, value addition and social inclusiveness, with a focus on women. New York and Geneva, UNCTAD. 54pp.

UNDP. 2019. United Nations Development Programme, Human Development Reports. <http://hdr.undp.org/en/content/2019-human-development-index-ranking>

Vélez-Belchí, P., González-Carballo, M., Pérez-Hernández, M., and A. Hernández-Guerra. 2015. “Open ocean temperature and salinity trends in the Canary Current Large Marine Ecosystem,” in *Oceanographic and biological features in the Canary Current Large Marine Ecosystem. IOC Technical Series, No. 115*, eds. L. Valdés and I. Déniz-González (IOC-UNESCO, Paris), pp. 299–308.

Van Vliet, M.T.H., Ludwig F. and P. Kabat. 2013. Global streamflow and thermal habitats of freshwater fishes under climate change. *Climatic Change*: 121:739–754. doi:10.1007/s10584-013-0976-0

WCRP (World Climate Research Program). 2018. Global Sea-level Budget 1993-present. *Earth System Science Data* Vol. 10(3): 1551-1590.

Appendix 1A. Vulnerability scores for the temperature attribute

Scores range from 2 to -2 indicating a highly positive to highly negative value.

Habitat	Species	Species relevant values	Biological response	Category rating	Exposure Score
Oceanic	Deep-water rose shrimp <i>P. longirostris</i>	Catch levels are low when temperature is minimal (Benboucha et al. 2008)	High SST favours abundance/catch level.	Highly positive	+2
	Guinean shrimp <i>P. atlantica</i>	Unknown species-specific values but recruitment is negatively impacted by temperature (Ramirez et al. 2006)	High SST affects recruitment.	Highly negative	-2
	Pink shrimp <i>P. notialis</i>	Unknown species-specific values but recruitment is negatively impacted by temperature (Ramirez et al. 2006)	High SST affects recruitment.	Highly negative	-2
	Striped shrimp <i>P. kerathurus</i>	Preferred temperature range: 17.75–22.59°C (Aquamaps). Above 28°C hatching rates are nil (Nwamo et al. 2014).	High SST affects hatching.	Highly negative	-2
	Giant tiger shrimp <i>P. monodon</i>	Optimum growth rate: 28–35°C. Above 38°C is critical (Ze-Ping et al. 2005).	High SST affects growth.	Highly negative	-2
	Octopus <i>Octopus vulgaris</i>	16–21°C optimum temperature. Mortality at 19°C and more commonly at 25°C (Giménez & García, 2002; Repolho et al. 2014). CPUE negatively influenced by SST (Chédia et al. 2009)	High SST affects growth and survival.	Highly negative	-2
	cuttlefish <i>Sepia officinalis hierredda</i>	Temperature limit: 10–30°C; 24°C embryogenesis decreases (Bloor, 2016). SST influences hatchling and growth rate (Pecl & Jackson, 2008) as well as in catch abundance (Vargas-Yáñez et al. 2009)	SST affects negatively hatchling and growth rate but favours abundance/catch level.	Moderately negative	-1
	Tuna <i>Thunnus</i> spp.	Temperature optimum for distribution/catches: 22.2–27.6°C. Lowest catches coincide with temperatures above 27.5°C (Agyekum et al. 2018).	High SST affects distribution and catches.	Highly negative	-2

Sea breams <i>Dentex</i> spp.	Catches of <i>D. macrophthalmus</i> significantly correlated with SST in Portuguese waters, lower catches during warm years (Teixeira et al., 2014). Peak spawning observed during December and January in Angola, although individuals with ripe gonads were found during most of the year (Potts et al., 2010). Highest catches of <i>D. angolensis</i> during the cold season off the Congo coast (Fontana, 1981). Preferred maximum SST is ~ 27.8 °C (Aquamaps).	Likely decrease in biomass due to warming	Moderately negative	-1
Groupers <i>Epinephelus aeneus</i>	Preferred thermal range from 20 – 27.9 °C for <i>E. aeneus</i> (Aquamaps). Under experimental conditions, juvenile white grouper exposed to 27 °C had a larger proportion of inflated swim bladders compared to individuals in the 23°C treatment (Elsadin et al., 2018). Spawning observed between 24-24.7 °C in the western Mediterranean Sea (Desiderà et al., 2019)	Likely decrease in biomass or condition of individuals during their juvenile stage due to warming	Moderately negative	-1
Snappers <i>Lutjanus</i> spp.	Preferred thermal range from 25.3 – 27.9 °C for <i>L. agennes</i> and 24.7 – 27.9 °C for <i>L. goreensis</i> (Aquamaps). Spawning in tropical lutjanids take place year-round with peaks in spawning during warm water temperatures (Thresher, 1984)	Due to their preference for warmer temperatures, a neutral or positive effect of increased SST may be expected in the near future, but a likely decrease in biomass in the long-term depending on the warming rate per decade.	Neutral	0
Hake <i>Merluccius</i> spp.	Spawning season from Sep-March, with peak spawning between November and February off Mauritania (Fernández-Peralta et al., 2011). This coincides with the warm-cool season (Nov-Dec), and beginning of the cold season (Jan-May). Bathymetric differences indicate that	Due to their preference for colder temperatures, a distributional shift or a decrease in biomass may be expected due to increased sea temperature assuming that the bottom	Moderately negative	-1

	M. polli spawns at greater depths (300–500 m or more) than M. senegalensis (100–400 m or less).	sea temperature will increase at a similar rate as SST.		
Round sardinella <i>Sardinella</i> spp.	Preferred thermal range from 18.58 – 27.93 °C (Aquamaps). Positive effect of SST on S. aurita recruitment between 22-28.5°C (Diankha et al., 2018).	Likely decrease in recruitment and biomass due to increased SST, depending on the warming rate per decade.	Moderately negative	-1
Flat sardinella <i>Sardinella maderensis</i>	Preferred thermal range from 20.74 – 27.89 °C (Aquamaps). High recruitment associated with high SST, above 25 °C (Diankha et al., 2018).	Positive effect of increased SST in the short-term but a likely decrease in recruitment and biomass in the long-term, depending on the warming rate per decade.	Neutral	0
Mackerel <i>Scomber colias</i>	Preferred thermal range from 15.81 – 26.51 °C (Aquamaps). A literature review indicated that larvae are observed at 14-24 °C (Castro Hernández and Santana Ortega, 2000). Spawning mostly observed at temperatures of 15-22° C (Collette and Nauen., 1983, Tchetach et al., 2019).	Likely decrease in recruitment and biomass due to warming or distribution change e.g. migrating to deeper waters	Moderately negative	-1
Atlantic horse mackerel <i>Trachurus</i> spp.	Preferred thermal range from 10.2 – 19.7 °C for T. trachurus and 20.7-27.8 for T. trecae (Aquamaps). Spawning season of T. trecae extends from October to April (Overko and Mylnikov, 1979).	Likely decrease in recruitment and biomass due to warming or distributional change e.g. migrating to deeper waters	Moderately negative	-1
Blue spotted seabream <i>Pagrus</i> spp./ <i>Sparus</i> spp.	Prefers cooler waters (<15°C) and generally lives on hard (rocky) sandy or sandy-muddy bottoms, below the thermocline (FAO, 2016). Found in waters temperatures ranging from 13.5 °C to a maximum of 32 °C (Aquamaps).	Due to their preference for colder temperatures, a distributional shift or a decrease in biomass may be expected	Moderately negative	-1

Coastal	solefish <i>Cynoglossus senegalensis</i> / <i>Daetichthys cadenati</i>	24.75–27.89 °C temperature range (Aquamaps).	The extent of the effect is uncertain but it is likely to affect survival and growth. Further research is required.	Moderately negative	-1
	Red pandora <i>Pagellus bellottii</i>	Preferred thermal range from 20.7 – 27.9 °C for <i>P. bellottii</i> (Aquamaps). Eurythermic species (Amponsah et al., 2016)	Due to their broad temperature tolerance, a neutral effect of increased SST can be expected in the short-term but a likely decrease in recruitment and biomass in the long-term, depending on the warming rate per decade.	Neutral	0
	False scad <i>Caranx rhonchus</i>	Spawning observed off Mauritania during the warm period (summer) during 1997-2008. Temperature considered the most important factor for spawning of false scad off Mauritania (Arkhipov, 2009). Preferred thermal range from 19.83– 27.88 °C (Aquamaps).	Due to their preference for warmer temperatures, a neutral or positive effect of increased SST can be expected in the short-term depending on the warming rate per decade.	Neutral	0
	Croakers <i>Pseudolithus</i> spp.	Condition factor of <i>P. senegalensis</i> and <i>P. typus</i> influenced by SST, <i>P. senegalensis</i> showed higher condition with lower SST while <i>P. typus</i> coincided with the peak in SST (Wehye et al., 2017). These species have been found to spawn during the warm season, <i>P. typus</i> spawns in waters of 27.5 °C or warmer (Wehye et al., 2017 and references therein).	Due to their preference for warmer temperatures, a neutral or positive effect of increased SST can be expected in the short-term depending on the warming rate per decade.	Neutral	0
Estuarine/Freshwater	West African mangrove oyster <i>Crassostrea gasar/tulipa</i>	23–31°C optimum temperature (Atindana et al. 2020).	The extent of the effect is uncertain but it is likely to affect survival and growth.	Uncertain	

		Further research is required.		
African catfish <i>Clarias gariepinus/anguillaris</i>	35°C maximum water temperature tolerance (Vliet et al. 2013). Increase in temperature depicts increased growth rates (Kawamura et al. 2017)	SST/AT benefits growth rates.	Highly positive	+2
African arowana fatango <i>Heterotis niloticus</i>	Species-specific values unknown. 28–31°C optimum temperature for Asian arowana in captivity (Yue et al. 2020).	The extent of the effect is uncertain but experiments in captivity of silver arowana have shown that high temperature affects survival and growth rate (Armando et al. 2018). Further research is required.	Moderately negative	–1
Nile tilapia <i>O. niloticus</i>	33°C maximum water temperature tolerance (Vliet et al. 2013) and 26–30°C optimum temperature for growth and survival (Beitinger & FitzPatrick, 1979, Nivelle et al. 2019).	High SST/AT affects growth and increases mortality.	Moderately positive	+1
Catfish/kosso <i>Synodontis schall</i>	Water temperature: 26.47–29.72°C (Bakari et al. 2016).	High SST may affect populations but the extent of its effect is still unknown. Further research is required.	Uncertain	
Bonga shad <i>Ethmalosa fimbriata</i>	Monthly population fecundity peaked at SST of 25°C during 2004–2012 (Baldé et al., 2019). Bonga shad has been found to spawn at temperatures between 18 and 23°C, with a maximum spawning temperature of 30.2 °C (Albaret and Gerlotto, 1976; Döring et al., 2017)	Due to their broad temperature tolerance, a neutral effect of increased SST can be expected in the near future but a likely decrease in recruitment and biomass in the long-	Neutral	0

		term, depending on the warming rate per decade.		
catfish <i>Arius</i> spp.	Preferred temperature for <i>A. heudolotii</i> ranges from 25-28°C, but observed in temperatures from 23-32°C (Aquamaps).	Due to their broad temperature tolerance, a neutral effect of increased temperature can be expected in the near future but a likely decrease in recruitment and biomass in the long-term, depending on the warming rate per decade.	Neutral	0

Appendix 1B. Vulnerability scores for salinity

Scores range from 2 to -2 indicating a highly positive to highly negative value.

Habitat	Species	Species relevant values	Biological response	Category rating	Exposure Score
Oceanic	Deep-water rose shrimp <i>P. longirostris</i>	Spawning: 36.2–36.4 psu in shallow and deep waters (Benboucha et al. 2008)	High salinity favours spawning.	Highly positive	+2
	Guinean shrimp <i>P. atlantica</i>	Emigration pattern of juveniles to offshore depends on low salinity levels. Adults are hypersaline preferred (Benfield et al. 04).	High salinity affects emigration to offshore but adults prefer higher salinity.	Moderately negative	–1
	Pink shrimp <i>P. notialis</i>	Emigration pattern of juveniles to offshore depends on low salinity levels. Adults are hypersaline preferred (Benfield et al. 04).	High salinity affects emigration to offshore but adults prefer higher salinity.	Moderately negative	–1
	Striped shrimp <i>P. kerathurus</i>	Preferred salinity range: above 36 psu for adults; 10–20psu for postlarvae (Moussa & Taha, 2003).	High salinity affects hatching and survival of postlarvae but adults prefer higher salinity.	Moderately negative	–1
	Giant tiger shrimp <i>P. monodon</i>	Preferred salinity range: 30.11–35.36 (Aquamaps). Optimum for growth: 25ppt. Below 5ppt and above 25ppt it reaches the critical survival.	High salinity affects hatching growth.	Highly negative	-2
	Octopus <i>Octopus vulgaris</i>	Preferred salinity range: 32.09–37.79psu (Aquamaps).	The effect of high salinity is unknown but it is likely to have a neutral effect as the species tolerates high salinity levels. Further research is required.	Neutral	0

cuttlefish <i>Sepia officinalis hierredda</i>	Hatchling terminates below 23–25psu and anomalies are observed at 22.4psu (Bloor, 2016)	High salinity benefits hatchling.	Highly positive	+2
Tuna <i>Thunnus</i> spp.	Salinity does not exceed 35ppt for tuna catches in the eastern equatorial Atlantic (Agyekum et al. 2018).	Likely increases in salinity may not affect this species as it tolerates high salinity levels in the Gambia.	Neutral	0
Sea breams <i>Dentex</i> spp.	Preferred salinity range: 26.5-35.5 for <i>D. angolensis</i> , 25.9-34.65 for <i>D. congoensis</i> , 28.5-38.4 for <i>D. macrophthalmus</i> (Aquamaps).	Likely increases in salinity as a result of climate change may not affect croakers.	Neutral	0
Groupers <i>Epinephelus aeneus</i>	Preferred salinity range: 27.3-38.7 for white grouper (Aquamaps). White grouper has been reared in salinities of 3 ppt, however, low salinities affect growth performance (Cnaani et al., 2012).	Likely increases in salinity as a result of climate change may not affect white grouper.	Neutral	0
Snappers <i>Lutjanus</i> spp.	Preferred salinity range: 24.1-35 for <i>L. agennes</i> and from 25-35 for <i>L. goreensis</i> (Aquamaps).	Likely increases in salinity as a result of climate change may not affect snappers	Neutral	0
Hake <i>Merluccius</i> spp.	Preferred salinity range: 25.9-35.8 for <i>M. polli</i> and from 34-37 for <i>M. senegalensis</i> (Aquamaps).	Likely increases in salinity as a result of climate change may not affect snappers	Neutral	0
Round sardinella <i>Sardinella</i> spp.	Preferred salinity range: 30.7-37.39 (Aquamaps)	Likely increases in salinity as a result of climate change may not affect <i>S. aurita</i> due to their preference for oceanic salinity waters (Cury and Fontana, 1988)	Neutral	0
Flat sardinella <i>Sardinella maderensis</i>	Preferred salinity range: 25.33-37.75 (Aquamaps)	Likely increases in salinity as a result of climate change may not affect <i>S. maderensis</i> .	Neutral	0

	Mackerel <i>Scomber colias</i>	Preferred salinity range: 31.72-37.23 (Aquamaps)	Likely increases in salinity as a result of climate change may not affect <i>S. colias</i> .	Neutral	0
	Atlantic horse mackerel <i>Trachurus</i> spp.	Preferred salinity range: 32.5-36.9 for <i>T. trachurus</i> and 27.1-37 for <i>T. trecae</i> . (Aquamaps)	Likely increases in salinity as a result of climate change may not affect horse mackerel	Neutral	0
	Blue spotted seabream <i>Pagrus</i> spp./ <i>Sparus</i> spp.	Preferred salinity range: 27.6-38.4 for blue-spotted seabream (Aquamaps).	Likely increases in salinity as a result of climate change may not affect snappers	Neutral	0
Coastal	solefish <i>Cynoglossus senegalensis</i> / <i>Dagetichthys cadenati</i>	Salinity range during spawning: 0.0–38.0psu (Panfili et al. 2006).	High salinity benefits spawning.	Highly positive	+2
	False scad <i>Caranx rhonchus</i>	Entering brackish-water lagoons and estuaries (Bauchot, M.-L., 2003. Carangidae). Preferred salinity range: 27.52-37.5 (Aquamaps).	Due to their broad salinity range, Likely increases in salinity as a result of climate change may not affect false scad	Neutral	0
	Red pandora <i>Pagellus bellottii</i>	Preferred salinity range: 26.7-36.1 (Aquamaps).	Likely increases in salinity as a result of climate change may not affect red pandora.	Neutral	0
	Croakers <i>Pseudolithus</i> spp.	Preferred salinity range: 25.1-34.9 for <i>P. typus</i> (Aquamaps). <i>P. elongatus</i> has been found in salinities from 0.1-35.5 (FAO, 1995)	Likely increases in salinity as a result of climate change may not affect croakers.	Neutral	0
Estuarine/Freshwater	West African mangrove oyster <i>Crassostrea gasar/tulipa</i>	Preferred salinity: 4–40g/L but "intolerable" below 4g/L and above 50g/L (Horodesky et al. 2019). Filtration rates are lower at high salinity (Sutton et al. 2016).	High salinity affects survival.	Moderately negative	–1
	African catfish <i>Clarias gariepinus/anguillaris</i>	Optimum salinity: 4–6psu; It is a stenohaline species (Kawamura et al. 2017).	High salinity affects survival, growth and induce to cannibalism.	Moderately negative	–1

	African arowana fatango <i>Heterotis niloticus</i>	Unknown species-specific values.	The extent of the effect is uncertain. Further research is required.	Uncertain	
	Nile tilapia <i>O. niloticus</i>	Optimum salinity: 0.0–19psu but tolerates up to 36psu (Schofield et al. 2011)	High salinity affects on growth and survival if above the 20psu lethal limit.	Moderately negative	–1
	Catfish/kosso <i>Synodontis schall</i>	Salinity range: 1.49–9.70‰ but also recorded at 26.77‰. Species prefer habitats with no environmental fluctuations such as salinity (Bakari et al. 2016)	High salinity may affect populations but the extent of the effect is still unknown.	Uncertain	
	Bonga shad <i>Ethmalosa fimbriata</i>	Spawns in salinities from 3.5-38 ppt (Abowei, 2009). Bonga shad can tolerate salinities of up to 90 psu, their preferred range is 35-60 psu (Panfili et al., 2004).	Likely increases in salinity as a result of climate change may not affect bonga shad.	Neutral	0
	catfish <i>Arius</i> spp.	Preferred salinity range: 25-34 for <i>Arius heudolotii</i> (Aquamaps). These species inhabit shallow water systems and estuaries.	Likely increases in salinity as a result of climate change may not affect snappers	Neutral	0

Appendix 1C. Vulnerability scores for oxygen

Scores range from 2 to -2 indicating a highly positive to highly negative value. NA: Projections not available for freshwater environments.

Habitat	Species	Species relevant values	Biological response	Category rating	Exposure Score
Oceanic	Deep-water rose shrimp <i>P. longirostris</i>	Unknown species-specific thresholds. Penaeid shrimps are tolerant to hypoxic conditions (Benfield et al. 04).	Deoxygenation benefits shrimp populations.	Moderately positive	+1
	Guinean shrimp <i>P. atlantica</i>	Unknown species-specific thresholds. Penaeid shrimps are tolerant to hypoxic conditions (Benfield et al. 04).	Deoxygenation benefits shrimp populations.	Moderately positive	+1
	Pink shrimp <i>P. notialis</i>	Unknown species-specific thresholds. Penaeid shrimps are tolerant to hypoxic conditions (Benfield et al. 04).	Deoxygenation benefits shrimp populations.	Moderately positive	+1
	Striped shrimp <i>P. kerathurus</i>	Distribution records correspond to preferred bottom oxygen (mol m ⁻³) values from 189.29–248.66 (Aquamaps).	Likely impacts uncertain, further research is required.	Uncertain	
	Giant tiger shrimp <i>P. monodon</i>	Distribution records correspond to preferred bottom oxygen (mol m ⁻³) values from 185.87–214.50 (Aquamaps).	Likely impacts uncertain, further research is required.	Uncertain	
	Octopus <i>Octopus vulgaris</i>	Premature hatching occurs under hypoxic conditions (Repolho et al. 2014).	Deoxygenation promotes premature hatchings.	Moderately negative	–1
	cuttlefish <i>Sepia officinalis hierredda</i>	Oceanic pH decrease has negative effect on oxygen affinity by respiratory proteins, reducing metabolism and consequently growth and reproduction (Pecl & Jackson, 2008)	Deoxygenation affects growth and reproduction.	Highly positive	+2
	Tuna <i>Thunnus</i> spp.	DO lethal range in larvae: 2.65mg/L (Wexler et al. 2011)	Deoxygenation affects growth and dispersal of larvae.	Highly negative	–2

Sea breams <i>Dentex</i> spp.	Distribution records correspond to preferred bottom oxygen (mol m ⁻³) values from 59.7-230.4 for <i>D. angolensis</i> , 48.95-235.21 for <i>D. congoensis</i> and from 59.62-235 for <i>D. macrophthalmus</i> (Aquamaps).	Likely impacts uncertain, further research is required.	Uncertain	
Groupers <i>Epinephelus aeneus</i>	White grouper distribution records correspond to preferred bottom oxygen (mol m ⁻³) values from 88.6-235.4 (Aquamaps).	Likely impacts uncertain, further research is required.	Uncertain	
Snappers <i>Lutjanus</i> spp.	Distribution records correspond to preferred bottom oxygen (mol m ⁻³) values from 74.4-220.3 for <i>L. agennes</i> and from 72.6-221.7 for <i>L. goreensis</i> (Aquamaps).	Likely impacts uncertain, further research is required.	Uncertain	
Hake <i>Merluccius</i> spp.	Distribution records correspond to preferred preferred bottom oxygen (mol m ⁻³) values from 60.7-230.4 for <i>M. polli</i> and from 64.5-238.8 for <i>M. senegalensis</i> (Aquamaps).	Likely impacts uncertain, further research is required.	Uncertain	
Round sardinella <i>Sardinella</i> spp.	<i>S. aurita</i> distribution records correspond to preferred bottom oxygen (mol m ⁻³) values from 161.88-245.21.	Likely impacts uncertain, further research is required.	Uncertain	
Flat sardinella <i>Sardinella maderensis</i>	<i>S. maderensis</i> distribution records correspond to preferred bottom oxygen (mol m ⁻³) values from 71.32-233.3.	Likely impacts uncertain, further research is required.	Uncertain	
Mackerel <i>Scomber colias</i>	<i>S. colias</i> distribution records correspond to preferred bottom oxygen (mol m ⁻³) values from 189.37-269.38.	Likely impacts uncertain, further research is required.	Uncertain	
Atlantic horse mackerel <i>Trachurus</i> spp.	Horse mackerel distribution records correspond to preferred bottom oxygen (mol m ⁻³) values from 193.1-288.8 for <i>T. trachurus</i> and from 45.21-227.57 for <i>T. trecae</i> .	Likely impacts uncertain, further research is required.	Uncertain	

	Blue spotted seabream <i>Pagrus</i> spp./ <i>Sparus</i> spp.	Distribution records correspond to preferred preferred bottom oxygen (mol m ⁻³) values from 77-241.3 for blue-spotted seabream (Aquamaps).	Likely impacts uncertain, further research is required.	Uncertain	
Coastal	solefish <i>Cynoglossus senegalensis</i> / <i>Dagetichthys cadenati</i>	DO range: 83.75–220.98 mmol/m ³ (Aquamaps).	The extent of the effect is uncertain. Further research is required.	Uncertain	
	False scad <i>Caranx rhonchus</i>	Distribution records correspond to preferred bottom oxygen of 72.56-236.25 mmol m ⁻³	Likely impacts uncertain, further research is required.	Uncertain	
	Red pandora <i>Pagellus bellottii</i>	Red pandora distribution records correspond to preferred bottom oxygen (mol m ⁻³) values from 67.7-235.4 (Aquamaps).	Likely impacts uncertain, further research is required.	Uncertain	
	Croakers <i>Pseudolithus</i> spp.	<i>P. elongatus</i> and <i>P. typus</i> distribution records correspond to preferred bottom oxygen (mol m ⁻³) values from 94.3-220.3 and 71.3-221.7 (Aquamaps).	Likely impacts uncertain, further research is required.	Uncertain	
Estuarine/Freshwater	West African mangrove oyster <i>Crassostrea gasar/tulipa</i>		NA		
	African catfish <i>Clarias gariepinus/anguillaris</i>		NA		
	African arowana fatango <i>Heterotis niloticus</i>		NA		
	Nile tilapia <i>O. niloticus</i>		NA		
	Catfish/kosso <i>Synodontis schall</i>		NA		

	Bonga shad <i>Ethmalosa fimbriata</i>		NA		
	catfish <i>Arius</i> spp.		NA		

Appendix 1D. Vulnerability scores for pH

Scores range from 2 to -2 indicating a highly positive to highly negative value. NA: Projections not available for freshwater environments.

Habitat	Species	Species relevant values	Biological response	Category rating	Exposure Score
Oceanic	Deep-water rose shrimp <i>P. longirostris</i>	Shell-forming species relies on the availability of aragonite levels (Chapter CC and Oceanic Environment).	Low pH affects aragonite stability.	Highly negative	-2
	Guinean shrimp <i>P. atlantica</i>	Shell-forming species relies on the availability of aragonite levels (Chapter CC and Oceanic Environment).	Low pH affects aragonite stability.	Highly negative	-2
	Pink shrimp <i>P. notialis</i>	Shell-forming species relies on the availability of aragonite levels (Chapter CC and Oceanic Environment).	Low pH affects aragonite stability.	Highly negative	-2
	Striped shrimp <i>P. kerathurus</i>	Unknown species-specific values.	Likely impacts uncertain, further research is required.	Uncertain	
	Giant tiger shrimp <i>P. monodon</i>	Optimum pH for growth: 7.5–8.5 (Tendencia & Verreth, 2011)	Low pH affects growth.	Highly negative	-2
	Octopus <i>Octopus vulgaris</i>	Oceanic pH decrease has negative effect on oxygen affinity by respiratory proteins, reducing metabolism and consequently growth and reproduction (Pecl & Jackson, 2008).	Low pH affects growth and reproduction.	Highly negative	-2
	cuttlefish <i>Sepia officinalis hierredda</i>	7.5 pH observed premature hatching. Survival rates are lower at lower pH (Bloor, 2016).	Low pH affects survival and hatchling.	Highly negative	-2

	Tuna <i>Thunnus</i> spp.	Below pH 7.56 affects larvae survival and growth rates, and reduce larval absorption (Bromhead et al. 2015).	Low pH affects larvae survival and growth, and prey detection.	Highly negative	-2
	Sea breams <i>Dentex</i> spp.	Unknown species-specific values.	Likely impacts uncertain, further research is required.	Uncertain	
	Groupers <i>Epinephelus aeneus</i>	High CO ₂ concentrations have been found to reduce swimbladder volume and body weight of white grouper, and affect skeletal development (Elsadin et al., 2018).	Experimental studies suggest that acidification will negatively influence white grouper	Moderate negative	-1
	Snappers <i>Lutjanus</i> spp.	Unknown species-specific values.	Likely impacts uncertain, further research is required.	Uncertain	
	Hake <i>Merluccius</i> spp.	Unknown species-specific values.	Likely impacts uncertain, further research is required.	Uncertain	
	Round sardinella <i>Sardinella</i> spp.	Unknown species-specific values.	Likely impacts uncertain, further research is required.	Uncertain	
	Flat sardinella <i>Sardinella maderensis</i>	Unknown species-specific values.	Likely impacts uncertain, further research is required.	Uncertain	
	Mackerel <i>Scomber colias</i>	Unknown species-specific values.	Likely impacts uncertain, further research is required.	Uncertain	
	Atlantic horse mackerel <i>Trachurus</i> spp.	Unknown species-specific values.	Likely impacts uncertain, further research is required.	Uncertain	
	Blue spotted seabream <i>Pagrus</i> spp./ <i>Sparus</i> spp.	Unknown species-specific values.	Likely impacts uncertain, further research is required.	Uncertain	
Coastal	solefish <i>Cynoglossus senegalensis</i> / <i>Dagetichthys cadenati</i>	Unknown species-specific values.	Likely impacts uncertain, further research is required.	Uncertain	

	False scad <i>Caranx rhonchus</i>	Unknown species-specific values.	Likely impacts uncertain, further research is required.	Uncertain	
	Red pandora <i>Pagellus bellottii</i>	Unknown species-specific values.	Likely impacts uncertain, further research is required.	Uncertain	
	Croakers <i>Pseudolithus</i> spp.	Unknown species-specific values.	Likely impacts uncertain, further research is required.	Uncertain	
Estuarine/Freshwater	West African mangrove oyster <i>Crassostrea gasar/tulipa</i>		NA		
	African catfish <i>Clarias gariepinus/anguillaris</i>		NA		
	African arowana fatango <i>Heterotis niloticus</i>		NA		
	Nile tilapia <i>O. niloticus</i>		NA		
	Catfish/kosso <i>Synodontis schall</i>		NA		
	Bonga shad <i>Ethmalosa fimbriata</i>		NA		
	catfish <i>Arius</i> spp.		NA		

Appendix 1E. Vulnerability scores for ocean circulation and productivity

Scores range from 2 to -2 indicating a highly positive to highly negative value. NA: Projections not available for freshwater environments.

Habitat	Species	Species relevant values	Biological response	Category rating	Exposure Score
Oceanic	Deep-water rose shrimp <i>P. longirostris</i>	Bathymetrics: 50–500m depth (Sobrino et al. 2005), with greatest biomass density along 200–500m (Muñoz et al. 2012)	Stratification affects survival.	Highly negative	–2
	Guinean shrimp <i>P. atlantica</i>	Bathymetrics: 22–25m depth with greatest biomass below 50m (Muñoz et al. 2012). Larval dispersal relies on circulation and mixing (Benfield et al. 04).	Stratification affects larval dispersal.	Highly negative	–2
	Pink shrimp <i>P. notialis</i>	Bathymetrics: 22–24m depth with greatest biomass below 50m (Muñoz et al. 2012). Algal filaments and diatoms are the main feeding components (Taiwo et al. 2014).	Stratification affects larval survival and dispersal.	Highly negative	–2
	Striped shrimp <i>P. kerathurus</i>	Bathymetrics: 9–46m depth (Aquamaps). Larval dispersal relies on circulation and mixing (Benfield et al. 04).	Stratification affects larval survival and dispersal.	Highly negative	-2
	Giant tiger shrimp <i>P. monodon</i>	Bathymetrics: 16–60m depth (Aquamaps). Larval dispersal relies on circulation and mixing (Benfield et al. 04).	Stratification affects larval survival and dispersal.	Highly negative	-2
	Octopus <i>Octopus vulgaris</i>	Larvae hatches at the end of the upwelling event, contributing to food quality for survival (Otero et al. 2008).	Stratification affects larval survival.	Highly negative	–2
	cuttlefish <i>Sepia officinalis hierredda</i>	Feeding rates increase with SST and larvae requires more food within shorter period of time (Pecl & Jackson, 2008).	Stratification affects larval survival.	Highly negative	–2

	Tuna <i>Thunnus</i> spp.	High catches coincide with after intensive seasonal upwelling (Agyekum et al. 2018).	Stratification affects distribution and catches.	Highly negative	-2
	Sea breams <i>Dentex</i> spp.	Preferred primary Production ($\text{mgC}\cdot\text{m}^{-3}\cdot\text{d}^{-1}$) ranges from 4.04 – 57.26 for <i>D. angolensis</i> , from 3.9-49.9 for <i>D. congensis</i> and from 0.69-63.2 for <i>D. macrophthalmus</i> .	Decreased upwelling likely to affect abundance of Dentex species	Moderately negative	-1
	Groupers <i>Epinephelus aeneus</i>	Preferred primary Production ($\text{mgC}\cdot\text{m}^{-3}\cdot\text{d}^{-1}$) ranges from 0.74-51.4 for white grouper. Seasonal migration of white grouper from Mauritania to Senegal is related to the onset of productivity in Senegalese waters and decreased productivity in Mauritania (Cury and Roy, 1988).	The reduction in productivity may negatively affect the phenology and biomass of white grouper.	Moderately negative	-1
	Snappers <i>Lutjanus</i> spp.	Preferred primary Production ($\text{mgC}\cdot\text{m}^{-3}\cdot\text{d}^{-1}$) ranges from 6.25 – 50.9 for <i>L. agennes</i> and from 5.6-49.9 for <i>L. goreensis</i> (Aquamaps).	Decreased upwelling likely to affect abundance of snappers due to a reduction in food availability	Moderately negative	-1
	Hake <i>Merluccius</i> spp.	Large assemblages of <i>M. senegalensis</i> breeders are found in central and southern Mauritania (south of Cape Timiris), where significant winter upwelling occurs but breeding grounds are not located on the permanent upwelling zone off Cape Blanc (Fernández-Peralta et al., 2011). Meiners et al., (2010) suggested that black hake abundance is inversely related with intensified and extended upwelling along the Mauritanian and Senegalese coast	Decreased upwelling likely to affect the timing of the reproductive migration of black hakes	Moderately negative	-1
	Round sardinella <i>Sardinella</i> spp.	Production ($\text{mgC}\cdot\text{m}^{-3}\cdot\text{d}^{-1}$) ranges from 0.58-34.58 (Aquamaps). Positive effect of Chl-a on recruitment under low values ($\leq 3.3 \text{ mg m}^{-3}$) and high values ($\geq 10 \text{ mg m}^{-3}$)	The reduction in productivity may not negatively affect round sardinella, since high recruitment has been observed at low Chl-a values	Neutral	0

Coastal	Flat sardinella <i>Sardinella maderensis</i>	Preferred primary Production ($\text{mgC}\cdot\text{m}^{-3}\cdot\text{d}^{-1}$) ranges from 1.9-53.78 (Aquamaps). Positive effect of Chl-a on recruitment under low values ($\leq 4.4 \text{ mg m}^{-3}$)	The reduction in productivity may not negatively affect flat sardinella in the near future, since high recruitment has been observed at low Chl-a values	Neutral	0
	Mackerel <i>Scomber colias</i>	Preferred primary Production ($\text{mgC}\cdot\text{m}^{-3}\cdot\text{d}^{-1}$) ranges from 0.44-14.8 (Aquamaps). Food availability and quality were found to have a greater effect on growth of <i>S. japonicus</i> than temperature (Perrotta et al., 2005).	The reduction in productivity may negatively affect <i>S. colias</i> through a reduction in food availability	Moderately negative	-1
	Atlantic horse mackerel <i>Trachurus</i> spp.	Preferred primary Production ($\text{mgC}\cdot\text{m}^{-3}\cdot\text{d}^{-1}$) ranges from 1.05-23.6 for <i>T. trachurus</i> and 9.92-67.88 for <i>T. trecae</i> (Aquamaps).	The reduction in productivity may negatively affect horse mackerel through a reduction in food availability	Moderately negative	-1
	Blue spotted seabream <i>Pagrus</i> spp./ <i>Sparus</i> spp.	Preferred primary Production ($\text{mgC}\cdot\text{m}^{-3}\cdot\text{d}^{-1}$) ranges from 0.6-58 (Aquamaps).	Due to their broad range of preferred primary production, this species may not be strongly affected by decrease upwelling	Neutral	0
	solefish <i>Cynoglossus senegalensis</i> / <i>Dagetichthys cadenati</i>	Bathymetrics: 20–60m depth (Aquamaps).	Stratification may affect population but the effect is unknown. Further research is required.	Uncertain	
	False scad <i>Caranx rhonchus</i>	Abundance related to upwelling (Diallo, 2000). Preferred primary Production ($\text{mgC}\cdot\text{m}^{-3}\cdot\text{d}^{-1}$) ranges from 1.22-60.41.	The reduction in productivity may negatively affect <i>C. rhonchus</i> since their abundance is related to upwelling	Moderately negative	-1
	Red pandora <i>Pagellus bellottii</i>	Preferred primary Production ($\text{mgC}\cdot\text{m}^{-3}\cdot\text{d}^{-1}$) ranges from 3.12-60.4 for red pandora. Seasonal migration of red pandora in Ghanaian waters, moving inshore up to 18 m depth during the upwelling months (Amponsah et al., 2016). Spawning occurred during the upwelling season (Jun- Sep) in Ghanaian waters (Asabere-Ameyaw, 2000)	The reduction in productivity may negatively affect the phenology and biomass of red pandora	Moderately negative	-1

	Croakers <i>Pseudolithus</i> spp.	Preferred primary Production ($\text{mgC}\cdot\text{m}^{-3}\cdot\text{d}^{-1}$) ranges from 6.41 – 45.2 for <i>P. elongatus</i> and from 7.9-51.4 for <i>P. typus</i> .	No studies have been found indicating a relationship between spawning or recruitment and upwelling.	Uncertain	
Estuarine/Freshwater	West African mangrove oyster <i>Crassostrea gasar/tulipa</i>		NA		
	African catfish <i>Clarias gariepinus/anguillaris</i>		NA		
	African arowana fatango <i>Heterotis niloticus</i>		NA		
	Nile tilapia <i>O. niloticus</i>		NA		
	Catfish/kosso <i>Synodontis schall</i>		NA		
	Bonga shad <i>Ethmalosa fimbriata</i>		NA		
	catfish <i>Arius</i> spp.		NA		

Appendix 1F. Vulnerability scores for Sea level rise

Scores range from 2 to -2 indicating a highly positive to highly negative value.

Habitat	Species	Species relevant values	Biological response	Category rating	Exposure Score
Oceanic	Deep-water rose shrimp <i>P. longirostris</i>	Two spawning zones: 75–200m depth (coastal); 250–500m depth (deep water) (Benboucha et al. 2008).	SLR benefits spawning by favouring saline intrusion in the Gambia river watershed.	Moderately positive	+1
	Guinean shrimp <i>P. atlantica</i>	Unknown species-specific threshold. Adults spawning at the sea, with hypersaline conditions (Benfield et al. 04).	SLR benefits spawning by favouring hypersaline intrusion in the Gambia river watershed.	Moderately positive	+1
	Pink shrimp <i>P. notialis</i>	Unknown species-specific threshold. Adults spawning at the sea, with hypersaline conditions (Benfield et al. 04).	SLR benefits spawning by favouring hypersaline intrusion in the Gambia river watershed.	Moderately positive	+1
	Striped shrimp <i>P. kerathurus</i>	Unknown species-specific values. Hatching rates is influenced by salinity, in which below 28‰ salinity reduces hatching rates (Nwamo et al. 2014).	SLR benefits spawning by favouring hypersaline intrusion in the Gambia river watershed.	Moderately positive	+1
	Giant tiger shrimp <i>P. monodon</i>	Unknown species-specific values. Low growth rates is observed in salinities above 25ppt (Ye et al. 2009)	SLR affects growth.	Highly negative	-2
	Octopus <i>Octopus vulgaris</i>	Bathymetrics: 0–200m depth; Site fidelity throughout the whole life with no latitudinal migration (Balguerías et al. 2002).	The extent of the effect is uncertain but it is likely to have no effect due to site fidelity. Further research is required.	Neutral	0
	cuttlefish <i>Sepia officinalis hierredda</i>	Bathymetrics: 2–200m depth (more commonly found at 100m) with shell implosion beyond this limit. SLR due to SST may expand dispersal in the Arctic with over 2500km migration at depths	SLR is likely to benefit dispersal.	Highly positive	+2

		deeper than 200m and above 9.5°C (Xavier et al.2016).			
	Tuna <i>Thunnus</i> spp.	Highest occurrence of tuna occurs in regions of increased SLR (above -0.03 but below 0.05m) (Agyekum et al. 2018).	SLR may benefit distribution.	Moderately positive	+1
	Sea breams <i>Dentex</i> spp.	Unknown species-specific threshold.	No information has been found suggesting impacts on the species	Neutral	0
	Groupers <i>Epinephelus aeneus</i>	Unknown species-specific threshold.	No information has been found suggesting impacts on the species	Neutral	0
	Snappers <i>Lutjanus</i> spp.	Unknown species-specific threshold.	No information has been found suggesting impacts on the species	Neutral	0
	Hake <i>Merluccius</i> spp.	Unknown species-specific threshold.	No information has been found suggesting impacts on the species	Neutral	0
	Round sardinella <i>Sardinella</i> spp.	Unknown species-specific threshold.	No information has been found suggesting impacts on the species	Neutral	0
	Flat sardinella <i>Sardinella maderensis</i>	Unknown species-specific threshold.	No information has been found suggesting impacts on the species	Neutral	0
	Mackerel <i>Scomber colias</i>	Unknown species-specific threshold.	No information has been found suggesting impacts on the species	Neutral	0
	Atlantic horse mackerel <i>Trachurus</i> spp.	Unknown species-specific threshold.	No information has been found suggesting impacts on the species	Neutral	0
	Blue spotted seabream <i>Pagrus</i> spp./ <i>Sparus</i> spp.	Unknown species-specific threshold.	No information has been found suggesting impacts on the species	Neutral	0

Coastal	solefish <i>Cynoglossus senegalensis/ Dagetichthys cadenati</i>	Bathymetrics:20–60m depth (Aquamaps).	SLR may benefit dispersal but may affect spawning in estuaries. Further research is required.	Neutral	0
	False scad <i>Caranx rhonchus</i>	They occur frequently near the bottom, mostly in depths of 30 to 50 m. Also pelagic and found near the surface at times.	No information has been found suggesting impacts on the species	Neutral	
	Red pandora <i>Pagellus bellottii</i>	Unknown species-specific threshold.	No information has been found suggesting impacts on the species	Neutral	0
	Croakers <i>Pseudolithus</i> spp.	Unknown species-specific threshold.	No information has been found suggesting impacts on the species	Neutral	0
Estuarine/Freshwater	West African mangrove oyster <i>Crassostrea gasar/tulipa</i>	SLR allows salinity intrusion that affects survival.	SLR affects survival.	Moderately negative	–1
	African catfish <i>Clarias gariepinus/anguillaris</i>	Unknown species-specific values.	The extent of the effect is uncertain. Further research is required.	Uncertain	
	African arowana fatango <i>Heterotis niloticus</i>	Unknown species-specific values but this species prefer habitats as floodplains, deep river and lagoons.	The extent of the effect is uncertain. Further research is required.	Uncertain	
	Nile tilapia <i>O. niloticus</i>	Unknown species-specific values but it is tolerant to high salinities although it may affect growth and survival when above 20 psu.	SLR may affect growth and survival by salinity intrusion.	Moderately negative	–1
	Catfish/kosso <i>Synodontis schall</i>	Unknown species-specific values but species is intolerant to salinity fluctuations.	The extent of the effect is uncertain due to salinity intrusion. Further research is required.	Uncertain	
	Bonga shad <i>Ethmalosa fimbriata</i>	Unknown species-specific threshold.	No information has been found suggesting impacts on the species	Neutral	0

	catfish <i>Arius</i> spp.	Unknown species-specific threshold.	No information has been found suggesting impacts on the species	Neutral	0
--	---------------------------	-------------------------------------	---	---------	---

Appendix 1G. Vulnerability scores for extreme events

Scores range from 2 to -2 indicating a highly positive to highly negative value.

Habitat	Species	Species relevant values	Biological response	Category rating	Exposure Score
Oceanic	Deep-water rose shrimp <i>P. longirostris</i>	Maximum spawning relies on maximum salinity (Benboucha et al. 2008).	Droughts benefits salinity intrusion in the Gambia River watershed.	Highly positive	+2
	Guinean shrimp <i>P. atlantica</i>	Unknown species-specific values. Penaeids prefer hypersaline habitats (Benfield et al. 04).	Droughts benefits salinity intrusion in the Gambia River watershed.	Highly positive	+2
	Pink shrimp <i>P. notialis</i>	Unknown species-specific values. Penaeids prefer hypersaline habitats (Benfield et al. 04).	Droughts benefits salinity intrusion in the Gambia River watershed.	Highly positive	+2
	Striped shrimp <i>P. kerathurus</i>	Unknown species-specific values. This species is more abundant during the wet season (Eyo et al. 2016).	Floods affects catches.	Highly negative	-2
	Giant tiger shrimp <i>P. monodon</i>	Unknown species-specific values. This species is more abundant during the wet season (Eyo et al. 2016).	Floods affects catches.	Highly negative	-2
	Octopus <i>Octopus vulgaris</i>	There is a positive correlation between rainfall rates and catches of this species (Chédia et al. 2009; Vargas-Yáñez et al. 2014).	Floods benefits catches.	Highly positive	+2
	cuttlefish <i>Sepia officinalis hierredda</i>	Correlation between rainfall and catches are contradictory, showing positive and negative effects (Guerra 2006).	The extent of the effect is uncertain. Further research is required.	Uncertain	
	Tuna <i>Thunnus</i> spp.	Low catches coincides with regions of intensive discharges (Agyekum et al. 2018).	Floods affect distribution.	Highly negative	-2
	Sea breams <i>Dentex</i> spp.	No studies have assessed the effect of HABs or marine heatwaves on this species		Uncertain	

	Groupers <i>Epinephelus aeneus</i>	No studies have assessed the effect of HABs or marine heatwaves on this species		Uncertain	
	Snappers <i>Lutjanus</i> spp.	No studies have assessed the effect of HABs or marine heatwaves on this species		Uncertain	
	Hake <i>Merluccius</i> spp.	No studies have assessed the effect of HABs or marine heatwaves on this species		Uncertain	
	Round sardinella <i>Sardinella</i> spp.	No studies have assessed the effect of HABs or marine heatwaves on this species	While no studies have assessed the effect of HABs in <i>S. aurita</i> . HABs may negatively impact <i>Sardinella</i> 's condition as observed for South African sardine	Uncertain	
	Flat sardinella <i>Sardinella maderensis</i>	No studies have assessed the effect of HABs or marine heatwaves on this species	While no studies have assessed the effect of HABs in <i>S. maderensis</i> . HABs may negatively impact <i>Sardinella</i> 's condition as observed for South African sardine	Uncertain	
	Mackerel <i>Scomber colias</i>	No studies have assessed the effect of HABs or marine heatwaves on this species	While no studies have assessed the effect of HABs in mackerel. HABs may negatively impact mackerel through a decrease in food availability (i.e. zooplankton)	Uncertain	
	Atlantic horse mackerel <i>Trachurus</i> spp.	No studies have assessed the effect of HABs or marine heatwaves on this species	While no studies have assessed the effect of HABs in horse mackerel. HABs may negatively impact mackerel through a decrease in food availability (i.e. zooplankton)	Uncertain	
	Blue spotted seabream <i>Pagrus</i> spp./ <i>Sparus</i> spp.	No studies have assessed the effect of HABs or marine heatwaves on this species		Uncertain	

Coastal	solefish <i>Cynoglossus senegalensis/ Dagetichthys cadenati</i>	Unknown species-specific values.	The extent of the effect is uncertain. Further research is required.	Uncertain	
	False scad <i>Caranx rhonchus</i>	No studies have assessed the effect of HABs or marine heatwaves on this species	While no studies have assessed the effect of HABs in false scad, HABs may negatively impact it through a decrease in food availability (i.e. zooplankton)	Uncertain	
	Red pandora <i>Pagellus bellottii</i>	No studies have assessed the effect of HABs or marine heatwaves on this species		Uncertain	
	Croakers <i>Pseudolithus</i> spp.	No studies have assessed the effect of HABs or marine heatwaves on this species		Uncertain	
Estuarine/Freshwater	West African mangrove oyster <i>Crassostrea gasar/tulipa</i>	Low survival rates under 5ppt and over 50ppt (Horodesky et al. 2019)	High and low salinity due to effects of droughts/floods affect survival.	Highly negative	-2
	African catfish <i>Clarias gariepinus/anguillaris</i>	Peak spawning and fecundity coincide with floods and wet season (Mark, 2015). Hybernation adapted to dry seasons (Mark, 2015).	Floods benefits spawning.	Highly positive	+2
	African arowana fatango <i>Heterotis niloticus</i>	It inhabits lakes, deep swamps and rivers, and flooded forests with slow current and dense vegetation (Medipally et al. 2015).	Droughts affects species habitats.	Highly negative	-2
	Nile tilapia <i>O. niloticus</i>	Peak catches coincide with rises in water level (Kolding, 1993).	Floods benefits catches.	Highly positive	+2
	Catfish/kosso <i>Synodontis schall</i>	Spawning and slow growth take place during flooding season (Akombo et al.2015).	Floods benefits reproduction.	Highly positive	+2
	Bonga shad <i>Ethmalosa fimbriata</i>	No studies have assessed the effect of HABs or marine heatwaves on this species	While no studies have assessed the effect of HABs in bonga shad. HABs may negatively impact it through a	Uncertain	

			decrease in food availability (i.e. zooplankton)		
	catfish <i>Arius</i> spp.	No studies have assessed the effect of HABs or marine heatwaves on this species		Uncertain	

Appendix 1H. Vulnerability scores for precipitation

Scores range from 2 to -2 indicating a highly positive to highly negative value.

Habitat	Species	Species relevant values	Biological response	Category rating	Exposure Score
Oceanic	Deep-water rose shrimp <i>P. longirostris</i>	Maximum spawning relies on maximum salinity (Benboucha et al. 2008)	Decrease in freshwater discharge maintains the maximum salinity levels for spawning.	Highly positive	+2
	Guinean shrimp <i>P. atlantica</i>	Unknown species-specific preferences. Penaeids generally prefer high salinity levels (Benfield et al. 04)	Decrease in freshwater discharge maintains the maximum salinity levels for spawning.	Highly positive	+2
	Pink shrimp <i>P. notialis</i>	Unknown species-specific preferences. Penaeids generally prefer high salinity levels (Benfield et al. 04)	The extent of the effect is uncertain. Further research is required.	Uncertain	
	Striped shrimp <i>P. kerathurus</i>	Unknown species-specific preferences. Catch abundance are influenced by river flow. Catches are high when there is reduced freshwater flow (Belmar et al. 2019).	Decrease in freshwater discharge benefits catch rates.	Highly positive	+2
	Giant tiger shrimp <i>P. monodon</i>	Unknown species-specific preferences. Catch abundance are influenced by river flow. Catches are high when there is reduced freshwater flow (Belmar et al. 2019).	Decrease in freshwater discharge benefits catch rates.	Highly positive	+2
	Octopus <i>Octopus vulgaris</i>	There is a positive correlation between rainfall rates and catches of this species (Chédia et al. 2009; Vargas-Yáñez et al. 2014).	Decrease in precipitation affects catches.	Highly negative	-2
	cuttlefish <i>Sepia officinalis hierredda</i>	Correlation between rainfall and catches are contradictory, showing positive and negative effects (Guerra XX).	The extent of the effect is uncertain. Further research is required.	Moderately negative	-1

Tuna <i>Thunnus</i> spp.	Low catches coincide with regions of intensive discharges (Agyekum et al. 2018).	Decrease in precipitation benefits occurrences.	Highly positive	+2
Sea breams <i>Dentex</i> spp.	Unknown species-specific preferences	The extent of the effect is uncertain. Further research is required.	Uncertain	
Groupers <i>Epinephelus aeneus</i>	Unknown species-specific preferences	The extent of the effect is uncertain. Further research is required.	Uncertain	
Snappers <i>Lutjanus</i> spp.	A peak in the breeding season of <i>L. goreensis</i> was observed during the heavy rains (May to September) in Nigeria (Fakoya and Anetekha, 2019)	Likely decrease in breeding and spawning due to declines in precipitation	Moderately negative	–1
Hake <i>Merluccius</i> spp.	Unknown species-specific preferences. Oceanic species	The extent of the effect is uncertain. Further research is required.	Uncertain	
Round sardinella <i>Sardinella</i> spp.	The availability of these two sardinella species to coastal fisheries is associated with flooding scenarios, and alternates depending of the location of the low salinity waters (Binet et al., 2001). When the plume is advancing in the vicinity of the coastline, flat sardinella would become the main target species of coastal fisheries (Ostrowski and Barradas, undated).	Decrease in precipitation may benefit round sardinella distribution and abundance	Moderately positive	+1
Flat sardinella <i>Sardinella maderensis</i>	The availability of these two sardinella species to coastal fisheries is associated with flooding scenarios, and alternates depending of the location of the low salinity waters (Binet et al., 2001). When the plume is advancing in the vicinity of the coastline, flat sardinella would	Decrease in precipitation may negatively affect flat sardinella distribution and abundance	Moderately negative	–1

		become the main target species of coastal fisheries (Ostrowski and Barradas, undated).			
	Mackerel <i>Scomber colias</i>	Unknown species-specific preferences	The extent of the effect is uncertain. Further research is required.	Uncertain	
	Atlantic horse mackerel <i>Trachurus</i> spp.	Unknown species-specific preferences	The extent of the effect is uncertain. Further research is required.	Uncertain	
	Blue spotted seambream <i>Pagrus</i> spp./ <i>Sparus</i> spp.	Unknown species-specific preferences	The extent of the effect is uncertain. Further research is required.	Uncertain	
Coastal	solefish <i>Cynoglossus senegalensis</i> / <i>Dagetichthys cadenati</i>	Decrease in precipitation allows salinity intrusion that benefits populations.	The extent of the effect is uncertain. Further research is required.	Moderately positive	+1
	False scad <i>Caranx rhonchus</i>	Unknown species-specific preferences. However, species have a broad salinity preference and thus a decrease in precipitation may benefit the population	The extent of the effect is uncertain. Further research is required.	Uncertain	
	Red pandora <i>Pagellus bellottii</i>	Unknown species-specific preferences	The extent of the effect is uncertain. Further research is required.	Uncertain	
	Croakers <i>Pseudolithus</i> spp.	<i>P. elongatus</i> observed to have reduced spawning from August to October and peak spawning from December to February, this peak corresponding with the dry season (Watts, 1958 in Longhurst, 1969)	Peak spawning during the dry season	Moderately positive	+1
Estuarine/Freshwater	West African mangrove oyster <i>Crassostrea gasar/tulipa</i>	Unknown species-specific values.	Decrease in precipitation allows salinity intrusion that affects survival.	Moderately negative	-1

African catfish <i>Clarias gariepinus/anguillaris</i>	Lower precipitation rates coincides with higher catches (Mark, 2015).	Decrease in precipitation benefits catches.	Highly positive	+2
African arowana fatango <i>Heterotis niloticus</i>	It inhabits lakes, deep swamps and rivers, and flooded forests with slow current and dense vegetation (Medipally et al. 2015).	Decrease in river discharge affects populations by impeding the formation of swamps and flooded forests but also benefits them by decreasing formation of currents.	Neutral	0
Nile tilapia <i>O. niloticus</i>	Decrease in precipitation increases salinity intrusion that affects survival and growth.	The extent of the effect is uncertain but high salinity affects survival and growth.	Uncertain	
Catfish/kosso <i>Synodontis schall</i>	Species are abundant in rainy and flooding habitats (Bakari et al. 2016). Spawning and slow growth take place during flooding season (Akombo et al.2015).	Decrease in precipitation affects spawning.	Moderately negative	-1
Bonga shad <i>Ethmalosa fimbriata</i>	Decrease in precipitation increases salinity intrusion.	Hypersaline condition are found to affect growth and fecundity. These hypersaline conditions not predicted for the Gambia Estuary	Neutral	
catfish <i>Arius</i> spp.	Onset of the rainy season coincides with breeding season in Guinean waters, as well as seasonal movement from relatively deep water (10-20m) during the dry season, to estuaries and very coastal areas during the monsoon (Conand et al., 1995).	Likely declines in precipitation may affect the timing of the breeding season and migration.	Moderately negative	-1

Appendix 2. Examples of adaptive models/activities applied to different systems in the fisheries and aquaculture sectors.

Classification according to Poulain et al. 2018.

System	Model/Parties	Description	Actions	Nature	Mitigation	Adaptation	Response	Time line	Source
<i>Management</i>	Carbon Offset Project/Mexico and Kenya	Conservation of mangroove forest by planting and seeding in order to ensure reasonable carbon sequestration rates as well as maintenance of nursery grounds and shoreline protection	community-based participation; ecosystem rehabilitation	Institutional	yes	Transformational	Direct CC impact	long-term	Gross et al.2016
	Fishing safety and training/ Pacific Islands	Safety audits of longline vessels and any purse-seine vessels operating within the cyclone belt	capacity building	Risk reduction and resilience	–	Incremental	Indirect CC impact	short-term	Bell et al. 2011b
	Kosrae Shoreline Management Plan/ Micronesia	Relocate coastal infrastructure and restrict new development away from coastal hazards	ecosystem rehabilitation	Risk reduction and resilience	–	Incremental	Direct CC impact	long-term	Poulain et al. 2018
	Translocation of fish population/ USA	Translocation of a wild population of bull trout from downstream to upstream in order to establish a new population in the Glacier National Park due to invasive species and impacts from climate change (e.g., increasing water temperatures, altered precipitation and runoff patterns, reduced late-season snow- and ice-melt) in order to conserve the genetic diversity and life history traits.	adaptive operations	Livelihood	yes	Transformational	Indirect CC impact	long-term	Gross et al. 2016
	Risk reduction/ Malawai and Caribbean	Safety at the Sea in order to reduce exposure to risks at sea, such as storms and winds.	capacity building; risk management	Risk reduction and resilience	–	Transformational	Direct CC impact	short-term	Johnson et al. 2013

	Water management/ Uganda	Promoting water conservation during drought periods through regulated water harvesting techniques and sustainable agricultural and aquaculture practices in order to form reservoirs for storing water for usage in fish ponds.	community-based participation; capacity building;	Institutional –	Incremental	Direct CC impact	short-term	Muchuru & Nhamo (2018)
	ClimaPesca, ClimeFish/ South America and USA	Early warning systems for storms, weather, disease, sea scape or temperature extremes reduce exposure in order to connect marine researchers, fisheries organizations and policy decision-makers.	capacity building	Risk reduction and resilience yes	Incremental	Indirect CC impact	short-term	Poulain et al. 2018
<i>Scientific and technological</i>	Monitoring, control and surveillance (MCS)/South Africa	Develop geographical information systems (GIS) that identify fish hot spots vulnerable to climate change, determine coastal erosion and drawing up shoreline management plans.	integrated science	Institutional –	Transformational	Direct CC impact	long-term	Muchuru & Nhamo (2018)
	Multi-trophic farming or pokkali cum fish	Usage and development of novel technologies such as microalgal food development	integrated science; capacity building	Livelihood –	Transformational	Direct CC impact	long-term	Poulain et al. 2018
	Fishing Aggregating Device (FAD)/Melanesia	Increase access to protein in coastal and rural areas through consumption of pelagic species, and reduce pressure on inshore and coral reef habitats. FAD siting, construction and management to increase skills, with local fishers trained in monitoring and identification of species at FADs to collect data in data-poor areas.	community-based participation; capacity building; business development	Livelihood –	Incremental	Direct CC impact	short-term	Poulain et al. (2018); Johnson et al. 2013 (SPC/FAO)
	Fish breeding/Nigeria	Support breeding programmes of research institutions through funding their relevant fish-based research and development and dissemination of findings in order to Adopt and breed hardier and early maturing fish	integrated science; capacity building	Livelihood –	Transformational	Direct CC impact	long-term	Muchuru & Nhamo (2018)

Social		species or salt-tolerant species for increasing the fish production							
	No name/Vanuatu, Brazil	Develop ecotourism and/or craft marketing (e.g. seashells, fish scale fashion and design) in coastal communities in order to reduce reliance on potentially vulnerable systems such as mangrove or coral reef habitats.	business development and planning; community-based participation	Livelihood	–	Transformational impact	Direct CC long-term	Johnson et al. 2013	
	Government compensation/UK, Viet Nam	compensation to individual fishers and fishing industry (e.g. farms) in the form of grants to replace damaged or lost static gear and allowed temporary flexibility on allocation rules to make up lost income when conditions returned to normal. Insurance provision, co-financed by governments, is also an important tool to compensate fishers and farmers and build back better after a disaster.	risk insurance and social protection	Risk reduction and resilience	–	Incremental	Direct CC impact	FAO, 2016; Poulain et al. (2018)	
	Strengthening of the Gambia's Climate Change Early Warning Systems/ Gambia	enhance the capacity of hydro-meteorological services and networks to predict climate events and risk factors; develop a more effective, efficient and targeted delivery of climate information including early warnings; and contribute to improved and timely preparedness and responses of various stakeholders to climate linked risks and vulnerabilities.	capacity building; community-based participation	Risk reduction and resilience	–	Incremental	Indirect CC impact	Twinomuhangi & Ouma (2015)	
	Social networking/ Ghana	Social networks are important for livelihood strategies and livelihood diversification, which is a crucial component of adaptation to climate change in resource-dependent communities in developing countries. In	community-based participation	Risk reduction and resilience	–	Incremental	Direct CC impact	short-term Dapilah et al. 2020	

Economic		Bangladesh, communities share gear and fishing tactics together after storm events.								
	Vessel Day Scheme (VDS)/Pacific Islands	The 'cap and trade' provisions of the vessel day scheme (VDS) enable members of the parties to receive benefits, regardless of where tuna are concentrated. Periodic adjustment of allocated vessels days within the VDS will reduce the need for members in the east to purchase days from those in the west.	diversifying fishing activities	Livelihood	–	Transformational impact	Direct CC	long-term	Bell et al. 2011	
	Weather-based index insurance/Seychelles	Public-private partnership arrangement that provides an insurance to small-scale and industrial fishers by providing inputs (fish feed) on credit, technical support and marketing or covers loss or damage caused to fishing vessels.	risk insurance and social protection	Risk reduction and resilience	–	Incremental	Indirect CC impact	short-term	Muchuru & Nhamo (2018)	
	Buy-back scheme/Mauritius	Net fishing license holders were encouraged to surrender their net license on the basis of an inducement package made up of financial compensation, conversion and training to join other fisheries.	alternative livelihood strategy	Livelihood	–	Incremental	Direct CC impact	short-term	Muchuru & Nhamo (2018)	
	Adaptation to Climate Change in Arid Lands/ Kenya	Fingerlings to be produced by specialized farmers who sell it as fish feed, and set up and manage fishpond in fingerlings farms to be sold in local markets and traders.	alternative livelihood strategy	Livelihood	–	Transformational impact	Direct CC	long-term	GEF/UNDP, 2018	